

# HEAT TRANSFER

SECOND EDITION



A. F. MILLS

MASIMO 2159  
Apple v. Masimo  
IPR2022-01299

# HEAT TRANSFER

---

**Second Edition**

**A. F. MILLS**

University of California at Los Angeles  
Los Angeles, California 90024-5197



Prentice Hall, Upper Saddle River, New Jersey 07458

**MASIMO 2159**  
**Apple v. Masimo**  
**IPR2022-01299**

**Library of Congress Cataloging-in-Publication Data**

Mills, A. F.

Basic Heat and Mass Transfer 2/E by A. F. Mills  
p. cm.

Includes bibliographical references and index.  
ISBN 0-13-947624-5

CIP data available.

General Library System  
University of Wisconsin - Madison  
728 State Street  
Madison, WI 53706-1494  
U.S.A.

**Acquisitions Editor:** *Bill Stenquist*

**Editorial/Production Supervision:** *Sharyn Vitrano*

**Editor-in-Chief:** *Marcia Horton*

**Managing Editor:** *Eileen Clark*

**Cover Director:** *Jayne Conte*

**Director of Production and Manufacturing:** *David W. Riccardi*

**Manufacturing Buyer:** *Pat Brown*

**Editorial Assistant:** *Meg Weist*



©1999 by Prentice-Hall, Inc.

Simon & Schuster/A Viacom Company

Upper Saddle River, New Jersey 07458

The author and publisher of this book have used their best efforts in preparing this book. These efforts include the development, research, and test of the theories and programs to determine their effectiveness. The author and publisher make no warranty of any kind, expressed or implied, with regard to these programs or the documentation contained in this book. The author and publisher shall not be liable in any event for incidental or consequential damages in connection with, or arising out of, the furnishing, performance, or use of these programs.

All rights reserved. No part of this book may be reproduced in any form or by any means, without permission in writing from the publisher.

Printed in the United States of America

10 9 8 7 6 5 4 3 2 1

**ISBN 0-13-947624-5**

Prentice-Hall International (U.K.) Limited, *London*

Prentice-Hall of Australia Pty. Limited, *Sydney*

Prentice-Hall Canada Inc., *Toronto*

Prentice-Hall Hispanoamericana, S.A., *Mexico*

Prentice-Hall of India Private Limited, *New Delhi*

Prentice-Hall of Japan, Inc., *Tokyo*

Simon & Schuster Asia Pte. Ltd., *Singapore*

Editora Prentice-Hall do Brasil, Ltda., *Rio de Janeiro*

About the Cover: The columns supporting portions of the trans-Alaska oil pipeline system are gravity-flow ammonia heatpipes (see Chapter 7). In winter, the ground underneath the columns is warmer than the environment. Ammonia liquid evaporates inside the base of a column and condenses at the top, with the enthalpy of vaporization dissipated to the environment by convection and radiation from the cooling fins. The heat extracted from the ground causes a large volume of ice to form underneath the columns and provides a solid foundation for the pipeline. The Arctic summer is not warm enough to completely melt this permafrost before the next winter.

**MASIMO 2159**  
**Apple v. Masimo**  
**IPR2022-01299**

Wendt

7087744

TJ

260

M52

1999

*To Brigid  
For your patience and understanding.*

---

# PREFACE

---

---

*Heat Transfer* has been written for undergraduates in mechanical, aerospace, nuclear, and chemical engineering programs. Apart from the usual lower-division mathematics and science courses, the preparation required of the student is introductory courses in fluid mechanics and thermodynamics, and preferably the usual junior-level engineering mathematics course. The ordering of the material and the pace at which it is presented have been carefully chosen so that the beginning student can proceed from the most elementary concepts to those that are more difficult. As a result, the book should prove to be quite versatile. It can be used as the text for an introductory course during the junior or senior year, although the coverage is sufficiently comprehensive for use as a reference work in laboratory and design courses, and by the practicing engineer.

Throughout the text, the emphasis is on engineering calculations, and each topic is developed to a point that will provide students with the tools needed to practice the art of design. The worked examples not only illustrate the use of relevant equations but also teach modeling as both an art and science. A supporting feature of *Heat Transfer* is the fully integrated software available from the Prentice-Hall website at [www.prenhall.com](http://www.prenhall.com). The software is intended to serve primarily as a tool for the student, both at college and after graduation in engineering practice. The programs are designed to reduce the effort required to obtain reliable numerical results and thereby increase the efficiency and effectiveness of the engineer. I have found the impact of the software on the educational process to be encouraging. It is now possible to assign more meaningful and interesting problems, because the students need not get bogged down in lengthy calculations. Parametric studies, which are the essence of engineering design, are relatively easily performed. Of course, computer programs are not a substitute for a proper understanding. The instructor is free to choose the extent to which the software is used by students because of the unique exact correspondence between the software and the text material. My practice has been to initially require students to perform various hand calculations, using the

computer to give immediate feedback. For example, they do not have to wait a week or two until homework is returned to find that a calculated convective heat transfer coefficient was incorrect because a property table was misread.

The extent to which engineering design should be introduced in a heat transfer course is a controversial subject. It is my experience that students can be best introduced to design methodology through an increased focus on equipment such as heat exchangers: *Heat Transfer* presents more extensive coverage of exchanger design than do comparable texts. In the context of such equipment one can conveniently introduce topics such as synthesis, parametric studies, trade-offs, optimization, economics, and material constraints. The computer program HEX2 assists the student to explore the consequences of changing the many parameters involved in a design process. If an appropriate selection of this material is taught, I am confident that Accreditation Board for Engineering and Technology guidelines for design content will be met. More important, I believe that engineering undergraduates are well served by being exposed to this material, even if it means studying somewhat less heat transfer science.

More than 300 new exercises have been added for this edition. They fall into two categories: (1) relatively straightforward exercises designed to help students understand fundamental concepts, and (2) exercises that introduce new heat transfer technology and that have a practical flavor. The latter play a very important role in motivating students; considerable care has been taken to ensure that they are realistic in terms of parameter values and focus on significant aspects of real engineering problems. The practical exercises are first steps in the engineering design process and many have substantial design content. Since environmental considerations have required the phasing out of CFC refrigerants, R-12 and R-113 property data, worked examples and exercises, have been replaced with corresponding material for R-22 and R-134a.

*Heat Transfer* contains the following chapters and appendixes:

1. Elementary Heat Transfer
2. Steady One-Dimensional Heat Conduction
3. Multidimensional and Unsteady Conduction
4. Convection Fundamentals and Correlations
5. Convection Analysis
6. Thermal Radiation
7. Condensation, Evaporation, and Boiling
8. Heat Exchangers
- A. Property Data
- B. Units, Conversion Factors, and Mathematics
- C. Charts

In a first course, the focus is always on the key topics of conduction, convection, radiation, and heat exchangers. Particular care has been taken to order the material on these topics from simpler to more difficult concepts. In Chapter 2 one-dimensional conduction and fins are treated before deriving the general partial differential heat conduction equation in Chapter 3. In Chapter 4 the student is taught how to use convection correlations before encountering the partial differential equations governing momentum and energy conservation in Chapter 5. In Chapter 6 radiation properties are introduced on a total energy basis and the shape factor is introduced as a geometrical concept to allow engineering problem solving before having to deal with the directional and spectral aspects of radiation. Also, wherever possible, advanced topics are located at the ends of chapters, and thus can be easily omitted in a first course.

Chapter 1 is a brief but self-contained introduction to heat transfer. Students are given an overview of the subject and some material needed in subsequent chapters. Interesting and relevant engineering problems can then be introduced at the earliest opportunity, thereby motivating student interest. All the exercises can be solved without accessing the property data in Appendix A.

Chapters 2 and 3 present a relatively conventional treatment of heat conduction, though the outdated and approximate Heissler and Gröber charts are replaced by exact charts and the computer program COND2. The treatment of finite-difference numerical methods for conduction has been kept concise and is based on finite-volume energy balances. Students are encouraged to solve the difference equations by writing their own computer programs, or by using standard mathematics software such as Mathcad or MATLAB.

In keeping with the overall philosophy of the book, the objective of Chapter 4 is to develop the students' ability to calculate convective heat transfer coefficients. The physics of convection is explained in a brief introduction, and the heat transfer coefficient is defined. Dimensional analysis using the Buckingham pi theorem is used to introduce the required dimensional groups and to allow a discussion of the importance of laboratory experiments. A large number of correlation formulas follow; instructors can discuss selected geometrical configurations as class time allows, and students can use the associated computer program CONV to reliably calculate heat transfer coefficients and skin friction coefficients or pressure drop for a wide range of configurations. Being able to do parametric studies with a wide variety of correlations enhances the students' understanding more than can be accomplished by hand calculations. Design alternatives can also be explored using CONV.

Analysis of convection is deferred to Chapter 5: simple laminar flows are considered, and high-speed flows are treated first in Section 5.2, since an understanding of the recovery temperature concept enhances the students' problem-solving capabilities. Each of the topics in Sections 5.3 through 5.8 are essentially self-contained, and the instructor can select as few or as many as required.

Chapter 6 focuses on thermal radiation. Radiation properties are initially defined on a total energy basis, and the shape factor is introduced as a simple geometrical concept. This approach allows students to immediately begin solving engineering radiation exchange problems. Only subsequently need they tackle the more difficult di-

rectional and spectral aspects of radiation. For gas radiation, the ubiquitous Hottel charts have been replaced by the more accurate methods developed by Edwards; the accompanying computer program RAD3 makes their use particularly simple.

The treatment of condensation and evaporation heat transfer in Chapter 7 has novel features, while the treatment of pool boiling is quite conventional. Forced convection boiling and condensation is taken far enough to facilitate calculation of both pressure drop and heat transfer. Heatpipes are dealt with in some detail, enabling students to calculate the wicking limit and to analyze the performance of simple gas-controlled heatpipes.

Chapter 8 expands the presentation of the thermal analysis of heat exchangers beyond the customary and includes regenerators and the effect of axial conduction on thermal performance. The treatment of heat exchanger design includes the calculation of exchanger pressure drop, thermal-hydraulic design, heat transfer surface selection for compact heat exchangers, and economic analysis leading to the calculation of the benefit-cost differential associated with heat recovery operations. The computer program HEX2 serves to introduce students to computer-aided design of heat exchangers.

The author and publisher appreciate the efforts of all those who provided input that helped develop and improve the text. We remain dedicated to further refining the text in future editions, and encourage you to contact us with any suggestions or comments you might have.

A. F. Mills  
amills@ucla.edu

Bill Stenquist  
Executive Editor  
william\_stenquist@prenhall.com



---

# ACKNOWLEDGMENTS

---

---

Reviewers commissioned for the previous edition, published by Richard D. Irwin, Inc., provided helpful feedback. The author would like to thank the following for their contributions to the first edition.

David Antoniuk, TRW Systems, Inc.

Theodore Bergman, University of Texas at Austin

Robert F. Boehm, University of Nevada—Las Vegas

John M. Boyd, Worcester Polytechnic Institute

Harry Buchberg, University of California—Los Angeles

Vernon E. Denny, Science Applications International Corporation

Creighton A. Depew, University of Washington

A. M. Dhanak, Michigan State University

Thomas E. Diller, Virginia Polytechnic Institute & State University

D. K. Edwards, University of California—Irvine

L. W. Florschuetz, Arizona State University

J. C. Han, Texas A&M University

B. K. Hodge, Mississippi State University

Sukhyun Kim, Kukmin University, Korea

V. V. Klimenko, Nuclear Safety Institute, USSR

Allan Kirkpatrick, Colorado State University

Adrienne Lavine, University of California—Los Angeles

Gordon D. Mallinson, University of Auckland, New Zealand

Atila Mertol, LSI Logic Corporation

Ronald S. Mullisen, California Polytechnic State University—San Luis Obispo  
M. Ohadi, University of Maryland  
Calvin C. Oliver, University of Florida—Gainesville  
Patrick H. Oosthuizen, Queen's University, Kingston, Ontario  
Peter Othmer, California State University—Fullerton  
Gerald Pomraning, University of California—Los Angeles  
John P. Renie, Indiana University/Purdue University at Fort Wayne  
Frank W. Schmidt, Pennsylvania State University  
Terry Simon, University of Minnesota  
E. M. Sparrow, University of Minnesota  
J. Edward Sunderland, University of Massachusetts  
John A. Tichy, Rensselaer Polytechnic Institute  
Brian Vick, Virginia Polytechnic & State University  
Andrew Wortman, California State Air Resources Board  
Walter W. Yuen, University of California—Santa Barbara

Some of the material in *Heat Transfer*, in the form of examples and exercises, has been adapted from an earlier text by my former colleagues at UCLA, D. K. Edwards and V. E. Denny (*Transfer Processes* 1/e, Holt, Rinehart & Winston, 1973; 2/e Hemisphere-McGraw-Hill, 1979). I have also drawn on material in radiation heat transfer from a more recent text by D. K. Edwards (*Radiation Heat Transfer Notes*, Hemisphere, 1981). I gratefully acknowledge the contributions of these gentlemen, both to this book and to my professional career. The computer software was expertly written by Baek Youn. I would also like to thank former students S. W. Hiebert, H. Choi, R. Tsai, B. Cowan, E. Myhre, B. H. Chang, D. C. Weatherly, A. Gopinath, J. I. Rodriguez, B. P. Dooher, and M. A. Friedman.

In preparing the second edition, I have had useful input from a number of people, including Professor F. Forster, University of Washington; Professor N. Shamsundar, University of Houston; Professor S. Kim, Kukmin University; and Professor A. Lavine, UCLA. Students who have helped include P. Hwang, M. Tari, B. Tan, J. Sigler, M. Fabri, and A. Na-Nakornpanom.

My special thanks to the secretarial staff at UCLA and the University of Auckland: Phyllis Gilbert, Joy Wallace, and Julie Austin provided enthusiastic and expert typing of the manuscript. Mrs. Gilbert also provided expert typing of the solutions manual.

---

# NOTES TO THE INSTRUCTOR AND STUDENT

---




---

These notes have been prepared to assist the instructor and student and should be read before the text is used. Topics covered include conventions for artwork and mathematics, the format for example problems, organization of the exercises, comments on the thermophysical property data in Appendix A, and a guide for use of the accompanying computer software.

## ARTWORK

---

Conventions used in the figures are as follows.

-  Conduction or convection heat flow
-  Radiation heat flow
-  Fluid flow

## MATHEMATICAL SYMBOLS

---

Symbols that may need clarification are as follows.

- $\approx$  Nearly equal
- $\sim$  Of the same order of magnitude
- $|_x$  All quantities in the term to the left of the bar are evaluated at  $x$

## EXAMPLES

---

Use of standard format for presenting the solutions of engineering problems is a good practice. The format used for the examples in *Heat Transfer*, which is but one possible approach, is as follows.

### Problem statement

### Solution

#### *Given:*

#### *Required:*

#### *Assumptions:* 1.

2. etc.

*Sketch* (when appropriate)

*Analysis* (diagrams when appropriate)

*Properties evaluation*

*Calculations*

*Results* (tables or graphs when appropriate)

### Comments

1.

2. etc.

It is always assumed that the problem statement precedes the solution (as in the text) or that it is readily available (as in the *Solutions Manual*). Thus, the *Given* and *Required* statements are concise and focus on the essential features of the problem. Under *Assumptions*, the main assumptions required to solve the problem are listed; when appropriate, they are discussed further in the body of the solution. A sketch of the physical system is included when the geometry requires clarification; also, expected temperature profiles are given when appropriate. (Schematics that simply repeat the information in the problem statements are used sparingly. I know that many instructors always require a schematic. My view is that students need to develop an appreciation of when a figure or graph is necessary, because artwork is usually an expensive component of engineering reports. For example, I see little use for a schematic that shows a 10 m length of straight 2 cm–O.D. tube.) The analysis may consist simply of listing some formulas from the text, or it may require setting up a differential equation and its solution. Strictly speaking, a property should not be evaluated until its need is identified by the analysis. However, in routine calculations, such as evaluation of convective heat transfer coefficients, it is often convenient

to list all the property values taken from an Appendix A table in one place. The calculations then follow with results listed, tabulated, or graphed as appropriate. Under *Comments*, the significance of the results can be discussed, the validity of assumptions further evaluated, or the broader implications of the problem noted.

In presenting calculations for the examples in *Heat Transfer*, I have rounded off results at each stage of the calculation. If additional figures are retained for the complete calculations, discrepancies in the last figure will be observed. Since many of the example calculations are quite lengthy, I believe my policy will facilitate checking a particular calculation step of concern. As is common practice, I have generally given results to more significant figures than is justified, so that these results can be conveniently used in further calculations. It is safe to say that no engineering heat transfer calculation will be accurate to within 1%, and that most experienced engineers will be pleased with results accurate to within 10% or 20%. Thus, preoccupation with a third or fourth significant figure is misplaced (unless required to prevent error magnification in operations such as subtraction).

## EXERCISES

---

The diskette logo next to an exercise statement indicates that it should be solved using the *Heat Transfer* software, and that the sample solution provided to the instructor has been prepared accordingly. There are many additional exercises that can be solved using the software but that do not have the logo designation. These exercises are intended to give the student practice in hand calculations, and thus the sample solutions were also prepared manually.

The exercises have been ordered to correspond with the order in which the material is presented in the text, rather than in some increasing degree of difficulty. Since the range of difficulty of the exercises is considerable, the instructor is urged to give students guidance in selecting exercises for self-study. Answers to all exercises are listed in the *Solutions Manual* provided to instructors. Odd- and even-numbered exercises are listed separately; the instructor may choose to give either list to students to assist self-study.

## PROPERTY DATA

---

A considerable quantity of property data has been assembled in Appendix A. Key sources are given as references or are listed in the bibliography. Since *Heat Transfer* is a textbook, my primary objective in preparing Appendix A was to provide the student with a wide range of data in an easily used form. Whenever possible, I have used the most accurate data that I could obtain, but accuracy was not always the primary concern. For example, the need to have consistent data over a wide range of temperature often dictated the choice of source. All the tables are in SI units, with temperature in kelvins. The computer program UNITS can be used for conversions to other systems of units. Appendix A should serve most needs of the

student, as well as of the practicing engineer, for doing routine calculations. If a heat transfer research project requires accurate and reliable thermophysical property data, the prudent researcher should carefully check relevant primary data sources.

## SOFTWARE

---

The *Heat Transfer* software has a menu that describes the content of each program. The programs are also described at appropriate locations in the text. The input format and program use are demonstrated in example problems in the text. Use of the text index is recommended for locating the program descriptions and examples. There is a one-to-one correspondence between the text and the software. In principle, all numbers generated by the software can be calculated manually from formulas, graphs, and data given in the text. Small discrepancies may be seen when interpolation in graphs or property tables is required, since some of the data are stored in the software as polynomial curve fits.

The software facilitates self-study by the student. Practice hand calculations can be immediately checked using the software. When programs such as CONV, PHASE, and BOIL are used, properties evaluation and intermediate calculation steps can also be checked when the final results do not agree.

Since there is a large thermophysical property database stored in the software package, the programs can also be conveniently used to evaluate these properties for other purposes. For example, in CONV both the wall and fluid temperatures can be set equal to the desired temperature to obtain property values required for convection calculations. We can even go one step further when evaluating a convective heat transfer coefficient from a new correlation not contained in CONV: if a corresponding item is chosen, the values of relevant dimensionless groups can also be obtained from CONV, further simplifying the calculations.

---

# CONTENTS

---

---

## CHAPTER

---

- 1 ELEMENTARY HEAT TRANSFER 1**
  - 1.1 Introduction 2**
  - 1.2 Heat Transfer and Its Relation to Thermodynamics 3**
  - 1.3 Modes of Heat Transfer 7**
    - 1.3.1 Heat Conduction 8
    - 1.3.2 Thermal Radiation 13
    - 1.3.3 Heat Convection 17
  - 1.4 Combined Modes of Heat Transfer 24**
    - 1.4.1 Thermal Circuits 24
    - 1.4.2 Surface Energy Balances 27
  - 1.5 Transient Thermal Response 29**
    - 1.5.1 The Lumped Thermal Capacity Model 29
    - 1.5.2 Combined Convection and Radiation 34
  - 1.6 Heat Exchangers 37**
    - 1.6.1 Single- and Two-Stream Exchangers 38
    - 1.6.2 Analysis of a Condenser 40
    - 1.6.3 Other Single-Stream Exchangers 45
  - 1.7 Dimensions and Units 45**
  - 1.8 Closure 47**
    - Exercises 48
  
- 2 STEADY ONE-DIMENSIONAL HEAT CONDUCTION 67**
  - 2.1 Introduction 68**
  - 2.2 Fourier's Law of Heat Conduction 68**
    - 2.2.1 Thermal Conductivity 69
    - 2.2.2 Contact Resistance 71

<b>2.3</b>	<b>Conduction across Cylindrical and Spherical Shells</b>	<b>73</b>
2.3.1	Conduction across a Cylindrical Shell	73
2.3.2	Critical Thickness of Insulation on a Cylinder	77
2.3.3	Conduction across a Spherical Shell	80
2.3.4	Conduction with Internal Heat Generation	82
<b>2.4</b>	<b>Fins</b>	<b>86</b>
2.4.1	The Pin Fin	86
2.4.2	Fin Resistance and Surface Efficiency	94
2.4.3	Other Fin Type Analyses	95
2.4.4	Fins of Varying Cross-Sectional Area	100
2.4.5	The Similarity Principle and Dimensional Analysis	108
<b>2.5</b>	<b>Closure</b>	<b>111</b>
	References	112
	Exercises	112
<b>3</b>	<b>MULTIDIMENSIONAL AND UNSTEADY CONDUCTION</b>	<b>143</b>
<b>3.1</b>	<b>Introduction</b>	<b>144</b>
<b>3.2</b>	<b>The Heat Conduction Equation</b>	<b>144</b>
3.2.1	Fourier's Law as a Vector Equation	145
3.2.2	Derivation of the Heat Conduction Equation	145
3.2.3	Boundary and Initial Conditions	150
3.2.4	Solution Methods	153
<b>3.3</b>	<b>Multidimensional Steady Conduction</b>	<b>154</b>
3.3.1	Steady Conduction in a Rectangular Plate	154
3.3.2	Steady Conduction in a Rectangular Block	161
3.3.3	Conduction Shape Factors	164
<b>3.4</b>	<b>Unsteady Conduction</b>	<b>167</b>
3.4.1	The Slab with Negligible Surface Resistance	168
3.4.2	The Semi-Infinite Solid	175
3.4.3	Convective Cooling of Slabs, Cylinders, and Spheres	187
3.4.4	Product Solutions for Multidimensional Unsteady Conduction	198
<b>3.5</b>	<b>Moving-Boundary Problems</b>	<b>203</b>
3.5.1	Solidification from a Melt	203
3.5.2	Steady-State Melting Ablation	207
<b>3.6</b>	<b>Numerical Solution Methods</b>	<b>212</b>
3.6.1	A Finite-Difference Method for Two-Dimensional Steady Conduction	213
3.6.2	Finite-Difference Methods for One-Dimensional Unsteady Conduction	221
3.6.3	Resistance-Capacitance ( $RC$ ) Formulation	230
3.6.4	A Finite-Difference Method for Moving-Boundary Problems	237
<b>3.7</b>	<b>Closure</b>	<b>242</b>
	References	243
	Exercises	244



<b>4</b>	<b>CONVECTION FUNDAMENTALS AND CORRELATIONS</b>	<b>275</b>
4.1	<b>Introduction</b>	<b>276</b>
4.2	<b>Fundamentals</b>	<b>276</b>
4.2.1	The Convective Heat Transfer Coefficient	277
4.2.2	Dimensional Analysis	283
4.2.3	Correlation of Experimental Data	295
4.2.4	Evaluation of Fluid Properties	299
4.3	<b>Forced Convection</b>	<b>301</b>
4.3.1	Forced Flow in Tubes and Ducts	301
4.3.2	External Forced Flows	312
4.4	<b>Natural Convection</b>	<b>325</b>
4.4.1	External Natural Flows	325
4.4.2	Internal Natural Flows	333
4.4.3	Mixed Forced and Natural Flows	340
4.5	<b>Tube Banks and Packed Beds</b>	<b>347</b>
4.5.1	Flow through Tube Banks	348
4.5.2	Flow through Packed Beds	355
4.6	<b>Rotating Surfaces</b>	<b>362</b>
4.6.1	Rotating Disks, Spheres, and Cylinders	362
4.7	<b>Rough Surfaces</b>	<b>365</b>
4.7.1	Effect of Surface Roughness	366
4.8	<b>The Computer Program CONV</b>	<b>375</b>
4.9	<b>Closure</b>	<b>375</b>
	<b>References</b>	<b>384</b>
	<b>Exercises</b>	<b>387</b>
<b>5</b>	<b>CONVECTION ANALYSIS</b>	<b>413</b>
5.1	<b>Introduction</b>	<b>414</b>
5.2	<b>High-Speed Flows</b>	<b>415</b>
5.2.1	A Couette Flow Model	415
5.2.2	The Recovery Factor Concept	420
5.3	<b>Laminar Flow in a Tube</b>	<b>422</b>
5.3.1	Momentum Transfer in Hydrodynamically Fully Developed Flow	423
5.3.2	Fully Developed Heat Transfer for a Uniform Wall Heat Flux	426
5.4	<b>Laminar Boundary Layers</b>	<b>432</b>
5.4.1	The Governing Equations for Forced Flow along a Flat Plate	433
5.4.2	The Plug Flow Model	435
5.4.3	Integral Solution Method	437
5.4.4	Self-Similar Solutions	446
5.4.5	Natural Convection on an Isothermal Vertical Wall	455
5.5	<b>Turbulent Flows</b>	<b>461</b>
5.5.1	The Prandtl Mixing Length and the Eddy Diffusivity Model	462

	5.5.2	Forced Flow along a Flat Plate	465
	5.5.3	Flow in a Tube	478
	5.5.4	More Advanced Turbulence Models	486
<b>5.6</b>		<b>Similarity and Modeling</b>	<b>486</b>
	5.6.1	Dimensionless Equations and Boundary Conditions	486
	5.6.2	Modeling	492
<b>5.7</b>		<b>The General Conservation Equations</b>	<b>493</b>
	5.7.1	Conservation of Mass	493
	5.7.2	Conservation of Momentum	495
	5.7.3	Conservation of Energy	499
	5.7.4	Use of the Conservation Equations	503
<b>5.8</b>		<b>Scale Analysis</b>	<b>504</b>
	5.8.1	Forced-Convection Laminar Boundary Layers	504
	5.8.2	Natural-Convection Laminar Boundary Layer on a Vertical Wall	510
<b>5.9</b>		<b>Closure</b>	<b>515</b>
		<b>References</b>	<b>516</b>
		<b>Exercises</b>	<b>517</b>
<b>6</b>		<b>THERMAL RADIATION</b>	<b>531</b>
	<b>6.1</b>	<b>Introduction</b>	<b>532</b>
	<b>6.2</b>	<b>The Physics of Radiation</b>	<b>532</b>
	6.2.1	The Electromagnetic Spectrum	533
	6.2.2	The Black Surface	534
	6.2.3	Real Surfaces	536
	<b>6.3</b>	<b>Radiation Exchange between Surfaces</b>	<b>538</b>
	6.3.1	Radiation Exchange between Black Surfaces	538
	6.3.2	Shape Factors and Shape Factor Algebra	540
	6.3.3	Electrical Network Analogy for Black Surfaces	547
	6.3.4	Radiation Exchange between Two Diffuse Gray Surfaces	550
	6.3.5	Radiation Exchange between Many Diffuse Gray Surfaces	557
	6.3.6	Radiation Transfer through Passages	565
	<b>6.4</b>	<b>Solar Radiation</b>	<b>568</b>
	6.4.1	Solar Irradiation	568
	6.4.2	Atmospheric Radiation	570
	6.4.3	Solar Absorptance and Transmittance	572
	<b>6.5</b>	<b>Directional Characteristics of Surface Radiation</b>	<b>577</b>
	6.5.1	Radiation Intensity and Lambert's Law	578
	6.5.2	Shape Factor Determination	581
	6.5.3	Directional Properties of Real Surfaces	584
	<b>6.6</b>	<b>Spectral Characteristics of Surface Radiation</b>	<b>590</b>
	6.6.1	Planck's Law and Fractional Functions	590
	6.6.2	Spectral Properties	592
	<b>6.7</b>	<b>Radiation Transfer through Gases</b>	<b>599</b>
	6.7.1	The Equation of Transfer	600
	6.7.2	Gas Radiation Properties	601

- 6.7.3 Effective Beam Lengths for an Isothermal Gas 609
- 6.7.4 Radiation Exchange between an Isothermal Gas and a Black Enclosure 614
- 6.7.5 Radiation Exchange between an Isothermal Gray Gas and a Gray Enclosure 615
- 6.7.6 Radiation Exchange between an Isothermal Nongray Gas and a Single-Gray-Surface Enclosure 619
- 6.8 Closure 622**
- References 623**
- Exercises 624**

## **7 CONDENSATION, EVAPORATION, AND BOILING 651**

- 7.1 Introduction 652**
- 7.2 Film Condensation 652**
  - 7.2.1 Laminar Film Condensation on a Vertical Wall 654
  - 7.2.2 Wavy Laminar and Turbulent Film Condensation on a Vertical Wall 662
  - 7.2.3 Laminar Film Condensation on Horizontal Tubes 668
  - 7.2.4 Effects of Vapor Velocity and Vapor Superheat 674
- 7.3 Film Evaporation 681**
  - 7.3.1 Falling Film Evaporation on a Vertical Wall 681
- 7.4 Pool Boiling 685**
  - 7.4.1 Regimes of Pool Boiling 685
  - 7.4.2 Boiling Inception 688
  - 7.4.3 Nucleate Boiling 691
  - 7.4.4 The Peak Heat Flux 693
  - 7.4.5 Film Boiling 696
- 7.5 Forced-Convection Boiling and Condensation 702**
  - 7.5.1 Two-Phase Flow Patterns 702
  - 7.5.2 Pressure Drop 708
  - 7.5.3 Internal Forced-Convection Boiling 712
  - 7.5.4 Internal Forced-Convection Condensation 716
- 7.6 Phase Change at Low Pressures 719**
  - 7.6.1 Kinetic Theory of Phase Change 719
  - 7.6.2 Interfacial Heat Transfer Resistance 723
  - 7.6.3 Nusselt Analysis Including Interfacial Resistance 725
  - 7.6.4 Engineering Significance of the Interfacial Resistance 728
- 7.7 Heatpipes 730**
  - 7.7.1 Capillary Pumping 733
  - 7.7.2 Sonic, Entrainment, and Boiling Limitations 738
  - 7.7.3 Gas-Loaded Heatpipes 740
- 7.8 Closure 744**
- References 745**
- Exercises 748**

<b>8</b>	<b>HEAT EXCHANGERS</b>	<b>761</b>
8.1	Introduction	762
8.2	Types of Heat Exchangers	762
8.2.1	Geometric Flow Configurations	764
8.2.2	Fluid Temperature Behavior	767
8.2.3	Heat Transfer Surfaces	769
8.2.4	Direct-Contact Exchangers	769
8.3	Energy Balances and the Overall Heat Transfer Coefficient	770
8.3.1	Exchanger Energy Balances	770
8.3.2	Overall Heat Transfer Coefficients	772
8.4	Single-Stream Steady-Flow Heat Exchangers	777
8.4.1	Analysis of an Evaporator	778
8.5	Two-Stream Steady-Flow Heat Exchangers	781
8.5.1	The Logarithmic Mean Temperature Difference	781
8.5.2	Effectiveness and Number of Transfer Units	786
8.5.3	Balanced-Flow Exchangers	794
8.5.4	Effect of Axial Conduction	797
8.6	Regenerators	805
8.6.1	Balanced Counterflow Regenerators	805
8.7	Elements of Heat Exchanger Design	811
8.7.1	Exchanger Pressure Drop	813
8.7.2	Thermal-Hydraulic Exchanger Design	820
8.7.3	Surface Selection for Compact Heat Exchangers	827
8.7.4	Economic Analysis	830
8.7.5	Computer-Aided Heat Exchanger Design: HEX2	835
8.8	Closure	846
	References	847
	Exercises	848

---

**APPENDIX**

<b>A</b>	<b>PROPERTY DATA</b>	<b>871</b>
Table A.1a	Solid metals: Melting point and thermal properties at 300 K	873
Table A.1b	Solid metals: Temperature dependence of thermal conductivity $k$ [W/m K]	875
Table A.1c	Solid metals: Temperature dependence of specific heat capacity $c$ [J/kg K]	876
Table A.2	Solid dielectrics: Thermal properties	877
Table A.3	Insulators and building materials: Thermal properties	879
Table A.4	Thermal conductivity of selected materials at cryogenic temperatures	881
Table A.5a	Total hemispherical emittance of surfaces at $T_s \approx 300$ K, and solar absorptance	882

<b>Table A.5b</b>	Temperature variation of total hemispherical emittance for selected surfaces 885
<b>Table A.6a</b>	Spectral and total absorptances of metals for normal incidence 886
<b>Table A.6b</b>	Spectral absorptances at room temperature and an angle of incidence of $25^\circ$ from the normal [for nonconductors $\alpha(25^\circ) \approx \alpha$ (hemispherical)] 887
<b>Table A.7</b>	Gases: Thermal properties 888
<b>Table A.8</b>	Dielectric liquids: Thermal properties 892
<b>Table A.9</b>	Liquid metals: Thermal properties 895
<b>Table A.10a</b>	Volume expansion coefficients for liquids 896
<b>Table A.10b</b>	Density and volume expansion coefficient of water 897
<b>Table A.11</b>	Surface tension 898
<b>Table A.12a</b>	Thermodynamic properties of saturated steam 899
<b>Table A.12b</b>	Thermodynamic properties of saturated ammonia 902
<b>Table A.12c</b>	Thermodynamic properties of saturated nitrogen 903
<b>Table A.12d</b>	Thermodynamic properties of saturated mercury 904
<b>Table A.12e</b>	Thermodynamic properties of saturated refrigerant-22 (chlorodifluoromethane) 905
<b>Table A.12f</b>	Thermodynamic properties of saturated refrigerant-134a (tetrafluoroethane) 906
<b>Table A.13a</b>	Aqueous ethylene glycol solutions: Thermal properties 907
<b>Table A.13b</b>	Aqueous sodium chloride solutions: Thermal properties 908
<b>Table A.14a</b>	Dimensions of commercial pipes [mm] (ASA standard) 909
<b>Table A.14b</b>	Dimensions of commercial tubes [mm] (ASTM standard) 910
<b>Table A.14c</b>	Dimensions of seamless steel tubes for tubular heat exchangers [mm] (DIN 28 180) 911
<b>Table A.14d</b>	Dimensions of wrought copper and copper alloy tubes for condensers and heat exchangers [mm] (DIN 1785-83) 911
<b>Table A.14e</b>	Dimensions of seamless cold drawn stainless steel tubes [mm] (LN 9398) 912
<b>Table A.14f</b>	Dimensions of seamless drawn wrought aluminum alloy tubes [mm] (LN 9223) 912
<b>Table A.15</b>	U.S. standard atmosphere 913
<b>Table A.16</b>	Selected physical constants 914

## **B UNITS, CONVERSION FACTORS, AND MATHEMATICS 915**

<b>Table B.1a</b>	Base and supplementary SI units 916
<b>Table B.1b</b>	Derived SI units 916
<b>Table B.1c</b>	Recognized non-SI units 917
<b>Table B.1d</b>	Multiples of SI units 917
<b>Table B.2</b>	Conversion factors 918
<b>Table B.3</b>	Bessel functions 919
<i>a.</i>	Bessel functions of the first and second kinds, orders 0 and 1 920

	<i>b.</i> Modified Bessel functions of the first and second kinds, orders 0 and 1	922
<b>Table B.4</b>	The complementary error function	924
<b>C</b>	<b>CHARTS</b>	<b>925</b>
<b>Figure C.1a</b>	Centerplane temperature response for a convectively cooled slab	926
<b>Figure C.1b</b>	Centerline temperature response for a convectively cooled cylinder	927
<b>Figure C.1c</b>	Center temperature response for a convectively cooled sphere	927
<b>Figure C.2a</b>	Fractional energy loss for a convectively cooled slab	928
<b>Figure C.2b</b>	Fractional energy loss for a convectively cooled cylinder	928
<b>Figure C.2c</b>	Fractional energy loss for a convectively cooled sphere	929
<b>Figure C.3a</b>	Shape (view) factor for coaxial parallel disks	929
<b>Figure C.3b</b>	Shape (view) factor for opposite rectangles	930
<b>Figure C.3c</b>	Shape (view) factor for adjacent rectangles	930
<b>Figure C.4a</b>	LMTD correction factor for a heat exchanger with one shell pass and 2, 4, 6, . . . tube passes	931
<b>Figure C.4b</b>	LMTD correction factor for a cross-flow heat exchanger with both fluids unmixed	931
<b>Figure C.4c</b>	LMTD correction factor for a cross-flow heat exchanger with both fluids mixed	932
<b>Figure C.4d</b>	LMTD correction factor for a cross-flow heat exchanger with two tube passes (unmixed) and one shell pass (mixed)	932
<b>Bibliography</b>		<b>933</b>
<b>Nomenclature</b>		<b>941</b>
<b>Index</b>		<b>947</b>

# ELEMENTARY HEAT TRANSFER

---

CONTENTS

- 1.1 INTRODUCTION
- 1.2 HEAT TRANSFER AND ITS RELATION TO THERMODYNAMICS
- 1.3 MODES OF HEAT TRANSFER
- 1.4 COMBINED MODES OF HEAT TRANSFER
- 1.5 TRANSIENT THERMAL RESPONSE
- 1.6 HEAT EXCHANGERS
- 1.7 DIMENSIONS AND UNITS
- 1.8 CLOSURE

## 1.1 INTRODUCTION

The process of heat transfer is familiar to us all. On a cold day we put on more clothing to reduce heat transfer from our warm body to cold surroundings. To make a cup of coffee we may plug in a kettle, inside which heat is transferred from an electrical resistance element to the water, heating the water until it boils. The engineering discipline of **heat transfer** is concerned with methods of calculating **rates** of heat transfer. These methods are used by engineers to design components and systems in which heat transfer occurs. Heat transfer considerations are important in almost all areas of technology. Traditionally, however, the discipline that has been most concerned with heat transfer is mechanical engineering because of the importance of heat transfer in energy conversion systems, from coal-fired power plants to solar water heaters.

Many *thermal design* problems require reducing heat transfer rates by providing suitable *insulation*. The insulation of buildings in extreme climates is a familiar example, but there are many others. The space shuttle has thermal tiles to insulate the vehicle from high-temperature air behind the bow shock wave during reentry into the atmosphere. Cryostats, which maintain the cryogenic temperatures required for the use of superconductors, must be effectively insulated to reduce the cooling load on the refrigeration system. Often, the only way to ensure protection from severe heating is to provide a fluid flow as a heat "sink." Nozzles of liquid-fueled rocket motors are cooled by pumping the cold fuel through passages in the nozzle wall before injection into the combustion chamber. A critical component in a fusion reactor is the "first wall" of the containment vessel, which must withstand intense heating from the hot plasma. Such walls may be cooled by a flow of helium gas or liquid lithium.

A common thermal design problem is the transfer of heat from one fluid to another. Devices for this purpose are called *heat exchangers*. A familiar example is the automobile radiator, in which heat is transferred from the hot engine coolant to cold air blowing through the radiator core. Heat exchangers of many different types are required for power production and by the process industries. A power plant, whether the fuel be fossil or nuclear, has a *boiler* in which water is evaporated to produce steam to drive the turbines, and a *condenser* in which the steam is condensed to provide a low back pressure on the turbines and for water recovery. The condenser patented by James Watt in 1769 more than doubled the efficiency of steam engines then being used and set the Industrial Revolution in motion. The common vapor cycle refrigeration or air-conditioning system has an *evaporator* where heat is absorbed at low temperature and a *condenser* where heat is rejected at a higher temperature. On a domestic refrigerator, the condenser is usually in the form of a tube coil with cooling *fins* to assist transfer of heat to the surroundings. An oil refinery has a great variety of heat transfer equipment, including rectification columns and thermal crackers. Many heat exchangers are used to transfer heat from one process stream to another, to reduce the total energy consumption by the refinery.

Often the design problem is one of *thermal control*, that is, maintaining the operating temperature of temperature-sensitive components within a specified range. Cooling of all kinds of electronic gear is an example of thermal control. The development



of faster computers is now severely constrained by the difficulty of controlling the temperature of very small components, which dissipate large amounts of heat. Thermal control of temperature-sensitive components in a communications satellite orbiting the earth is a particularly difficult problem. Transistors and diodes must not overheat, batteries must not freeze, telescope optics must not lose alignment due to thermal expansion, and photographs must be processed at the proper temperature to ensure high resolution. Thermal control of space stations of the future will present even greater problems, since reliable life-support systems also will be necessary.

From the foregoing examples, it is clear that heat transfer involves a great variety of physical phenomena and engineering systems. The phenomena must first be understood and quantified before a methodology for the thermal design of an engineering system can be developed. Chapter 1 is an overview of the subject and introduces key topics at an elementary level. In Section 1.2, the distinction between the subjects of heat transfer and thermodynamics is explained. The first law of thermodynamics is reviewed, and closed- and open-system forms required for heat transfer analysis are developed. Section 1.3 introduces the three important modes of heat transfer: **heat conduction**, **thermal radiation**, and **heat convection**. Some formulas are developed that allow elementary heat transfer calculations to be made. In practical engineering problems, these modes of heat transfer usually occur simultaneously. Thus, in Section 1.4, the analysis of heat transfer by combined modes is introduced. The remainder of Chapter 1 deals with changes that occur in engineering systems as a result of heat transfer processes. In Section 1.5, the first law is applied to a very simple model closed system to determine the temperature response of the system with time. In Section 1.6, the first law for an open system is used to determine the change in temperature of a fluid flowing through a simple heat exchanger. Appropriate relations are developed that allow the design engineer to evaluate the exchanger performance. Finally, in Section 1.7, the International System of units (SI) is reviewed, and the units policy that is followed in the text is discussed.

## 1.2 HEAT TRANSFER AND ITS RELATION TO THERMODYNAMICS

When a hot object is placed in cold surroundings, it cools: the object loses internal energy, while the surroundings gain internal energy. We commonly describe this interaction as a *transfer of heat* from the object to the surrounding region. Since the caloric theory of heat has been long discredited, we do not imagine a "heat substance" flowing from the object to the surroundings. Rather, we understand that internal energy has been transferred by complex interactions on an atomic or subatomic scale. Nevertheless, it remains common practice to describe these interactions as transfer, transport, or flow, of heat. The engineering discipline of heat transfer is concerned with calculation of the rate at which heat flows within a medium, across an interface, or from one surface to another, as well as with the calculation of associated temperatures.

It is important to understand the essential difference between the engineering discipline of heat transfer and what is commonly called thermodynamics. Classical thermodynamics deals with systems in equilibrium. Its methodology may be used

to calculate the energy required to change a system from one equilibrium state to another, but it cannot be used to calculate the rate at which the change may occur. For example, if a 1 kg ingot of iron is quenched from 1000°C to 100°C in an oil bath, thermodynamics tells us that the loss in internal energy of the ingot is mass (1 kg)  $\times$  specific heat ( $\sim 450$  J/kg K)  $\times$  temperature change (900 K), or approximately 405 kJ. But thermodynamics cannot tell us how long we will have to wait for the temperature to drop to 100°C. The time depends on the temperature of the oil bath, physical properties of the oil, motion of the oil, and other factors. An appropriate heat transfer analysis will consider all of these.

Analysis of heat transfer processes does require using some thermodynamics concepts. In particular, the **first law of thermodynamics** is used, generally in particularly simple forms since work effects can often be ignored. The first law is a statement of the *principle of conservation of energy*, which is a basic law of physics. This principle can be formulated in many ways by excluding forms of energy that are irrelevant to the problem under consideration, or by simply redefining what is meant by energy. In heat transfer, it is common practice to refer to the first law as the *energy conservation principle* or simply as an *energy* or *heat balance* when no work is done. However, as in thermodynamics, it is essential that the correct form of the first law be used. The student must be able to define an appropriate system, recognize whether the system is *open* or *closed*, and decide whether a steady state can be assumed. Some simple forms of the energy conservation principle, which find frequent use in this text, follow.

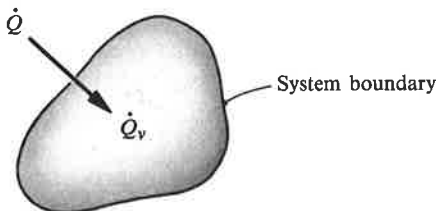
A closed system containing a fixed mass of a solid is shown in Fig. 1.1. The system has a volume  $V$  [m<sup>3</sup>], and the solid has a density  $\rho$  [kg/m<sup>3</sup>]. There is heat transfer into the system at a rate of  $\dot{Q}$  [J/s or W], and heat may be generated within the solid, for example, by nuclear fission or by an electrical current, at a rate  $\dot{Q}_v$  [W]. Solids may be taken to be incompressible, so no work is done by or on the system. The principle of conservation of energy requires that over a time interval  $\Delta t$  [s],

$$\begin{array}{l} \text{Change in internal energy} \\ \text{within the system} \end{array} = \begin{array}{l} \text{Heat transferred} \\ \text{into the system} \end{array} + \begin{array}{l} \text{Heat generated} \\ \text{within the system} \end{array}$$

$$\Delta U = \dot{Q}\Delta t + \dot{Q}_v\Delta t \quad (1.1)$$

Dividing by  $\Delta t$  and letting  $\Delta t$  go to zero gives

$$\frac{dU}{dt} = \dot{Q} + \dot{Q}_v$$

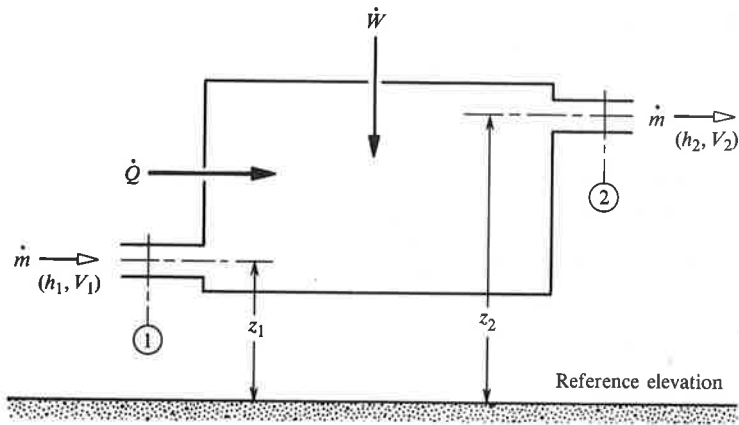


**Figure 1.1** Application of the energy conservation principle to a closed system.

The system contains a fixed mass ( $\rho V$ ); thus, we can write  $dU = \rho V du$ , where  $u$  is the specific internal energy [J/kg]. Also, for an incompressible solid,  $du = c_v dT$ , where  $c_v$  is the constant-volume specific heat [J/kg K], and  $T$  [K] is temperature. Since the solid has been taken to be incompressible, the constant-volume and constant-pressure specific heats are equal, so we simply write  $du = c dT$  to obtain

$$\rho V c \frac{dT}{dt} = \dot{Q} + \dot{Q}_v \quad (1.2)$$

Equation (1.2) is a special form of the first law of thermodynamics that will be used often in this text. It is written on a *rate* basis; that is, it gives the rate of change of temperature with time. For some purposes, however, it will prove convenient to return to Eq. (1.1) as a statement of the first law.



**Figure 1.2** Application of the energy conservation principle to a steady-flow open system.

Figure 1.2 shows an *open system* (or *control volume*), for which a useful form of the first law is the **steady-flow energy equation**. It is used widely in the thermodynamic analysis of equipment such as turbines and compressors. Then

$$\dot{m} \Delta \left( h + \frac{V^2}{2} + gz \right) = \dot{Q} + \dot{W} \quad (1.3)$$

where  $\dot{m}$  [kg/s] is the mass flow rate,  $h$  [J/kg] is the specific enthalpy,  $V$  [m/s] is velocity,  $g$  [ $\text{m/s}^2$ ] is the gravitational acceleration,  $z$  is elevation [m],  $\dot{Q}$  [W] is the rate of heat transfer, as before, and  $\dot{W}$  [W] is the rate at which external (shaft) work is done on the system.<sup>1</sup> Notice that the sign convention here is that external work done *on* the system is positive; the opposite sign convention is also widely used. The symbol  $\Delta X$  means  $X_{\text{out}} - X_{\text{in}}$ , or the change in  $X$ . Equation (1.3) applies to a pure

<sup>1</sup> Equation (1.3) has been written as if  $h$ ,  $V$ , and  $z$  are uniform in the streams crossing the control volume boundary. Often such an assumption can be made; if not, an integration across each stream is required to give appropriate average values.

substance when conditions within the system, such as temperature and velocity, are unchanging over some appropriate time interval. Heat generation within the system has not been included. In many types of heat transfer equipment, no external work is done, and changes in kinetic and potential energy are negligible; Eq. (1.3) then reduces to

$$\dot{m}\Delta h = \dot{Q} \quad (1.4)$$

The specific enthalpy  $h$  is related to the specific internal energy  $u$  as

$$h = u + Pv \quad (1.5)$$

where  $P$  [N/m<sup>2</sup> or Pa] is pressure, and  $v$  is specific volume [m<sup>3</sup>/kg]. Two limit forms of  $\Delta h$  are useful. If the fluid enters the system at state 1 and leaves at state 2:

1. For ideal gases with  $Pv = RT$ ,

$$\Delta h = \int_{T_1}^{T_2} c_p dT \quad (1.6a)$$

where  $R$  [J/kg K] is the gas constant and  $c_p$  [J/kg K] is the constant-pressure specific heat.

2. For incompressible liquids with  $\rho = 1/v = \text{constant}$

$$\Delta h = \int_{T_1}^{T_2} c dT + \frac{P_2 - P_1}{\rho} \quad (1.6b)$$

where  $c = c_v = c_p$ . The second term in Eq. (1.6b) is often negligible.

Equation (1.4) is the usual starting point for the heat transfer analysis of steady-state open systems.

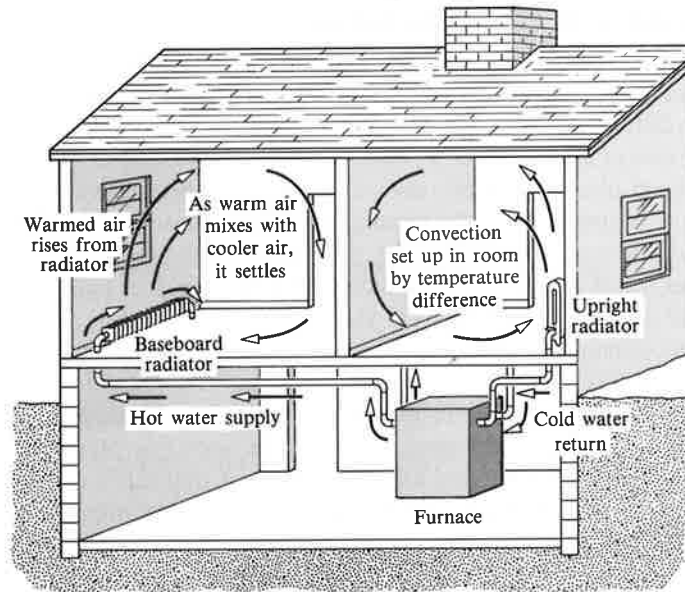
The *second law of thermodynamics* tells us that if two objects at temperatures  $T_1$  and  $T_2$  are connected, and if  $T_1 > T_2$ , then heat will flow spontaneously and irreversibly from object 1 to object 2. Also, there is an entropy increase associated with this heat flow. As  $T_2$  approaches  $T_1$ , the process approaches a reversible process, but simultaneously the rate of heat transfer approaches zero, so the process is of little practical interest. All heat transfer processes encountered in engineering are irreversible and generate entropy. With the increasing realization that energy supplies should be conserved, efficient use of available energy is becoming an important consideration in thermal design. Thus, the engineer should be aware of the irreversible processes occurring in the system under development and understand that the optimal design may be one that minimizes entropy generation due to heat transfer and fluid flow. Most often, however, energy conservation is simply a consideration in the overall economic evaluation of the design. Usually there is an important trade-off between energy costs associated with the operation of the system and the capital costs required to construct the equipment.

### 1.3 MODES OF HEAT TRANSFER

In thermodynamics, *heat* is defined as energy transfer due to temperature gradients or differences. Consistent with this viewpoint, thermodynamics recognizes only two modes of heat transfer: *conduction* and *radiation*. For example, heat transfer across a steel pipe wall is by conduction, whereas heat transfer from the sun to the earth or to a spacecraft is by thermal radiation. These modes of heat transfer occur on a molecular or subatomic scale. In air at normal pressure, conduction is by molecules that travel a very short distance ( $\sim 0.65 \mu\text{m}$ ) before colliding with another molecule and exchanging energy. On the other hand, radiation is by photons, which travel almost unimpeded through the air from one surface to another. Thus, an important distinction between conduction and radiation is that the energy carriers for conduction have a short *mean free path*, whereas for radiation the carriers have a long mean free path. However, in air at the very low pressures characteristic of high-vacuum equipment, the mean free path of molecules can be much longer than the equipment dimensions, so the molecules travel unimpeded from one surface to another. Then heat transfer by molecules is governed by laws analogous to those for radiation.

A fluid, by virtue of its mass and velocity, can transport momentum. In addition, by virtue of its temperature, it can transport energy. Strictly speaking, *convection* is the transport of energy by bulk motion of a medium (a moving solid can also convect energy in this sense). In the steady-flow energy equation, Eq. (1.3), convection of internal energy is contained in the term  $\dot{m}\Delta h$ , which is on the left-hand side of the equation, and heat transfer by conduction and radiation is on the right-hand side, as  $\dot{Q}$ . However, it is common engineering practice to use the term *convection* more broadly and describe heat transfer from a surface to a moving fluid also as convection, or *convective heat transfer*, even though conduction and radiation play a dominant role close to the surface, where the fluid is stationary. In this sense, convection is usually regarded as a distinct mode of heat transfer. Examples of convective heat transfer include heat transfer from the radiator of an automobile or to the skin of a hypersonic vehicle. Convection is often associated with a change of phase, for example, when water boils in a kettle or when steam condenses in a power plant condenser. Owing to the complexity of such processes, boiling and condensation are often regarded as distinct heat transfer processes.

The hot water home heating system shown in Fig. 1.3 illustrates the modes of heat transfer. Hot water from the furnace in the basement flows along pipes to radiators located in individual rooms. Transport of energy by the hot water from the basement is true convection as defined above; we do not call this a heat transfer process. Inside the radiators, there is convective heat transfer from the hot water to the radiator shell, conduction across the radiator shell, and both convective and radiative heat transfer from the hot outer surface of the radiator shell into the room. The convection is *natural* convection: the heated air adjacent to the radiator surface rises due to its buoyancy, and cooler air flows in to take its place. The radiators are heat exchangers. Although commonly used, the term *radiator* is misleading since



**Figure 1.3** A hot-water home heating system illustrating the modes of heat transfer.

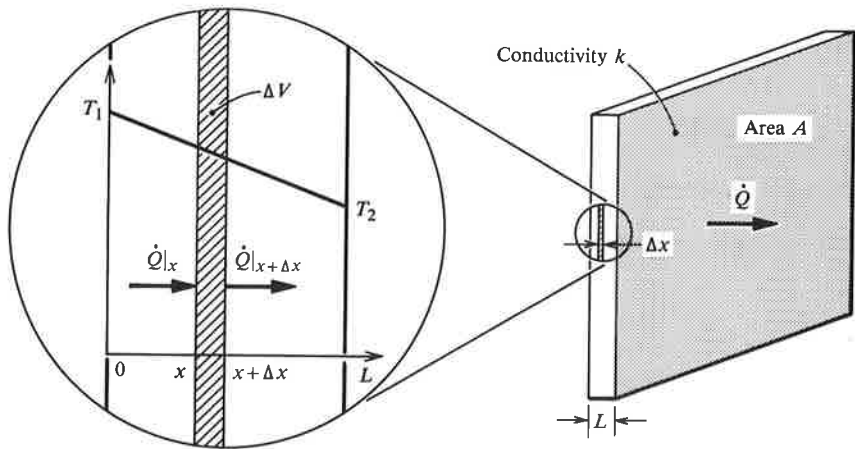
heat transfer from the shell surface can be predominantly by convection rather than by radiation (see Exercise 1–20). Heaters that transfer heat predominantly by radiation are, for example, electrical resistance wire units.

Each of the three important subject areas of heat transfer will now be introduced: conduction, in Section 1.3.1; radiation, in Section 1.3.2; and convection, in Section 1.3.3.

### 1.3.1 Heat Conduction

On a microscopic level, the physical mechanisms of conduction are complex, encompassing such varied phenomena as molecular collisions in gases, lattice vibrations in crystals, and flow of free electrons in metals. However, if at all possible, the engineer avoids considering processes at the microscopic level, preferring to use *phenomenological laws*, at a macroscopic level. The phenomenological law governing heat conduction was proposed by the French mathematical physicist J. B. Fourier in 1822. This law will be introduced here by considering the simple problem of one-dimensional heat flow across a plane wall—for example, a layer of insulation.<sup>2</sup> Figure 1.4 shows a plane wall of surface area  $A$  and thickness  $L$ , with its face at  $x = 0$  maintained at temperature  $T_1$  and the face at  $x = L$  maintained at  $T_2$ . The heat flow  $\dot{Q}$  through the wall is in the direction of decreasing temperature: if

<sup>2</sup> In thermodynamics, the term *insulated* is often used to refer to a *perfectly* insulated (zero-heat-flow or adiabatic) surface. In practice, insulation is used to *reduce* heat flow and seldom can be regarded as perfect.



**Figure 1.4** Steady one-dimensional conduction across a plane wall, showing the application of the energy conservation principle to an elemental volume  $\Delta x$  thick.

$T_1 > T_2$ ,  $\dot{Q}$  is in the positive  $x$  direction.<sup>3</sup> The phenomenological law governing this heat flow is **Fourier's law of heat conduction**, which states that in a homogeneous substance, the local heat flux is proportional to the negative of the local temperature gradient:

$$\frac{\dot{Q}}{A} = q \quad \text{and} \quad q \propto -\frac{dT}{dx} \quad (1.7)$$

where  $q$  is the heat flux, or heat flow per unit area perpendicular to the flow direction [ $\text{W}/\text{m}^2$ ],  $T$  is the local temperature [ $\text{K}$  or  $^\circ\text{C}$ ], and  $x$  is the coordinate in the flow direction [ $\text{m}$ ]. When  $dT/dx$  is negative, the minus sign in Eq. (1.7) gives a positive  $q$  in the positive  $x$  direction. Introducing a constant of proportionality  $k$ ,

$$q = -k \frac{dT}{dx} \quad (1.8)$$

where  $k$  is the **thermal conductivity** of the substance and, by inspection of the equation, must have units [ $\text{W}/\text{m K}$ ]. Notice that temperature can be given in kelvins or degrees Celsius in Eq. (1.8): the temperature gradient does not depend on which of these units is used since one kelvin equals one degree Celsius ( $1 \text{ K} = 1^\circ\text{C}$ ). Thus, the units of thermal conductivity could also be written [ $\text{W}/\text{m }^\circ\text{C}$ ], but this is not the recommended practice when using the SI system of units. The magnitude of the thermal conductivity  $k$  for a given substance very much depends on its microscopic structure and also tends to vary somewhat with temperature; Table 1.1 gives some selected values of  $k$ .

<sup>3</sup> Notice that this  $\dot{Q}$  is the heat flow in the  $x$  direction, whereas in the first law, Eqs. (1.1)–(1.4),  $\dot{Q}$  is the heat transfer into the whole system. In linking thermodynamics to heat transfer, some ambiguity in notation arises when common practice in both subjects is followed.

**Table 1.1** Selected values of thermal conductivity at 300 K ( $\sim 25^\circ\text{C}$ ).

Material	$k$ W/m K
Copper	386
Aluminum	204
Brass (70% Cu, 30% Zn)	111
Mild steel	64
Stainless steel, 18-8	15
Mercury	8.4
Concrete	1.4
Pyrex glass	1.09
Water	0.611
Neoprene rubber	0.19
Engine oil, SAE 50	0.145
White pine, perpendicular to grain	0.10
Polyvinyl chloride (PVC)	0.092
Freon 12	0.071
Cork	0.043
Fiberglass (medium density)	0.038
Polystyrene	0.028
Air	0.027

Note: Appendix A contains more comprehensive data.

Figure 1.4 shows an elemental volume  $\Delta V$  located between  $x$  and  $x + \Delta x$ ;  $\Delta V$  is a closed system, and the energy conservation principle in the form of Eq. (1.2) applies. If we consider a steady state, then temperatures are unchanging in time and  $dT/dt = 0$ ; also, if there is no heat generated within the volume,  $\dot{Q}_v = 0$ . Then Eq. (1.2) states that the net heat flow into the system is zero. Since heat is flowing into  $\Delta V$  across the face at  $x$ , and out of  $\Delta V$  across the face at  $x + \Delta x$ ,

$$\dot{Q}|_x = \dot{Q}|_{x+\Delta x}$$

or

$$\dot{Q} = \text{Constant}$$

But from Fourier's law, Eq. (1.8),

$$\dot{Q} = qA = -kA \frac{dT}{dx}$$

The variables are separable: rearranging and integrating across the wall,

$$\frac{\dot{Q}}{A} \int_0^L dx = - \int_{T_1}^{T_2} k dT$$

where  $\dot{Q}$  and  $A$  have been taken outside the integral signs since both are constants. If the small variation of  $k$  with temperature is ignored for the present we obtain



$$\dot{Q} = \frac{kA}{L}(T_1 - T_2) = \frac{T_1 - T_2}{L/kA} \quad (1.9)$$

Comparison of Eq. (1.9) with Ohm's law,  $I = E/R$ , suggests that  $\Delta T = T_1 - T_2$  can be viewed as a driving potential for flow of heat, analogous to voltage being the driving potential for current. Then  $R \equiv L/kA$  can be viewed as a **thermal resistance** analogous to electrical resistance.

If we have a composite wall of two slabs of material, as shown in Fig. 1.5, the heat flow through each layer is the same:

$$\dot{Q} = \frac{T_1 - T_2}{L_A/k_A A} = \frac{T_2 - T_3}{L_B/k_B A}$$

Rearranging,

$$\dot{Q} \left( \frac{L_A}{k_A A} \right) = T_1 - T_2$$

$$\dot{Q} \left( \frac{L_B}{k_B A} \right) = T_2 - T_3$$

Adding eliminates the interface temperature  $T_2$ :

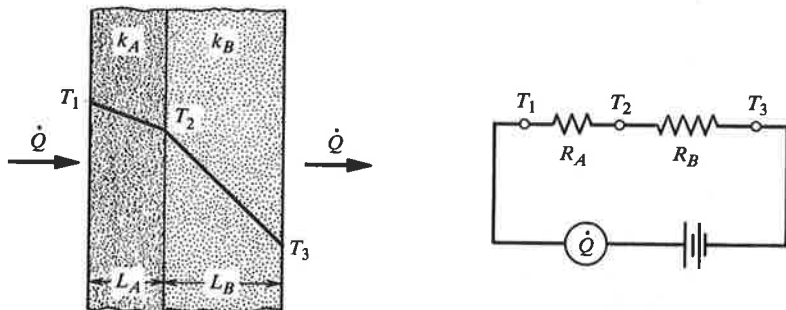
$$\dot{Q} \left( \frac{L_A}{k_A A} + \frac{L_B}{k_B A} \right) = T_1 - T_3$$

or

$$\dot{Q} = \frac{T_1 - T_3}{L_A/k_A A + L_B/k_B A} = \frac{\Delta T}{R_A + R_B} \quad (1.10a)$$

Using the electrical resistance analogy, we would view the problem as two resistances in series forming a **thermal circuit**, and immediately write

$$\dot{Q} = \frac{\Delta T}{R_A + R_B} \quad (1.10b)$$



**Figure 1.5** The temperature distribution for steady conduction across a composite plane wall and the corresponding thermal circuit.

**EXAMPLE 1.1** Heat Transfer through Insulation

A refrigerated container is in the form of a cube with 2 m sides and has 5 mm-thick aluminum walls insulated with a 10 cm layer of cork. During steady operation, the temperatures on the inner and outer surfaces of the container are measured to be  $-5^{\circ}\text{C}$  and  $20^{\circ}\text{C}$ , respectively. Determine the cooling load on the refrigerator.

**Solution**

**Given:** Aluminum container insulated with 10 cm-thick cork.

**Required:** Rate of heat gain.

**Assumptions:** 1. Steady state.  
2. One-dimensional heat conduction (ignore corner effects).

Equation (1.10) applies:

$$\dot{Q} = \frac{\Delta T}{R_A + R_B} \quad \text{where } R = \frac{L}{kA}$$

Let subscripts  $A$  and  $B$  denote the aluminum wall and cork insulation, respectively. Table 1.1 gives  $k_A = 204 \text{ W/mK}$ ,  $k_B = 0.043 \text{ W/mK}$ . We suspect that the thermal resistance of the aluminum wall is negligible, but we will calculate it anyway. For one side of area  $A = 4 \text{ m}^2$ , the thermal resistances are

$$R_A = \frac{L_A}{k_A A} = \frac{(0.005 \text{ m})}{(204 \text{ W/mK})(4 \text{ m}^2)} = 6.13 \times 10^{-6} \text{ K/W}$$

$$R_B = \frac{L_B}{k_B A} = \frac{(0.10 \text{ m})}{(0.043 \text{ W/mK})(4 \text{ m}^2)} = 0.581 \text{ K/W}$$

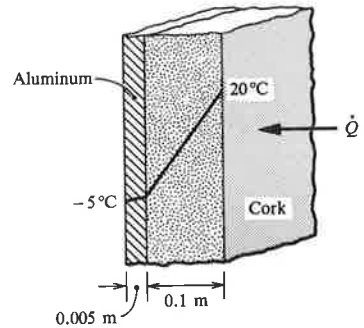
Since  $R_A$  is five orders of magnitude less than  $R_B$ , it can be ignored. The heat flow for a temperature difference of  $T_1 - T_2 = 20 - (-5) = 25 \text{ K}$ , is

$$\dot{Q} = \frac{\Delta T}{R_B} = \frac{25 \text{ K}}{0.581 \text{ K/W}} = 43.0 \text{ W}$$

For six sides, the total cooling load on the refrigerator is  $6.0 \times 43.0 = 258 \text{ W}$ .

**Comments**

1. In the future, when it is obvious that a resistance in a series network is negligible, it can be ignored from the outset (no effort should be expended to obtain data for its calculation).
2. The assumption of one-dimensional conduction is good because the 0.1 m insulation thickness is small compared to the 2 m-long sides of the cube.



3. Notice that the temperature difference  $T_1 - T_2$  is expressed in kelvins, even though  $T_1$  and  $T_2$  were given in degrees Celsius.
4. We have assumed perfect thermal contact between the aluminum and cork; that is, there is no thermal resistance associated with the interface between the two materials (see Section 2.2.2).

### 1.3.2 Thermal Radiation

All matter and space contains electromagnetic radiation. A particle, or *quantum*, of electromagnetic energy is a photon, and heat transfer by radiation can be viewed either in terms of electromagnetic waves or in terms of photons. The flux of radiant energy incident on a surface is its **irradiation**,  $G$  [ $\text{W}/\text{m}^2$ ]; the energy flux leaving a surface due to emission and reflection of electromagnetic radiation is its **radiosity**,  $J$  [ $\text{W}/\text{m}^2$ ]. A **black surface** (or **blackbody**) is defined as a surface that absorbs all incident radiation, reflecting none. As a consequence, all of the radiation leaving a black surface is emitted by the surface and is given by the **Stefan-Boltzmann law** as

$$J = E_b = \sigma T^4 \quad (1.11)$$

where  $E_b$  is the **blackbody emissive power**,  $T$  is absolute temperature [K], and  $\sigma$  is the Stefan-Boltzmann constant ( $\approx 5.67 \times 10^{-8} \text{ W}/\text{m}^2 \text{ K}^4$ ). Table 1.2 shows how  $E_b = \sigma T^4$  increases rapidly with temperature.

**Table 1.2** Blackbody emissive power  $\sigma T^4$  at various temperatures.

Surface Temperature K	Blackbody Emissive Power $\text{W}/\text{m}^2$
300 (room temperature)	459
1000 (cherry-red hot)	56,700
3000 (lamp filament)	4,590,000
5760 (sun temperature)	62,400,000

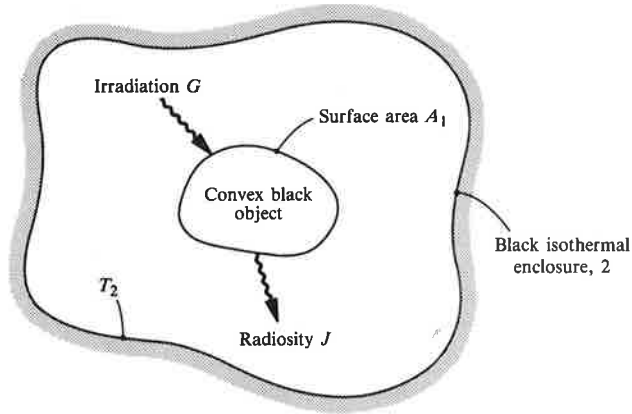
Figure 1.6 shows a convex black object of surface area  $A_1$  in a black isothermal enclosure at temperature  $T_2$ . At equilibrium, the object is also at temperature  $T_2$ , and the radiation flux incident on the object must equal the radiation flux leaving:

$$G_1 A_1 = J_1 A_1 = \sigma T_2^4 A_1$$

Hence

$$G_1 = \sigma T_2^4 \quad (1.12)$$

and is uniform over the area. If the temperature of the object is now raised to  $T_1$ , its radiosity becomes  $\sigma T_1^4$  while its irradiation remains  $\sigma T_2^4$  (because the enclosure reflects no radiation). Then the net radiant heat flux through the surface,  $q_1$ , is the



**Figure 1.6** A convex black object (surface 1) in a black isothermal enclosure (surface 2).

radiosity minus the irradiation:

$$q_1 = J_1 - G_1 \tag{1.13}$$

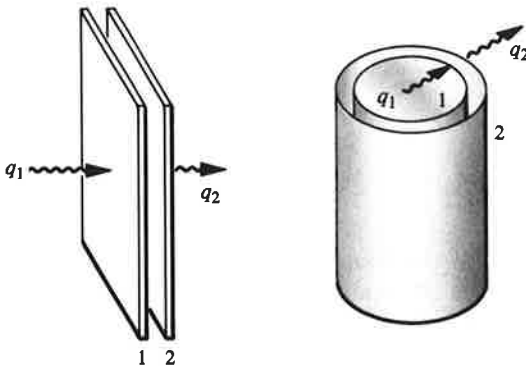
or

$$q_1 = \sigma T_1^4 - \sigma T_2^4 \tag{1.14}$$

where the sign convention is such that a net flux away from the surface is positive. Equation (1.14) is also valid for two large black surfaces facing each other, as shown in Fig. 1.7.

The blackbody is an ideal surface. Real surfaces absorb less radiation than do black surfaces. The fraction of incident radiation absorbed is called the absorptance (or absorptivity),  $\alpha$ . A widely used model of a real surface is the **gray surface**, which is defined as a surface for which  $\alpha$  is a constant, irrespective of the nature of the incident radiation. The fraction of incident radiation reflected is the **reflectance** (or reflectivity),  $\rho$ . If the object is opaque, that is, not transparent to electromagnetic radiation, then

$$\rho = 1 - \alpha \tag{1.15}$$



**Figure 1.7** Examples of two large surfaces facing each other.

**Table 1.3** Selected approximate values of emittance,  $\varepsilon$  (total hemispherical values at normal temperatures).

Surface	Emittance, $\varepsilon$
Aluminum alloy, unoxidized	0.035
Black anodized aluminum	0.80
Chromium plating	0.16
Stainless steel, type 312, lightly oxidized	0.30
Inconel X, oxidized	0.72
Black enamel paint	0.78
White acrylic paint	0.90
Asphalt	0.88
Concrete	0.90
Soil	0.94
Pyrex glass	0.80

Note: More comprehensive data are given in Appendix A. Emittance is very dependent on surface finish; thus, values obtained from various sources may differ significantly.

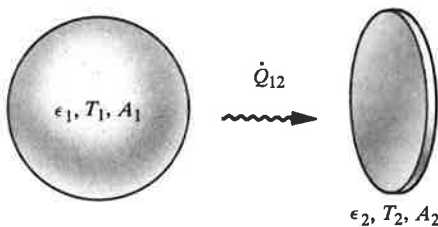
Real surfaces also emit less radiation than do black surfaces. The fraction of the blackbody emissive power  $\sigma T^4$  emitted is called the **emittance** (or emissivity),  $\varepsilon$ .<sup>4</sup> A gray surface also has a constant value of  $\varepsilon$ , independent of its temperature, and, as will be shown in Chapter 6, the emittance and absorptance of a gray surface are equal:

$$\varepsilon = \alpha \quad (\text{gray surface}) \quad (1.16)$$

Table 1.3 shows some typical values of  $\varepsilon$  at normal temperatures. Bright metal surfaces tend to have low values, whereas oxidized or painted surfaces tend to have high values. Values of  $\alpha$  and  $\rho$  can also be obtained from Table 1.3 by using Eqs. (1.15) and (1.16).

If heat is transferred by radiation between two gray surfaces of finite size, as shown in Fig. 1.8, the rate of heat flow will depend on temperatures  $T_1$  and  $T_2$  and emittances  $\varepsilon_1$  and  $\varepsilon_2$ , as well as the geometry. Clearly, some of the radiation leaving surface 1 will not be intercepted by surface 2, and vice versa. Determining the rate of heat flow is usually quite difficult. In general, we may write

$$\dot{Q}_{12} = A_1 \mathcal{F}_{12} (\sigma T_1^4 - \sigma T_2^4) \quad (1.17)$$

**Figure 1.8** Radiation heat transfer between two finite gray surfaces.

<sup>4</sup> Both the endings *-ance* and *-ivity* are commonly used for radiation properties. In this text, *-ance* will be used for surface radiation properties. In Chapter 6, *-ivity* will be used for gas radiation properties.

where  $\dot{Q}_{12}$  is the net radiant energy interchange (heat transfer) from surface 1 to surface 2, and  $\mathcal{F}_{12}$  is a **transfer factor**, which depends on emittances and geometry. For the special case of surface 1 surrounded by surface 2, where either area  $A_1$  is small compared to area  $A_2$ , or surface 2 is nearly black,  $\mathcal{F}_{12} \approx \varepsilon_1$  and Eq. (1.17) becomes

$$\dot{Q}_{12} = \varepsilon_1 A_1 (\sigma T_1^4 - \sigma T_2^4) \quad (1.18)$$

Equation (1.18) will be derived in Chapter 6. It is an important result and is often used for quick engineering estimates.

The  $T^4$  dependence of radiant heat transfer complicates engineering calculations. When  $T_1$  and  $T_2$  are not too different, it is convenient to linearize Eq. (1.18) by factoring the term  $(\sigma T_1^4 - \sigma T_2^4)$  to obtain

$$\begin{aligned} \dot{Q}_{12} &= \varepsilon_1 A_1 \sigma (T_1^2 + T_2^2)(T_1 + T_2)(T_1 - T_2) \\ &\approx \varepsilon_1 A_1 \sigma (4T_m^3)(T_1 - T_2) \end{aligned}$$

for  $T_1 \approx T_2$ , where  $T_m$  is the mean of  $T_1$  and  $T_2$ . This result can be written more concisely as

$$\dot{Q}_{12} \approx A_1 h_r (T_1 - T_2) \quad (1.19)$$

where  $h_r = 4\varepsilon_1 \sigma T_m^3$  is called the **radiation heat transfer coefficient** [ $\text{W}/\text{m}^2 \text{K}$ ]. At  $25^\circ\text{C}$  ( $= 298 \text{ K}$ ),

$$h_r = (4)\varepsilon_1 (5.67 \times 10^{-8} \text{ W}/\text{m}^2 \text{K}^4)(298 \text{ K})^3$$

or

$$h_r \approx 6\varepsilon_1 \text{ W}/\text{m}^2 \text{K}$$

This result can be easily remembered: The radiation heat transfer coefficient at room temperature is about six times the surface emittance. For  $T_1 = 320 \text{ K}$  and  $T_2 = 300 \text{ K}$ , the error incurred in using the approximation of Eq. (1.19) is only 0.1%; for  $T_1 = 400 \text{ K}$  and  $T_2 = 300 \text{ K}$ , the error is 2%.

### EXAMPLE 1.2 Heat Loss from a Transistor

An electronic package for an experiment in outer space contains a transistor capsule, which is approximately spherical in shape with a 2 cm diameter. It is contained in an evacuated case with nearly black walls at  $30^\circ\text{C}$ . The only significant path for heat loss from the capsule is radiation to the case walls. If the transistor dissipates 300 mW, what will the capsule temperature be if it is (i) bright aluminum and (ii) black anodized aluminum?

#### Solution

**Given:** 2 cm-diameter transistor capsule dissipating 300 mW.

**Required:** Capsule temperature for (i) bright aluminum and (ii) black anodized aluminum.

**Assumptions:** Model as a small gray body in large, nearly black surroundings.

Equation (1.18) is applicable with

$$\dot{Q}_{12} = 300 \text{ mW}$$

$$T_2 = 30^\circ\text{C} = 303 \text{ K}$$

and  $T_1$  is the unknown.

$$\dot{Q}_{12} = \varepsilon_1 A_1 (\sigma T_1^4 - \sigma T_2^4)$$

$$0.3 \text{ W} = (\varepsilon_1)(\pi)(0.02 \text{ m})^2 [\sigma T_1^4 - (5.67 \times 10^{-8} \text{ W/m}^2 \text{ K}^4)(303 \text{ K})^4]$$

Solving,

$$\sigma T_1^4 = 478 + \frac{239}{\varepsilon_1}$$

(i) For bright aluminum ( $\varepsilon = 0.035$  from Table 1.3),

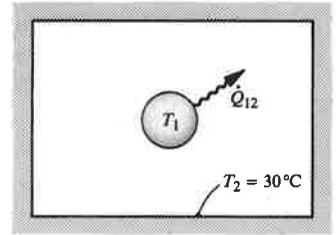
$$\sigma T_1^4 = 478 + 6828 = 7306 \text{ W/m}^2$$

$$T_1 = 599 \text{ K} (326^\circ\text{C})$$

(ii) For black anodized aluminum ( $\varepsilon = 0.80$  from Table 1.3),

$$\sigma T_1^4 = 478 + 298 = 776 \text{ W/m}^2$$

$$T_1 = 342 \text{ K} (69^\circ\text{C})$$

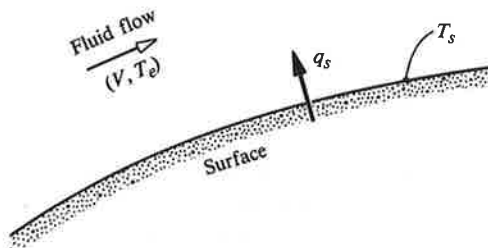


### Comments

1. The anodized aluminum gives a satisfactory operating temperature, but a bright aluminum capsule could not be used since  $326^\circ\text{C}$  is far in excess of allowable operating temperatures for semiconductor devices.
2. Note the use of kelvins for temperature in this radiation heat transfer calculation.

### 1.3.3 Heat Convection

As already explained, *convection* or *convective heat transfer* is the term used to describe heat transfer from a surface to a moving fluid, as shown in Fig. 1.9. The surface may be the inside of a pipe, the skin of a hypersonic aircraft, or a water-air interface in a cooling tower. The flow may be *forced*, as in the case of a liquid pumped



**Figure 1.9** Schematic of convective heat transfer to a fluid at temperature  $T_e$ , flowing at velocity  $V$  past a surface at temperature  $T_s$ .

through the pipe or air on the flight vehicle propelled through the atmosphere. On the other hand, the flow could be *natural* (or *free*), driven by buoyancy forces arising from a density difference, as in the case of a natural-draft cooling tower. Either type of flow can be *internal*, such as the pipe flow, or *external*, such as flow over the vehicle. Also, both forced and natural flows can be either *laminar* or *turbulent*, with laminar flows being predominant at lower velocities, for smaller sizes, and for more viscous fluids. Flow in a pipe becomes turbulent when the dimensionless group called the **Reynolds number**,  $Re_D = VD/\nu$ , exceeds about 2300, where  $V$  is the velocity [m/s],  $D$  is the pipe diameter [m], and  $\nu$  is the kinematic viscosity of the fluid [ $m^2/s$ ]. Heat transfer rates tend to be much higher in turbulent flows than in laminar flows, owing to the vigorous mixing of the fluid. Figure 1.10 shows some commonly encountered flows.

The rate of heat transfer by convection is usually a complicated function of surface geometry and temperature, the fluid temperature and velocity, and fluid thermophysical properties. In an external forced flow, the rate of heat transfer is approximately proportional to the difference between the surface temperature  $T_s$  and the temperature of the free stream fluid  $T_e$ . The constant of proportionality is called the **convective heat transfer coefficient**  $h_c$ :

$$q_s = h_c \Delta T \quad (1.20)$$

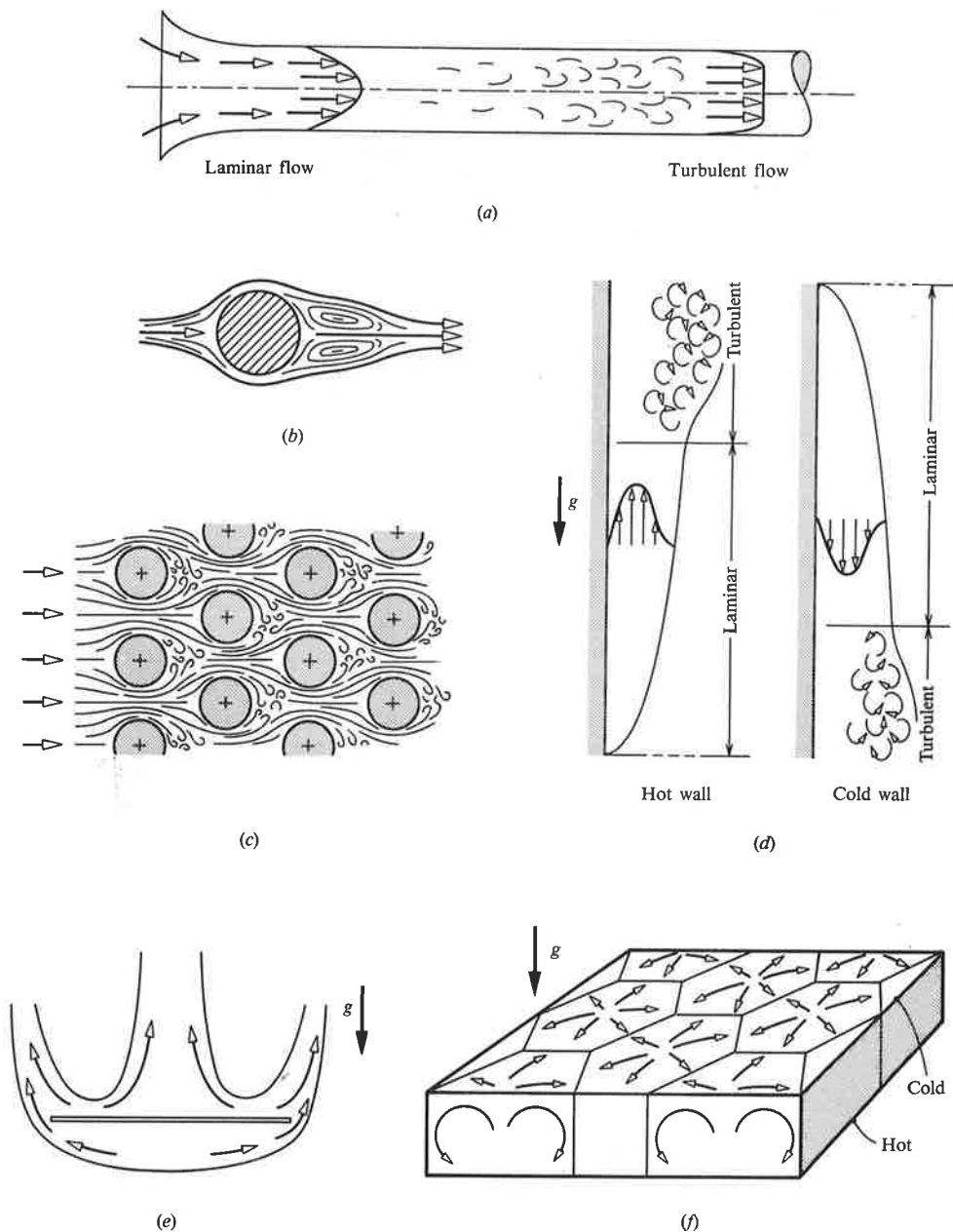
where  $\Delta T = T_s - T_e$ ,  $q_s$  is the heat flux from the surface into the fluid [ $W/m^2$ ], and  $h_c$  has units [ $W/m^2 K$ ]. Equation (1.20) is often called *Newton's law of cooling* but is a definition of  $h_c$  rather than a true physical law. For natural convection, the situation is more complicated. If the flow is laminar,  $q_s$  varies as  $\Delta T^{5/4}$ ; if the flow is turbulent, it varies as  $\Delta T^{4/3}$ . However, we still find it convenient to define a heat transfer coefficient by Eq. (1.20); then  $h_c$  varies as  $\Delta T^{1/4}$  for laminar flows and as  $\Delta T^{1/3}$  for turbulent ones.

An important practical problem is convective heat transfer to a fluid flowing in a tube, as may be found in heat exchangers for heating or cooling liquids, in condensers, and in various kinds of boilers. In using Eq. (1.20) for internal flows,  $\Delta T = T_s - T_b$ , where  $T_b$  is a properly averaged fluid temperature called the **bulk temperature** or mixed mean temperature and is defined in Chapter 4. Here it is sufficient to note that enthalpy in the steady-flow energy equation, Eq. (1.4), is also the bulk value, and  $T_b$  is the corresponding temperature. If the pipe has a uniform wall temperature  $T_s$  along its length, and the flow is laminar ( $Re_D \lesssim 2300$ ), then sufficiently far from the pipe entrance, the heat transfer coefficient is given by the exact relation

$$h_c = 3.66 \frac{k}{D} \quad (1.21)$$

where  $k$  is the fluid thermal conductivity and  $D$  is the pipe diameter. Notice that the heat transfer coefficient is directly proportional to thermal conductivity, inversely proportional to pipe diameter, and—perhaps surprisingly— independent of flow velocity. On the other hand, for fully turbulent flow ( $Re_D \gtrsim 10,000$ ),  $h_c$  is given





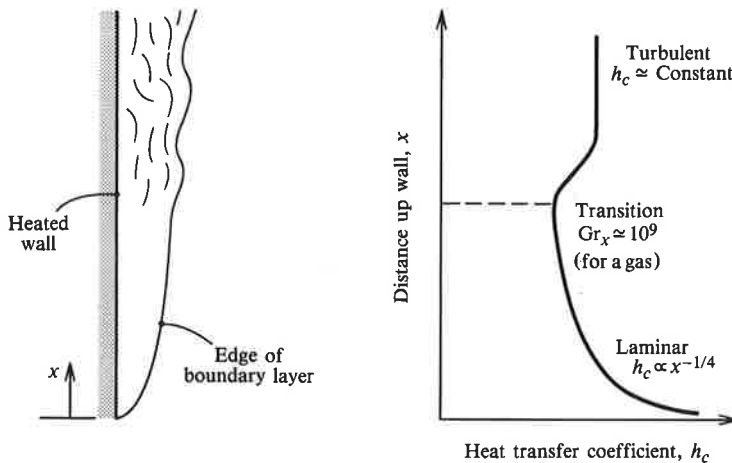
**Figure 1.10** Some commonly encountered flows. (a) Forced flow in a pipe,  $Re_D \approx 50,000$ . The flow is initially laminar because of the "bell-mouth" entrance but becomes turbulent downstream. (b) Laminar forced flow over a cylinder,  $Re_D \approx 25$ . (c) Forced flow through a tube bank as found in a shell-and-tube heat exchanger. (d) Laminar and turbulent natural convection boundary layers on vertical walls. (e) Laminar natural convection about a heated horizontal plate. (f) Cellular natural convection in a horizontal enclosed fluid layer.

approximately by the following, rather complicated correlation of experimental data:

$$h_c = 0.023 \frac{V^{0.8} k^{0.6} (\rho c_p)^{0.4}}{D^{0.2} \nu^{0.4}} \quad (1.22)$$

In contrast to laminar flow,  $h_c$  is now strongly dependent on velocity,  $V$ , but only weakly dependent on diameter. In addition to thermal conductivity, other fluid properties involved are the kinematic viscosity,  $\nu$ ; density,  $\rho$ ; and specific heat,  $c_p$ . In Chapter 4 we will see how Eq. (1.22) can be rearranged in a more compact form by introducing appropriate dimensionless groups. Equations (1.21) and (1.22) are only valid at some distance from the pipe entrance and indicate that the heat transfer coefficient is then independent of position along the pipe. Near the pipe entrance, heat transfer coefficients tend to be higher, due to the generation of large-scale vortices by upstream bends or sharp corners and the effect of suddenly heating the fluid.

Figure 1.11 shows a natural convection flow on a heated vertical surface, as well as a schematic of the associated variation of  $h_c$  along the surface. Transition from a laminar to a turbulent boundary layer is shown. In gases, the location of the transition is determined by a critical value of a dimensionless group called the **Grashof number**. The Grashof number is defined as  $Gr_x = (\beta \Delta T) g x^3 / \nu^2$ , where  $\Delta T = T_s - T_e$ ,  $g$  is the gravitational acceleration [ $m/s^2$ ],  $x$  is the distance from the bottom of the surface where the boundary layer starts, and  $\beta$  is the volumetric coefficient of expansion, which for an ideal gas is simply  $1/T$ , where  $T$  is absolute temperature [K]. On a vertical wall, transition occurs at  $Gr_x \approx 10^9$ . For air, at normal temperatures, experiments show that the heat transfer coefficient for natural convection on a vertical wall can be approximated by the following formulas:



**Figure 1.11** A natural-convection boundary layer on a vertical wall, showing the variation of local heat transfer coefficient. For gases, transition from a laminar to turbulent flow occurs at a Grashof number of approximately  $10^9$ ; hence  $x_{tr} \approx [10^9 \nu^2 / \beta \Delta T g]^{1/3}$ .

$$\text{Laminar flow: } h_c = 1.07(\Delta T/x)^{1/4} \text{ W/m}^2 \text{ K} \quad 10^4 < Gr_x < 10^9 \quad (1.23a)$$

$$\text{Turbulent flow: } h_c = 1.3(\Delta T)^{1/3} \text{ W/m}^2 \text{ K} \quad 10^9 < Gr_x < 10^{12} \quad (1.23b)$$

Since these are dimensional equations, it is necessary to specify the units of  $h_c$ ,  $\Delta T$ , and  $x$ , which are  $[\text{W/m}^2 \text{ K}]$ ,  $[\text{K}]$ , and  $[\text{m}]$ , respectively. Notice that  $h_c$  varies as  $x^{-1/4}$  in the laminar region but is independent of  $x$  in the turbulent region.

Usually the engineer requires the total heat transfer from a surface and is not too interested in the actual variation of heat flux along the surface. For this purpose, it is convenient to define an average heat transfer coefficient  $\bar{h}_c$  for an *isothermal* surface of area  $A$  by the relation

$$\dot{Q} = \bar{h}_c A (T_s - T_e) \quad (1.24)$$

so that the total heat transfer rate,  $\dot{Q}$ , can be obtained easily. The relation between  $\bar{h}_c$  and  $h_c$  is obtained as follows: For flow over a surface of width  $W$  and length  $L$ , as shown in Fig. 1.12,

$$d\dot{Q} = h_c (T_s - T_e) W dx$$

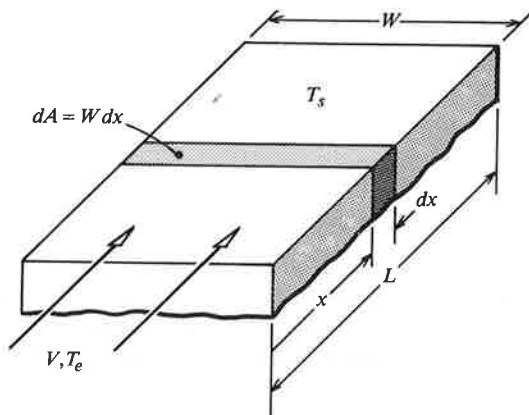
$$\dot{Q} = \int_0^L h_c (T_s - T_e) W dx$$

or

$$\dot{Q} = \left( \frac{1}{A} \int_0^A h_c dA \right) A (T_s - T_e), \quad \text{where } A = WL, \quad dA = W dx \quad (1.25)$$

if  $(T_s - T_e)$  is independent of  $x$ . Since  $T_e$  is usually constant, this condition requires an isothermal wall. Thus, comparing Eqs. (1.24) and (1.25),

$$\bar{h}_c = \frac{1}{A} \int_0^A h_c dA \quad (1.26)$$



**Figure 1.12** An isothermal surface used to define the average convective heat transfer coefficient  $\bar{h}_c$ .

**Table 1.4** Orders of magnitude of average convective heat transfer coefficients.

Flow and Fluid	$\bar{h}_c$ W/m <sup>2</sup> K
Free convection, air	3–25
Free convection, water	15–1000
Forced convection, air	10–200
Forced convection, water	50–10,000
Forced convection, liquid sodium	10,000–100,000
Condensing steam	5000–50,000
Boiling water	3000–100,000

The surface may not be isothermal; for example, the surface may be electrically heated to give a uniform flux  $q_s$  along the surface. In this case, defining an average heat transfer coefficient is more difficult and will be dealt with in Chapter 4. Table 1.4 gives some order-of-magnitude values of average heat transfer coefficients for various situations. In general, high heat transfer coefficients are associated with high fluid thermal conductivities, high flow velocities, and small surfaces. The high heat transfer coefficients shown for boiling water and condensing steam are due to another cause: as we will see in Chapter 7, a large enthalpy of phase change (latent heat) is a contributing factor.

The complexity of most situations involving convective heat transfer precludes exact analysis, and *correlations* of experimental data must be used in engineering practice. For a particular situation, a number of correlations from various sources might be available, for example, from research laboratories in different countries. Also, as time goes by, older correlations may be superseded by newer correlations based on more accurate or more extensive experimental data. Heat transfer coefficients calculated from various available correlations usually do not differ by more than about 20%, but in more complex situations, much larger discrepancies may be encountered. Such is the nature of engineering calculations of convective heat transfer, in contrast to the more exact nature of the analysis of heat conduction or of elementary mechanics, for example.

---

### EXAMPLE 1.3 Heat Loss through Glass Doors

The living room of a ski chalet has a pair of glass doors 2.3 m high and 4.0 m wide. On a cold morning, the air in the room is at 10°C, and frost partially covers the inner surface of the glass. Estimate the convective heat loss to the doors. Would you expect to see the frost form initially near the top or the bottom of the doors? Take  $\nu = 14 \times 10^{-6}$  m<sup>2</sup>/s for the air.

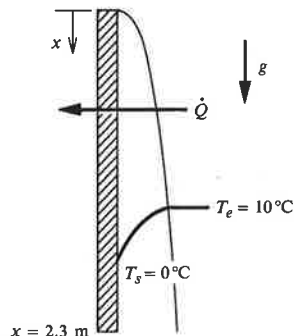
**Solution**

**Given:** Glass doors, width  $W = 4$  m, height  $L = 2.3$  m.

**Required:** Estimate of convective heat loss to the doors.

**Assumptions:** 1. Inner surface isothermal at  $T_s \approx 0^\circ\text{C}$ .  
2. The laminar to turbulent flow transition occurs at  $\text{Gr}_x \approx 10^9$ .

Equation (1.24) will be used to estimate the heat loss. The inner surface will be at approximately  $0^\circ\text{C}$  since it is only partially covered with frost. If it were warmer, frost couldn't form; and if it were much colder, frost would cover the glass completely. There is a natural convection flow down the door since  $T_e = 10^\circ\text{C}$  is greater than  $T_s = 0^\circ\text{C}$ . Transition from a laminar boundary layer to a turbulent boundary layer occurs when the Grashof number is about  $10^9$ . For transition at  $x = x_{tr}$ ,



$$\text{Gr} = 10^9 = \frac{(\beta\Delta T)gx_{tr}^3}{\nu^2}; \quad \beta = 1/T \text{ for an ideal gas}$$

$$x_{tr} = \left[ \frac{10^9 \nu^2}{(\Delta T/T)g} \right]^{1/3} = \left[ \frac{(10^9)(14 \times 10^{-6} \text{ m}^2/\text{s}^2)}{(10/278)(9.81 \text{ m/s}^2)} \right]^{1/3} = 0.82 \text{ m}$$

where the average of  $T_s$  and  $T_e$  has been used to evaluate  $\beta$ . The transition is seen to take place about one third of the way down the door.

We find the average heat transfer coefficient,  $\bar{h}_c$ , by substituting Eqs. (1.23a,b) in Eq. (1.26):

$$\begin{aligned} \bar{h}_c &= \frac{1}{A} \int_0^A h_c dA; \quad A = WL, \quad dA = W dx \\ &= \frac{1}{L} \int_0^L h_c dx \\ &= \frac{1}{L} \left[ \int_0^{x_{tr}} 1.07(\Delta T/x)^{1/4} dx + \int_{x_{tr}}^L 1.3(\Delta T)^{1/3} dx \right] \\ &= (1/L)[(1.07)(4/3)\Delta T^{1/4}x_{tr}^{3/4} + (1.3)(\Delta T)^{1/3}(L - x_{tr})] \\ &= (1/2.3)[(1.07)(4/3)(10)^{1/4}(0.82)^{3/4} + (1.3)(10)^{1/3}(2.3 - 0.82)] \\ &= (1/2.3)[2.19 + 4.15] \\ &= 2.75 \text{ W/m}^2 \text{ K} \end{aligned}$$

Then, from Eq. (1.24), the total heat loss to the door is

$$\dot{Q} = \bar{h}_c A \Delta T = (2.75 \text{ W/m}^2 \text{ K})(2.3 \times 4.0 \text{ m}^2)(10 \text{ K}) = 253 \text{ W}$$

### Comments

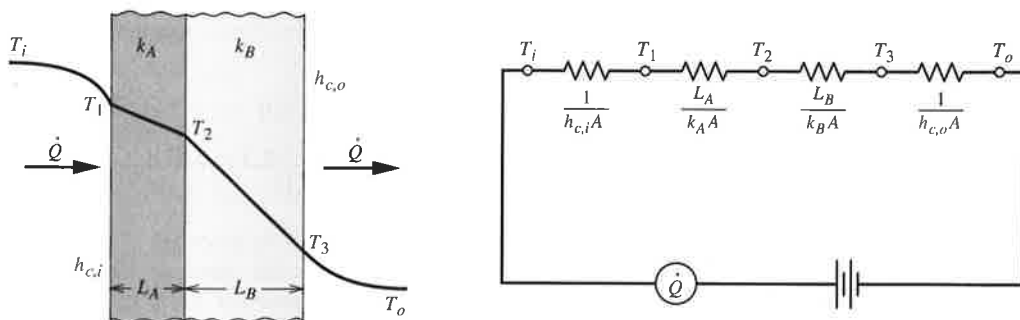
1. The local heat transfer coefficient is larger near the top of the door, so that the relatively warm room air will tend to cause the glass there to be at a higher temperature than further down the door. Thus, frost should initially form near the bottom of the door.
2. In addition, interior surfaces in the room will lose heat by radiation through the glass doors.

## 1.4 COMBINED MODES OF HEAT TRANSFER

Heat transfer problems encountered by the design engineer almost always involve more than one mode of heat transfer occurring simultaneously. For example, consider the nighttime heat loss through the roof of the house shown in Fig. 1.3. Heat is transferred to the ceiling by convection from the warm room air, and by radiation from the walls, furniture, and occupants. Heat transfer across the ceiling and its insulation is by conduction, across the attic crawlspace by convection and radiation, and across the roof tile by conduction. Finally, the heat is transferred by convection to the cold ambient air, and by radiation to the nighttime sky. To consider realistic engineering problems, it is necessary at the outset to develop the theory required to handle *combined modes* of heat transfer.

### 1.4.1 Thermal Circuits

The electrical circuit analogy for conduction through a composite wall was introduced in Section 1.3.1. We now extend this concept to include convection and radiation as well. Figure 1.13 shows a two-layer composite wall of cross-sectional area  $A$  with the layers  $A$  and  $B$  having thickness and conductivity  $L_A, k_A$  and  $L_B, k_B$ , respectively. Heat is transferred from a hot fluid at temperature  $T_i$  to the inside of the wall with a convective heat transfer coefficient  $h_{c,i}$ , and away from the outside of the wall to a cold fluid at temperature  $T_o$  with heat transfer coefficient  $h_{c,o}$ .



**Figure 1.13** The temperature distribution for steady heat transfer across a composite plane wall, and the corresponding thermal circuit.

Newton's law of cooling, Eq. (1.20), can be rewritten as

$$\dot{Q} = \frac{\Delta T}{1/h_c A} \quad (1.27)$$

with  $1/h_c A$  identified as a convective thermal resistance. At steady state, the heat flow through the wall is constant. Referring to Fig. 1.13 for the intermediate temperatures,

$$\dot{Q} = \frac{T_i - T_1}{1/h_{c,i} A} = \frac{T_1 - T_2}{L_A/k_A A} = \frac{T_2 - T_3}{L_B/k_B A} = \frac{T_3 - T_o}{1/h_{c,o} A} \quad (1.28)$$

Equation (1.28) is the basis of the thermal circuit shown in Fig. 1.13. The total resistance is the sum of four resistances in series. If we define the **overall heat transfer coefficient**  $U$  by the relation

$$\dot{Q} = UA(T_i - T_o) \quad (1.29)$$

then  $1/UA$  is an overall resistance given by

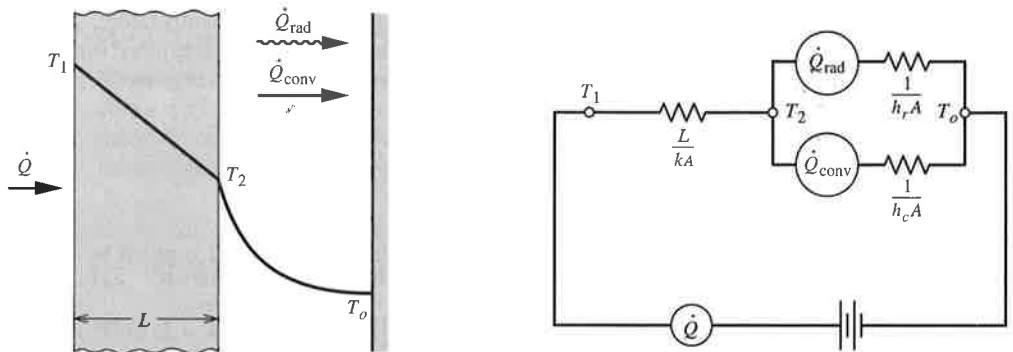
$$\frac{1}{UA} = \frac{1}{h_{c,i} A} + \frac{L_A}{k_A A} + \frac{L_B}{k_B A} + \frac{1}{h_{c,o} A} \quad (1.30a)$$

or, since the cross-sectional area  $A$  is constant for a plane wall,

$$\frac{1}{U} = \frac{1}{h_{c,i}} + \frac{L_A}{k_A} + \frac{L_B}{k_B} + \frac{1}{h_{c,o}} \quad (1.30b)$$

Equation (1.29) is simple and convenient for use in engineering calculations. Typical values of  $U$  [ $\text{W}/\text{m}^2 \text{K}$ ] vary over a wide range for different types of walls and convective flows.

Figure 1.14 shows a wall whose outer surface loses heat by both convection and radiation. For simplicity, assume that the fluid is at the same temperature as the surrounding surfaces,  $T_o$ . Using the approximate linearized Eq. (1.19),



**Figure 1.14** A wall that loses heat by both conduction and radiation; the thermal circuit shows resistances in parallel.

$$\dot{Q}_{\text{rad}} = \frac{\Delta T}{1/h_r A} \quad (1.31)$$

with  $1/h_r A$  identified as a radiative thermal resistance. We now have two resistances in parallel, as shown in Fig. 1.14. The sum of the resistances is

$$\sum R = \frac{L}{kA} + \frac{1}{h_c A + h_r A}$$

or

$$\frac{1}{UA} = \frac{L}{kA} + \frac{1}{(h_c + h_r)A} \quad (1.32)$$

so that the convective and radiative heat transfer coefficients can simply be added. However, often the fluid and surrounding temperatures are not the same, or the simple linearized representation of radiative transfer [Eq. (1.19)] is invalid, so the thermal circuit is then more complex. When appropriate, we will write  $h = h_c + h_r$  to account for combined convection and radiation.<sup>5</sup>

#### EXAMPLE 1.4 Heat Loss through a Composite Wall

The walls of a sparsely furnished single-room cabin in a forest consist of two layers of pine wood, each 2 cm thick, sandwiching 5 cm of fiberglass insulation. The cabin interior is maintained at 20°C when the ambient air temperature is 2°C. If the interior and exterior convective heat transfer coefficients are 3 and 6 W/m<sup>2</sup> K, respectively, and the exterior surface is finished with a white acrylic paint, estimate the heat flux through the wall.

#### Solution

**Given:** Pine wood cabin wall insulated with 5 cm of fiberglass.

**Required:** Estimate of heat loss through wall.

- Assumptions:**
1. Forest trees and shrubs are at the ambient air temperature,  $T_e = 2^\circ\text{C}$ .
  2. Radiation transfer inside cabin is negligible since inner surfaces of walls, roof, and floor are at approximately the same temperature.

From Eq. (1.29), the heat flux through the wall is

$$q = \frac{\dot{Q}}{A} = U(T_i - T_o)$$

From Eqs. (1.30) and (1.32), the overall heat transfer coefficient is given by

$$\frac{1}{U} = \frac{1}{h_{c,i}} + \frac{L_A}{k_A} + \frac{L_B}{k_B} + \frac{L_C}{k_C} + \frac{1}{(h_{c,o} + h_{r,o})}$$

<sup>5</sup> Notice that the notation used for this combined heat transfer coefficient,  $h$ , is the same as that used for enthalpy. The student must be careful not to confuse these two quantities. Other notation is also in common use, for example,  $\alpha$  for the heat transfer coefficient and  $i$  for enthalpy.



The thermal conductivities of pine wood, perpendicular to the grain, and of fiberglass are given in Table 1.1 as 0.10 and 0.038 W/m K, respectively. The exterior radiation heat transfer coefficient is given by Eq. (1.19) as

$$h_{r,o} = 4\varepsilon\sigma T_m^3$$

where  $\varepsilon = 0.9$  for white acrylic paint, from Table 1.3, and  $T_m \approx 2^\circ\text{C} = 275\text{ K}$  (since we expect the exterior resistance to be small). Thus,

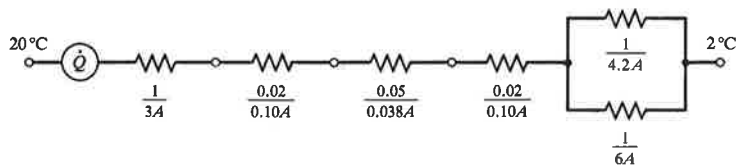
$$\begin{aligned} h_{r,o} &= 4(0.9)(5.67 \times 10^{-8} \text{ W/m}^2 \text{ K}^4)(275 \text{ K})^3 \\ &= 4.2 \text{ W/m}^2 \text{ K} \end{aligned}$$

$$\begin{aligned} \frac{1}{U} &= \frac{1}{3} + \frac{0.02}{0.10} + \frac{0.05}{0.038} + \frac{0.02}{0.10} + \frac{1}{6 + 4.2} \\ &= 0.333 + 0.200 + 1.316 + 0.200 + 0.098 \\ &= 2.15 \text{ (W/m}^2 \text{ K)}^{-1} \end{aligned}$$

$$U = 0.466 \text{ W/m}^2 \text{ K}$$

Then the heat flux  $q = U(T_i - T_o) = 0.466(20 - 2) = 8.38 \text{ W/m}^2$ .

The thermal circuit is shown below.

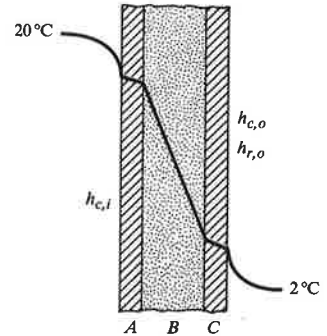


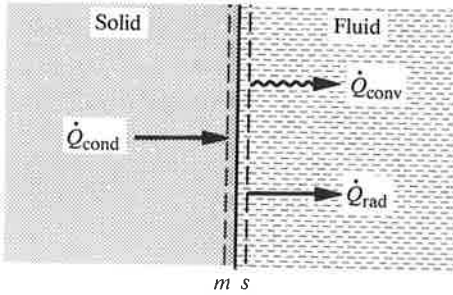
### Comments

1. The outside resistance is seen to be  $0.098/2.15 \approx 5\%$  of the total resistance; hence, the outside wall of the cabin is only about 1 K above the ambient air, and our assumption of  $T_m = 275\text{ K}$  for the evaluation of  $h_{r,o}$  is adequate.
2. The dominant resistance is that of the fiberglass insulation; therefore, an accurate calculation of  $q$  depends mainly on having accurate values for the fiberglass thickness and thermal conductivity. Poor data or poor assumptions for the other resistances have little impact on the result.

### 1.4.2 Surface Energy Balances

Section 1.4.1 assumed that the energy flow  $\dot{Q}$  across the wall surfaces is continuous. In fact, we used a procedure commonly called a *surface energy balance*, which is used in various ways. Some examples follow. Figure 1.15 shows an opaque solid that is losing heat by convection and radiation to its surroundings. Two imaginary surfaces are located on each side of the real solid-fluid interface: an *s*-surface





**Figure 1.15** Schematic of a surface energy balance, showing the  $m$ - and  $s$ -surface in the solid and fluid, respectively.

in the fluid just adjacent to the interface, and an  $m$ -surface in the solid located such that all radiation is emitted or absorbed between the  $m$ -surface and the interface. Thus, energy is transferred across the  $m$ -surface by conduction only. (The choice of  $s$  and  $m$  to designate these surfaces follows an established practice. In particular, the use of the  $s$  prefix is consistent with the use of the subscript  $s$  to denote a surface temperature  $T_s$  in convection analysis.) The first law as applied to the closed system located between  $m$ - and  $s$ -surfaces requires that  $\sum \dot{Q} = 0$ ; thus,

$$\dot{Q}_{\text{cond}} - \dot{Q}_{\text{conv}} - \dot{Q}_{\text{rad}} = 0 \quad (1.33)$$

or, for a unit area,

$$q_{\text{cond}} - q_{\text{conv}} - q_{\text{rad}} = 0 \quad (1.34)$$

where the sign convention for the fluxes is shown in Fig. 1.15. If the solid is isothermal, Eq. (1.33) reduces to

$$\dot{Q}_{\text{conv}} + \dot{Q}_{\text{rad}} = 0 \quad (1.35)$$

which is a simple energy balance on the solid. Notice that these surface energy balances remain valid for unsteady conditions, in which temperatures change with time, provided the mass contained between the  $s$ - and  $m$ -surfaces is negligible and cannot store energy.

### EXAMPLE 1.5 Air Temperature Measurement

A machine operator in a workshop complains that the air-heating system is not keeping the air at the required minimum temperature of 20°C. To support his claim, he shows that a mercury-in-glass thermometer suspended from a roof truss reads only 17°C. The roof and walls of the workshop are made of corrugated iron and are not insulated; when the thermometer is held against the wall, it reads only 5°C. If the average convective heat transfer coefficient for the suspended thermometer is estimated to be 10 W/m<sup>2</sup> K, what is the true air temperature?

#### Solution

**Given:** Thermometer reading a temperature of 17°C.

**Required:** True air temperature.

**Assumptions:** Thermometer can be modeled as a small gray body in large, nearly black surroundings at 5°C.

Let  $T_i$  be the thermometer reading,  $T_e$  the air temperature, and  $T_w$  the wall temperature. Equation (1.35) applies,

$$\dot{Q}_{\text{conv}} + \dot{Q}_{\text{rad}} = 0$$

since at steady state there is no conduction within the thermometer. Substituting from Eqs. (1.24) and (1.18),

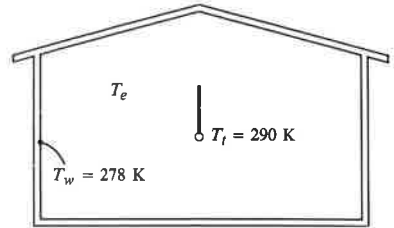
$$\bar{h}_c A (T_i - T_e) + \varepsilon \sigma A (T_i^4 - T_w^4) = 0$$

From Table 1.3,  $\varepsilon = 0.8$  for pyrex glass. Canceling  $A$ ,

$$10(290 - T_e) + (0.8)(5.67)(2.90^4 - 2.78^4) = 0$$

Solving,

$$T_e = 295 \text{ K} \approx 22^\circ\text{C}$$



### Comments

1. Since  $T_e > 20^\circ\text{C}$ , the air-heating system appears to be working satisfactorily.
2. Our model assumes that the thermometer is completely surrounded by a surface at  $5^\circ\text{C}$ : actually, the thermometer also receives radiation from machines, workers, and other sources at temperatures higher than  $5^\circ\text{C}$ , so that our calculated value of  $T_e = 22^\circ\text{C}$  is somewhat high.

## 1.5 TRANSIENT THERMAL RESPONSE

The heat transfer problems described in Examples 1.1 through 1.5 were *steady-state* problems; that is, temperatures were not changing in time. In Example 1.2, the transistor temperature was steady with the resistance ( $I^2R$ ) heating balanced by the radiation heat loss. *Unsteady-state* or *transient* problems occur when temperatures change with time. Such problems are often encountered in engineering practice, and the engineer may be required to predict the temperature-time response of a system involved in a heat transfer process. If the system, or a component of the system, can be assumed to have a spatially uniform temperature, analysis involves a relatively simple application of the energy conservation principle, as will now be demonstrated.

### 1.5.1 The Lumped Thermal Capacity Model

If a system undergoing a transient thermal response to a heat transfer process has a nearly uniform temperature, we may ignore small differences of temperature within the system. Changes in internal energy of the system can then be specified in terms of changes of the assumed uniform (or average) temperature of the system. This approximation is called the **lumped thermal capacity** model.<sup>6</sup> The system might be

<sup>6</sup> The term *capacitance* is also used, in analogy to an equivalent electrical circuit.

a small solid component of high thermal conductivity that loses heat slowly to its surroundings via a large external thermal resistance. Since the thermal resistance to conduction in the solid is small compared to the external resistance, the assumption of a uniform temperature is justified. Alternatively, the system might be a well-stirred liquid in an insulated tank losing heat to its surroundings, in which case it is the mixing of the liquid by the stirrer that ensures a nearly uniform temperature. In either case, once we have assumed uniformity of temperature, we have no further need for details of the heat transfer within the system—that is, of the conduction in the solid component or the convection in the stirred liquid. Instead, the heat transfer process of concern is the interaction of the system with the surroundings, which might be by conduction, radiation, or convection.

### *Governing Equation and Initial Condition*

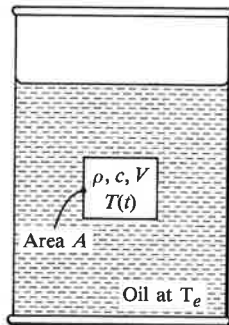
For purposes of analysis, consider a metal forging removed from a furnace at temperature  $T_0$  and suddenly immersed in an oil bath at temperature  $T_e$ , as shown in Fig. 1.16. The forging is a closed system, so the energy conservation principle in the form of Eq. (1.2) applies. Heat is transferred out of the system by convection. Using Eq. (1.24) the rate of heat transfer is  $\bar{h}_c A(T - T_e)$ , where  $\bar{h}_c$  is the heat transfer coefficient averaged over the forging surface area  $A$ , and  $T$  is the forging temperature. There is no heat generated within the forging, so that  $\dot{Q}_v = 0$ . Substituting in Eq. (1.2):

$$\rho V c \frac{dT}{dt} = -\bar{h}_c A(T - T_e)$$

$$\frac{dT}{dt} = -\frac{\bar{h}_c A}{\rho V c}(T - T_e) \quad (1.36)$$

which is a first-order ordinary differential equation for the forging temperature,  $T$ , as a function of time,  $t$ . One initial condition is required:

$$t = 0: \quad T = T_0 \quad (1.37)$$



**Figure 1.16** A forging immersed in an oil bath for quenching.

### Solution for the Temperature Response

A simple analytical solution can be obtained provided we assume that the bath is large, so  $T_e$  is independent of time, and that  $\bar{h}_c A / \rho V c$  is approximated by a constant value independent of temperature. The variables in Eq. (1.36) can then be separated:

$$\frac{dT}{T - T_e} = -\frac{\bar{h}_c A}{\rho V c} dt$$

Writing  $dT = d(T - T_e)$ , since  $T_e$  is constant, and integrating with  $T = T_0$  at  $t = 0$ ,

$$\int_{T_0}^T \frac{d(T - T_e)}{T - T_e} = -\frac{\bar{h}_c A}{\rho V c} \int_0^t dt$$

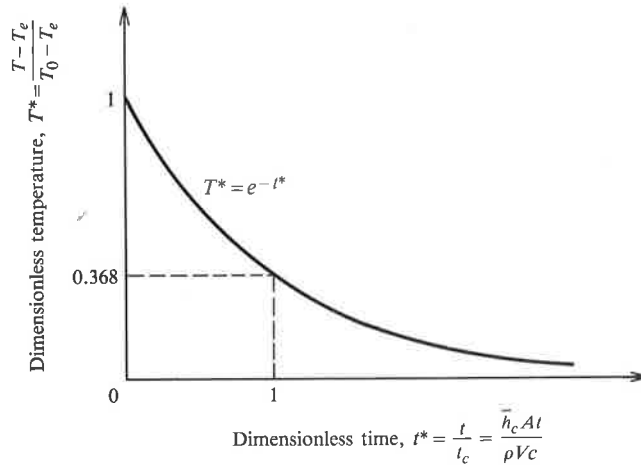
$$\ln \frac{T - T_e}{T_0 - T_e} = -\frac{\bar{h}_c A}{\rho V c} t$$

$$\frac{T - T_e}{T_0 - T_e} = e^{-(\bar{h}_c A / \rho V c)t} = e^{-t/t_c} \quad (1.38)$$

where  $t_c = \rho V c / \bar{h}_c A$  [s] is called the **time constant** of the process. When  $t = t_c$ , the temperature difference  $(T - T_e)$  has dropped to be 36.8% of the initial difference  $(T_0 - T_e)$ . Our result, Eq. (1.38), is a relation between two dimensionless parameters: a dimensionless temperature,  $T^* = (T - T_e) / (T_0 - T_e)$ , which varies from 1 to 0; and a dimensionless time,  $t^* = t / t_c = \bar{h}_c A t / \rho V c$ , which varies from 0 to  $\infty$ . Equation (1.38) can be written simply as

$$T^* = e^{-t^*} \quad (1.39)$$

and a graph of  $T^*$  versus  $t^*$  is a single curve, as illustrated in Fig. 1.17.



**Figure 1.17** Lumped thermal capacity temperature response in terms of dimensionless variables  $T^*$  and  $t^*$ .

Methods introduced in Chapter 2 can be used to deduce directly from Eqs. (1.36) and (1.37) that  $T^*$  must be a function of  $t^*$  alone [i.e.,  $T^* = f(t^*)$ ] without solving the equation. Of course, the solution also gives us the form of the function. Thus, the various parameters,  $\bar{h}_c$ ,  $c$ ,  $\rho$ , and so on, only affect the temperature response in the combination  $t^*$ , and not independently. If both  $\bar{h}_c$  and  $c$  are doubled, the temperature at time  $t$  is unchanged. This dimensionless parameter  $t^*$  is a dimensionless group in the same sense as the Reynolds number, but it does not have a commonly used name.

### Validity of the Model

We would expect our assumption of negligible temperature gradients within the system to be valid when the internal resistance to heat transfer is small compared with the external resistance. If  $L$  is some appropriate characteristic length of a solid body, for example,  $V/A$  (which for a plate is half its thickness), then

$$\frac{\text{Internal conduction resistance}}{\text{External convection resistance}} \approx \frac{L/k_s A}{1/\bar{h}_c A} = \frac{\bar{h}_c L}{k_s} \quad (1.40)$$

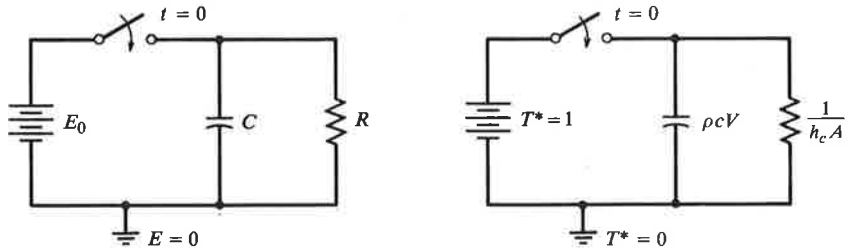
where  $k_s$  is the thermal conductivity of the solid material. The quantity  $\bar{h}_c L/k_s$  [ $\text{W/m}^2 \text{K}][\text{m}]/[\text{W/m K}]$  is a dimensionless group called the **Biot number**,  $Bi$ . More exact analyses of transient thermal response of solids indicate that, for bodies resembling a plate, cylinder, or sphere,  $Bi < 0.1$  ensures that the temperature at the center will not differ from that at the surface by more than 5%; thus,  $Bi < 0.1$  is a suitable criterion for determining if the assumption that the body has a uniform temperature is justified. If the heat transfer is by radiation, the convective heat transfer coefficient in Eq. (1.40) can be replaced by the approximate radiation heat transfer coefficient  $h_r$  defined in Eq. (1.19).

In the case of the well-stirred liquid in an insulated tank, it will be necessary to evaluate the ratio

$$\frac{\text{Internal convection resistance}}{\text{External resistance}} \approx \frac{1/h_{c,i} A}{1/UA} = \frac{U}{h_{c,i}} \quad (1.41)$$

where  $U$  is the overall heat transfer coefficient, for heat transfer from the inner surface of the tank, across the tank wall and insulation, and into the surroundings. If this ratio is small relative to unity, the assumption of a uniform temperature in the liquid is justified.

The approximation or model used in the preceding analysis is called a lumped thermal capacity approximation since the thermal capacity is associated with a single temperature. There is an electrical analogy to the lumped thermal capacity model, owing to the mathematical equivalence of Eq. (1.36) to the equation governing the voltage in the simple resistance-capacitance electrical circuit shown



**Figure 1.18** Equivalent electrical and thermal circuits for the lumped thermal capacity model of temperature response.

in Fig. 1.18,

$$\frac{dE}{dt} = -\frac{E}{RC} \quad (1.42)$$

with the initial condition  $E = E_0$  at  $t = 0$  if the capacitor is initially charged to a voltage  $E_0$ . The solution is identical in form to Eq. (1.38),

$$\frac{E}{E_0} = e^{-t/RC}$$

and the time constant is  $RC$ , the product of the resistance and capacitance [or  $C/(1/R)$ , the ratio of capacitance to conductance, to be exactly analogous to Eq. (1.38)].

### EXAMPLE 1.6 Quenching of a Steel Plate

A steel plate 1 cm thick is taken from a furnace at 600°C and quenched in a bath of oil at 30°C. If the heat transfer coefficient is estimated to be 400 W/m<sup>2</sup> K, how long will it take for the plate to cool to 100°C? Take  $k$ ,  $\rho$ , and  $c$  for the steel as 50 W/m K, 7800 kg/m<sup>3</sup>, and 450 J/kg K, respectively.

#### Solution

**Given:** Steel plate quenched in an oil bath.

**Required:** Time to cool from 600°C to 100°C.

**Assumptions:** Lumped thermal capacity model valid.

First the Biot number will be checked to see if the lumped thermal capacity approximation is valid. For a plate of width  $W$ , height  $H$ , and thickness  $L$ ,

$$\frac{V}{A} \approx \frac{WHL}{2WH} = \frac{L}{2}$$

where the surface area of the edges has been neglected.

$$\begin{aligned} \text{Bi} &= \frac{\bar{h}_c(L/2)}{k_s} \\ &= \frac{(400 \text{ W/m}^2 \text{ K})(0.005 \text{ m})}{50 \text{ W/m K}} \\ &= 0.04 < 0.1 \end{aligned}$$

so the lumped thermal capacity model is applicable. The time constant  $t_c$  is

$$t_c = \frac{\rho Vc}{\bar{h}_c A} = \frac{\rho(L/2)c}{\bar{h}_c} = \frac{(7800 \text{ kg/m}^3)(0.005 \text{ m})(450 \text{ J/kg K})}{(400 \text{ W/m}^2 \text{ K})} = 43.9 \text{ s}$$

Substituting  $T_e = 30^\circ\text{C}$ ,  $T_0 = 600^\circ\text{C}$ ,  $T = 100^\circ\text{C}$  in Eq. (1.38) gives

$$\frac{100 - 30}{600 - 30} = e^{-t/43.9}$$

Solving,

$$t = 92 \text{ s}$$

### Comments

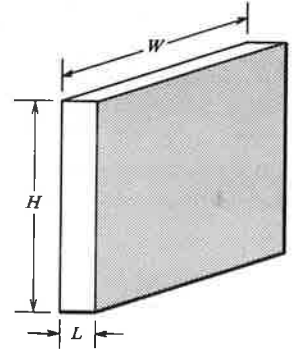
The use of a constant value of  $h_c$  may be inappropriate for heat transfer by natural convection or radiation (see Section 1.5.2).

## 1.5.2 Combined Convection and Radiation

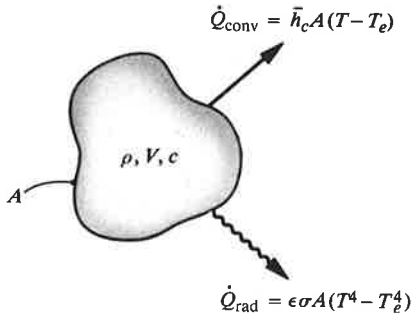
The analysis of Section 1.5.1 assumes that the heat transfer coefficient was constant during the cooling period. This assumption is adequate for forced convection but is less appropriate for natural convection, and when thermal radiation is significant. Equation (1.23) shows that the natural convection heat transfer coefficient  $\bar{h}_c$  is proportional to  $\Delta T^{1/4}$  for laminar flow and to  $\Delta T^{1/3}$  for turbulent flow. The temperature difference  $\Delta T = T - T_e$  decreases as the body cools, as does  $\bar{h}_c$ . Radiation heat transfer is proportional to  $(T^4 - T_e^4)$  and hence cannot be represented exactly by Newton's law of cooling. We now extend our lumped thermal capacity analysis to allow both for a variable convective heat transfer coefficient and for situations where both convection and radiation are important.

### Governing Equation and Initial Condition

Figure 1.19 shows a body that loses heat by both convection and radiation. For a small gray body in large, nearly black surroundings also at temperature  $T_e$ , the radiation heat transfer is obtained from Eq. (1.18) as  $\dot{Q} = \varepsilon A \sigma (T^4 - T_e^4)$ . As in







**Figure 1.19** Schematic of a body losing heat by convection and radiation for a lumped thermal capacity model.

Section 1.5.1, the energy conservation principle Eq. (1.2) becomes

$$\rho V c \frac{dT}{dt} = -\bar{h}_c A (T - T_e) - \epsilon A \sigma (T^4 - T_e^4)$$

or

$$\frac{dT}{dt} = -\frac{\bar{h}_c A}{\rho V c} (T - T_e) - \frac{\epsilon A \sigma}{\rho V c} (T^4 - T_e^4) \quad (1.43)$$

The initial condition is again

$$t = 0: \quad T = T_0 \quad (1.44)$$

This first-order ordinary differential equation has no convenient analytical solution even when the convective heat transfer coefficient  $h_c$  is constant as in forced convection. However, Eq. (1.43) can be solved easily using a numerical integration procedure. For this purpose, it can be rearranged as

$$\frac{dT}{dt} + \frac{hA}{\rho V c} (T - T_e) = 0 \quad (1.45)$$

$$h = \bar{h}_c + h_r = B(T - T_e)^n + \sigma \epsilon (T^2 + T_e^2)(T + T_e) \quad (1.46)$$

where  $(T^4 - T_e^4)$  has been factored, as was done in deriving Eq. (1.19). For forced convection,  $n = 0$ ,  $B = \bar{h}_c$ ; for laminar natural convection  $n = 1/4$  and  $B$  is a constant [for example, for a plate of height  $L$ , Eq. (1.23a) gives  $B = (4/3)(1.07)/L^{1/4}$ ]. Equation (1.46) defines a total heat transfer coefficient that accounts for both convection and radiation and changes continuously as the body cools. To put Eq. (1.45) in dimensionless form, we use the dimensionless variables introduced in Section 1.5.1:

$$T^* = \frac{T - T_e}{T_0 - T_e}, \quad t^* = \frac{t}{t_c} \quad (1.47a,b)$$

The definition of the time constant  $t_c$  poses a problem since  $h$  is not a constant as before. We choose to define  $t_c$  in terms of the value of  $h$  at time  $t = 0$ , when the body temperature is  $T_0$ ,

$$t_c = \frac{\rho V c}{h_0 A} = \frac{\rho V c}{[B(T_0 - T_e)^n + \sigma \epsilon (T_0^2 + T_e^2)(T_0 + T_e)]A} \quad (1.48)$$

Equation (1.45) then becomes

$$\frac{dT^*}{dt^*} + \frac{h(T^*)}{h_0} T^* = 0 \quad (1.49)$$

with the initial condition

$$t^* = 0: T^* = 1 \quad (1.50)$$

### Computer Program LUMP

Numerical integration is appropriate for this problem. The computer program LUMP has been prepared accordingly. LUMP solves Eq. (1.49), that is, it obtains the temperature response of a body that loses heat by convection and/or radiation, based on the lumped thermal capacity model. The required input constant  $B$  is defined in Eq. (1.46). Any consistent system of units can be used. The output can be obtained either as a graph or as numerical data.

---

### EXAMPLE 1.7 Quenching of an Alloy Sphere

A materials processing experiment under microgravity conditions on the space shuttle requires quenching in a forced flow of an inert gas. A 1 cm-diameter metal alloy sphere is removed from a furnace at 800°C and is to be cooled to 500°C by a flow of nitrogen gas at 25°C. Determine the effect of the convective heat transfer coefficient on cooling time for  $10 < \bar{h}_c < 100 \text{ W/m}^2 \text{ K}$ . Properties of the alloy include:  $\rho = 14,000 \text{ kg/m}^3$ ;  $c = 140 \text{ J/kg K}$ ;  $\varepsilon = 0.1$ . The surrounds can be taken as nearly black at 25°C.

#### Solution

**Given:** A metal alloy sphere to be quenched.

**Required:** Effect of convective heat transfer coefficient on cooling time.

**Assumptions:** 1. Lumped thermal capacity model valid.  
2. Constant convective heat transfer coefficient.

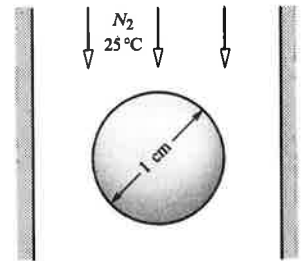
The computer code LUMP can be used to solve this problem.

The required inputs are:

$$\begin{aligned} T_0 \text{ and } T_e &= 1073, 298 \\ B = \bar{h}_c &= 10 \text{ (repeat for 20, 30, 50, 100)} \\ n &= 0 \\ \sigma &= 5.67 \times 10^{-8} \\ \varepsilon &= 0.1 \\ \text{Final value of } t^* &: \text{ try } t^* = 1 \end{aligned}$$

The required dimensionless temperature is

$$T^* = \frac{T - T_e}{T_0 - T_e} = \frac{773 - 298}{1073 - 298} = 0.613$$



and the code is used to obtain the corresponding dimensionless time  $t^*$ . For a sphere  $V/A = (\pi D^3/6)/(\pi D^2) = D/6$ , so that the time constant is

$$t_c = \frac{\rho V c}{h_0 A} = \frac{\rho(D/6)c}{h_0} = \frac{(14,000)(0.01/6)(140)}{\bar{h}_c + (5.67 \times 10^{-8})(0.1)(1073^2 + 298^2)(1073 + 298)}$$

$$= \frac{3267}{\bar{h}_c + 9.64} \text{ s}$$

The actual time is  $t = t^* t_c$ . Results obtained using LUMP are tabulated below.

$\bar{h}_c$ W/m <sup>2</sup> K	$t^*$	$t_c$ s	$t$ s
10	0.59	166	98
20	0.55	110	61
30	0.53	82	43
50	0.52	55	29
100	0.51	30	15

### Comments

1. Only two significant figures have been given since high accuracy is not warranted for the problem.
2. The heat transfer coefficient does not have a strong effect on  $t^*$ . Why?
3. For the lumped thermal capacity model to be valid, the Biot number should be less than 0.1. The worst case is with  $\bar{h}_c = 100 \text{ W/m}^2 \text{ K}$  at time  $t = 0$ , giving  $h_0 = 109.6$  and  $0.1 > (109.6)(0.01/6)/k_s$ , that is,  $k_s > 1.8 \text{ W/m K}$ , which certainly will be true for a metal alloy.

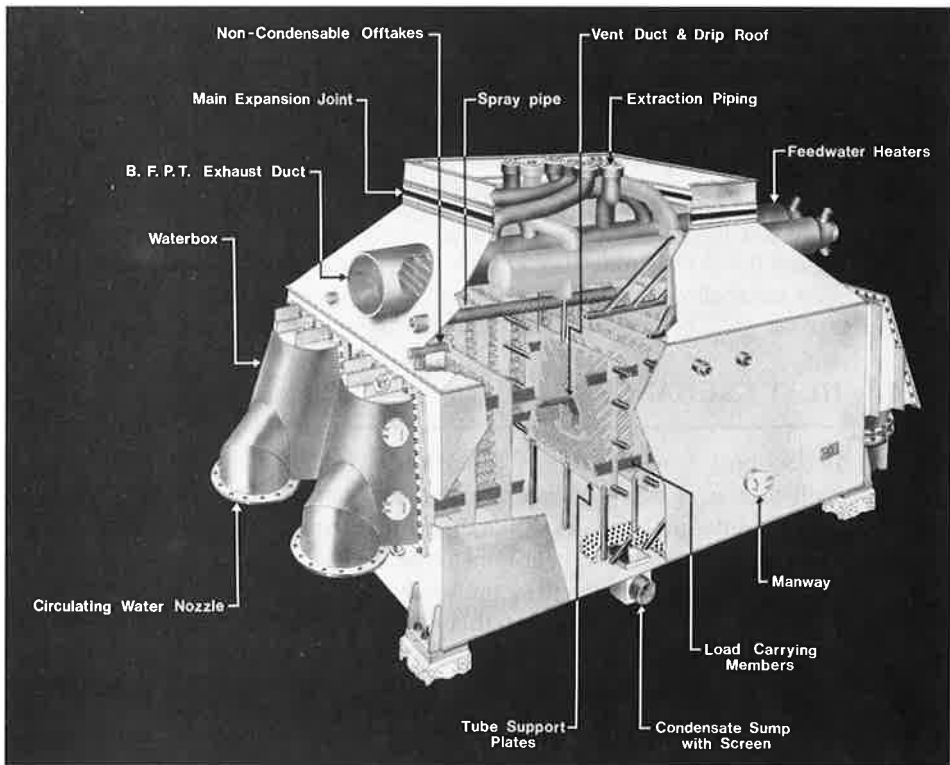
## 1.6 HEAT EXCHANGERS

In Section 1.5, we considered problems in which the temperature of a system changed with time as a result of heat transfer between the system and its surroundings. We now consider problems in which the temperature of a fluid changes as it flows through a passage as a result of heat transfer between the passage walls and the fluid. These problems are encountered in the analysis of heat exchanger performance. A *heat exchanger* is a device that facilitates transfer of heat from one fluid stream to another. Power production, refrigeration, heating and air conditioning, food processing, chemical processing, oil refining, and the operation of almost all vehicles depends on heat exchangers of various types. The analysis and design of heat exchangers is the subject of Chapter 8. The analysis of a very simple heat exchanger configuration is presented here to introduce some of the basic concepts underlying heat exchanger analysis and associated terminology. These concepts will prove useful in the development and application of heat transfer theory in chapters preceding Chapter 8—particularly in Chapters 4 and 5, which deal with convection.

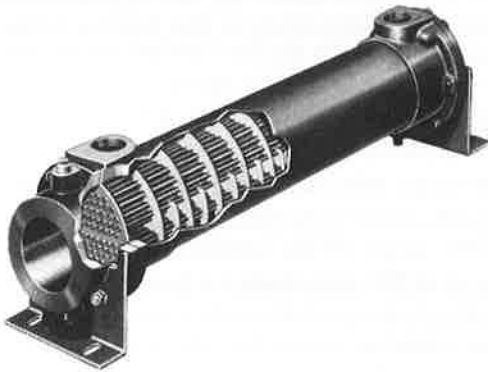
### 1.6.1 Single- and Two-Stream Exchangers

One important classification of heat exchangers is into **single-stream exchangers** and **two-stream exchangers**. A single-stream exchanger is one in which the temperature of only one stream changes in the exchanger; examples include many types of evaporators and condensers found in power plants and refrigeration systems. A power plant condenser is shown in Fig. 1.20. A two-stream exchanger is one in which the temperatures of both streams change in the exchanger; examples include radiators and intercoolers for automobile engines, and oil coolers for aircraft engines. Figure 1.21 shows an oil cooler, which has a **counterflow** configuration; that is, the streams flow in opposite directions in the exchanger.

In the analysis of heat exchangers, a useful first step is to draw a sketch of the expected fluid temperature variations along the exchanger. Figure 1.22*a* is such a sketch for the power plant condenser. The hot stream is steam returning from the turbines, which condenses at a constant temperature  $T_H$ . This is the saturation temperature corresponding to the pressure maintained in the condenser shell. The cold stream is cold water from a river, ocean, or cooling tower, and its temperature



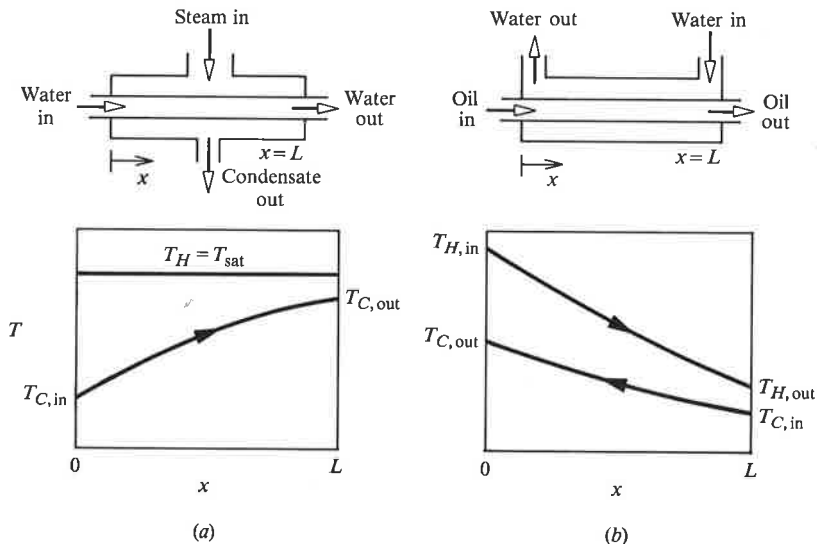
**Figure 1.20** A power plant condenser. (Courtesy Senior Engineering Co. [formerly Southwestern Engineering], Los Angeles, California.)



**Figure 1.21** A small single-pass shell-and-tube two-stream heat exchanger, typically used for cooling oil or water. (Photograph courtesy of the Young Radiator Company, Racine, Wis.)

$T_C$  increases as it flows through the exchanger. Figure 1.22b shows the sketch for the oil cooler. The hot stream is oil from the engine, and the cold stream is coolant water. Notice that in this counterflow configuration, the cold stream can leave the exchanger at a higher temperature than the hot stream!

A point that might confuse the beginning student is that there are actually two streams in many single-stream exchangers. The definition simply requires that the temperature of only one stream changes in a single-stream exchanger. It is this feature that makes the analysis of single-stream exchangers particularly simple, as will now be demonstrated. In Section 1.5, the system analysis was based on the

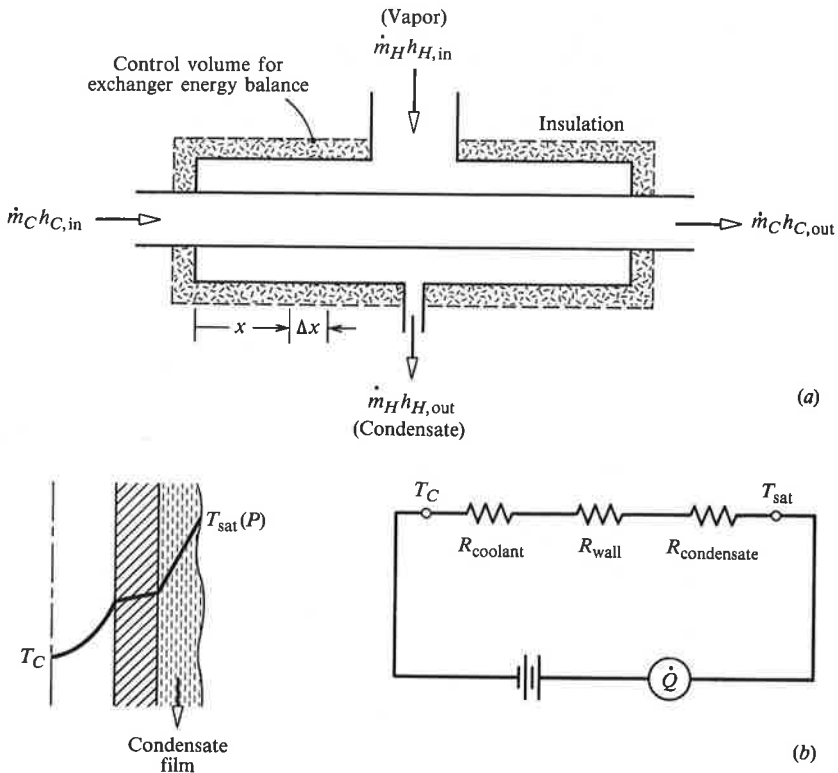


**Figure 1.22** Temperature variations along heat exchangers. (a) A power plant condenser. (b) A counterflow oil cooler.

energy conservation principle in the form of the first law of thermodynamics applied to a *closed system*. In contrast, the system analysis that follows is based on the first law applied to an *open system*.

### 1.6.2 Analysis of a Condenser

Figure 1.23a shows a simple single-tube condenser. Pure saturated vapor enters the shell at the top and condenses on a single horizontal tube. The condensate forms a thin film on the outside of the tube, drops off the bottom, and leaves the shell through a drain. The vapor condenses at the saturation temperature corresponding to the pressure in the shell. Hence, the condensate film surface temperature is  $T_{\text{sat}}(P)$ . Figure 1.23b shows the temperature variation across the tube wall and the corresponding thermal circuit. The enthalpy of condensation is transferred by conduction across the thin condensate film, by conduction across the tube wall; and by convection into the coolant. As a result, the coolant temperature rises as it gains energy flowing along the tube. The vapor flow rate is denoted  $\dot{m}_H$  [kg/s] and the coolant flow rate  $\dot{m}_C$  (the *hot* and *cold* streams, respectively).



**Figure 1.23** (a) Schematic of a single-tube condenser. (b) The temperature variation across the tube wall and the thermal circuit for heat transfer across the tube wall.

### The Exchanger Energy Balance

An energy balance on the exchanger as a whole is formulated by writing down the steady-flow energy equation for a control volume enclosing the exchanger (the dashed line in Fig. 1.23a). If the exchanger is well insulated, there is no heat loss to the surroundings, and Eq. (1.4) requires that the enthalpy inflow equal the enthalpy outflow:

$$\dot{m}_H h_{H,\text{in}} + \dot{m}_C h_{C,\text{in}} = \dot{m}_H h_{H,\text{out}} + \dot{m}_C h_{C,\text{out}}$$

where  $h$  is specific enthalpy [J/kg] and subscripts “in” and “out” denote inlet and outlet values, respectively. Rearranging gives

$$\dot{m}_C (h_{C,\text{out}} - h_{C,\text{in}}) = \dot{m}_H (h_{H,\text{in}} - h_{H,\text{out}}) \quad (1.51)$$

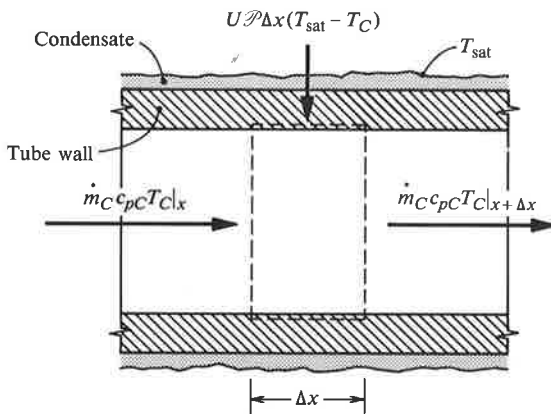
If we assume a constant specific heat for the coolant and that the condensate leaves at the saturation temperature, Eq. (1.51) becomes

$$\dot{m}_C c_{pC} (T_{C,\text{out}} - T_{C,\text{in}}) = \dot{m}_H h_{\text{fg}} \quad (1.52)$$

where  $h_{\text{fg}}$  is the enthalpy of vaporization for the vapor. When the coolant flow rate  $\dot{m}_C$  and inlet temperature  $T_{C,\text{in}}$  are known, Eq. (1.52) relates the coolant outlet temperature  $T_{C,\text{out}}$  to the amount of vapor condensed  $\dot{m}_H$ .

### Governing Equation and Boundary Condition

To determine the variation of coolant temperature along the exchanger, we make an energy balance on a differential element of the exchanger  $\Delta x$  long and so derive a differential equation with  $x$  as the independent variable and  $T_C$  as the dependent variable. When the steady-flow energy equation, Eq. (1.4), is applied to the control volume of length  $\Delta x$ , shown in Fig. 1.24 as a dotted line, the contribution to  $\dot{Q}$  due to  $x$ -direction conduction in the coolant is small and can be neglected. Thus, the



**Figure 1.24** An elemental control volume  $\Delta x$  long for application of the steady-flow energy equation to a condenser coolant stream.

coolant flow rate times its enthalpy increase must equal the heat transfer across the tube wall:

$$\dot{m}_C c_{pC} (T_C|_{x+\Delta x} - T_C|_x) = U\mathcal{P}\Delta x (T_{\text{sat}} - T_C)$$

where  $U$  [ $\text{W}/\text{m}^2 \text{K}$ ] is the overall heat transfer coefficient for heat transfer from the vapor to the coolant, and  $\mathcal{P}$  [ $\text{m}$ ] is the perimeter of the tube wall. Thus,  $\mathcal{P}\Delta x$  is the surface area of the tube element with length  $\Delta x$ . For a circular tube  $\mathcal{P} = \pi D$  where  $D$  is the pipe diameter. Dividing by  $\Delta x$ ,

$$\dot{m}_C c_{pC} \left( \frac{T_C|_{x+\Delta x} - T_C|_x}{\Delta x} \right) = U\mathcal{P} (T_{\text{sat}} - T_C)$$

and letting  $\Delta x \rightarrow 0$ , gives

$$\dot{m}_C c_{pC} \frac{dT_C}{dx} = U\mathcal{P} (T_{\text{sat}} - T_C)$$

Rearranging,

$$\frac{dT_C}{dx} - \frac{U\mathcal{P}}{\dot{m}_C c_{pC}} (T_{\text{sat}} - T_C) = 0 \quad (1.53)$$

Equation (1.53) is a first-order ordinary differential equation for  $T_C(x)$ ; it requires one boundary condition, which is

$$x = 0: T_C = T_{C,\text{in}} \quad (1.54)$$

### Temperature Variation

To integrate Eq. (1.53), let  $\theta = T_{\text{sat}} - T_C$ ; then  $dT_C/dx = -d\theta/dx$ , and the equation becomes

$$\frac{d\theta}{dx} + \frac{U\mathcal{P}}{\dot{m}_C c_{pC}} \theta = 0$$

If  $U$  is assumed constant along the exchanger, the solution is

$$\theta = Ae^{-(U\mathcal{P}/\dot{m}_C c_{pC})x}$$

where  $A$  is the integration constant. Substituting for  $\theta$  and using the boundary condition, Eq. (1.54) gives the integration constant:

$$T_{\text{sat}} - T_{C,\text{in}} = Ae^0 = A$$

Thus, the solution of Eq. (1.53) is

$$T_{\text{sat}} - T_C = (T_{\text{sat}} - T_{C,\text{in}})e^{-(U\mathcal{P}/\dot{m}_C c_{pC})x} \quad (1.55)$$

which is the desired relation  $T_C(x)$ , showing an exponential variation along the exchanger. Of particular interest is the coolant outlet temperature  $T_{C,\text{out}}$  which is obtained by letting  $x = L$ , the length of the exchanger, in Eq. (1.55):

$$T_{\text{sat}} - T_{C,\text{out}} = (T_{\text{sat}} - T_{C,\text{in}})e^{-(U\mathcal{P}L/\dot{m}_C c_{pC})} \quad (1.56)$$



### Exchanger Performance Parameters

The product of perimeter and length  $\mathcal{P}L$  is the area of the heat transfer surface. The exponent in Eq. (1.56) is, of course, dimensionless,

$$\left[ \frac{U\mathcal{P}L}{\dot{m}_C c_{pC}} \right] = \frac{[\text{W/m}^2 \text{K}][\text{m}][\text{m}]}{[\text{kg/s}][\text{J/kg K}]} = \left[ \frac{\text{W s}}{\text{J}} \right] = 1$$

since a watt is a joule per second. This dimensionless group is called the **number of transfer units**, with abbreviation NTU and symbol  $N_{tu}$ .<sup>7</sup> For a given  $\dot{m}_C c_{pC}$ , the larger  $U$ ,  $\mathcal{P}$ , or  $L$ , the greater the NTU of the exchanger. Thus, the NTU can be viewed as a measure of the heat transfer “size” of the exchanger. Equation (1.56) can then be rearranged as

$$\frac{T_{\text{sat}} - T_{C,\text{out}}}{T_{\text{sat}} - T_{C,\text{in}}} = e^{-N_{tu}} \quad (1.57)$$

Thus, if  $T_{\text{sat}}$ ,  $T_{C,\text{in}}$ , and the NTU of the exchanger are known,  $T_{C,\text{out}}$  can be calculated. But we find it convenient to rearrange Eq. (1.57) by subtracting each side from unity to obtain

$$1 - \frac{T_{\text{sat}} - T_{C,\text{out}}}{T_{\text{sat}} - T_{C,\text{in}}} = 1 - e^{-N_{tu}}$$

or

$$\frac{T_{C,\text{out}} - T_{C,\text{in}}}{T_{\text{sat}} - T_{C,\text{in}}} = 1 - e^{-N_{tu}} \quad (1.58)$$

Now, even if the exchanger were infinitely long, the maximum outlet temperature of the coolant would be  $T_{\text{sat}}$  (see Fig. 1.22a). Thus, the left-hand side of Eq. (1.58) is the ratio of the actual temperature rise of the coolant ( $T_{C,\text{out}} - T_{C,\text{in}}$ ) divided by the maximum possible rise for an infinitely long exchanger ( $T_{\text{sat}} - T_{C,\text{in}}$ ) and can be viewed as the **effectiveness** of the exchanger, for which we use the symbol  $\varepsilon$ . Our result is therefore

$$\varepsilon = 1 - e^{-N_{tu}} \quad (1.59)$$

Equation (1.59) indicates that the larger the number of transfer units of the exchanger, the higher its effectiveness. Although a high effectiveness is desirable, as the length of an exchanger increases, so does the cost of materials for its construction and the pumping power required by the coolant flow. Thus, the goal of the design engineer is to maximize the effectiveness subject to the constraints of construction (capital) costs and power (operating) costs. In practice, values of  $\varepsilon$  between 0.6 and 0.9 are typical.

<sup>7</sup> NTU is also widely used as the symbol for number of transfer units.

**EXAMPLE 1.8** Performance of a Steam Condenser

A steam condenser is 4 m long and contains 2000, 5/8 inch nominal-size, 18 gage brass tubes (1.59 cm O.D., 1.25 mm wall thickness). In a test 120 kg/s of coolant water at 300 K is supplied to the condenser, and when the steam pressure in the shell is 10,540 Pa, condensate is produced at a rate of 3.02 kg/s. Determine the effectiveness of the exchanger and the overall heat transfer coefficient. Take the specific heat of the water to be 4174 J/kg K.

**Solution**

**Given:** A shell-and-tube steam condenser.

**Required:** The effectiveness,  $\varepsilon$ , and overall heat transfer coefficient,  $U$ .

**Assumptions:**  $U$  is constant along the exchanger so that Eq. (1.59) applies.

The hot-stream temperature  $T_H$  is the saturation temperature corresponding to the given steam pressure of 10,540 Pa; from steam tables (see Table A.12a in Appendix A of this text)  $T_{\text{sat}} = 320.0$  K. We first find the coolant water outlet temperature from the exchanger energy balance Eq. (1.52):

$$\dot{m}_C c_{pC} (T_{C,\text{out}} - T_{C,\text{in}}) = \dot{m}_H h_{fg}$$

From steam tables, the enthalpy of vaporization at  $T_{\text{sat}} = 320$  K is  $h_{fg} = 2.389 \times 10^6$  J/kg.

$$(120 \text{ kg/s})(4174 \text{ J/kg K})(T_{C,\text{out}} - 300 \text{ K}) = (3.02 \text{ kg/s})(2.389 \times 10^6 \text{ J/kg})$$

Solving gives  $T_{C,\text{out}} = 314.4$  K.

The effectiveness,  $\varepsilon$ , is then obtained from Eq. (1.58) as

$$\varepsilon = \frac{T_{C,\text{out}} - T_{C,\text{in}}}{T_{\text{sat}} - T_{C,\text{in}}} = \frac{314.4 - 300}{320 - 300} = 0.720$$

and the number of transfer units, from Eq. (1.59), is

$$N_{\text{tu}} = \ln \frac{1}{1 - \varepsilon} = \ln \frac{1}{1 - 0.720} = 1.27 = \frac{U \mathcal{P}L}{\dot{m}_C c_{pC}}$$

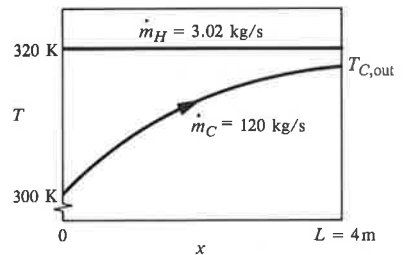
Solving for the  $U \mathcal{P}L$  product,

$$U \mathcal{P}L = 1.27 \dot{m}_C c_{pC} = (1.27)(120 \text{ kg/s})(4174 \text{ J/kg K}) = 6.36 \times 10^5 \text{ W/K}$$

If we choose to base the overall heat transfer coefficient on the outside of the tubes, then, for  $N$  tubes, the heat transfer area  $\mathcal{P}L$  is

$$\mathcal{P}L = N\pi DL = (2000)(\pi)(1.59 \times 10^{-2} \text{ m})(4 \text{ m}) = 400 \text{ m}^2$$

Hence,  $U = U \mathcal{P}L / \mathcal{P}L = 6.36 \times 10^5 / 400 = 1590 \text{ W/m}^2 \text{ K}$

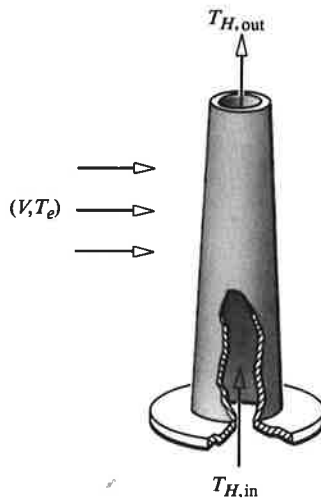


### Comments

We could have performed these calculations by considering a single tube of the tube bundle, for which the coolant flow is  $(120/2000)$  kg/s and the heat transfer area is simply  $\pi DL$ . But common practice is always to consider the exchanger as a whole, as we have done here.

### 1.6.3 Other Single-Stream Exchangers

Simple evaporators and boilers are also single-stream exchangers, where the cold stream is an evaporating or boiling liquid and the hot stream supplies the enthalpy of vaporization. Such exchangers will be analyzed in Chapter 8. Heat transfer to a fluid stream may also be a concern in problems that do not involve heat exchangers. The exhaust gas stack cooled by a crosswind, shown in Fig. 1.25, can also be viewed as a single-stream heat exchanger, since only the exhaust gas temperature changes with location up the stack. Thus, the analysis of Section 1.6.2, properly interpreted, applies (see Exercise 1–52). Single-stream heat exchanger theory also will be used in Chapters 4 and 5 in the examination of convective heat transfer in internal flows.



**Figure 1.25** An exhaust gas stack cooled by a crosswind.

## 1.7 DIMENSIONS AND UNITS

*Dimensions* are physical properties that are measurable—for example, length, time, mass, and temperature. A system of *units* is used to give numerical values to dimensions. The system most widely used throughout the world in science and industry is the International System of units (SI), from the French name *Système International*

*d'Unités*. This system was recommended at the General Conference on Weights and Measures of the International Academy of Sciences in 1960 and was adopted by the U.S. National Bureau of Standards in 1964. In the United States, the transition from the older English system of units to the SI system has been slow and is not complete. The SI system is used in science education, by engineering professional societies, and by many industries. However, engineers in some more mature industries still prefer to use English units, and, of course, commerce and trade in the United States remains dominated by the English system. We buy pounds of vegetables, quarts of milk, drive miles to work, and say that it is a hot day when the temperature exceeds 80°F. (Wine is now sold in 750 ml bottles, though, which is a modest step forward!)

In this text, we will use the SI system, with which the student has become familiar from physics courses. For convenience, this system is summarized in the tables of Appendix B. Base and supplementary units, such as length, time, and plane angle, are given in Table B.1*a*; and derived units, such as force and energy, are given in Table B.1*b*. Recognized non-SI units (e.g., hour, bar) that are acceptable for use with the SI system are listed in Table B.1*c*. Multiples of SI units (e.g., kilo, micro) are defined in Table B.1*d*. Accordingly, the property data given in the tables of Appendix A are in SI units. The student should review this material and is urged to be careful when writing down units. For example, notice that the unit of temperature is a kelvin (not Kelvin) and has the symbol K (not °K). Likewise, the unit of power is the watt (not Watt). The symbol for a kilogram is kg (not KG). An issue that often confuses the student is the correct use of Celsius temperature. Celsius temperature is defined as  $(T - 273.15)$  where  $T$  is in kelvins. However, the unit "degree Celsius" is equal to the unit "kelvin" ( $1^\circ\text{C} = 1\text{ K}$ ).

Notwithstanding the wide acceptance of the SI system of units, there remains a need to communicate with those engineers (or lawyers!) who are still using English units. Also, component dimensions, or data for physical properties, may be available only in English or cgs units. For example, most pipes and tubes used in the United States conform to standard sizes originally specified in English units. A 1 inch nominal-size tube has an outside diameter of 1 in. For convenience, selected dimensions of U.S. commercial standard pipes and tubes are given in SI units in Appendix A as Tables A.14*a* and A.14*b*, respectively. The engineer must be able to convert dimensions from one system of units to another. Table B.2 in Appendix B gives the conversion factors required for most heat transfer applications. The program UNITS is based on Table B.2 and contains all the conversion factors in the table. With the input of a quantity in one system of units, the output is the same quantity in the alternative units listed in Table B.2. It is recommended that the student or engineer perform all problem solving using the SI system so as to efficiently use the Appendix A property data and the computer software. If a problem is stated in English units, the data should be converted to SI units using UNITS; if a customer requires results in units other than SI, UNITS will give the required values.

## 1.8 CLOSURE

---

Chapter 1 had two main objectives:

1. To introduce the three important modes of heat transfer, namely, conduction, radiation, and convection.
2. To demonstrate how the first law of thermodynamics is applied to engineering systems to obtain the consequences of a heat transfer process.

For each mode of heat transfer, some working equations were developed, which, though simple, allow heat transfer calculations to be made for a wide variety of problems. Equations (1.9), (1.18), and (1.20) are probably the most frequently used equations for thermal design. An electric circuit analogy was shown to be a useful aid for problem solving when more than one mode of heat transfer is involved. In applying the first law to engineering systems, both a closed system and an open system were considered. In the first case, the variation of temperature with time was determined for a solid of high conductivity or a well-stirred fluid. In the second case, the variation of fluid temperature with position along a heat exchanger tube was determined.

The student should be familiar with some of the Chapter 1 concepts from previous physics, thermodynamics, and fluid mechanics courses. A review of texts for such courses is appropriate at this time. Many new concepts were introduced, however, which will take a little time and effort to master. Fortunately, the mathematics in this chapter is simple, involving only algebra, calculus, and the simplest first-order differential equation, and should present no difficulties to the student. After successfully completing a selection of the following exercises, the student will be well equipped to tackle subsequent chapters.

A feature of this text is an emphasis on real engineering problems as examples and exercises. Thus, Chapter 1 has somewhat greater scope and detail than the introductory chapters found in most similar texts. With the additional material, more realistic problems can be treated in subsequent chapters. Conduction problems in Chapters 2 and 3 have more realistic convection and radiation boundary conditions. Convective heat transfer coefficients for flow over tube bundles in Chapter 4 are calculated in the appropriate context of a heat exchanger. Similarly, condensation heat transfer coefficients in Chapter 7 can be discussed in the context of condenser performance. Throughout the text are exercises that require application of the first law to engineering systems, for it is always the consequences of a heat transfer process that motivate the engineer's concern with the subject.

Two computer programs accompany Chapter 1. The program LUMP calculates temperature response using the lumped thermal capacity model of Section 1.5. When heat loss is by convection and radiation simultaneously, the problem does not have an analytical solution. However, a numerical solution is easily obtained; LUMP demonstrates the value of writing a computer program in such situations. It is most important that the

engineer be aware of the potential of the PC as an engineering tool and take the initiative to use the PC when appropriate. The program UNITS is a simple units conversion tool that allows unit conversions to be made quickly and reliably.

---

## EXERCISES

1-1. Solve the following ordinary differential equations:

$$(i) \frac{dy}{dx} + \beta y = 0$$

$$(ii) \frac{dy}{dx} + \beta y + \alpha = 0$$

$$(iii) \frac{d^2y}{dx^2} - \lambda^2 y = 0$$

$$(iv) \frac{d^2y}{dx^2} + \lambda^2 y = 0$$

$$(v) \frac{d^2y}{dx^2} - \lambda^2 y + \alpha = 0$$

where  $\alpha$ ,  $\beta$ , and  $\lambda$  are constants.

1-2. A low-pressure heat exchanger transfers heat between two helium streams, each with a flow rate of  $\dot{m} = 5 \times 10^{-3}$  kg/s. In a performance test the cold stream enters at a pressure of 1000 Pa and a temperature of 50 K, and exits at 730 Pa and 350 K.

- (i) If the flow cross-sectional area for the cold stream is  $0.019 \text{ m}^2$ , calculate the inlet and outlet velocities.
- (ii) If the exchanger can be assumed to be perfectly insulated, determine the heat transfer in the exchanger. For helium,  $c_p = 5200 \text{ J/kg K}$ .

1-3. A shell-and-tube condenser for an ocean thermal energy conversion and fresh water plant is tested with a water feed rate to the tubes of 4000 kg/s. The water inlet and outlet conditions are measured to be  $P_1 = 129 \text{ kPa}$ ,  $T_1 = 280 \text{ K}$ ; and  $P_2 = 108 \text{ kPa}$ ,  $T_2 = 285 \text{ K}$ .

- (i) Calculate the heat transferred to the water.
- (ii) If saturated steam condenses in the shell at 1482 Pa, calculate the steam condensation rate.

For the feed water, take  $\rho = 1000 \text{ kg/m}^3$ ,  $c_v = 4192 \text{ J/kg K}$ . (Steam tables are given as Table A.12a in Appendix A.)

1-4. A pyrex glass vessel has a 5 mm-thick wall and is protected with a 1 cm-thick layer of neoprene rubber. If the inner and outer surface temperatures are  $40^\circ\text{C}$

# MULTIDIMENSIONAL AND UNSTEADY CONDUCTION

CONTENTS

- 3.1 INTRODUCTION
- 3.2 THE HEAT CONDUCTION EQUATION
- 3.3 MULTIDIMENSIONAL STEADY CONDUCTION
- 3.4 UNSTEADY CONDUCTION
- 3.5 MOVING-BOUNDARY PROBLEMS
- 3.6 NUMERICAL SOLUTION METHODS
- 3.7 CLOSURE

### 3.1 INTRODUCTION

---

The analyses of steady one-dimensional heat conduction in Chapter 2 were relatively simple but nevertheless gave results that are widely used by engineers for the design of thermal systems. In general, however, heat conduction can be **unsteady**; that is, temperatures change with time. An example is heat flow through the cylinder wall of an automobile engine. Also, heat conduction can be **multidimensional**; that is, temperatures vary significantly in more than one coordinate direction. An example is heat loss from a hot oil line buried underneath the ground. Heat conduction can also be simultaneously unsteady and multidimensional, for example, when a rectangular block forging is quenched.

In Chapter 2, each new analysis commenced with the application of the first law to an elemental volume to yield the governing differential equation. In Chapter 3, our approach will be different. We will derive a partial differential equation that governs the temperature distribution in a solid under very general conditions; we will then start each analysis by choosing the form of this equation appropriate to the problem under consideration. This **general heat conduction equation** is derived in Section 3.2, where boundary and initial conditions as well as solution methods are discussed. Solution methods are broadly divided into two groups: (1) classical mathematical methods, and (2) numerical methods. Classical mathematical methods are demonstrated in Section 3.3 for multidimensional steady conduction, and in Section 3.4 for unsteady conduction. In particular, the method of separation of variables is used, which leads to the need to construct Fourier series expansions. Section 3.5 introduces the analysis of a special class of conduction problems, in which there is a moving boundary—for example, solidification of ice from water. Numerical methods commonly used to solve the heat conduction equation include the finite-difference method, the finite-element method, and the boundary-element method. In Section 3.6, use of the finite-difference method is demonstrated for steady two-dimensional conduction, unsteady one-dimensional conduction, and a moving-boundary problem.

The classical mathematical methods used to solve the heat conduction equation might at first appear intimidating to the student. However, these methods rely on concepts normally studied in freshman- and sophomore-level mathematics courses, such as partial differentiation, integration, and second-order ordinary differential equations. Sufficient detail is given in the analyses for the student to proceed step by step without having to refer to a text on advanced engineering mathematics. Those students who have already had a junior- or senior-level engineering mathematics course should find the mathematics straightforward (and even perhaps old-fashioned!).

### 3.2 THE HEAT CONDUCTION EQUATION

---

In this section, the energy conservation principle and Fourier's law of heat conduction are used to derive various forms of the differential equation governing the temperature distribution in a stationary medium. The types of boundary and initial conditions encountered in practical problems are then discussed and classified. Finally, various methods available for solving the equation are introduced.



### 3.2.1 Fourier's Law as a Vector Equation

Chapter 2 used one-dimensional forms of Fourier's law of conduction. In general, the temperature in a body may vary in all three coordinate directions, which requires a more general form of Fourier's law. For simplicity, we will restrict our attention to *isotropic* media, for which the conductivity is the same in all directions. Most materials are isotropic. Exceptions include timber, which has different values of thermal conductivity  $k$  along and perpendicular to the grain, and pyrolytic graphite, for which the value of  $k$  can vary by an order of magnitude in different directions. For an isotropic medium, Fourier's law in terms of Cartesian coordinates is

$$q_x = -k \frac{\partial T}{\partial x}; \quad q_y = -k \frac{\partial T}{\partial y}; \quad q_z = -k \frac{\partial T}{\partial z} \quad (3.1)$$

where  $q_x$  is the component of the heat flux in the  $x$  direction,  $\partial T/\partial x$  is the *partial derivative* of  $T(x, y, z, t)$  with respect to  $x$ , and so on. As indicated in Fig. 3.1, Eq. (3.1) can be written more compactly in vector form as

$$\mathbf{q} = -k \nabla T \quad (3.2)$$

where  $\mathbf{q}$  is the conduction heat flux vector, and  $\nabla T$  is the gradient of the scalar temperature field. In Cartesian coordinates,

$$\mathbf{q} = \mathbf{i}q_x + \mathbf{j}q_y + \mathbf{k}q_z$$

$$\nabla T = \mathbf{i} \frac{\partial T}{\partial x} + \mathbf{j} \frac{\partial T}{\partial y} + \mathbf{k} \frac{\partial T}{\partial z}$$

where  $\mathbf{i}$ ,  $\mathbf{j}$ , and  $\mathbf{k}$  are the unit vectors in the  $x$ ,  $y$ , and  $z$  directions, respectively.

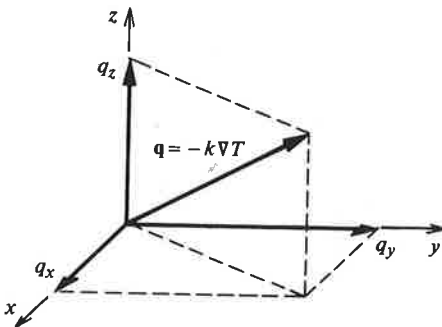


Figure 3.1 Vector representation of Fourier's law of heat conduction.

### 3.2.2 Derivation of the Heat Conduction Equation

The general heat conduction equation will first be derived in a Cartesian coordinate system. Subsequently, the result will be written in cylindrical and spherical coordinates.

### Derivation in Cartesian Coordinates

Figure 3.2 depicts an elemental volume  $\Delta x$  by  $\Delta y$  by  $\Delta z$  located in a solid. The energy conservation principle, Eq. (1.2), applied to the elemental volume as a closed system gives

$$\rho(\Delta x \Delta y \Delta z) c \frac{\partial T}{\partial t} = \dot{Q} + \dot{Q}_v \quad (3.3)$$

where the time derivative is a partial derivative, since  $T$  is also a function of the spatial coordinates  $x$ ,  $y$ , and  $z$ .

The term  $\dot{Q}$  represents heat transfer across the volume boundaries by conduction. The rate of heat inflow across the face at  $x$  is

$$q_x|_x \Delta y \Delta z$$

and the outflow across the face at  $x + \Delta x$  is

$$q_x|_{x+\Delta x} \Delta y \Delta z$$

The net inflow in the  $x$  direction is then

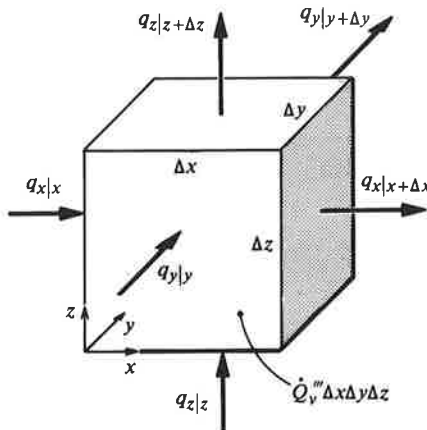
$$(q_x|_x - q_x|_{x+\Delta x}) \Delta y \Delta z$$

The outflow heat flux can be expanded in a Taylor series as

$$q_x|_{x+\Delta x} = q_x|_x + \frac{\partial q_x}{\partial x} \Delta x + \text{Higher-order terms}$$

Substituting and dropping the higher-order terms gives the net inflow in the  $x$  direction as

$$-\frac{\partial q_x}{\partial x} \Delta x \Delta y \Delta z$$



**Figure 3.2** Three-dimensional Cartesian elemental volume in a solid for derivation of the heat conduction equation.

Similar terms arise from conduction in the  $y$  and  $z$  directions. Thus, the net heat transfer into the volume by conduction is

$$\left( -\frac{\partial q_x}{\partial x} - \frac{\partial q_y}{\partial y} - \frac{\partial q_z}{\partial z} \right) \Delta x \Delta y \Delta z$$

The rate of generation of thermal energy within the volume  $\dot{Q}_v$  is simply

$$\dot{Q}_v''' \Delta x \Delta y \Delta z$$

where  $\dot{Q}_v'''$  [W/m<sup>3</sup>] is the rate of internal or volumetric heat generation introduced in Section 2.3.4. Substituting in Eq. (3.3) and dividing by  $\Delta x \Delta y \Delta z$  gives

$$\rho c \frac{\partial T}{\partial t} = - \left( \frac{\partial q_x}{\partial x} + \frac{\partial q_y}{\partial y} + \frac{\partial q_z}{\partial z} \right) + \dot{Q}_v'''$$

Introducing Fourier's law, Eq. (3.1), for  $q_x$ ,  $q_y$ , and  $q_z$ ,

$$\rho c \frac{\partial T}{\partial t} = \frac{\partial}{\partial x} \left( k \frac{\partial T}{\partial x} \right) + \frac{\partial}{\partial y} \left( k \frac{\partial T}{\partial y} \right) + \frac{\partial}{\partial z} \left( k \frac{\partial T}{\partial z} \right) + \dot{Q}_v'''$$
 (3.4)

Notice that the thermal conductivity  $k$  has been left inside the derivatives since, in general,  $k$  is a function of temperature. However, we usually simplify heat conduction analysis by taking  $k$  to be independent of temperature;  $k$  is then also independent of position, and Eq. (3.4) becomes

$$\rho c \frac{\partial T}{\partial t} = k \left( \frac{\partial^2 T}{\partial x^2} + \frac{\partial^2 T}{\partial y^2} + \frac{\partial^2 T}{\partial z^2} \right) + \dot{Q}_v'''$$
 (3.5)

When there is no internal heat generation,  $\dot{Q}_v''' = 0$ , and Eq. (3.5) reduces to

$$\frac{\partial T}{\partial t} = \alpha \left( \frac{\partial^2 T}{\partial x^2} + \frac{\partial^2 T}{\partial y^2} + \frac{\partial^2 T}{\partial z^2} \right)$$
 (3.6)

where  $\alpha \equiv k/\rho c$  [m<sup>2</sup>/s] is a thermophysical property of the material called the **thermal diffusivity**. Table 3.1 gives selected values of the thermal diffusivity. Additional data are given in Appendix A, as are values for  $k$ ,  $\rho$ , and  $c$ , from which  $\alpha$  can be calculated. Equation (3.6) is called **Fourier's equation** (or the *heat or diffusion equation*) and governs the temperature distribution  $T(x, y, z, t)$  in a solid. The relevance of the thermal diffusivity can be seen in Fourier's equation: when there is no internal heat generation, it is the only physical property that influences temperature changes in the solid. The thermal diffusivity is the ratio of thermal conductivity to a volumetric heat capacity: the larger  $\alpha$ , the faster temperature changes will propagate through the solid.

For a timewise steady state,  $\partial/\partial t = 0$ , and Eq. (3.5) reduces to *Poisson's equation*:

$$\frac{\partial^2 T}{\partial x^2} + \frac{\partial^2 T}{\partial y^2} + \frac{\partial^2 T}{\partial z^2} = -\frac{\dot{Q}_v'''}{k}$$
 (3.7)

**Table 3.1** Selected values of thermal diffusivity at 300 K (~25°C). (Other values may be calculated from the data given in Appendix A.)

Material	$\alpha$ m <sup>2</sup> /s × 10 <sup>6</sup>
Copper	112
Aluminum	84
Brass, 70% Cu, 30% Zn	34.2
Air at 1 atm pressure	22.5
Mild steel	18.8
Mercury	4.43
Stainless steel, 18-8	3.88
Fiberglass (medium density)	1.6
Concrete	0.75
Pyrex glass	0.51
Cork	0.16
Water	0.147
Engine oil, SAE 50	0.086
Neoprene rubber	0.079
White pine, perpendicular to grain	0.071
Refrigerant R-12	0.056
Polyvinylchloride (PVC)	0.051

Note: This table should be read as  $\alpha \times 10^6$  m<sup>2</sup>/s = Listed value; for example, for copper  $\alpha = 112 \times 10^{-6}$  m<sup>2</sup>/s.

Finally, for a steady state and no internal heat generation,  $\partial/\partial t = 0$ ,  $\dot{Q}_v''' = 0$ , so

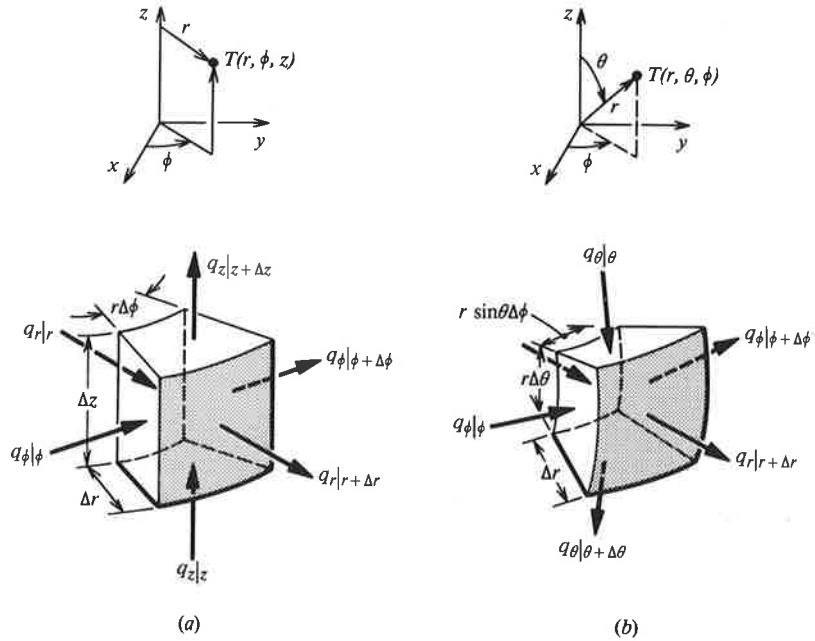
$$\frac{\partial^2 T}{\partial x^2} + \frac{\partial^2 T}{\partial y^2} + \frac{\partial^2 T}{\partial z^2} = 0 \quad (3.8)$$

which is **Laplace's equation**.

The Fourier, Poisson, and Laplace equations are *partial differential equations* and have been thoroughly studied by mathematicians [1,2,3]. They are important because each is the governing equation for many different physical phenomena in fields as diverse as heat conduction, mass diffusion, electrostatics, and fluid mechanics. Solutions of Laplace's equation are called *potential* or *harmonic* functions.

### Other Coordinate Systems

The solution of partial differential equations is simpler when boundary conditions are specified on *coordinate surfaces*, for example,  $x = \text{Constant}$  in the Cartesian coordinate system. Thus, for conduction problems in cylindrical or spherical bodies, the Cartesian coordinate system is inappropriate. Such problems require heat conduction equations in terms of the cylindrical and spherical coordinate systems shown in Fig. 3.3. We can proceed in a number of ways. The most direct approach



**Figure 3.3** (a) Cylindrical coordinate system,  $r$ ,  $\phi$ ,  $z$ , and an elemental volume. (b) Spherical coordinate system,  $r$ ,  $\theta$ ,  $\phi$ , and an elemental volume.

is to repeat our derivation using appropriate volume elements, as shown in Fig. 3.3. Alternatively, we can transform the equations already derived in Cartesian coordinates to cylindrical or spherical coordinates; Exercises 3-1, 3-2, and 3-4 illustrate these procedures. To present the results in compact form, we introduce the *del-squared* or *Laplacian operator*. In Cartesian coordinates,

$$\nabla^2 = \frac{\partial^2}{\partial x^2} + \frac{\partial^2}{\partial y^2} + \frac{\partial^2}{\partial z^2}$$

and Eq. (3.5) becomes

$$\rho c \frac{\partial T}{\partial t} = k \nabla^2 T + \dot{Q}_v''' \quad (3.9)$$

Writing the heat conduction equation in any coordinate system then simply requires the proper expression for  $\nabla^2$ . For cylindrical coordinates  $r$ ,  $\phi$ ,  $z$ ,

$$\nabla^2 = \frac{1}{r} \frac{\partial}{\partial r} \left( r \frac{\partial}{\partial r} \right) + \frac{1}{r^2} \frac{\partial^2}{\partial \phi^2} + \frac{\partial^2}{\partial z^2} \quad (3.10)$$

For spherical coordinates  $r, \theta, \phi$ ,

$$\nabla^2 = \frac{1}{r^2} \frac{\partial}{\partial r} \left( r^2 \frac{\partial}{\partial r} \right) + \frac{1}{r^2 \sin \theta} \frac{\partial}{\partial \theta} \left( \sin \theta \frac{\partial}{\partial \theta} \right) + \frac{1}{r^2 \sin^2 \theta} \frac{\partial^2}{\partial \phi^2} \quad (3.11)$$

Two additional useful relations are

$$\frac{1}{r} \frac{\partial}{\partial r} \left( r \frac{\partial}{\partial r} \right) = \frac{\partial^2}{\partial r^2} + \frac{1}{r} \frac{\partial}{\partial r} \quad (3.12a)$$

$$\frac{1}{r^2} \frac{\partial}{\partial r} \left( r^2 \frac{\partial}{\partial r} \right) = \frac{\partial^2}{\partial r^2} + \frac{2}{r} \frac{\partial}{\partial r} \quad (3.12b)$$

As a final comment regarding the heat conduction equation, it is noted that Fourier's law, Eq. (3.2), is a vector equation; thus, the heat conduction equation is most efficiently derived using the methods of vector calculus. Such a derivation is required as Exercise 3-3.

### 3.2.3 Boundary and Initial Conditions

In solving heat conduction problems in Chapters 1 and 2, boundary and initial conditions were used to evaluate integration constants. We now classify the types of boundary and initial conditions required to solve heat conduction problems.

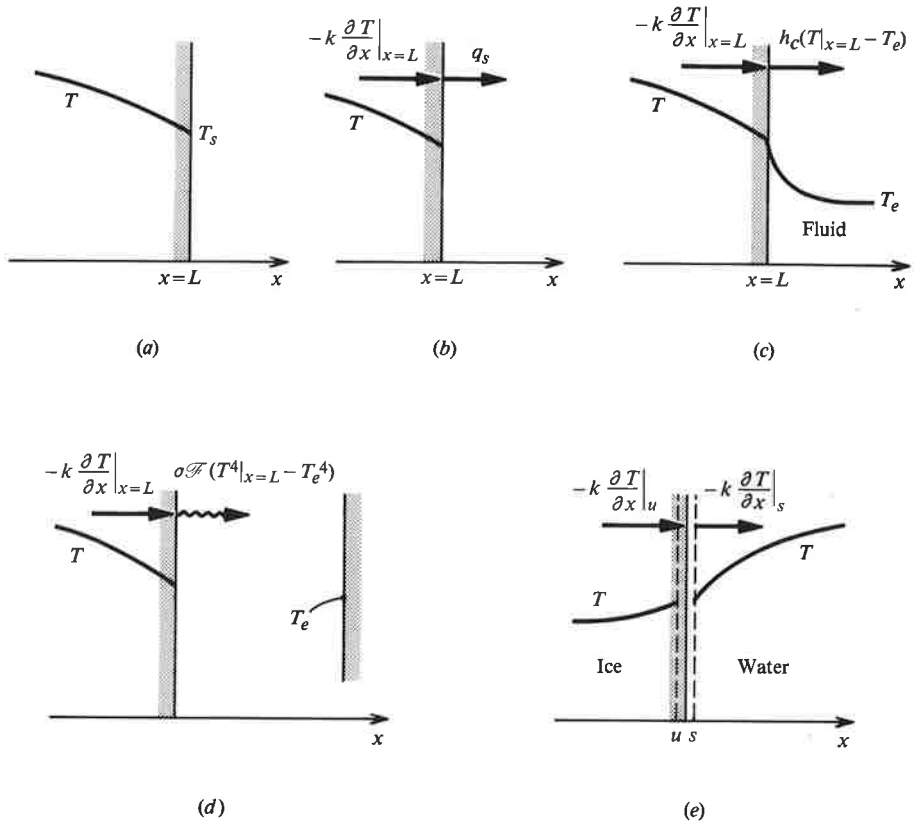
#### *Boundary Conditions*

In Chapters 1 and 2, it was shown how practical heat conduction problems involve adjacent regions that may be quite different. For example, in Example 2.4, a uranium oxide nuclear fuel rod is enclosed in a Zircaloy-4 sheath and cooled by flowing water. Heat is generated within the fuel and flows by conduction to the fuel-sheath interface, by conduction across the sheath to the sheath-water interface, and by convection into the water. To analyze such problems, it is necessary to specify thermal conditions at solid-solid and solid-liquid interfaces. In general, it is required that both the heat flux and the temperature be continuous across an interface (although when a contact resistance model is used, as described in Section 2.2.2, the effect is to have a discontinuity in temperature). Thus, the solutions of the heat conduction equation in each region are *coupled*.

When analyzing more difficult heat transfer problems, we often find it convenient to uncouple the regions and consider each region independently. The boundary condition is then simply one of specified temperature. Considering the coordinate surface  $x = L$  and referring to Fig. 3.4a,

$$T|_{x=L} = T_s \quad (3.13)$$

which is called a **first-kind** or **Dirichlet** boundary condition.



**Figure 3.4** Types of boundary conditions. (a) First kind, or Dirichlet. (b) Second kind, or Neumann. (c) Third kind, or mixed. (d) Fourth kind, or radiation. (e) Phase change.

Sometimes it is convenient to apply a boundary condition at a surface where the heat flux is known. Referring to Fig. 3.4*b*,

$$-k \left. \frac{\partial T}{\partial x} \right|_{x=L} = q_s \quad (3.14)$$

which is called a **second-kind** or **Neumann** boundary condition. Often the known heat flux is zero, such as at a plane of symmetry, or approximately zero, such as when the adjoining region is a good insulator.

Another commonly encountered situation is one in which the adjacent region is a fluid and we wish to describe heat transfer to the fluid using Newton's law of cooling. Referring to Fig. 3.4*c*,

$$-k \left. \frac{\partial T}{\partial x} \right|_{x=L} = h_c (T|_{x=L} - T_e) \quad (3.15)$$

which is the **third-kind** or **mixed** boundary condition. Notice that Eq. (3.15) involves both the value of the dependent variable and that of its derivative at the boundary. Similarly, if there is heat loss by thermal radiation into adjacent surroundings (see Fig. 3.4*d*), using Eq. (1.17),

$$-k \left. \frac{\partial T}{\partial x} \right|_{x=L} = \sigma \mathcal{F} (T|_{x=L}^4 - T_e^4) \quad (3.16)$$

which is a **fourth-kind** or **radiation** boundary condition.<sup>1</sup> (Note, however, that some texts refer to the third-kind boundary condition as a radiation boundary condition, a practice with historical precedent but preferably avoided.)

There are other, more complex boundary conditions encountered in practice. The contact resistance described in Section 2.2.2 is one example. Another example is when there is a change of phase at the interface, such as ice melting or steam condensing. Figure 3.4*e* represents the surface of a block of ice melting in warm water. The *s*- and *u*-surfaces are on either side and infinitesimally close to the actual water-ice interface. Thus, the *s*-surface is in water, and the *u*-surface is in solid ice. Only the temperature is the same at the *s*- and *u*-surfaces; in general, the physical properties and temperature gradients are different. If the ice is melting at a rate per unit area  $\dot{m}''$  [kg/m<sup>2</sup> s] and the interface is imagined to be fixed in space, then ice flows toward the interface, and water flows away at the melting rate. Application of the steady-flow energy equation to the control volume bounded by the *u*- and *s*-surfaces gives

$$\dot{m}''(h_s - h_u) = -k \left. \frac{\partial T}{\partial x} \right|_u - \left( -k \left. \frac{\partial T}{\partial x} \right|_s \right) \quad (3.17)$$

for  $\dot{m}''$  positive. Equation (3.17) can be rearranged as

$$k \left. \frac{\partial T}{\partial x} \right|_s = k \left. \frac{\partial T}{\partial x} \right|_u + \dot{m}'' h_{fs} \quad (3.18)$$

where  $h_{fs} = h_s - h_u$  is the enthalpy of fusion of the ice. Equation (3.18) can be interpreted as stating that the heat conducted from the warm water to the interface must balance both the heat conducted away from the interface into the cold ice and the heat required to melt the ice.

### Initial Conditions

Transient heat conduction problems usually require specification of an **initial condition**, which simply means that the temperature throughout the region must be known at some instant in time before its subsequent variation with time can be

<sup>1</sup> This simple form is strictly valid only when the surroundings are isothermal and have a uniform emittance. More general situations are treated in Chapter 6.



determined. An exception is when the temperature varies periodically, for example, conduction in a spacecraft orbiting the earth. Then a periodic condition must be imposed on the solution.

### 3.2.4 Solution Methods

During the 19th century, considerable progress was made in developing mathematical methods for solving the various forms of the heat conduction equation. The first major contribution was by J. Fourier. His book, published in 1822 [4], developed the use of the method of **separation of variables**, which leads to the need to express an arbitrary function in a **Fourier series expansion**. Subsequently, **transform methods**—particularly the use of the *Laplace transform*—as well as other methods of classical mathematics were widely used. The treatise on heat conduction by Carslaw and Jaeger [5] contains an extensive compilation of solutions obtained using classical mathematical methods. Use of these methods usually requires that (1) the bounding surfaces be of relatively simple shape, (2) the boundary conditions be of simple mathematical form, and (3) the thermophysical properties be constant. Notwithstanding these limitations, many analytical results have wide engineering utility. Analytical solutions are useful benchmarks for checking the accuracy of numerical methods of solution. Also, the exercise of obtaining an analytical solution gives valuable insight into the essential features of heat transfer by conduction.

More recently, numerical methods, including **finite-difference** and **finite-element** methods, have been developed that allow solutions to be easily obtained for problems involving unusual shapes, complicated boundary conditions, and variable thermophysical properties. An early example was the application of the numerical *relaxation* method to steady heat conduction by H. Emmons in 1943 [6]. However, with the advent of the modern high-speed computer in the 1960s, numerical methods have been greatly improved. The wide availability of the personal computer in the 1980s has led to the marketing of versatile computer programs. These can be used to solve a great variety of heat conduction problems without requiring the user to have detailed knowledge of the numerical methods involved.

Some other methods have been used to obtain solutions to heat conduction problems. Two graphical methods, the *flux plotting* method and the *Schmidt plot*, are described in some heat transfer texts. The first is used for steady two-dimensional conduction and involves the free-hand sketching of isotherms and lines of heat flow; the latter is used for transient conduction and is the graphical equivalent to a finite-difference numerical method. A number of *analog* methods have also been used. Since Laplace's equation also governs electrical potential fields, two-dimensional steady conduction problems have been solved by making voltage and current measurements in appropriate shapes cut out of graphite-coated paper of high electrical resistance [7]. Before digital computers were developed, the analog computer or "differential analyzer" was used to solve heat conduction problems [8].

Methods of mathematical analysis are demonstrated in Sections 3.3 through 3.5, and finite-difference methods are dealt with in Section 3.6.

### 3.3 MULTIDIMENSIONAL STEADY CONDUCTION

One-dimensional steady conduction was dealt with in Chapter 2. Although the simple analytical results obtained are very useful, they have obvious limitations. Often the heat flow is multidimensional, that is, in two or three directions. For example, consider the furnace shown in Fig. 3.5. If the insulation is thin compared to the furnace dimensions, the assumption of one-dimensional heat flow is adequate (see Example 1.1). High-temperature furnaces, however, require thick insulation to reduce heat loss; in these furnaces, the heat flow through the edges is two-dimensional, and through the corners it is three-dimensional. Multidimensional steady conduction with no internal heat generation is governed by Laplace's equation. The classical approach to solving Laplace's equation is the *separation of variables* method; Section 3.3.1 uses a simple two-dimensional problem to demonstrate this approach. Often we are concerned with conduction between two isothermal surfaces, all other surfaces present being adiabatic. A **conduction shape factor** can be defined for such configurations, and a compilation of useful shape factors is given in Section 3.3.3.

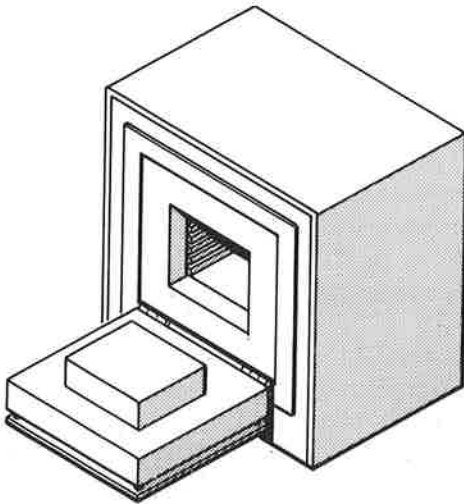


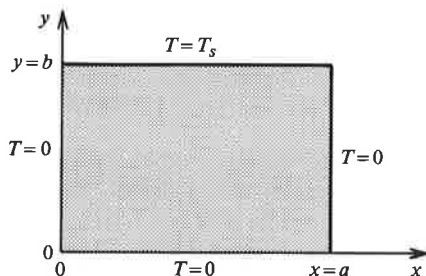
Figure 3.5 An insulated furnace.

#### 3.3.1 Steady Conduction in a Rectangular Plate

The relatively simple problem of two-dimensional steady heat conduction in a rectangular plate will be used to demonstrate the method of separation of variables for solving Laplace's equation.

##### *The Governing Equation and Boundary Conditions*

Figure 3.6 depicts a thin rectangular plate with negligible heat loss from its surface. Temperature variations across the plate in the  $z$  direction are assumed to be zero ( $\partial^2 T / \partial z^2 = 0$ ), and the thermal conductivity is assumed to be constant.



**Figure 3.6** Boundary conditions for two-dimensional steady conduction in a rectangular plate.

The temperature distribution  $T(x, y)$  is then governed by the two-dimensional form of Laplace's equation:

$$\frac{\partial^2 T}{\partial x^2} + \frac{\partial^2 T}{\partial y^2} = 0 \quad (3.19)$$

To demonstrate the method of solution, we will first consider a model problem and later demonstrate how our solution can also be used to construct solutions for practical situations. Thus, we choose the boundary conditions shown in Fig. 3.6, namely,

$$\begin{aligned} x=0, \quad 0 < y < b: \quad T=0 \\ y=0, \quad 0 < x < a: \quad T=0 \end{aligned} \quad (3.20a)$$

$$\begin{aligned} x=a, \quad 0 < y < b: \quad T=0 \\ y=b, \quad 0 < x < a: \quad T=T_s \end{aligned} \quad (3.20b)$$

The zero values for the boundary conditions, Eqs. (3.20a), will simplify the problem without loss of generality. Such boundary conditions are *homogeneous*. In general, a differential equation or boundary condition is said to be homogeneous if a constant times a solution is also a solution, that is, if  $T_1$  is a solution,  $CT_1$  is also a solution. The boundary condition Eq. (3.20b) looks simple, but we shall see that it actually makes solution of the problem quite difficult.

### *Solution for the Temperature Distribution*

To use the method of separation of variables, we first assume that the function  $T(x, y)$  can be expressed as the product of a function of  $x$  only,  $X(x)$ , and a function of  $y$  only,  $Y(y)$ :

$$T(x, y) = X(x)Y(y) \quad (3.21)$$

Substitution in Eq. (3.19) gives

$$Y \frac{d^2 X}{dx^2} + X \frac{d^2 Y}{dy^2} = 0$$

where total derivatives have replaced the partial derivatives, since  $X$  is a function of independent variable  $x$  only, and  $Y$  is a function of independent variable  $y$  only.

Rearranging,

$$-\frac{1}{X} \frac{d^2 X}{dx^2} = \frac{1}{Y} \frac{d^2 Y}{dy^2} \quad (3.22)$$

Since each side of Eq. (3.22) is a function of a single independent variable, the equality can hold only if both sides are equal to a constant, which can be positive, negative, or zero. Using hindsight, the constant will be chosen to be a positive number  $\lambda^2$ . The reason for this choice will be discussed later. Two ordinary differential equations are thus obtained,

$$\frac{d^2 X}{dx^2} + \lambda^2 X = 0 \quad \frac{d^2 Y}{dy^2} - \lambda^2 Y = 0$$

which have the solutions

$$X = B \cos \lambda x + C \sin \lambda x \quad Y = D e^{-\lambda y} + E e^{\lambda y}$$

Substituting in Eq. (3.21) gives a tentative solution for  $T(x, y)$ :

$$T(x, y) = (B \cos \lambda x + C \sin \lambda x)(D e^{-\lambda y} + E e^{\lambda y}) \quad (3.23)$$

Applying boundary conditions Eqs. (3.20a) and taking care to ensure that the  $x$ - and  $y$ -dependences remain,

$$x = 0: \quad B(D e^{-\lambda y} + E e^{\lambda y}) = 0; \quad \text{thus, } B = 0$$

$$y = 0: \quad C \sin \lambda x (D + E) = 0; \quad \text{thus, } E = -D$$

$$x = a: \quad CD \sin \lambda a (e^{-\lambda y} - e^{\lambda y}) = -2CD \sin \lambda a \sinh \lambda y = 0$$

This requires that  $\sin \lambda a = 0$ , which has the roots  $\lambda_n = n\pi/a$ , for  $n = 0, 1, 2, 3, \dots$ . These values of  $\lambda$  are called the **eigenvalues** or *characteristic values* of the problem. There is a distinct solution for each eigenvalue, each with its own constant. Writing the constant  $-2CD$  for the  $n$ th solution as  $A_n$ ,

$$T_n(x, y) = A_n \sin \frac{n\pi x}{a} \sinh \frac{n\pi y}{a}; \quad n = 0, 1, 2, 3, \dots \quad (3.24)$$

Equation (3.19) is a *linear* differential equation, so its general solution is a sum of the series of solutions given by Eq. (3.24):

$$T(x, y) = \sum_{n=1}^{\infty} A_n \sin \frac{n\pi x}{a} \sinh \frac{n\pi y}{a} \quad (3.25)$$

where the solution for  $n = 0$  has been deleted since  $\sinh 0 = 0$ . We now apply the last boundary condition, Eq. (3.20b), which requires that at  $y = b$ ,

$$T|_{y=b} = T_s = \sum_{n=1}^{\infty} A_n \sin \frac{n\pi x}{a} \sinh \frac{n\pi b}{a} \quad (3.26)$$

that is, the constant  $T_s$  must be expressed in terms of an infinite series of sine functions, or a *Fourier series*.

**Construction of a Fourier Series Expansion**

In general, the temperature distribution along the boundary  $y = b$  will be some arbitrary function  $f(x)$ , and the required expansion is then

$$f(x) = \sum_{n=1}^{\infty} C_n \sin \frac{n\pi x}{a}; \quad C_n = A_n \sinh \frac{n\pi b}{a} \quad (3.27)$$

The constants  $C_n$  are determined as follows. Multiply Eq. (3.27) by  $\sin n\pi x/a$ , and integrate term by term from  $x = 0$  to  $x = a$ :

$$\begin{aligned} \int_0^a f(x) \sin \frac{n\pi x}{a} dx &= \int_0^a C_1 \sin \frac{\pi x}{a} \sin \frac{n\pi x}{a} dx + \cdots + \int_0^a C_n \sin^2 \left( \frac{n\pi x}{a} \right) dx \\ &+ \cdots + \int_0^a C_m \sin \frac{m\pi x}{a} \sin \frac{n\pi x}{a} dx + \cdots \end{aligned} \quad (3.28)$$

Using standard integral tables, we find:

$$\begin{aligned} \int_0^a \sin \frac{n\pi x}{a} \sin \frac{m\pi x}{a} dx &= \left[ \frac{\sin(n\pi x/a - m\pi x/a)}{2(n\pi/a - m\pi/a)} - \frac{\sin(n\pi x/a + m\pi x/a)}{2(n\pi/a + m\pi/a)} \right]_0^a \\ &= 0 \text{ for } n \neq m \end{aligned}$$

$$\int_0^a \sin^2 \left( \frac{n\pi x}{a} \right) dx = \frac{a}{2n\pi} \left[ \frac{n\pi x}{a} - \frac{1}{2} \sin \frac{2n\pi x}{a} \right]_0^a = \frac{a}{2}$$

Thus, only the  $n$ th term on the right-hand side of Eq. (3.28) remains, and solving for  $C_n$  gives

$$C_n = \frac{2}{a} \int_0^a f(x) \sin \frac{n\pi x}{a} dx \quad (3.29)$$

The set of sine functions  $\sin \pi x/a, \sin 2\pi x/a, \dots, \sin n\pi x/a, \dots$  is said to be **orthogonal** over the interval  $0 \leq x \leq a$ , because the integral of  $\sin m\pi x/a \sin n\pi x/a$  is zero if  $m \neq n$ . As shown in texts on applied mathematics [2,3], if the function  $f(x)$  is piecewise continuous, it can always be expressed in terms of a uniformly converging series of orthogonal functions. The cosine function is also orthogonal over an appropriate interval, as are many other functions, including Bessel functions and Legendre polynomials.

**Temperature Distribution for  $f(x) = T_s$** 

For the function  $f(x)$  equal to a constant value  $T_s$ , the integral in Eq. (3.29) can be evaluated analytically:

$$C_n = \frac{2}{a} \left[ -\frac{T_s a}{n\pi} \cos \frac{n\pi x}{a} \right]_0^a = T_s \frac{2}{n\pi} [1 - (-1)^n]$$

and from Eq. (3.27),

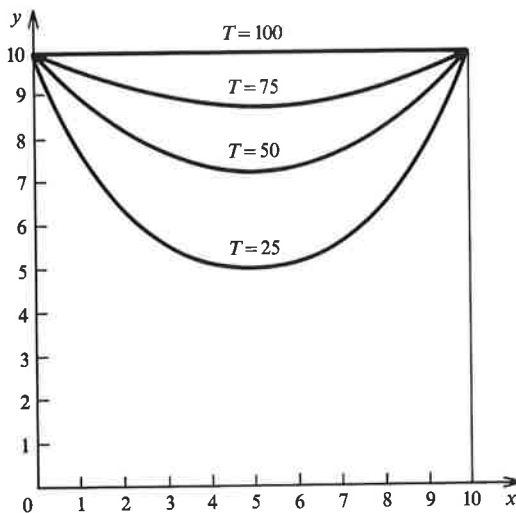
$$A_n = \frac{C_n}{\sinh(n\pi b/a)} = T_s \frac{2[1 - (-1)^n]}{n\pi \sinh(n\pi b/a)}$$

Substituting into Eq. (3.25) gives the desired temperature distribution for steady conduction in a rectangular plate:

$$T(x, y) = T_s \sum_{n=1}^{\infty} \frac{2[1 - (-1)^n]}{n\pi \sinh(n\pi b/a)} \sin \frac{n\pi x}{a} \sinh \frac{n\pi y}{a} \quad (3.30)$$

Lines of constant temperature, or *isotherms*, are shown in Fig. 3.7. The temperature discontinuities at the top corners are physically unrealistic since an infinite heat flow is implied. In fact, the heat flow across the plate edge at  $y = b$ , evaluated from Eq. (3.30) using Fourier's law, is infinite. Thus, the isotherms in the vicinity of these corners correspond to a mathematical problem only; in real physical problems, there might be a very marked variation in temperature along the edges near these corners, but there cannot be an actual discontinuity.

Since the variables in the partial differential equation, Eq. (3.19), did separate, and because a solution could be found to satisfy the boundary conditions, the method of solution has been successful. If a negative constant is chosen for Eq. (3.22), the boundary conditions cannot be satisfied. Use of a negative constant just reverses the roles of the independent variables  $x$  and  $y$ , and the negative constant is appropriate if the temperature  $T_s$  is specified on the edge  $x = a$ .



**Figure 3.7** Isotherms for conduction in a rectangular plate obtained from Eq. (3.30);  $a = b = 10$ ,  $T_s = 100$ .

### Generalization Using the Principle of Superposition

Laplace's equation is a *linear* differential equation. A useful consequence of this property is that the solution of a problem with complicated boundary conditions can be constructed by adding solutions for problems having simpler boundary conditions.

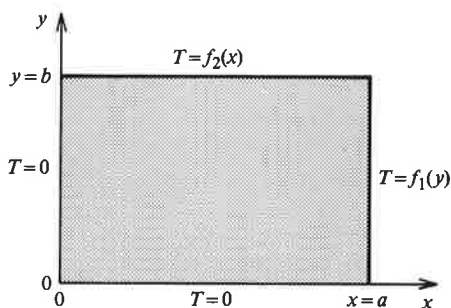
To illustrate the procedure, consider a problem where the plate temperature is specified along two edges. If the boundary conditions Eqs. (3.20) are replaced by those shown in Fig. 3.8,

$$\begin{aligned}x = 0, \quad 0 < y < b: \quad T &= 0 \\y = 0, \quad 0 < x < a: \quad T &= 0 \\x = a, \quad 0 < y < b: \quad T &= f_1(y) \\y = b, \quad 0 < x < a: \quad T &= f_2(x)\end{aligned}$$

the *superposition principle* can be used as follows. Let  $T(x, y) = T_1(x, y) + T_2(x, y)$ , where  $T_1$  and  $T_2$  satisfy

$$\begin{aligned}\frac{\partial^2 T_1}{\partial x^2} + \frac{\partial^2 T_1}{\partial y^2} &= 0 & \frac{\partial^2 T_2}{\partial x^2} + \frac{\partial^2 T_2}{\partial y^2} &= 0 \\x = 0, y = 0, y = b: T_1 &= 0 & x = 0, y = 0, x = a: T_2 &= 0 \\x = a: T_1 &= f_1(y) & y = b: T_2 &= f_2(x)\end{aligned}$$

Addition of the equations and boundary conditions shows that  $T = T_1 + T_2$  satisfies the original problem. Clearly, this approach can be extended to a problem where the temperature is specified on three or all four sides.



**Figure 3.8** Rectangular plate with nonhomogeneous boundary conditions specified on two edges.

### EXAMPLE 3.1 Heat Flow across a Neoprene Rubber Pad

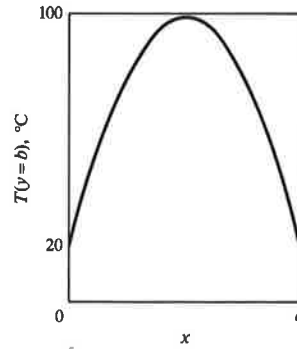
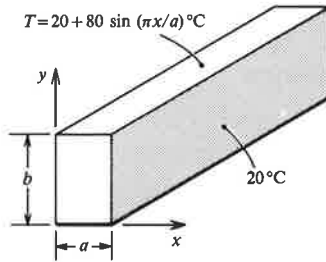
A long neoprene rubber pad of width  $a = 2$  cm and height  $b = 4$  cm is a component of a spacecraft structure. Its sides and bottom are bonded to a metal channel at temperature  $T_e = 20^\circ\text{C}$ , and the temperature distribution along the top can be approximated as a simple sine curve,  $T = T_e + T_m \sin(\pi x/a)$ , where  $T_m = 80$  K. Determine the heat flow across the pad per meter length.

#### Solution

**Given:** Long rubber pad with a rectangular cross section.

**Required:** Heat flow across pad for given boundary conditions.

**Assumptions:** Two-dimensional, steady conduction.



Conservation of energy requires that at steady state, the heat flow across the top surface equal the heat flow out across the sides and bottom; thus,

$$\dot{Q} = (1) \int_0^a q_y|_{y=b} dx = \int_0^a -k \frac{\partial T}{\partial y} \Big|_{y=b} dx$$

The sides and bottom of the pad can be taken to have a temperature of 20°C. Thus,  $T$  is the solution of Laplace's equation that satisfies the boundary conditions

$$x = 0, x = a, y = 0: T = T_e$$

$$y = b: T = T_e + T_m \sin \frac{\pi x}{a}$$

Let  $T_1 = T - T_e$ ; then  $T_1$  satisfies the boundary conditions

$$x = 0, x = a, y = 0: T_1 = 0$$

$$y = b: T_1 = T_m \sin \frac{\pi x}{a}$$

Equation (3.25) satisfies the homogeneous boundary conditions. Applying the boundary condition at  $y = b$  gives

$$T_1|_{y=b} = T_m \sin \frac{\pi x}{a} = \sum_{n=1}^{\infty} A_n \sin \frac{n\pi x}{a} \sinh \frac{n\pi b}{a}$$

which can be satisfied if

$$A_1 = \frac{T_m}{\sinh(\pi b/a)}; \quad A_2 = A_3 = \dots = 0$$

That is, only the first term of the infinite series is required. Hence,

$$T - T_e = T_1 = T_m \sin \frac{\pi x}{a} \frac{\sinh(\pi y/a)}{\sinh(\pi b/a)}$$

$$\frac{\partial T}{\partial y} \Big|_{y=b} = T_m \frac{(\pi/a) \sin(\pi x/a)}{\tanh(\pi b/a)}$$



$$\dot{Q} = \int_0^a -k \frac{\partial T}{\partial y} \Big|_{y=b} dx = \frac{T_m k}{\tanh(\pi b/a)} (\cos \pi - \cos 0) = -\frac{2T_m k}{\tanh(\pi b/a)} \text{ W/m}$$

For  $T_m = 80 \text{ K}$ ,  $k = 0.19 \text{ W/m K}$  (Table A.2), and  $b/a = 2.0$ , the heat flow is

$$\dot{Q} = -\frac{(2)(80)(0.19)}{\tanh 2\pi} = -\frac{30.4}{1.0000} = -30.4 \text{ W/m}$$

### Comments

Notice that in the limit of large  $b/a$ ,  $\tanh \pi b/a \rightarrow 1$  and  $\dot{Q}$  is independent of  $b/a$ ; even for a square pad,  $b/a = 1$ ,  $\tanh \pi = 0.996$ . In the opposite limit of  $b/a \rightarrow 0$ , we can use the expansion  $\tanh x = x - x^3/3 + \dots$  to obtain

$$\dot{Q} = -\frac{2T_m k a}{\pi b} = -\frac{(2)(80)(0.19)(0.02)}{(\pi)(0.04)} = -4.83 \text{ W/m}$$

which is the result for one-dimensional heat flow across a thin wall. For a 1 m length of pad,

$$\begin{aligned} \dot{Q} &= \int_0^a q dx = -\int_0^a \frac{k}{b} \left( T_e + T_m \sin \frac{\pi x}{a} - T_e \right) dx \\ &= -\frac{k T_m}{b} \int_0^a \sin \frac{\pi x}{a} dx = -\frac{2T_m k a}{\pi b} \end{aligned}$$

which agrees with the result obtained above.

### 3.3.2 Steady Conduction in a Rectangular Block

Consider a rectangular block with boundary conditions, which cause the temperature to vary in all three coordinate directions,  $x$ ,  $y$ , and  $z$ . For an assumed constant thermal conductivity, the temperature distribution  $T(x, y, z)$  is governed by the three-dimensional form of Laplace's equation:

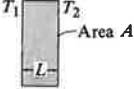
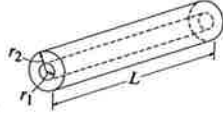

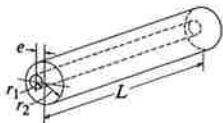
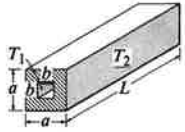
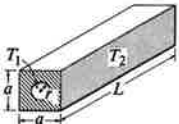
$$\frac{\partial^2 T}{\partial x^2} + \frac{\partial^2 T}{\partial y^2} + \frac{\partial^2 T}{\partial z^2} = 0 \quad (3.31)$$

Again the method of separation of variables can be used and  $T(x, y, z)$  taken to have the form

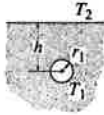
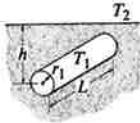
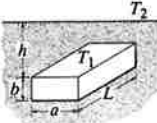
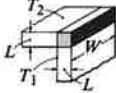
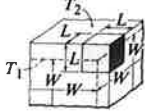

$$T(x, y, z) = X(x)Y(y)Z(z)$$

The analysis proceeds as for the rectangular plate in Section 3.3.1, but the mathematics is very cumbersome, even for the simplest of boundary conditions. In practice, one cannot expect a simple behavior of the boundary conditions over a three-dimensional object, and the numerical methods of solution described in Section 3.6 are more appropriate than analytical methods.

**Table 3.2** Shape factors for steady-state conduction for use in Eq. (3.32),  $\dot{Q} = kS\Delta T$ ;  $\Delta T = T_1 - T_2$ . (See also the bibliography for Chapter 3.)

Configuration	Shape Factor
1. Plane wall 	$\frac{A}{L}$
2. Concentric cylinders  <p style="text-align: center;"><math>L \gg r_2</math></p>	$\frac{2\pi L}{\ln(r_2/r_1)}$ <p>Note there is no steady-state solution for <math>r_2 \rightarrow \infty</math>, i.e., for a cylinder in an infinite medium.</p>
3. Concentric spheres 	(a) $\frac{4\pi}{1/r_1 - 1/r_2}$ (b) $4\pi r_1$ for $r_2 \rightarrow \infty$
4. Eccentric cylinders  <p style="text-align: center;"><math>L \gg r_2</math></p>	$\frac{2\pi L}{\cosh^{-1}\left(\frac{r_2^2 + r_1^2 - e^2}{2r_1 r_2}\right)}$
5. Concentric square cylinders  <p style="text-align: center;"><math>L \gg a</math></p>	$\frac{2\pi L}{0.93 \ln(a/b) - 0.0502} \quad \text{for } \frac{a}{b} > 1.4$ $\frac{2\pi L}{0.785 \ln(a/b)} \quad \text{for } \frac{a}{b} < 1.4$
6. Concentric circular and square cylinders 	$\frac{2\pi L}{\ln(0.54a/r)} \quad a > 2r$

**Table 3.2** (Concluded)

Configuration	Shape Factor
7. Buried sphere	$\frac{4\pi r_1}{1 - r_1/2h}$
	For $h \rightarrow \infty$ , the result for item 3(b) is recovered
Medium at infinity also at $T_2$	
8. Buried cylinder	$\frac{2\pi L}{\cosh^{-1}(h/r_1)}$
	$\frac{2\pi L}{\ln(2h/r_1)} \quad \text{for } h > 3r_1$
Medium at infinity also at $T_2$	$L \gg r_1$
9. Buried rectangular beam	$2.756L \left[ \ln \left( 1 + \frac{h}{a} \right) \right]^{-0.59} \left( \frac{h}{b} \right)^{-0.078}$
	
Medium at infinity also at $T_2$	$L \gg h, a, b$
10. The edge of adjoining walls	$0.54W \quad \text{for } W > L/5$ <p>(<math>W</math> is the inner edge)</p>
	
11. The corner of three adjoining walls	$0.15L \quad \text{for } W > L/5$
	
12. Disk area on the adiabatic surface of a semi-infinite solid	$4r$
	
Medium at infinity at $T_2$	

### 3.3.3 Conduction Shape Factors

Many multidimensional conduction problems involve heat flow between two surfaces, each of uniform temperature, with any other surfaces present being adiabatic. The conduction *shape factor*,  $S$ , is defined such that the heat flow between the surfaces,  $\dot{Q}$ , is

$$\dot{Q} = kS\Delta T \quad (3.32)$$

where  $k$  is the thermal conductivity and  $\Delta T$  is the difference in surface temperatures;  $S$  is seen to have the dimensions of length. The results we have already obtained for one-dimensional conduction can also be expressed in terms of the shape factor. For example, a plane slab of area  $A$  and thickness  $L$  has  $S = A/L$  from Eq. (1.9). Table 3.2 lists shape factors for various configurations.

Some points to note when using Table 3.2 are:

1. There is no internal heat generation:  $\dot{Q}_v''' = 0$ .
2. The thermal conductivity,  $k$ , is constant.
3. The two surfaces should be isothermal. If these temperatures are not prescribed, but are intermediate temperatures in a series thermal circuit, the isothermal condition may not be satisfied. The surfaces will generally be isothermal when the component in question has the dominant thermal resistance. Example 3.3 illustrates this point.
4. Special care must be taken with the configurations involving an infinite medium. For example, in item 7, not only the plane surface but also the medium at infinity must be at temperature  $T_2$ .
5. Item 8 is often used incorrectly for calculating heat loss or gain from buried pipelines. It is essential that the deep soil be at the same temperature as the surface, which is a condition seldom met in reality. Also, the buried pipeline problem often involves transient conduction.
6. The shape factors given in items 10 and 11 were developed by the physicist I. Langmuir and coworkers in 1913 for calculating the heat loss from furnaces. Example 3.2 illustrates their use.

---

#### EXAMPLE 3.2 Heat Loss from a Laboratory Furnace

A small laboratory furnace is in the form of a cube and is insulated with a 10 cm layer of fiberglass insulation, with an inside edge 30 cm long. If the only significant resistance to heat flow across the furnace wall is this insulation, determine the power required for steady operation at a temperature of 600 K when the outer casing temperature is 350 K. The thermal conductivity of the fiberglass insulation at the mean temperature of 475 K is approximately 0.11 W/m K.

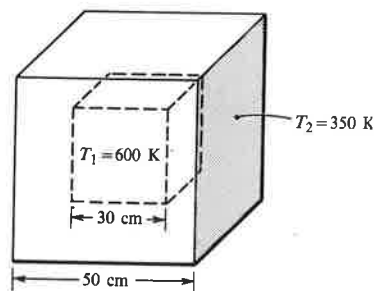
**Solution**

**Given:** Insulated laboratory furnace.

**Required:** Power required for operation at 600 K.

**Assumptions:** 1. Steady state.  
2. The outer convective resistance is negligible.

The shape factors given as items 1, 10, and 11 of Table 3.2 should be used, assuming independent parallel paths for heat flow through the 6 sides, 12 edges, and 8 corners of the enclosure. Thus, if  $L$  is the insulation thickness and  $W$  the inside edge,



$$\begin{aligned}\dot{Q} &= k\Delta T S \\ &= k(T_1 - T_2)[6W^2/L + (12)(0.54)W + (8)(0.15)L] \\ &= (0.11)(600 - 350)[(6)(0.3)^2/(0.1) + (12)(0.54)(0.3) + (8)(0.15)(0.1)] \\ &= (0.11)(250)[5.40 + 1.94 + 0.12] \\ &= 205 \text{ W}\end{aligned}$$

**Comments**

If an effective area for heat flow  $A_{\text{eff}}$  is defined by the equation for one-dimensional heat flow,

$$\dot{Q} = \frac{kA_{\text{eff}}(T_1 - T_2)}{L}$$

then  $A_{\text{eff}} = 6W^2 + (12)(0.54)WL + (8)(0.15)L^2 = 0.746 \text{ m}^2$ . Notice that  $A_{\text{eff}}$  is significantly less than either the arithmetic average of the inner and outer areas,  $1.02 \text{ m}^2$ , or the value midway through the wall,  $0.96 \text{ m}^2$ .

**EXAMPLE 3.3 Heat Loss from a Buried Oil Line**

An oil pipeline has an outside diameter of 30 cm and is buried with its centerline 1 m below ground level in damp soil. The line is 5000 m long, and the oil flows at 2.5 kg/s. If the inlet temperature of the oil is 120°C and the ground level soil is at 23°C, estimate the oil outlet temperature and the heat loss (i) for an uninsulated pipe, and (ii) if the pipe is insulated with a 15 cm layer of insulation with conductivity  $k = 0.03 \text{ W/m K}$ . Take the soil thermal conductivity as 1.5 W/m K and the oil specific heat as 2000 J/kg K.

**Solution**

**Given:** Buried oil pipeline.

**Required:** Oil outlet temperature and heat loss if (i) uninsulated, (ii) insulated.

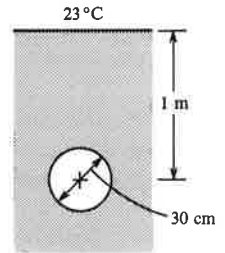
- Assumptions:**
1. Steady state.
  2. Deep ground temperature same as surface temperature.
  3. Negligible resistance of the pipe wall and for convection from the oil.
  4. Isothermal surface exposed to soil.

(i) Equation (3.32),  $\dot{Q} = kS\Delta T$ , can be used for the heat loss, with the shape factor obtained from Table 3.2, item 8:

$$\frac{h}{r_1} = \frac{1.0}{0.15} = 6.67 > 3$$

Hence,

$$S = \frac{2\pi L}{\ln(2h/r_1)} = \frac{(2\pi)(5000)}{\ln(2 \times 1/0.15)} = 12,130 \text{ m}$$

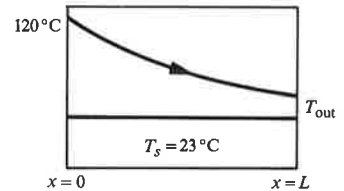


The temperature difference between the oil and the ground surface  $\Delta T$  decreases continuously in the flow direction, so how do we use Eq. (3.32)? We recognize that this problem is similar to the single-stream heat exchanger analyzed in Section 1.6 because the ground temperature is constant along the pipeline. We could easily perform an analysis similar to that of Section 1.6.2; however, with a little thought, we can simply reinterpret the results of Section 1.6.2 for the problem at hand. Equation (1.59), for the effectiveness, is

$$\varepsilon = 1 - e^{-N_{tu}}$$

where now

$$\varepsilon = \frac{\text{Actual temperature change}}{\text{Maximum possible temperature change}} = \frac{T_{in} - T_{out}}{T_{in} - T_s}$$



To specify the number of transfer units,  $N_{tu} = U\mathcal{P}L/\dot{m}c_p$ , recall that the heat transfer for an element of exchanger  $\Delta x$  long was

$$\Delta\dot{Q} = U\mathcal{P}\Delta x\Delta T$$

while for the pipeline it is

$$\Delta\dot{Q} = k\Delta S\Delta T; \quad \Delta S = \frac{2\pi\Delta x}{\ln(2h/r_1)}$$

Thus,  $U\mathcal{P}\Delta x$  can be replaced by  $k\Delta S$ , or  $U\mathcal{P}L$  by  $kS$ :

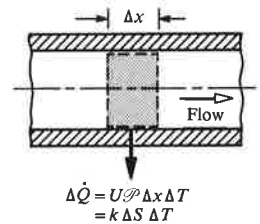
$$N_{tu} = \frac{U\mathcal{P}L}{\dot{m}c_p} = \frac{kS}{\dot{m}c_p} = \frac{(1.5)(12,130)}{(2.5)(2000)} = 3.64$$

$$\varepsilon = 1 - e^{-3.64} = 0.974$$

$$T_{out} = T_{in} - \varepsilon(T_{in} - T_s) = 120 - 0.974(120 - 23) = 25.5^\circ\text{C}$$

The heat loss is equal to the enthalpy given up by the oil,

$$\dot{Q} = \dot{m}c_p(T_{in} - T_{out}) = (2.5)(2000)(120 - 25.5) = 472 \text{ kW}$$



(ii) This problem cannot be solved exactly using the shape factor concept, since, when the insulation is added to the pipe, the outer surface of the insulation will not be isothermal. However, to get some idea of the effect of the insulation, we will assume an isothermal surface. Then for two resistances in series,

$$\frac{1}{U\mathcal{P}L} = \frac{\ln(r_2/r_1)}{2\pi k_{\text{ins}}L} + \frac{1}{k_{\text{soil}}S}$$

$$\frac{\ln(r_2/r_1)}{2\pi k_{\text{ins}}L} = \frac{\ln(0.30/0.15)}{(2\pi)(0.03)(5000)} = 7.35 \times 10^{-4} \text{ (W/K)}^{-1}$$

$$\frac{h}{r_2} = \frac{1.0}{0.3} = 3.33 > 3; \text{ hence}$$

$$S = \frac{2\pi L}{\ln(2h/r_2)} = \frac{(2\pi)(5000)}{\ln(2 \times 1/0.3)} = 16,560 \text{ m}$$

$$\frac{1}{k_{\text{soil}}S} = \frac{1}{(1.5)(16,560)} = 0.403 \times 10^{-4} \text{ (W/K)}^{-1}$$

$$\frac{1}{U\mathcal{P}L} = (7.35 + 0.40)10^{-4}; \quad U\mathcal{P}L = 1290 \text{ W/K}$$

$$N_{\text{tu}} = \frac{1290}{(2.5)(2000)} = 0.258; \quad \varepsilon = 1 - e^{-0.258} = 0.227$$

$$T_{\text{out}} = 120 - 0.227(120 - 23) = 98.0^\circ\text{C}$$

$$\dot{Q} = (2.5)(2000)(120 - 98.0) = 110 \text{ kW}$$

### Comments

The pipeline is located on a tropical island where the annual ground temperature variation is relatively small, so a steady-state analysis is reasonably valid. Problems concerning the freezing of buried water pipes often require a transient analysis because of ground temperature variations (see Exercise 3–39).

## 3.4 UNSTEADY CONDUCTION

In unsteady or *transient* conduction, temperature is a function of both time and spatial coordinates. In the absence of internal heat generation, the temperature response of a body is governed by Fourier's equation. Again the method of separation of variables is useful, and examples of its use are given in Sections 3.4.1 and 3.4.3. The method, however, fails under certain circumstances—for example, when the medium extends to infinity. Then possible methods include the use of *Laplace transforms* or a **similarity** transformation of the partial differential equation into an ordinary differential equation. The latter method is demonstrated in Section 3.4.2. Analytical results of unsteady conduction tend to be complicated and awkward to use. Thus, where possible, approximate solutions of adequate accuracy will be indicated. Often the results are conveniently presented in graphical form for rapid engineering calculations.

### 3.4.1 The Slab with Negligible Surface Resistance

Figure 3.9 shows a slab  $2L$  thick. It is initially at a uniform temperature  $T_0$ , and at time  $t = 0$  the surfaces at  $x = +L$  and  $x = -L$  are suddenly lowered to temperature  $T_s$ . Such a situation is encountered in practice when a poorly conducting slab is suddenly immersed in a liquid for which the convective heat transfer coefficient is very large, that is, under conditions where the convective resistance to heat transfer is negligible. Note that this situation is the opposite limit to that considered in Section 1.5, for which the lumped thermal capacity model was applicable. In that case, the Biot number  $Bi = h_c L/k$  had to be small; for this case, the Biot number must be large. In addition to its practical utility, the solution of this problem allows a simple demonstration of some important features of transient conduction.

#### *The Governing Equation and Conditions*

With no internal heat generation and an assumed constant thermal conductivity, Fourier's equation, Eq. (3.6), applies. Since the temperature does not vary in the  $y$  and  $z$  directions,

$$\frac{\partial T}{\partial t} = \alpha \frac{\partial^2 T}{\partial x^2} \quad (3.33)$$

which is the governing differential equation for  $T(x, t)$  and must be solved subject to the initial condition

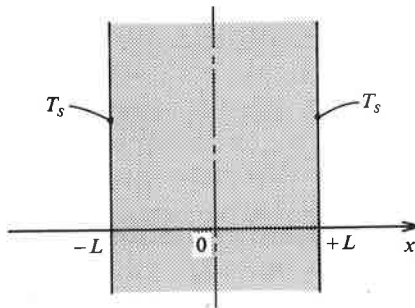
$$t = 0: \quad T = T_0 \quad (3.34a)$$

The symmetry of the problem allows the differential equation to be solved in the region  $0 \leq x \leq L$ , for which the appropriate boundary conditions are

$$x = 0: \quad \frac{\partial T}{\partial x} = 0 \quad (3.34b)$$

$$x = L: \quad T = T_s \quad (3.34c)$$

Equation (3.34b) follows from the symmetry of the temperature profile about the plane  $x = 0$ , or equivalently, from the condition that there can be no heat flow across this plane.



**Figure 3.9** Coordinate system for the analysis of unsteady conduction in an infinite slab.



### Dimensional Analysis

Before an attempt is made to solve Eq. (3.33), it is helpful to perform a dimensional analysis. We begin by constructing suitable dimensionless independent and dependent variables. Suitable choices for  $x$  and  $T$  are  $\eta = x/L$  and  $\theta = (T - T_s)/(T_0 - T_s)$ , since  $\eta$  and  $\theta$  will both vary between zero and unity. However, there is no obvious time scale for the problem that can be used to make  $t$  dimensionless, so we will let the differential equation itself indicate an appropriate choice. Transforming Eq. (3.33) with

$$\begin{aligned}x &= L\eta; & dx &= L d\eta \\T &= (T_0 - T_s)\theta + T_s; & dT &= (T_0 - T_s)d\theta\end{aligned}$$

gives

$$(T_0 - T_s) \frac{\partial \theta}{\partial t} = \frac{\alpha(T_0 - T_s)}{L^2} \frac{\partial^2 \theta}{\partial \eta^2}$$

or

$$\frac{\partial \theta}{\partial(\alpha t/L^2)} = \frac{\partial^2 \theta}{\partial \eta^2}$$

Thus, we choose  $\zeta = t/(L^2/\alpha)$  as dimensionless time, and the result is

$$\frac{\partial \theta}{\partial \zeta} = \frac{\partial^2 \theta}{\partial \eta^2} \quad (3.35)$$

The initial and boundary conditions transform into

$$\zeta = 0: \quad \theta = 1 \quad (3.36a)$$

$$\eta = 0: \quad \frac{\partial \theta}{\partial \eta} = 0 \quad (3.36b)$$

$$\eta = 1: \quad \theta = 0 \quad (3.36c)$$

There are no parameters in the transformed statement of the problem, so the solution is simply  $\theta(\zeta, \eta)$ . The dimensionless time variable  $\zeta$  is also commonly called the **Fourier number**,  $\text{Fo} = \alpha t/L^2$ . Notice that the Fourier number can also be written as  $\text{Fo} = t/t_c$ ;  $t_c = L^2/\alpha$  is a characteristic time (time constant) for this conduction problem. The behavior of the solution will depend on the value of  $t$  relative to  $t_c$ , that is, on whether  $\text{Fo}$  is much smaller than unity, of order unity, or much larger than unity. The relation  $\theta = \theta(\zeta, \eta)$  is a statement of the similarity principle for this problem, a concept introduced in Section 2.4.5. We now know that the solution for the dimensionless temperature  $\theta$  will be a function of dimensionless time  $\zeta$  and dimensionless position  $\eta$  only.

### Solution for the Temperature Response

As in Section 3.3.1, for steady conduction in a rectangular plate, the method of separation of variables will be used to solve the partial differential equation. We assume that the function  $\theta(\zeta, \eta)$  can be expressed as the product of a function of  $\zeta$

only,  $Z(\zeta)$ , and a function of  $\eta$  only,  $H(\eta)$ :

$$\theta(\zeta, \eta) = Z(\zeta)H(\eta) \quad (3.37)$$

Substitution in Eq. (3.35) yields

$$H \frac{dZ}{d\zeta} = Z \frac{d^2H}{d\eta^2}$$

where total derivatives have replaced partial derivatives, since  $Z$  is a function of independent variable  $\zeta$  only, and  $H$  is a function of independent variable  $\eta$  only. Rearranging gives

$$\frac{1}{Z} \frac{dZ}{d\zeta} = \frac{1}{H} \frac{d^2H}{d\eta^2} \quad (3.38)$$

Since each side of Eq. (3.38) is a function of a single independent variable, the equality can hold only if both sides are equal to a constant. To satisfy the boundary conditions, this constant must be a negative number, which will be written  $-\lambda^2$ . Two ordinary differential equations are obtained:

$$\frac{dZ}{d\zeta} + \lambda^2 Z = 0 \quad \frac{d^2H}{d\eta^2} + \lambda^2 H = 0$$

which have the solutions

$$Z = C_1 e^{-\lambda^2 \zeta} \quad H = C_2 \cos \lambda \eta + C_3 \sin \lambda \eta$$

Hence,

$$\theta(\zeta, \eta) = e^{-\lambda^2 \zeta} (A \cos \lambda \eta + B \sin \lambda \eta)$$

where  $A = C_1 C_2$  and  $B = C_1 C_3$ . Applying boundary condition Eq. (3.36b),

$$\left. \frac{\partial \theta}{\partial \eta} \right|_{\eta=0} = e^{-\lambda^2 \zeta} (-A \lambda \sin \lambda \eta + B \lambda \cos \lambda \eta)_{\eta=0} = 0$$

which requires that  $B = 0$ . Next, applying boundary condition Eq. (3.36c) gives

$$\theta|_{\eta=1} = A e^{-\lambda^2 \zeta} \cos \lambda \eta|_{\eta=1} = 0$$

which requires that  $\cos \lambda = 0$ , or  $\lambda_n = (n + 1/2)\pi$ ,  $n = 0, 1, 2, 3, \dots$ . The  $\lambda_n$  are the eigenvalues for this problem, and the solution corresponding to the  $n$ th eigenvalue may be written as

$$\theta_n(\zeta, \eta) = A_n e^{-(n+1/2)^2 \pi^2 \zeta} \cos \left( n + \frac{1}{2} \right) \pi \eta \quad (3.39)$$

The general solution to Eq. (3.35) is the sum of the series of solutions given by Eq. (3.39):

$$\theta(\zeta, \eta) = \sum_{n=0}^{\infty} A_n e^{-(n+1/2)^2 \pi^2 \zeta} \cos \left( n + \frac{1}{2} \right) \pi \eta \quad (3.40)$$

The constants  $A_n$  are determined from the initial condition, Eq. (3.36a):

$$\theta|_{\zeta=0} = \sum_{n=0}^{\infty} A_n \cos\left(n + \frac{1}{2}\right) \pi \eta = 1$$

That is, a constant must be expressed in terms of an infinite series of cosine functions, which again is a Fourier series expansion. More generally,  $\theta|_{\zeta=0} = f(\eta)$  is an arbitrary function of  $\eta$ , and the required expansion is then

$$f(\eta) = \sum_{n=0}^{\infty} A_n \cos\left(n + \frac{1}{2}\right) \pi \eta \quad (3.41)$$

Determination of the constants  $A_n$  follows the procedure demonstrated in Section 3.3.1. The result is

$$A_n = 2 \int_0^1 f(\eta) \cos\left(n + \frac{1}{2}\right) \pi \eta d\eta \quad (3.42)$$

$$\text{For } f(\eta) = 1, A_n = \frac{2}{(n + 1/2)\pi} \left[ \sin\left(n + \frac{1}{2}\right) \pi \eta \right]_0^1 = \frac{2(-1)^n}{(n + 1/2)\pi}$$

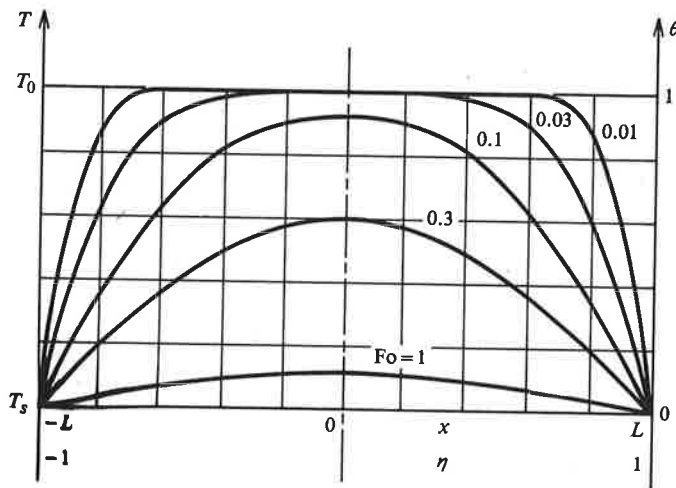
Substituting in Eq. (3.40) gives the solution for the temperature distribution,

$$\theta(\zeta, \eta) = \sum_{n=0}^{\infty} \frac{2(-1)^n}{(n + 1/2)\pi} e^{-(n+1/2)^2 \pi^2 \zeta} \cos\left(n + \frac{1}{2}\right) \pi \eta \quad (3.43)$$

or, in terms of temperature  $T(x, t)$ , Fourier number  $\text{Fo} = \alpha t/L^2$ , and  $x/L$ ,

$$\frac{T - T_s}{T_0 - T_s} = \sum_{n=0}^{\infty} \frac{2(-1)^n}{(n + 1/2)\pi} e^{-(n+1/2)^2 \pi^2 \text{Fo}} \cos\left(n + \frac{1}{2}\right) \pi \frac{x}{L} \quad (3.44)$$

which is plotted in Fig. 3.10.



**Figure 3.10** Temperature response in a slab with negligible surface resistance, calculated from Eq. (3.44).

### The Surface Heat Flux

Of particular interest is the rate of heat transfer out of the slab. The surface heat flux at  $x = L$  is obtained from Fourier's law and Eq. (3.44) as

$$\begin{aligned}
 q_s &= -k \left. \frac{\partial T}{\partial x} \right|_{x=L} \\
 &= -k(T_0 - T_s) \sum_{n=0}^{\infty} \frac{2(-1)^n}{(n + 1/2)\pi} e^{-(n+1/2)^2\pi^2 Fo} \frac{\partial}{\partial x} \left[ \cos \left( n + \frac{1}{2} \right) \pi \frac{x}{L} \right]_{x=L} \\
 &= -k(T_0 - T_s) \sum_{n=0}^{\infty} \frac{2(-1)^n}{(n + 1/2)\pi} e^{-(n+1/2)^2\pi^2 Fo} \left[ \frac{-(n + 1/2)\pi(-1)^n}{L} \right] \\
 &= \frac{2k(T_0 - T_s)}{L} \sum_{n=0}^{\infty} e^{-(n+1/2)^2\pi^2 Fo} \tag{3.45}
 \end{aligned}$$

or

$$q_s = \frac{2k(T_0 - T_s)}{L} \left[ e^{-(\pi/2)^2 Fo} + e^{-(3\pi/2)^2 Fo} + e^{-(5\pi/2)^2 Fo} + e^{-(7\pi/2)^2 Fo} + \dots \right]$$

Table 3.3 gives the first four terms in the series for values of the Fourier number  $Fo = \alpha t/L^2$  equal to 0.01, 0.1, 0.2, 0.3, and 1.0. It can be seen that the series converges rapidly unless the Fourier number is very small. For  $Fo \geq 0.2$ , only the first term in the series need be retained, and

$$q_s \approx \frac{2k(T_0 - T_s)}{L} e^{-(\pi/2)^2 Fo} \tag{3.46}$$

with an error of less than 2%. Since  $Fo = \alpha t/L^2$ , Eq. (3.46) is a solution valid for long times.

For small values of the Fourier number (that is, soon after the slab is immersed in the liquid), the series converges slowly, and sufficient terms must be retained for an accurate result. However, in the limit  $Fo \rightarrow 0$ , there is the simple mathematical result:

**Table 3.3** The first four terms of the series of Eq. (3.45) for the surface heat flux of a slab with negligible surface resistance.

Fo	$e^{-(\pi/2)^2 Fo}$	$e^{-(3\pi/2)^2 Fo}$	$e^{-(5\pi/2)^2 Fo}$	$e^{-(7\pi/2)^2 Fo}$
0.01	0.9756	0.8009	0.5396	0.2985
0.1	0.7813	0.1085	0.0021	$\sim 10^{-5}$
0.2	0.6105	0.0118	$\sim 10^{-6}$	
0.3	0.4770	0.0013		
1.0	0.0848	$\sim 10^{-10}$		

$$\sum_{n=0}^{\infty} e^{-(n+1/2)^2 \pi^2 Fo} = \frac{1}{2\pi^{1/2} Fo^{1/2}}; \quad Fo \rightarrow 0$$

Substituting in Eq. (3.45) gives

$$q_s \simeq \frac{k(T_0 - T_s)}{(\pi\alpha t)^{1/2}} \quad (3.47)$$

which can be used for  $Fo \lesssim 0.05$ . Equation (3.47) is thus a valid solution for *short times*. Figure 3.10 shows that for sufficiently short times, the temperature changes in a thin region near the surface only, while the temperature of the slab interior remains unaffected. The heat conduction process is confined to this thin region, and the thickness of the slab is of no consequence: notice that  $L$  does not appear in Eq. (3.47). It is this fact that motivates the analysis of the semi-infinite solid in Section 3.4.2.

### Nonsymmetrical Boundary Conditions

In our analysis, we specified the same temperature on both sides of the slab. Symmetry allowed the problem to be solved in the half slab,  $0 \leq x \leq L$ ; upon transformation, the boundary condition at  $\eta = 1$  was  $\theta = 0$ , that is, homogeneous. If we now specify a temperature  $T_s$  at  $x = L$  and  $T_{s'}$  at  $x = -L$ , as shown in Fig. 3.11, how do we proceed? It is not possible to define a dimensionless temperature  $\theta$  such that  $\theta = 0$  on both boundaries, and without homogeneous boundary conditions, it is not possible to obtain an eigenvalue problem as before. To get around this hurdle, we reduce the problem to the **superposition** of a steady and a transient problem. Let  $T(x, t) = T_1(x) + T_2(x, t)$  such that

$$\frac{d^2 T_1}{dx^2} = 0$$

$$\frac{\partial T_2}{\partial t} = \alpha \frac{\partial^2 T_2}{\partial x^2}$$

$$x = L: \quad T_1 = T_s$$

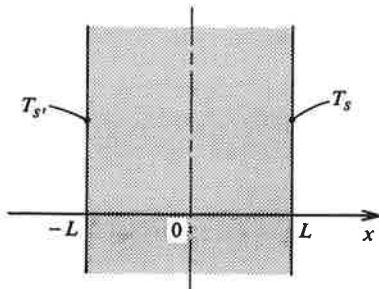
$$x = L, -L: \quad T_2 = 0$$

$$x = -L: \quad T_1 = T_{s'}$$

$$t = 0: \quad T_2 = T_0 - T_1$$

$$T_1 = \frac{T_s - T_{s'}}{2} \frac{x}{L} + \frac{T_s + T_{s'}}{2}$$

$$T_2 = \sum_{n=0}^{\infty} A_n e^{-(n+1/2)^2 \pi^2 Fo} \cos\left(n + \frac{1}{2}\right) \pi \frac{x}{L}$$

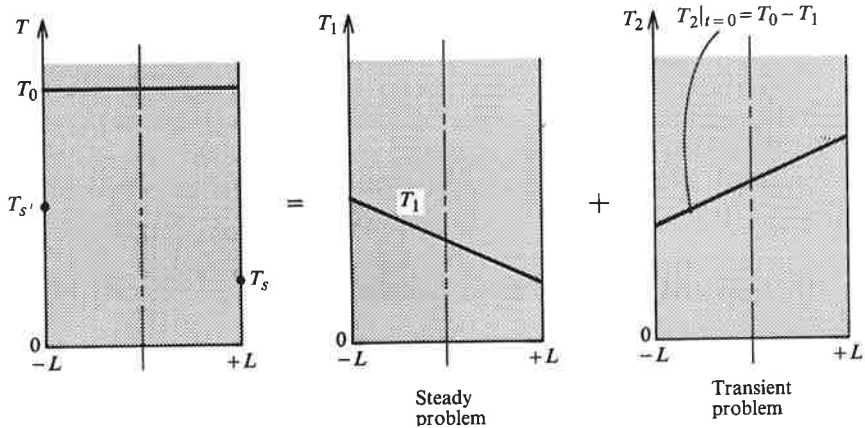


**Figure 3.11** Schematic for the analysis of unsteady conduction in a slab with unequal surface temperatures.

and the constants  $A_n$  must be determined from

$$\sum_{n=0}^{\infty} A_n \cos\left(n + \frac{1}{2}\right)\pi \frac{x}{L} = T_0 - \frac{T_s - T_{s'}}{2} \frac{x}{L} - \frac{T_s + T_{s'}}{2} \quad (3.48)$$

Figure 3.12 illustrates this superposition technique.



**Figure 3.12** Schematic of superposition of solutions for a slab with unequal surface temperatures.

### EXAMPLE 3.4 Transient Steam Condensation on a Concrete Wall

In a postulated nuclear reactor accident scenario, a concrete wall 20 cm thick at an initial temperature of 20°C is suddenly exposed on both sides to pure steam at atmospheric pressure. If the thermal resistance of the condensate flowing down the wall is negligible, estimate the rate of steam condensation on 160 m<sup>2</sup> wall area after (i) 10 s, (ii) 10 min, and (iii) 3 h.

#### Solution

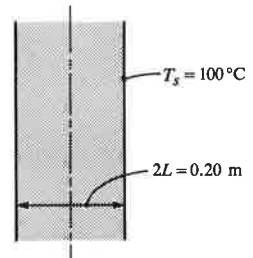
**Given:** Concrete wall suddenly exposed to steam.

**Required:** Rate of steam condensation at various times.

**Assumptions:** 1. Thermal resistance of condensate negligible.  
2. Pure steam,  $T_{\text{sat}}$  (1 atm) = 100°C.

The first step is to calculate the time constant for the wall,  $t_c = L^2/\alpha$ . From Table A.3, we take  $\alpha = 0.75 \times 10^{-6}$  m<sup>2</sup>/s for concrete. Then

$$t_c = \frac{L^2}{\alpha} = \frac{(0.1)^2}{0.75 \times 10^{-6}} = 1.33 \times 10^4 \text{ s (3.7 h)}$$



(i)  $t = 10$  s:

$Fo = t/t_c = 10/1.33 \times 10^4 = 7.5 \times 10^{-4} < 0.05$ . Thus, Eq. (3.47) applies. The condensation rate is  $\dot{m} = q_s A/h_{fg}$  where  $h_{fg}$  is the enthalpy of vaporization of steam at  $100^\circ\text{C}$ . From steam tables (for example, Table A.12a),  $h_{fg} = 2.257 \times 10^6$  J/kg. Also required is the conductivity of concrete, which from Table A.3 is  $1.4$  W/m K.

$$\dot{m} = \frac{q_s A}{h_{fg}} = \frac{k(T_s - T_0)A}{(\pi \alpha t)^{1/2} h_{fg}} = \frac{(1.4)(100 - 20)(160)}{[\pi(0.75 \times 10^{-6})(10)]^{1/2}(2.257 \times 10^6)} = 1.64 \text{ kg/s}$$

(ii)  $t = 10$  min:

$Fo = t/t_c = (10)(60)/1.33 \times 10^4 = 0.0451 < 0.05$ . Thus, Eq. (3.47) remains valid. Since  $q_s$  and, hence,  $\dot{m}$  decrease like  $t^{-1/2}$ , the condensation rate is now

$$\dot{m} = 1.64 \left( \frac{600}{10} \right)^{-1/2} = 0.212 \text{ kg/s}$$

(iii)  $t = 3$  h:

$Fo = t/t_c = (3)(3600)/1.33 \times 10^4 = 0.812 > 0.2$ . Equation (3.46) now applies, and the condensation rate is

$$\dot{m} = \frac{2k(T_s - T_0)A}{Lh_{fg}} e^{-(\pi/2)^2 Fo} = \frac{(2)(1.4)(100 - 20)(160)}{(0.10)(2.257 \times 10^6)} e^{-(\pi/2)^2(0.812)} = 0.0214 \text{ kg/s}$$

### Comments

These estimates may be regarded as upper limits: in practice the steam is likely to contain some noncondensables, such as air, and condense at a temperature lower than  $100^\circ\text{C}$ . The problem is then one involving simultaneous heat and mass transfer.

### 3.4.2 The Semi-Infinite Solid

In Section 3.4.1, we saw that for sufficiently short times, temperature changes did not penetrate far enough into the slab for the thickness of the slab to have any effect on the heat conduction process. Such situations are encountered in practice. One method of case-hardening tool steel involves rapid quenching from a high temperature for a short time. Only the metal close to the surface is rapidly cooled and hardened; the interior cools slowly after the quenching process and remains ductile. Thus, during the quenching process, the interior temperature remains unchanged, and the precise thickness and shape of the tool is irrelevant. The conduction process is confined to a thin region near the surface into which temperature changes have penetrated. Thus, it is useful to have formulas giving the temperature distribution and heat flow for various kinds of boundary conditions that are applicable to these *penetration* problems.

### The Governing Equation and Conditions

An appropriate model for penetration problems is transient conduction in a semi-infinite solid, as shown in Fig. 3.13. If we assume constant thermal conductivity, no internal heat generation, and negligible temperature variations in the  $y$  and  $z$  directions, Eq. (3.6) again reduces to

$$\frac{\partial T}{\partial t} = \alpha \frac{\partial^2 T}{\partial x^2} \quad (3.49)$$

If the solid is initially at a uniform temperature  $T_0$ , the appropriate initial condition is

$$t = 0: \quad T = T_0 \quad (3.50a)$$

The left face of the solid is suddenly raised to temperature  $T_s$  at time zero and held at that value. The two required boundary conditions are then

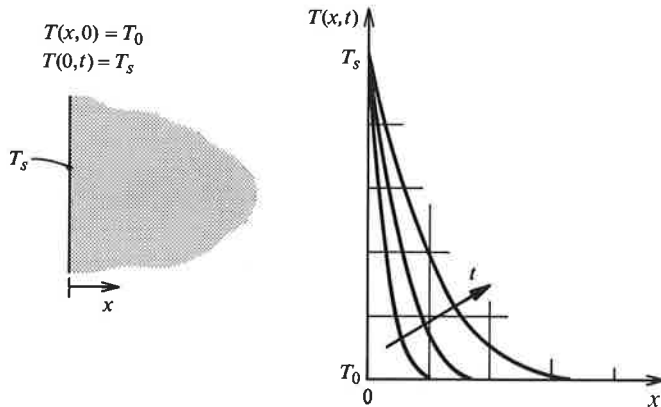
$$x = 0: \quad T = T_s \quad (3.50b)$$

$$x \rightarrow \infty: \quad T \rightarrow T_0 \quad (3.50c)$$

It is the second boundary condition, Eq. (3.50c), that makes this problem different from the slab problem of Section 3.4.1.

### Solution for the Temperature Distribution

It might at first appear that the *separation of variables* solution method can be used once again. As in the slab analysis of Section 3.4.1, the variables are separable in the differential equation, Eq. (3.49). However, a necessary requirement for completing the solution is that the boundary conditions of the eigenvalue problem be specified on *coordinate surfaces*, and  $x = \infty$  is not a coordinate surface of the Cartesian coordinate system. Instead, we proceed as follows.



**Figure 3.13** Coordinate system and expected temperature profiles for transient conduction in a semi-infinite solid with a step change in surface temperature.



We first normalize the dependent variable  $T(x, t)$  for algebraic convenience. Defining  $\theta = (T - T_0)/(T_s - T_0)$ , the problem statement transforms into

$$\frac{\partial \theta}{\partial t} = \alpha \frac{\partial^2 \theta}{\partial x^2} \quad (3.51)$$

$$t = 0: \quad \theta = 0 \quad (3.52a)$$

$$x = 0: \quad \theta = 1 \quad (3.52b)$$

$$x \rightarrow \infty: \quad \theta \rightarrow 0 \quad (3.52c)$$

This mathematical problem can be reduced to the solution of an ordinary differential equation for  $\theta$ . The independent variable in this equation is called a **similarity variable** and is an appropriate combination of  $x$  and  $t$ . One way to discover the combination is based on physical reasoning and dimensional considerations. Figure 3.13 shows the expected temperature profiles as a function of time as the heat penetrates into the solid. We can arbitrarily define some penetration depth  $\delta$ , for example, the location where  $\theta = 0.01$  or  $0.001$ . Then  $\delta$  is clearly a function of time  $t$  and thermal diffusivity  $\alpha$ : the larger  $\alpha$ , the deeper the penetration at a given time. Notice that the problem statement, Eqs. (3.51) and (3.52), contains no other quantities on which  $\delta$  can depend. Time has units [s], and thermal diffusivity has units [ $\text{m}^2/\text{s}$ ]. The only combination of these two variables that will give the required units of [m] for the penetration depth is  $(\alpha t)^{1/2}$ . For the temperature profile to be a function of a single variable, distances into the solid must be *scaled* to this penetration depth. Thus, we will choose

$$\eta = \frac{x}{(4\alpha t)^{1/2}} \quad (3.53)$$

where the factor of  $4^{1/2}$  has been inserted for future algebraic convenience. Eq. (3.51) is transformed by careful use of the rules of partial differentiation. The required differential operators are

$$\frac{\partial \theta}{\partial t} = \frac{d\theta}{d\eta} \frac{\partial \eta}{\partial t} \Big|_x = \frac{d\theta}{d\eta} \left( -\frac{x}{2t(4\alpha t)^{1/2}} \right)$$

$$\frac{\partial \theta}{\partial x} = \frac{d\theta}{d\eta} \frac{\partial \eta}{\partial x} \Big|_t = \frac{d\theta}{d\eta} \left( \frac{1}{(4\alpha t)^{1/2}} \right)$$

$$\frac{\partial^2 \theta}{\partial x^2} = \frac{1}{(4\alpha t)^{1/2}} \frac{d^2 \theta}{d\eta^2} \frac{\partial \eta}{\partial x} \Big|_t = \frac{1}{(4\alpha t)} \frac{d^2 \theta}{d\eta^2}$$

Notice that we have written the derivatives of  $\theta$  with respect to  $\eta$  as total derivatives since we have assumed that  $\theta$  is a function of  $\eta$  alone. Substituting in Eq. (3.51) gives

$$-\frac{x}{2t(4\alpha t)^{1/2}} \frac{d\theta}{d\eta} = \frac{\alpha}{(4\alpha t)} \frac{d^2 \theta}{d\eta^2}$$

which simplifies to

$$-2\eta \frac{d\theta}{d\eta} = \frac{d^2\theta}{d\eta^2} \quad (3.54)$$

Equation (3.54) is a second-order nonlinear ordinary differential equation, which requires two boundary conditions. Transforming Eqs. (3.52) gives

$$\eta = 0: \quad \theta = 1, \quad \text{since } \eta = 0 \text{ when } x = 0 \quad (3.55a)$$

$$\eta \rightarrow \infty: \quad \theta = 0, \quad \text{since } \eta \rightarrow \infty \text{ when } x \rightarrow \infty, \text{ or } t \rightarrow 0 \quad (3.55b)$$

Since both the transformed equation and conditions do not depend on  $x$  or  $t$ , the *similarity transformation* has been successful. Let  $d\theta/d\eta = p$ ; then Eq. (3.54) becomes the first-order equation

$$-2\eta p = \frac{dp}{d\eta}$$

or

$$\frac{dp}{p} = -2\eta d\eta = -d\eta^2$$

Integrating once,

$$p = \frac{d\theta}{d\eta} = C_1 e^{-\eta^2}$$

Integrating again,

$$\theta = C_1 \int_0^\eta e^{-u^2} du + C_2 \quad (3.56)$$

where  $u$  is a dummy variable for the integration. The integration constants are evaluated from the boundary conditions, Eq. (3.55). From Eq. (3.55a),  $\theta = 1$  at  $\eta = 0$ ; hence,  $C_2 = 1$ . From Eq. (3.55b),  $\theta \rightarrow 0$  as  $\eta \rightarrow \infty$ ,

$$0 = C_1 \int_0^\infty e^{-u^2} du + 1$$

The definite integral is given by standard integral tables as  $\pi^{1/2}/2$ ; hence,

$$0 = C_1 \frac{\pi^{1/2}}{2} + 1 \quad \text{or} \quad C_1 = -\frac{2}{\pi^{1/2}}$$

Substituting back in Eq. (3.56) gives the temperature distribution as

$$\theta = \frac{T - T_0}{T_s - T_0} = 1 - \frac{2}{\pi^{1/2}} \int_0^\eta e^{-u^2} du \quad (3.57)$$

The function  $(2/\pi^{1/2}) \int_0^\eta e^{-u^2} du$  is called the **error function**,  $\text{erf } \eta$ . For our purposes, it is more convenient to use the **complementary error function**,  $\text{erfc } \eta = 1 - \text{erf } \eta$ , which is tabulated as Table B.4 in Appendix B. Then

$$\frac{T - T_0}{T_s - T_0} = \text{erfc} \frac{x}{(4\alpha t)^{1/2}} \quad (3.58)$$

Equation (3.58) is plotted as Fig. 3.14. Since the temperature profiles at any time fall on a single curve when plotted as  $\theta(\eta)$ , they are said to be *self-similar*, which is why  $\eta$  is called the *similarity variable* for the problem.

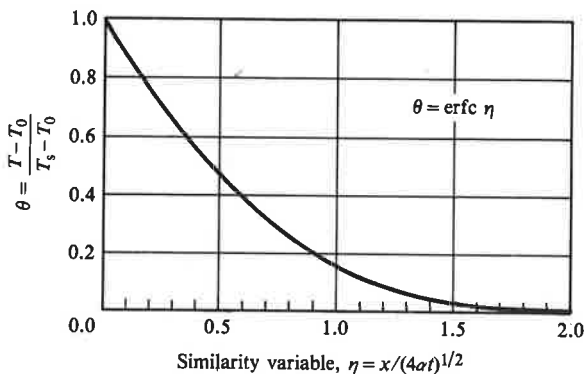
### The Surface Heat Flux

The heat flux at the surface is found from Eq. (3.58) using Fourier's law and the chain rule of differentiation,

$$\begin{aligned} q_s &= -k \left. \frac{\partial T}{\partial x} \right|_{x=0} \\ &= -k(T_s - T_0) \frac{\partial}{\partial x} \left[ 1 - \frac{2}{\pi^{1/2}} \int_0^\eta e^{-u^2} du \right]_{x=0} \\ &= -k(T_s - T_0) \left[ -\frac{2}{\pi^{1/2}} e^{-\eta^2} \frac{1}{(4\alpha t)^{1/2}} \right]_{\eta=0} \\ q_s &= \frac{k(T_s - T_0)}{(\pi\alpha t)^{1/2}} \end{aligned} \quad (3.59)$$

which is identical to the short-time solution for the slab problem, Eq. (3.47).

Solutions of the semi-infinite solid problem for other kinds of boundary conditions are also useful. A selection follows.



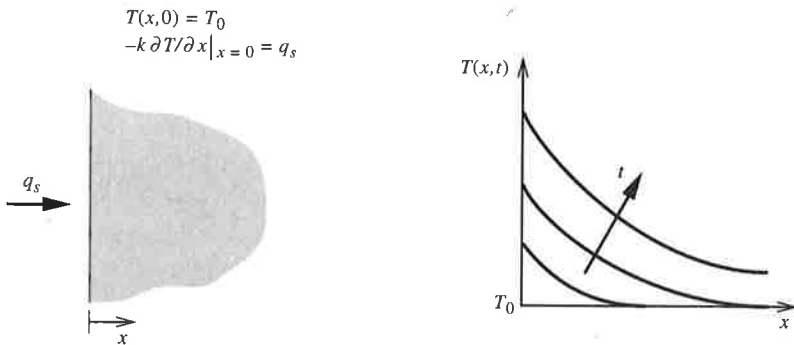
**Figure 3.14** Dimensionless temperature response in a semi-infinite solid with a step change in surface temperature, Eq. (3.58).

### Constant Surface Heat Flux

If at time  $t = 0$  the surface is suddenly exposed to a constant heat flux  $q_s$ —for example, by radiation from a high-temperature source—the resulting temperature response is

$$T - T_0 = \frac{q_s}{k} \left[ \left( \frac{4\alpha t}{\pi} \right)^{1/2} e^{-x^2/4\alpha t} - x \operatorname{erfc} \frac{x}{(4\alpha t)^{1/2}} \right] \quad (3.60)$$

This temperature response is shown in Fig. 3.15.



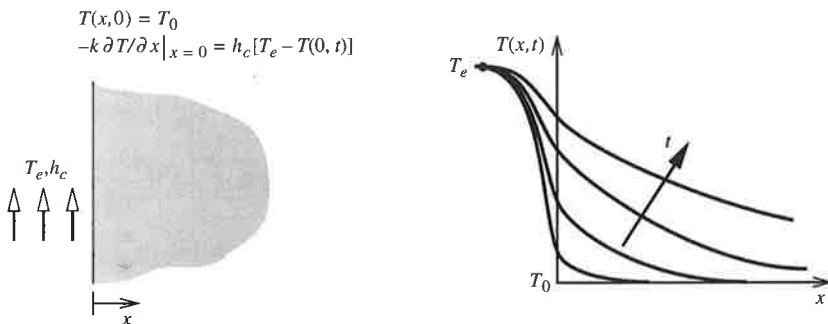
**Figure 3.15** Temperature response in a semi-infinite solid exposed to a constant surface heat flux, Eq. (3.60).

### Convective Heat Transfer to the Surface

If at time  $t = 0$  the surface is suddenly exposed to a fluid at temperature  $T_e$ , with a convective heat transfer coefficient  $h_c$ , the resulting temperature response is

$$\frac{T - T_0}{T_e - T_0} = \operatorname{erfc} \frac{x}{(4\alpha t)^{1/2}} - e^{h_c x/k + (h_c/k)^2 \alpha t} \operatorname{erfc} \left( \frac{x}{(4\alpha t)^{1/2}} + \frac{h_c}{k} (\alpha t)^{1/2} \right) \quad (3.61)$$

as shown in Fig. 3.16.



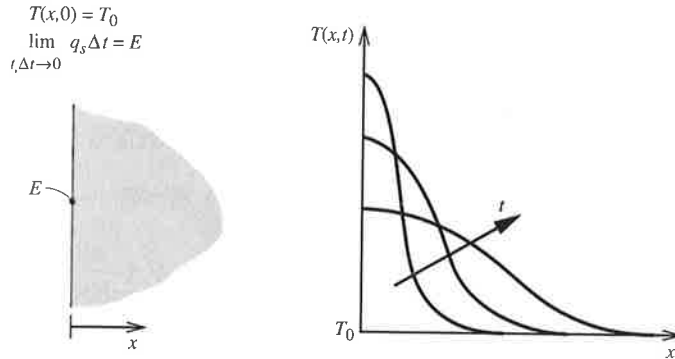
**Figure 3.16** Temperature response in a semi-infinite solid suddenly exposed to a fluid, Eq. (3.61).

### Surface Energy Pulse

If an amount of energy  $E$  per unit area is released instantaneously on the surface at  $t = 0$  (e.g., if the surface is exposed to an energy pulse from a laser), and none of this energy is lost from the surface, the resulting temperature response is

$$T - T_0 = \frac{E}{\rho c (\pi \alpha t)^{1/2}} e^{-x^2/4\alpha t} \quad (3.62)$$

as shown in Fig. 3.17.



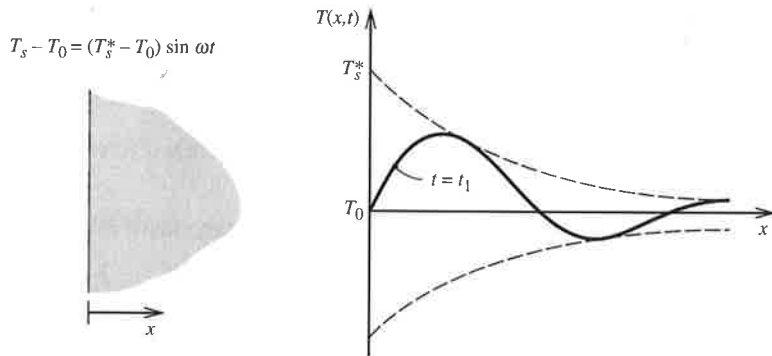
**Figure 3.17** Temperature response in a semi-infinite solid after an instantaneous release of energy on the surface, Eq. (3.62).

### Periodic Surface Temperature Variation

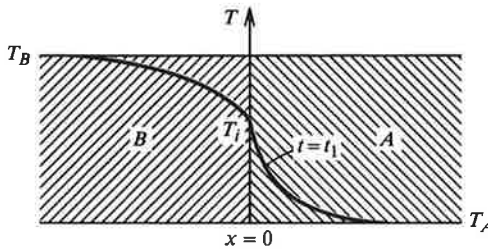
The surface temperature varies periodically as  $(T_s - T_0) = (T_s^* - T_0) \sin \omega t$ , as shown in Fig. 3.18. The resulting periodic (long-time) temperature response is

$$\frac{T - T_0}{T_s^* - T_0} = e^{-x(\omega/2\alpha)^{1/2}} \sin[\omega t - x(\omega/2\alpha)^{1/2}] \quad (3.63)$$

Notice how the amplitude of the temperature variation decays into the solid exponentially, while a phase lag  $x(\omega/2\alpha)^{1/2}$  develops.



**Figure 3.18** Periodic surface temperature variation for a semi-infinite solid: instantaneous temperature profile at  $t = t_1$ , Eq. (3.63).



**Figure 3.19** Contact of two semi-infinite solids: instantaneous temperature profile at  $t = t_1$  for  $k_B > k_A$ .

### Contact of Two Semi-Infinite Solids

Now consider two semi-infinite solids, A and B, of different materials with uniform temperatures  $T_A$  and  $T_B$ , brought together at time  $t = 0$ , as shown in Fig. 3.19. The solution of this problem shows that the interface temperature  $T_i$  is constant in time and is given by

$$\frac{T_A - T_i}{T_i - T_B} = \frac{k_B}{k_A} \left( \frac{\alpha_A}{\alpha_B} \right)^{1/2} = \left( \frac{(k\rho c)_B}{(k\rho c)_A} \right)^{1/2} \quad (3.64)$$

with corresponding erfc function temperature distributions in each solid. For example, if solid A is a carbon steel with  $k = 48$  W/m K and  $\alpha = 13.3 \times 10^{-6}$  m<sup>2</sup>/s at 100°C, and solid B is neoprene rubber with  $k = 0.19$  W/m K and  $\alpha = 0.079 \times 10^{-6}$  m<sup>2</sup>/s at 0°C, the interface temperature  $T_i$  is calculated to be 95.1°C. This is much closer to the initial temperature of the steel than to that of the rubber. Equation (3.64) shows why a high-conductivity material at room temperature feels colder to the touch than does a low-conductivity material at the same temperature.

The instantaneous heat flux at the surface  $q_s(t)$  can be found from Eqs. (3.61) through (3.63) by applying Fourier's law. The derivation of Eq. (3.63) is given as Exercise 3-37. The other solutions are best obtained using Laplace transforms [5,9].

### Computer Program CONDI

CONDI calculates the thermal response of a semi-infinite solid initially at temperature  $T_0$ . There is a choice of five boundary conditions imposed at time  $t = 0$ :

1. The surface temperature is changed to  $T_s$ .
2. A heat flux  $q_s$  is imposed on the surface.
3. The surface is exposed to a fluid at temperature  $T_e$ , with a convective heat transfer coefficient  $h_c$ .
4. An amount of energy  $E$  is released instantaneously at the surface.
5. The surface temperature varies periodically as  $T_s - T_0 = (T_s^* - T_0) \sin \omega t$ .

Plotting options include  $T(x)$ ,  $T_s(t)$ , or  $q_s(t)$ , which can be chosen appropriately. The analysis for boundary condition 1 was given in Section 3.4.2. The temperature responses for boundary conditions 2 through 5 are given as Eqs. (3.60) through (3.63), respectively.

**EXAMPLE 3.5** Cooling of a Concrete Slab

A thick concrete slab initially at 400 K is sprayed with a large quantity of water at 300 K. How long will the location 5 cm below the surface take to cool to 320 K?

**Solution**

**Given:** Hot concrete slab sprayed with water at 300 K.

**Required:** Rate of cooling 5 cm below surface.

**Assumptions:** 1. The rate of spraying is sufficient to maintain the surface at 300 K.  
2. The slab can be treated as a semi-infinite solid.

Equation (3.58) applies and can be written as

$$\theta = \operatorname{erfc} \eta \quad \text{where } \theta = \frac{T - T_0}{T_s - T_0}, \quad \eta = \frac{x}{(4\alpha t)^{1/2}}$$

$$\theta = \frac{320 - 400}{300 - 400} = 0.8$$

Thus,  $0.8 = \operatorname{erfc} \eta$ ; from Table B.4,  $\eta = 0.179$ .

$$t = \frac{x^2}{4\alpha\eta^2}$$

From Table A.3,  $\alpha$  for concrete is  $0.75 \times 10^{-6} \text{ m}^2/\text{s}$ . Thus, the required time is

$$t = \frac{(0.05)^2}{(4)(0.75 \times 10^{-6})(0.179)^2} = 2.60 \times 10^4 \text{ s} \approx 7 \text{ h}$$

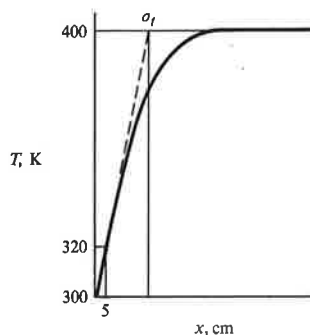
**Comments**

1. A temperature penetration depth  $\delta_i$  may be defined as the location where the tangent to the temperature profile at  $x = 0$  intercepts the line  $T = 400 \text{ K}$ , as shown in the figure. The temperature gradient at  $x = 0$  is found by differentiating Eq. (3.58):

$$-\left. \frac{\partial T}{\partial x} \right|_{x=0} = \frac{T_s - T_0}{(\pi\alpha t)^{1/2}} \equiv \frac{T_s - T_0}{\delta_i}$$

$$\text{Hence, } \delta_i = 1.772(\alpha t)^{1/2} = 1.772(0.75 \times 10^{-6} \times 2.60 \times 10^4)^{1/2} = 0.247 \text{ m.}$$

2. Check  $t$  using CONDI.

**EXAMPLE 3.6** Radiative Heating of a Firewall

A 15 cm-thick concrete firewall has a black silicone paint surface. The wall is suddenly exposed to a radiant heat source that can be approximated as a blackbody at 1000 K. How long will it take for the surface to reach 500 K if the initial temperature of the wall is 300 K?

**Solution**

**Given:** Concrete firewall exposed to radiant heat source.

**Required:** Temperature response of surface.

**Assumptions:** 1. Wall can be modeled as a semi-infinite solid.  
 2. Negligible temperature drop across the paint layer.  
 3. Negligible heat capacity of the paint layer.  
 4. An absorptance  $\alpha = 0.9$  for high-heat black silicone paint (Table A.5a); negligible radiation emitted by the wall.

Equation (3.60) evaluated at  $x = 0$  is

$$T_s - T_0 = \frac{q_s}{k} \left( \frac{4\alpha t}{\pi} \right)^{1/2}$$

or

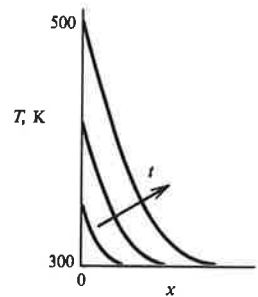
$$t = \frac{\pi}{\alpha} \left[ \frac{(T_s - T_0)k}{2q_s} \right]^2$$

From Table A.3, the required concrete properties are  $k = 1.4 \text{ W/m K}$  and  $\alpha = 0.75 \times 10^{-6} \text{ m}^2/\text{s}$ .

Since the surface temperature is low compared to the radiation source temperature, we can neglect radiation emitted by the surface, so

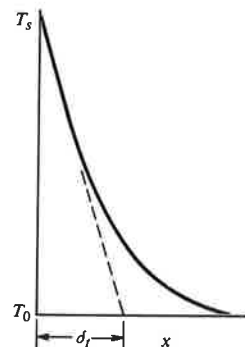
$$q_s \approx \alpha \sigma T^4 = (0.9)(5.67 \times 10^{-8})(1000)^4 = 51.0 \times 10^3 \text{ W/m}^2$$

$$t = \frac{\pi}{0.75 \times 10^{-6}} \left[ \frac{(500 - 300)(1.4)}{(2)(51.0 \times 10^3)} \right]^2 = 31.6 \text{ s}$$

**Comments**

1. At most,  $\epsilon \sigma T_s^4 = (0.9)(5.67 \times 10^{-8})(500^4) = 3.19 \times 10^3 \text{ W/m}^2$ , which is only 6% of  $q_s$  and is justifiably neglected in making this engineering estimate.
2. Check to see if the temperature drop and heat capacity of the paint layer are negligible. Choose an appropriate thickness and properties.
3. To check whether the assumption of a semi-infinite solid is valid, we estimate a penetration depth  $\delta_t$ :

$$\begin{aligned} \delta_t &= \frac{T_s - T_0}{-(\partial T / \partial x)_{x=0}} \\ &= \frac{T_s - T_0}{q_s / k} \\ &= \frac{500 - 300}{(51.0 \times 10^3) / (1.4)} \\ &= 0.0055 \text{ m (5.5 mm), which is small.} \end{aligned}$$





**Solution Using COND1**

The required input in SI units is:

- Boundary condition = 2
- Plot option = 2 ( $T_s$  versus  $t$ )
- $t$ -range for plot = 0, 60
- Thermal conductivity = 1.4
- Thermal diffusivity =  $0.75 \times 10^{-6}$
- Initial temperature  $T_0 = 300$
- Surface heat flux  $q_s = 51.0 \times 10^3$

From the graph of  $T_s$  versus  $t$ ,  $t \approx 32$  (seconds) when  $T_s = 500$  (kelvins).

**Comments**

1. A more accurate answer can be obtained from COND1 by adjusting the  $t$ -range.
2. Any consistent units can be used in COND1. With SI units, temperature may be in kelvins or degrees Celsius.

**EXAMPLE 3.7 Thermal Response of Soil**

On a tropical island, a large refrigerated shed has been operating at 5°C for a number of years. It is then put out of service; a wood floor is removed, and ambient air at 27°C is allowed to circulate freely through the shed. How long will it take for the ground 1 m below the surface to reach 15°C? Assume a convective heat transfer coefficient of 3.0 W/m<sup>2</sup> K, and use thermal properties of a wet soil ( $k = 2.6$  W/m K,  $\alpha = 0.45 \times 10^{-6}$  m<sup>2</sup>/s).

**Solution**

**Given:** Ground initially at 5°C, exposed to air at 27°C.

**Required:** Temperature response 1 m below surface.

- Assumptions:**
1. Semi-infinite solid model valid.
  2. The initial temperature is uniform (i.e., 5°C for an appreciable distance below the surface).

Equation (3.61) applies:

$$\frac{T - T_0}{T_e - T_0} = \operatorname{erfc} \frac{x}{(4\alpha t)^{1/2}} - e^{h_c x/k + (h_c/k)^2 \alpha t} \operatorname{erfc} \left( \frac{x}{(4\alpha t)^{1/2}} + \frac{h_c}{k} (\alpha t)^{1/2} \right)$$

$$\frac{T - T_0}{T_e - T_0} = \frac{15 - 5}{27 - 5} = 0.4545; \quad \frac{h_c}{k} = \frac{3.0}{2.6} = 1.154 \text{ m}^{-1}, \quad x = 1 \text{ m}$$

An iterative solution is required, but how do we make a reasonable first guess for  $t$ ? A lower limit is obtained if we use only the first term of Eq. (3.61), which corresponds to  $h_c \rightarrow \infty$ ,

$$T_s = T_e.$$

$$0.4545 = \operatorname{erfc} \eta$$

From Table B.4,  $\eta = 0.53$ .

$$0.53 = \frac{x}{(4\alpha t)^{1/2}} = \frac{1}{(4 \times 0.45 \times 10^{-6} t)^{1/2}}; \quad t = 2.0 \times 10^6 \text{ s}$$

The actual time will be greater than  $2.0 \times 10^6$  s; taking  $t = 4 \times 10^6$  s as a first guess, the following table summarizes the results:

Time, $t$ $\text{s} \times 10^{-6}$	$\frac{T - T_D}{T_e - T_D}$
4	0.368
5	0.415
6	0.452
6.05	0.4540
6.06	0.4545

Hence,  $t = 6.06 \times 10^6$  s ( $\sim 70$  days)

#### Comments

1. If the solution is done by hand, care must be taken to evaluate the erfc function accurately. COND1 will perform the required calculations rapidly and reliably.
2. The long time required suggests that problems involving conduction into the ground are almost always *transient* problems.

---

#### EXAMPLE 3.8 Temperature Fluctuations in a Diesel Engine Cylinder Wall

A thermocouple is installed in the 5 mm-thick cylinder wall of a stationary diesel engine, 1 mm below the inner surface. In a particular test, the engine operates at 1000 rpm, and the thermocouple reading is found to have a mean value of 322°C and an amplitude of 0.79°C. If the temperature variation can be assumed to be approximately sinusoidal, estimate the amplitude and phase difference of the inner-surface temperature variation. Take  $\alpha = 12.0 \times 10^{-6} \text{ m}^2/\text{s}$  and  $k = 40 \text{ W/m K}$  for the carbon steel wall.

#### Solution

**Given:** Thermocouple installed in diesel engine cylinder wall.

**Required:** Amplitude and phase difference of inner-surface temperature.

**Assumptions:** Model wall as a semi-infinite solid.

At first it would appear that the analysis of Section 3.4.2 does not apply to this problem. The cylinder wall is not very thick, and since the outer surface is cooled, there will be a temperature gradient through the wall. However, if the temperature wave is damped out in a very short distance from the surface, Eq. (3.63) can be used to estimate the amplitude decay and phase lag:

$$\frac{T - T_0}{T_s^* - T_0} = e^{-x(\omega/2\alpha)^{1/2}} \sin[\omega t - x(\omega/2\alpha)^{1/2}]$$

$$\omega = 2\pi \left( \frac{1000}{60} \right) = 104.7 \text{ rad/s}; \quad (\omega/2\alpha)^{1/2} = \left( \frac{104.7}{(2)(12.0 \times 10^{-6})} \right)^{1/2} = 2089 \text{ m}^{-1}$$

If  $(T^* - T_0)$  is the amplitude of the temperature variation,

$$\frac{T^* - T_0}{T_s^* - T_0} = e^{-x(\omega/2\alpha)^{1/2}} = e^{-(0.001)(2089)} = 0.124$$

Thus,

$$T_s^* - T_0 = \frac{T^* - T_0}{0.124} = \frac{0.79}{0.124} = 6.38^\circ\text{C}$$

The phase lag is  $x(\omega/2\alpha)^{1/2} = 2.09 \text{ rad} = 120 \text{ degrees}$ .

### Comments

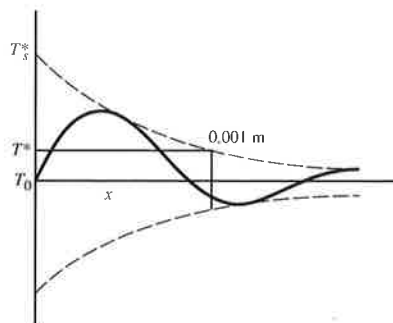
Use COND1 to examine some spatial and temporal temperature profiles.

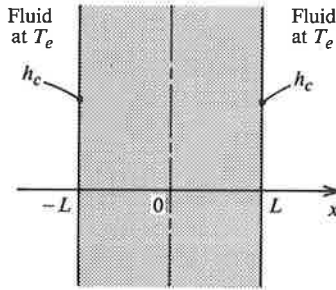
### 3.4.3 Convective Cooling of Slabs, Cylinders, and Spheres

We now consider the more general problem of transient conduction in three common shapes: the infinite slab, the infinite cylinder, and the sphere, with surface cooling (or heating) by convection. The slab problem will be analyzed first, and the results will be generalized to the cylinder and sphere.

#### *Analysis for the Slab*

In Section 3.4.1, we considered the temperature response  $T(x, t)$  of a slab suddenly immersed in a fluid under conditions where the convective heat transfer resistance is negligible, that is,  $\text{Bi} = h_c L/k$  is large. On the other hand, the lumped thermal capacity model of Section 1.5 applies when the conduction resistance in the slab is negligible, that is, the Biot number is small. We now consider the general case where the convection and conduction resistances are of comparable magnitudes, giving a Biot number of order unity. The slab and coordinate system are shown in





**Figure 3.20** Schematic of a slab suddenly immersed in a fluid.

Fig. 3.20. We again define  $\eta = x/L$  and  $\zeta = \alpha t/L^2$ , but now we define the dimensionless temperature  $\theta$  in terms of the initial slab temperature  $T_0$  and fluid temperature  $T_e$  as  $\theta = (T - T_e)/(T_0 - T_e)$ . The analysis proceeds as in Section 3.4.1 to obtain

$$\theta(\zeta, \eta) = e^{-\lambda^2 \zeta} (A \cos \lambda \eta + B \sin \lambda \eta)$$

The boundary condition, Eq. (3.36b), is as before; namely,  $\partial\theta/\partial\eta|_{\eta=0} = 0$ , so  $B = 0$  and

$$\theta(\zeta, \eta) = A e^{-\lambda^2 \zeta} \cos \lambda \eta \quad (3.65)$$

However, the second boundary condition is now obtained from the requirement that the heat conduction at the surface of the solid equal the heat convection into the fluid:

$$-k \left. \frac{\partial T}{\partial x} \right|_{x=L} = h_c (T|_{x=L} - T_e)$$

which transforms into

$$-\frac{k}{L} \left. \frac{\partial \theta}{\partial \eta} \right|_{\eta=1} = h_c \theta|_{\eta=1}$$

or

$$-\left. \frac{\partial \theta}{\partial \eta} \right|_{\eta=1} = \text{Bi} \theta|_{\eta=1} \quad (3.66)$$

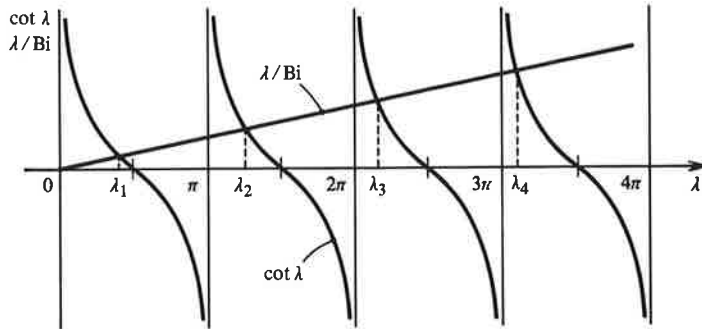
We see once again how the Biot number  $\text{Bi} = h_c L/k$  occurs naturally when the convective boundary condition is put in dimensionless form. Substituting Eq. (3.65) into Eq. (3.66) gives

$$A e^{-\lambda^2 \zeta} \lambda \sin \lambda = \text{Bi} A e^{-\lambda^2 \zeta} \cos \lambda$$

or

$$\cot \lambda = \frac{\lambda}{\text{Bi}} \quad (3.67)$$

which is a transcendental equation with an infinite number of roots or eigenvalues.



**Figure 3.21** Graphical solution of the transcendental equation, Eq. (3.67):  $\cot \lambda = \lambda/Bi$ .

Figure 3.21 shows a plot of Eq. (3.67); for a given value of the Biot number, the eigenvalues  $\lambda_n$  ( $n = 1, 2, 3, \dots$ ) can be calculated. To each of the eigenvalues corresponds a solution with eigenfunction  $\cos \lambda_n \eta$  and arbitrary constant  $A_n$ . Their sum is the general solution:

$$\theta(\zeta, \eta) = \sum_{n=1}^{\infty} A_n e^{-\lambda_n^2 \zeta} \cos \lambda_n \eta \quad (3.68)$$

The constants  $A_n$  are evaluated from the initial condition, Eq. (3.36a):

$$\theta(0, \eta) = \sum_{n=1}^{\infty} A_n \cos \lambda_n \eta = 1$$

Thus, a Fourier series expansion in terms of the eigenfunctions  $\cos \lambda_n \eta$  is required. The details are required as Exercise 3-56, and the result is

$$A_n = \frac{2 \sin \lambda_n}{\lambda_n + \sin \lambda_n \cos \lambda_n} \quad (3.69)$$

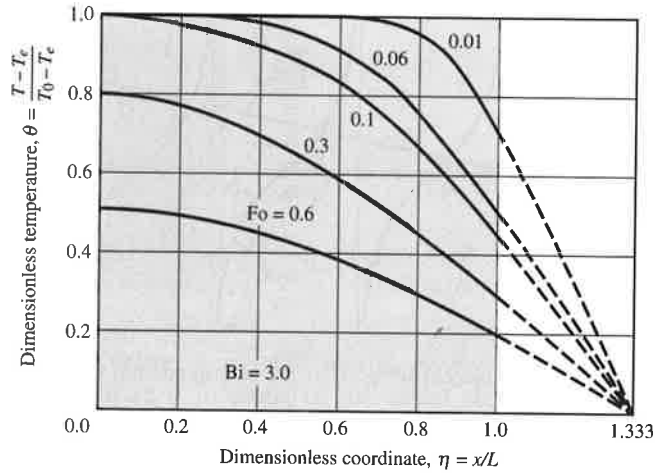
The solution in terms of temperature, Fourier number, and  $x/L$  is

$$\frac{T - T_e}{T_0 - T_e} = \sum_{n=1}^{\infty} e^{-\lambda_n^2 Fo} \frac{2 \sin \lambda_n}{\lambda_n + \sin \lambda_n \cos \lambda_n} \cos \lambda_n \frac{x}{L} \quad (3.70)$$

Figure 3.22 shows a plot of Eq. (3.70) for  $Bi = 3.0$ . Notice how the tangents to the temperature curves at the surface all intersect at a common point, the location of which is given by boundary condition, Eq. (3.66).

In addition to the temperature distribution, it is often useful to know the **fractional energy loss**  $\Phi$ , which is the actual energy loss in time  $t$  divided by the total loss in cooling completely to the ambient temperature. An energy balance on unit area of the half slab gives

$$\Phi = \frac{\int_0^t q_s dt}{\rho c L (T_0 - T_e)} = \frac{\rho c L (T_0 - \bar{T})}{\rho c L (T_0 - T_e)} = 1 - \frac{\bar{T} - T_e}{T_0 - T_e}$$

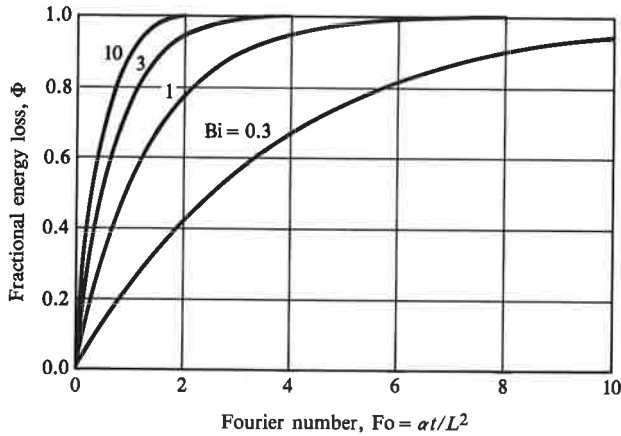


**Figure 3.22** Temperature profiles for convective cooling of a slab calculated from Eq. (3.70);  $Bi = 3.0$ .

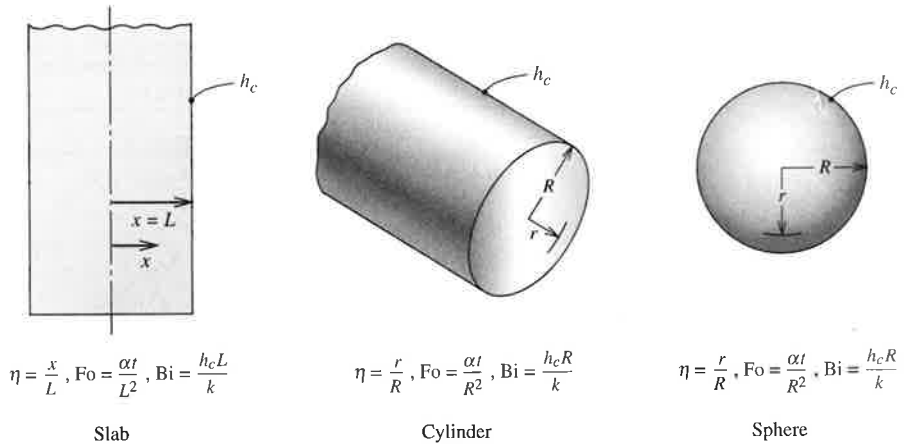
where  $\bar{T}$  is the volume-averaged temperature. Evaluating  $\bar{T}$  from Eq. (3.70) gives

$$\Phi = 1 - \sum_{n=1}^{\infty} e^{-\lambda_n^2 Fo} \frac{2 \sin \lambda_n}{\lambda_n + \sin \lambda_n \cos \lambda_n} \frac{\sin \lambda_n}{\lambda_n} \tag{3.71}$$

Figure 3.23 shows a plot of Eq. (3.71) for various values of the Biot number.



**Figure 3.23** Fractional energy loss  $\Phi$  as a function of Fourier number  $\alpha t/L^2$  for convective cooling of a slab calculated from Eq. (3.71). Biot number  $Bi = 0.3, 1, 3,$  and  $10$ .



**Figure 3.24** Schematic for the generalized solution of the temperature response of a convectively cooled slab, cylinder, or sphere.

### Generalized Form of the Solution

It is convenient to have a general form of the solution applicable to a slab, cylinder, or sphere. Referring to Fig. 3.24,

$$\theta = \sum_{n=1}^{\infty} A_n e^{-\lambda_n^2 Fo} f_n(\lambda_n \eta) \quad (3.72)$$

$$\Phi = 1 - \bar{\theta} = 1 - \sum_{n=1}^{\infty} A_n e^{-\lambda_n^2 Fo} B_n \quad (3.73)$$

with the eigenvalues given by

$$\text{Slab:} \quad \text{Bi} \cos \lambda - \lambda \sin \lambda = 0 \quad (3.74a)$$

$$\text{Cylinder:} \quad \lambda J_1(\lambda) - \text{Bi} J_0(\lambda) = 0 \quad (3.74b)$$

$$\text{Sphere:} \quad \lambda \cos \lambda + (\text{Bi} - 1) \sin \lambda = 0 \quad (3.74c)$$

For the slab,  $\eta = x/L$ ,  $Fo = \alpha t/L^2$ , and  $\text{Bi} = h_c L/k$ , as before; for the cylinder and sphere,  $\eta = r/R$ ,  $Fo = \alpha t/R^2$ , and  $\text{Bi} = h_c R/k$ . Table 3.4 gives  $A_n$ ,  $f_n$ , and  $B_n$ . In Eq. (3.74b)  $J_0$  and  $J_1$  are Bessel functions of the first kind, of orders 0 and 1, respectively. These functions are defined and tabulated in Appendix B.

Notice that the characteristic lengths used to define the Biot number are the slab half-width,  $L$ , and cylinder or sphere radius,  $R$ . Recall that in the lumped thermal capacity analysis of Section 1.5, we defined the characteristic length as volume/area,  $V/A$ . For a slab,  $V/A = L$ , so the Biot numbers are the same. However, for the cylinder and sphere,  $V/A = R/2$  and  $R/3$ , respectively, and the Biot number definitions are different.

**Table 3.4** The constants  $A_n$  and  $B_n$  and the function  $f_n$  for the transient thermal response of slabs, cylinders, and spheres.

Geometry	$A_n(\lambda_n)$	$B_n(\lambda_n)$	$f_n(\lambda_n, \eta)$
Slab	$2 \frac{\sin \lambda_n}{\lambda_n + \sin \lambda_n \cos \lambda_n}$	$\frac{\sin \lambda_n}{\lambda_n}$	$\cos\left(\lambda_n \frac{x}{L}\right)$
Cylinder	$2 \frac{J_1(\lambda_n)}{\lambda_n [J_0^2(\lambda_n) + J_1^2(\lambda_n)]}$	$2 \frac{J_1(\lambda_n)}{\lambda_n}$	$J_0\left(\lambda_n \frac{r}{R}\right)$
Sphere	$2 \frac{\sin \lambda_n - \lambda_n \cos \lambda_n}{\lambda_n - \sin \lambda_n \cos \lambda_n}$	$3 \frac{\sin \lambda_n - \lambda_n \cos \lambda_n}{\lambda_n^3}$	$\frac{\sin [\lambda_n (r/R)]}{\lambda_n (r/R)}$

**Computer Program COND2**

The generalized form of the solution described above is implemented in COND2. The program computes the eigenvalues from Eqs. (3.74) using Newton's method. Up to 40 eigenvalues are calculated in order to meet a specified accuracy of  $10^{-4}$  in the dimensionless temperature  $\theta$ . For very short times, more than 40 eigenvalues are required to obtain the desired accuracy. Thus, for Fourier number  $Fo < 10^{-3}$ , COND1 should be used, since the semi-infinite solid model is quite appropriate for such short times. The output can be obtained as numerical data, a plot of the temperature profile,  $\theta(\eta)$ , or a plot of the fractional energy loss as a function of time,  $\Phi(Fo)$ .

**Approximate Solutions for Long Times**

In Section 3.4.1, it was shown that the series solution converged rapidly for long times, and for  $Fo > 0.2$ , only the first term of the series need be retained for 2% accuracy. Usually we are most interested in the temperature at the center of the body ( $x = 0$  or  $r = 0$ ), where the response is slowest. Denoting the dimensionless center temperature as  $\theta_c = (T_c - T_e)/(T_0 - T_e)$  and retaining only the first term of Eq. (3.72) gives

$$\theta_c = A_1 e^{-\lambda_1^2 Fo}, \quad Fo > 0.2 \quad (3.75)$$

since  $f_1(\lambda_1 \eta) = 1$  for  $\eta = 0$ . When only the first term of the series is retained, the *shape* of the temperature distribution is unchanging with time. Thus, the temperature at any location is simply related to the center temperature as

$$\theta = \theta_c f_1(\lambda_1 \eta), \quad Fo > 0.2 \quad (3.76)$$

Similarly, retaining only one term in Eq. (3.73), the fractional energy loss is

$$\Phi = 1 - B_1 \theta_c, \quad Fo > 0.2 \quad (3.77)$$

Table 3.5 gives values of  $\lambda_1^2$ ,  $A_1$ , and  $B_1$  as a function of Biot number.



**Table 3.5** Constants in the one-term approximation for convective cooling of slabs, cylinders, and spheres.

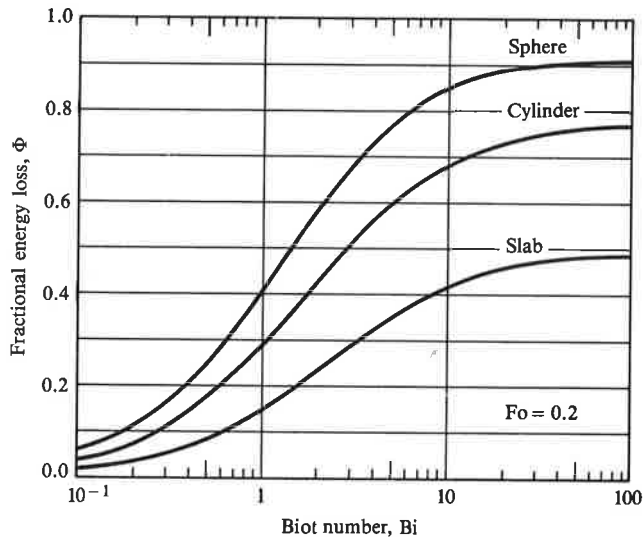
Slab							
Bi	$\lambda_1^2$	$A_1$	$B_1$	Bi	$\lambda_1^2$	$A_1$	$B_1$
0.02	0.01989	1.0033	0.9967	2	1.160	1.180	0.8176
0.04	0.03948	1.0066	0.9934	4	1.600	1.229	0.7540
0.06	0.05881	1.0098	0.9902	6	1.821	1.248	0.7229
0.08	0.07790	1.0130	0.9871	8	1.954	1.257	0.7047
0.10	0.09678	1.016	0.9839	10	2.042	1.262	0.6928
0.2	0.1873	1.031	0.9691	20	2.238	1.270	0.6665
0.4	0.3519	1.058	0.9424	30	2.311	1.272	0.6570
0.6	0.4972	1.081	0.9192	40	2.321	1.272	0.6521
0.8	0.6257	1.102	0.8989	50	2.371	1.273	0.6490
1.0	0.7401	1.119	0.8811	100	2.419	1.273	0.6429
				$\infty$	2.467	1.273	0.6366

Cylinder							
Bi	$\lambda_1^2$	$A_1$	$B_1$	Bi	$\lambda_1^2$	$A_1$	$B_1$
0.02	0.03980	1.0051	0.9950	2	2.558	1.338	0.7125
0.04	0.07919	1.010	0.9896	4	3.641	1.470	0.6088
0.06	0.1182	1.015	0.9844	6	4.198	1.526	0.5589
0.08	0.1568	1.020	0.9804	8	4.531	1.553	0.5306
0.10	0.1951	1.025	0.9749	10	4.750	1.568	0.5125
0.2	0.3807	1.049	0.9526	20	5.235	1.593	0.4736
0.4	0.7552	1.094	0.9112	30	5.411	1.598	0.4598
0.6	1.037	1.135	0.8753	40	5.501	1.600	0.4527
0.8	1.320	1.173	0.8430	50	5.556	1.601	0.4485
1.0	1.577	1.208	0.8147	100	5.669	1.602	0.4401
				$\infty$	5.784	1.602	0.4317

Sphere							
Bi	$\lambda_1^2$	$A_1$	$B_1$	Bi	$\lambda_1^2$	$A_1$	$B_1$
0.02	0.05978	1.0060	0.9940	2	4.116	1.479	0.6445
0.04	0.1190	1.012	0.9881	4	6.030	1.720	0.5133
0.06	0.1778	1.018	0.9823	6	7.042	1.834	0.4516
0.08	0.2362	1.024	0.9766	8	7.647	1.892	0.4170
0.10	0.2941	1.030	0.9710	10	8.045	1.925	0.3952
0.2	0.5765	1.059	0.9435	20	8.914	1.978	0.3500
0.4	1.108	1.116	0.8935	30	9.225	1.990	0.3346
0.6	1.599	1.171	0.8490	40	9.383	1.994	0.3269
0.8	2.051	1.224	0.8094	50	9.479	1.996	0.3223
1.0	2.467	1.273	0.7740	100	9.673	1.999	0.3131
				$\infty$	9.869	2.000	0.3040



**Figure 3.25** Fractional energy loss  $\Phi$  at a Fourier number (dimensionless time) of  $Fo = 0.2$  for the slab, cylinder, and sphere: effect of Biot number  $Bi$ . The one-term approximation is valid above each curve.

The single-term approximation is useful because it is valid during much of the cooling period. Figure 3.25 shows the fractional energy loss  $\Phi$  at  $Fo = 0.2$  as a function of  $Bi$  for the three shapes. The fraction of the cooling period over which the approximation is valid increases as the Biot number and surface-area/volume ratio (sphere-cylinder-slab) decrease. The single-term approximation is also used for problems in which the fluid temperature  $T_e$  changes slowly with time. It is then useful to define an *interior heat transfer coefficient* for conduction into the body for use in a thermal-circuit representation of the complete system. This concept is developed and used in Exercises 3–81 through 3–84.

### Temperature Response Charts

Graphs of the various solutions for convective cooling, known as *temperature response charts*, were indispensable to engineers until handheld calculators and personal computers became standard tools. Charts for the series solution were given by Gurney and Lurie [10] as early as 1923, but better examples are now available. Perhaps the best widely available selection of charts is found in the *Handbook of Heat Transfer Fundamentals* [11]. In addition to charts for the convective cooling problem discussed here, Reference [11] gives charts for numerous other cooling and heating problems. For example, there are charts for radiation heating, conduction with internal heat generation, and composite solids. These charts were first published by Schneider in 1963 [12].

Heisler published charts for the one-term approximate solution in 1947 [13]. Heisler-type charts are found in many textbooks and are widely used. However, such charts have three major limitations:

1. The charts are invalid for  $Fo < 0.2$ .
2. The charts are often difficult to read accurately for  $Fo \leq 1$ .
3. The cooling process is nearly complete over a large region of the charts. For example, for a sphere with  $Bi \geq 1$ , it is 90% complete for  $Fo \geq 1$ .

Appendix C contains temperature response charts for convective cooling. Two types of charts for the slab, cylinder, and sphere are given. Figure C.1 gives the temperature response of the body center ( $x = 0$  or  $r = 0$ ), and Fig. C.2 gives the fractional energy loss  $\Phi$  as a function of time. Both figures are based on the complete solution and are thus valid for all values of Fourier number. The curves for  $Bi = 1000$  in Fig. C.1 correspond to negligible convective resistance and, hence, to a prescribed surface temperature  $T_s = T_e$ .

### *Problem-Solving Strategy*

Our solutions for convective cooling (or heating) of slabs, cylinders, and spheres can be organized in the form of a problem-solving strategy. The basic problem is one where the heat transfer coefficient is known, and the temperature or fractional heat loss must be calculated at a given time. Then we may proceed as follows:

1. Calculate the lumped thermal capacity model Biot number.<sup>2</sup> If  $Bi < 0.1$ , the lumped thermal capacity solution of Section 1.5 applies.
2. If  $Bi > 0.1$ , calculate the Fourier number. If  $Fo < 0.05$ , the semi-infinite solid solution, Eq. (3.61), applies. A handheld calculator or COND1 can be used.
3. If  $Bi > 0.1$  and  $0.05 < Fo < 0.2$ , the complete series solution, Eqs. (3.72) and (3.73), applies. COND2 or the temperature response charts in Appendix C should be used.<sup>3</sup>
4. If  $Bi > 0.1$  and  $Fo > 0.2$ , the long-time approximate solution, Eqs. (3.75) through (3.77), applies. COND2 can be used if available. Otherwise, the temperature response charts or a handheld calculator will suffice.

Sometimes a problem may be posed in such a manner that the foregoing procedure cannot be followed exactly (as will be the case in Examples 3.9 and 3.10). Also, as in all engineering problem solving, the required accuracy of a particular calculation should be viewed in the context of the complete problem. It is of little value to obtain  $\theta$  or  $\Phi$  to even two-figure accuracy when the model is a poor simulation of

<sup>2</sup>  $Bi = h_c(V/A)/k$ ;  $V/A = L$  for an infinite slab,  $R/2$  for an infinite cylinder, and  $R/3$  for a sphere.

<sup>3</sup> For a slab, the required value of  $Bi$  was calculated in step 1. For a cylinder and sphere, the required values are two and three times larger, respectively.

the real engineering problem. The major source of error here is in the specification of the heat transfer coefficient. Not only is it difficult to specify a value of  $h_c$  with less than 10% error, but in many cooling problems,  $h_c$  is not a constant as assumed by the model. For example, when the cooling is by natural convection, Eq. (1.23) shows that  $h_c$  is proportional to  $(T_s - T_e)$  to the 1/4 power for laminar flow, and to the 1/3 power for turbulent flow. Thus,  $h_c$  must be estimated at some average temperature difference.

---

### EXAMPLE 3.9 Annealing of Steel Plate

When steel plates are thinned by rolling, periodic reheating is required. Plain carbon steel plate 8 cm thick, initially at 440°C, is to be reheated to a minimum temperature of 520°C in a furnace maintained at 600°C. If the sum of the convective and radiative heat transfer coefficients is estimated to be 200 W/m<sup>2</sup> K, how long will the reheating take? Take  $k = 40$  W/m K and  $\alpha = 8.0 \times 10^{-6}$  m<sup>2</sup>/s for the steel.

#### Solution

**Given:** Steel plate, thickness  $2L = 8$  cm.

**Required:** Temperature response of the center of the plate.

**Assumptions:** The heat transfer coefficient is constant at 200 W/m<sup>2</sup> K.

We first calculate the time constant for the heating process:

$$t_c = \frac{L^2}{\alpha} = \frac{(0.04)^2}{8 \times 10^{-6}} = 200 \text{ s}$$

which tells us the order of magnitude of the time required, namely, a few minutes (not seconds and not hours). Next we calculate the Biot number:

$$\text{Bi} = \frac{hL}{k} = \frac{(200)(0.040)}{40} = 0.2$$

Since  $\text{Bi} > 0.1$ , the lumped thermal capacity model should not be used. Since we cannot calculate the Fourier number yet (it is the answer to the problem), the complete series solution will be used. The minimum temperature is at the center of the plate, and the desired value of  $\theta$  is

$$\theta_c = \frac{T_c - T_e}{T_0 - T_e} = \frac{520 - 600}{440 - 600} = 0.50$$

Using the temperature response chart, Fig. C.1a in Appendix C,

$$\text{Fo} = 3.9; \quad t = t_c \text{Fo} = (200)(3.9) = 780 \text{ s (13 min)}$$

Since  $\text{Fo} > 0.2$ , we could have used the one-term approximation, Eq. (3.75):

$$\theta_c = 0.5 = A_1 e^{-\lambda_1^2 \text{Fo}}$$

From Table 3.5 for  $\text{Bi} = 0.2$ ,  $\lambda_1^2 = 0.1873$  and  $A_1 = 1.031$ . Solving,  $\text{Fo} = 3.86$ .

**Solution Using COND2**

The required inputs are:

$$\text{Geometry} = 1 \text{ (slab)}$$

$$\text{Bi} = 0.2$$

$$\text{Output option} = 2 \text{ } (\theta \text{ vs. } \eta \text{ plot})$$

$$\text{Fo} = \text{(must guess and iterate)}$$

$$\eta \text{ range} = 0, 1$$

A few iterations will give  $\text{Fo} = 3.9$  for  $\theta_c = 0.50$ .

**EXAMPLE 3.10** A Pebble Bed Air Heater

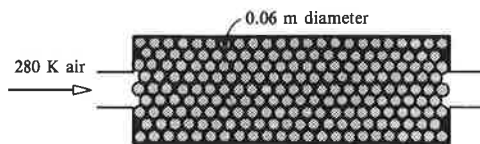
A pebble bed for storing thermal energy in a solar heating system has pebbles that can be approximated as 6 cm-diameter spheres. The bed is initially at 350 K before cold air at 280 K is admitted to the bed. If the heat transfer coefficient is  $80 \text{ W/m}^2 \text{ K}$ , how long will it take the pebbles at the inlet of the bed to lose 90% of their available energy? Take  $k = 1.6 \text{ W/m K}$  and  $\alpha = 0.7 \times 10^{-6} \text{ m}^2/\text{s}$  for the pebbles.

**Solution**

**Given:** Hot pebbles suddenly exposed to a cold air stream.

**Required:** Time for pebbles at inlet to lose 90% of their available energy.

**Assumptions:** Pebbles are spherical.



We first calculate the time constant for the cooling process:

$$t_c = \frac{R^2}{\alpha} = \frac{(0.03)^2}{0.7 \times 10^{-6}} = 1286 \text{ s (21 min)}$$

Next we calculate the lumped thermal capacity model Biot number:

$$\text{Bi} = \frac{h_c(R/3)}{k} = \frac{(80)(0.03/3)}{1.6} = 0.5$$

Since  $\text{Bi} > 0.1$ , the lumped thermal capacity method cannot be used. Although we suspect that  $\text{Fo} > 0.2$  for  $\Phi = 0.9$ , we can conveniently use the complete series solution given as the temperature response chart, Fig. C.2c of Appendix C. For  $\text{Bi} = h_c R/k = (3)(0.5) = 1.5$  and  $\Phi = 0.9$ , the chart gives  $\text{Bi}^2 \text{Fo} = 1.5$ . Thus,

$$\text{Fo} = 1.5/\text{Bi}^2 = 1.5/(1.5)^2 = 0.67$$

$$t = t_c \text{Fo} = (1286)(0.67) = 860 \text{ s } (\sim 14 \text{ min})$$

Since  $Fo > 0.2$ , we could have used the one-term approximate solution as follows. From Eq. (3.77),  $\Phi = 1 - B_1\theta_c$ . For  $Bi = 1.5$ , interpolation in Table 3.5 gives  $B_1 = 0.70$ . Thus,

$$0.9 = 1 - (0.70)\theta_c \quad \text{or} \quad \theta_c = 0.143$$

By Eq. (3.75),  $\theta_c = A_1 e^{-\lambda_1^2 Fo}$ . For  $Bi = 1.5$ , interpolation in Table 3.5 gives  $\lambda_1^2 = 3.33$ ,  $A_1 = 1.38$ .

$$0.143 = (1.38)e^{-(3.33)Fo} \quad \text{or} \quad Fo = 0.68$$

which agrees well with the chart solution.

### Solution using COND2

The required input is:

Geometry = 3 (sphere)

Bi = 1.5

Output option = 1 (Numerical data), or 3 ( $\Phi$  vs. Fo plot)

Fo range = 0, 1

Fo = 0.67 for  $\Phi = 0.9$ .

### Comments

The relatively short time of 14 min does not mean that warm air cannot be obtained for a long period. The bed is a regenerative heat exchanger (see Section 8.5): a temperature “wave” passes slowly through the bed, and the useful operating time is the time taken for this wave to break through the outlet end of the bed.

### 3.4.4 Product Solutions for Multidimensional Unsteady Conduction

Consider a long rectangular bar, with sides  $2L_1$  and  $2L_2$  wide, that is initially at temperature  $T_0$  and suddenly immersed in a fluid at temperature  $T_e$ . The heat transfer coefficients on the sides are  $h_{c1}$  and  $h_{c2}$ . The task is to determine the temperature distribution  $T(x, y, t)$ . Again, a dimensionless temperature  $\theta = (T - T_e)/(T_0 - T_e)$  is defined. The governing equation and appropriate initial and boundary conditions in a coordinate system such that  $-L_1 \leq x \leq L_1$ ,  $-L_2 \leq y \leq L_2$  are

$$\frac{\partial \theta}{\partial t} = \alpha \left( \frac{\partial^2 \theta}{\partial x^2} + \frac{\partial^2 \theta}{\partial y^2} \right) \quad (3.78)$$

$$t = 0: \quad \theta = 1$$

$$x = 0: \quad \frac{\partial \theta}{\partial x} = 0; \quad y = 0: \quad \frac{\partial \theta}{\partial y} = 0$$

$$x = L_1: \quad -k \frac{\partial \theta}{\partial x} = h_{c1} \theta; \quad y = L_2: \quad -k \frac{\partial \theta}{\partial y} = h_{c2} \theta$$

If the *separation of variables* method is to be used, one might assume a product solution of the form

$$\theta(t, x, y) = \mathcal{F}(t)X(x)Y(y)$$

where the functions  $\mathcal{F}(t)$ ,  $X(x)$ , and  $Y(y)$  are to be determined as before. However, it will now be shown that the solution can be expressed as the product of known solutions for the infinite slab. Consider two slabs of thickness  $2L_1$  and  $2L_2$ , for which the dimensionless temperature governing equations and boundary conditions are

$$\begin{aligned} \theta_1 &= \frac{T_1 - T_e}{T_0 - T_e} & \theta_2 &= \frac{T_2 - T_e}{T_0 - T_e} \\ \frac{\partial \theta_1}{\partial t} &= \alpha \frac{\partial^2 \theta_1}{\partial x^2} & \frac{\partial \theta_2}{\partial t} &= \alpha \frac{\partial^2 \theta_2}{\partial y^2} & (3.79a,b) \\ t = 0: \quad \theta_1 &= 1 & t = 0: \quad \theta_2 &= 1 \\ x = 0: \quad \frac{\partial \theta_1}{\partial x} &= 0 & y = 0: \quad \frac{\partial \theta_2}{\partial y} &= 0 \\ x = L_1: \quad -k \frac{\partial \theta_1}{\partial x} &= h_{c1} \theta_1 & y = L_2: \quad -k \frac{\partial \theta_2}{\partial y} &= h_{c2} \theta_2 \end{aligned}$$

The product of the solutions of these two problems satisfies the original problem. Let

$$\theta(t, x, y) = \theta_1(t, x)\theta_2(t, y)$$

Then

$$\frac{\partial^2 \theta}{\partial x^2} = \theta_2 \frac{\partial^2 \theta_1}{\partial x^2}; \quad \frac{\partial^2 \theta}{\partial y^2} = \theta_1 \frac{\partial^2 \theta_2}{\partial y^2} \quad (3.80a,b)$$

$$\frac{\partial \theta}{\partial t} = \theta_1 \frac{\partial \theta_2}{\partial t} + \theta_2 \frac{\partial \theta_1}{\partial t} \quad (3.81)$$

Substituting Eqs. (3.79a,b) into Eq. (3.81),

$$\frac{\partial \theta}{\partial t} = \alpha \left( \theta_1 \frac{\partial^2 \theta_2}{\partial y^2} + \theta_2 \frac{\partial^2 \theta_1}{\partial x^2} \right)$$

Then substituting from Eqs. (3.80a,b) gives

$$\frac{\partial \theta}{\partial t} = \alpha \left( \frac{\partial^2 \theta}{\partial x^2} + \frac{\partial^2 \theta}{\partial y^2} \right)$$

which is the original differential equation, Eq. (3.78). Also, the initial and boundary conditions become

$$\begin{aligned}
 t = 0: \quad & \theta(0, x, y) = \theta_1(0, x)\theta_2(0, y) = (1)(1) = 1 \\
 x = 0: \quad & \frac{\partial \theta}{\partial x} = \theta_2 \frac{\partial \theta_1}{\partial x} = \theta_2 \times 0 = 0 \\
 y = 0: \quad & \frac{\partial \theta}{\partial y} = \theta_1 \frac{\partial \theta_2}{\partial y} = \theta_1 \times 0 = 0 \\
 x = L_1: \quad & -k \frac{\partial \theta}{\partial x} = \theta_2 \left( -k \frac{\partial \theta_1}{\partial x} \right) = \theta_2 (h_{c1} \theta_1) = h_{c1} \theta \\
 y = L_2: \quad & -k \frac{\partial \theta}{\partial y} = \theta_1 \left( -k \frac{\partial \theta_2}{\partial y} \right) = \theta_1 (h_{c2} \theta_2) = h_{c2} \theta
 \end{aligned}$$

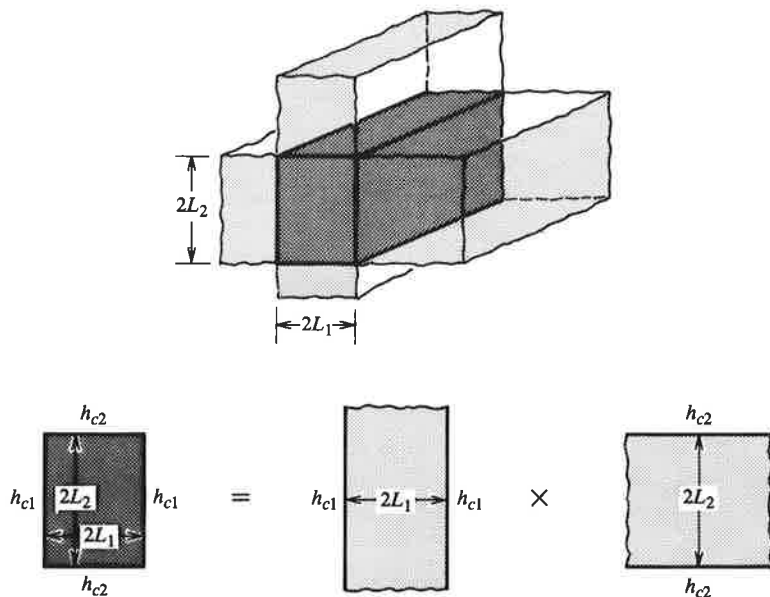
which are the original conditions. Figure 3.26 shows a schematic of the product solution.

Shapes amenable to product solutions of this type are shown in Table 3.6. Langston [14] has recently shown how the product rule can be applied to obtain the fractional energy loss. If the shape is formed by the intersection of two bodies, for example, the short cylinder of item 4 in Table 3.6, the fractional energy loss is

$$\Phi = \Phi_1 + \Phi_2(1 - \Phi_1) = \Phi_1 + \Phi_2 - \Phi_1\Phi_2 \quad (3.82a)$$

where subscripts 1 and 2 refer to the infinite slab and infinite cylinder, respectively. If the shape is formed by the intersection of three bodies, for example, the rectangular block of item 6 in Table 3.6, then

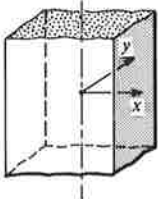
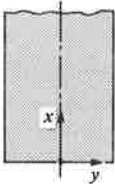
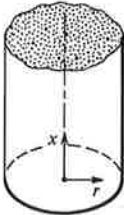
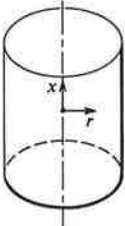
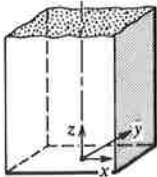
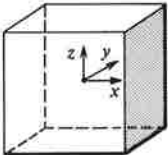
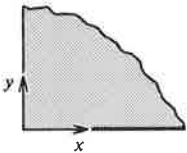
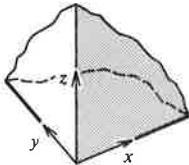
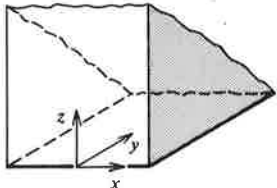
$$\Phi = \Phi_1 + \Phi_2(1 - \Phi_1) + \Phi_3(1 - \Phi_1)(1 - \Phi_2) \quad (3.82b)$$



**Figure 3.26** Schematic of the product solution procedure for the temperature response of a convectively cooled long rectangular bar.



**Table 3.6** Shapes amenable to product solutions. *Caution:* The dimensionless temperatures  $S$ ,  $P$ , and  $C$  are evaluated at the same value of actual time (not Fourier number).

Basic solutions		
Semi-infinite solid $S(x,t)$ Eq. (3.61); $1 - \frac{(T - T_0)}{(T_e - T_0)}$	Infinite plane slab $P(x,t)$ Eq. (3.70)	Infinite cylinder $C(r,t)$ Eq. (3.72)
1. Infinite rectangular bar $\theta = P(x,t)P(y,t)$ 	2. Semi-infinite plate $\theta = S(x,t)P(y,t)$ 	3. Semi-infinite cylinder $\theta = S(x,t)C(r,t)$ 
4. Finite cylinder $\theta = P(x,t)C(r,t)$ 	5. Semi-infinite rectangular bar $\theta = S(z,t)P(x,t)P(y,t)$ 	6. Rectangular block $\theta = P(x,t)P(y,t)P(z,t)$ 
7. Two-dimensional corner $\theta = S(x,t)S(y,t)$ 	8. Three-dimensional corner $\theta = S(x,t)S(y,t)S(z,t)$ 	9. Finite-width corner $\theta = P(x,t)S(y,t)S(z,t)$ 

Notice that these product solutions are not applicable when

1. The initial temperature of the body is nonuniform.
2. The fluid temperature  $T_e$  is not the same on all sides of the body.
3. The surface boundary conditions are of the second kind.

The requirement that the initial temperature of the body be uniform is, of course, the specified initial condition for the solutions given by Eqs. (3.72) and (3.73). However, the beginning student often overlooks this point in problem solving.

**EXAMPLE 3.11** Sterilization of a Can of Vegetables

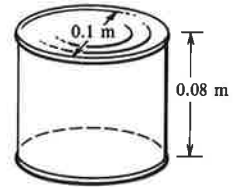
A can of vegetables 10 cm in diameter and 8 cm high is to be sterilized by immersion in saturated steam at 105°C. If the initial temperature is 40°C, what will be the minimum temperature in the can after 80 minutes? Also, calculate the total heat transfer to the can in this period.

**Solution**

**Given:** Can of vegetables to be sterilized in steam.

**Required:** (i) Minimum temperature in can after 80 minutes, and  
(ii) total heat transfer.

**Assumptions:** 1. The heat transfer coefficient for condensing steam is very large; hence,  $Bi \rightarrow \infty$ .  
2. No circulation inside can.  
3. Thermal diffusivity of contents approximates that of water.



(i) Since  $Bi \rightarrow \infty$ , the lumped thermal capacity model cannot be used. Item 4 of Table 3.6 applies, with the minimum temperature at the center of the can. The thermal diffusivity is evaluated at a guessed average temperature of 360 K; using the data in Table A.8 of Appendix A,  $k = 0.676$  W/m K,  $\rho = 967$  kg/m<sup>3</sup>,  $c = 4200$  J/kg K; hence,  $\alpha = k/\rho c = (0.676)/(967)(4200) = 0.166 \times 10^{-6}$  m<sup>2</sup>/s. The two Fourier numbers are:

$$\text{Slab with 4 cm half-width:} \quad Fo_1 = \frac{\alpha t}{L^2} = \frac{(0.166 \times 10^{-6})(4800)}{(0.04)^2} = 0.498$$

$$\text{Infinite cylinder of 5 cm radius:} \quad Fo_2 = \frac{\alpha t}{R^2} = \frac{(0.166 \times 10^{-6})(4800)}{(0.05)^2} = 0.319$$

Then  $\theta_c = P(0, t)C(0, t)$ , where  $P(0, t)$  and  $C(0, t)$  can be obtained from Fig. C.1a and b of Appendix C or by using COND2. Using the charts with  $Bi = 1000$ ,  $P(0, t) = 0.38$  and  $C(0, t) = 0.27$ .

$$\theta_c = \frac{T_c - T_e}{T_0 - T_e} = P(0, t)C(0, t)$$

$$\frac{T_c - 105}{40 - 105} = (0.38)(0.27); \quad \text{solving, } T_c = 98.3^\circ\text{C}$$

(ii) The total heat transfer is related to the fractional energy gain as

$$Q = \Phi \rho c V (T_e - T_0)$$

where  $V$  is the volume of the can and  $\Phi = \Phi_1 + \Phi_2 - \Phi_1 \Phi_2$  from Eq. (3.82a). Using COND2 or Fig. C.2a and b, with  $Bi = 50$ ,  $\Phi_1 = 0.75$ ,  $\Phi_2 = 0.88$ . Thus,

$$\Phi = 0.75 + 0.88 - (0.75)(0.88) = 0.97$$

$$Q = (0.97)(967)(4200)(\pi)(0.05)^2(0.08)(105 - 40) = 161 \text{ kJ}$$

### Comments

Although the heat transfer coefficient for condensing steam is large (see Chapter 7), it is not infinite. Using the curves for the largest values of  $Bi$  available in the charts gives satisfactory estimates for this problem.

## 3.5 MOVING-BOUNDARY PROBLEMS

There are many engineering problems that involve heat conduction in a region bounded by a moving surface. Examples include solidification of a melt to form a crystal, growth of a vapor bubble in a superheated liquid, and ablation of a heat shield on a reentry vehicle. There is usually either a phase change or chemical reaction at the surface. In the case of a phase change, a boundary condition of the form of Eq. (3.18) is appropriate. For a chemical reaction, the boundary condition is considerably more complicated and may involve mass transfer as well as heat transfer considerations. In this brief introduction to the analysis of *moving-boundary problems*, exact solutions to two rather simple problems are demonstrated.

### 3.5.1 Solidification from a Melt

Consider a liquid, initially at its solidification temperature  $T_s$ , suddenly exposed to a surface at temperature  $T_i < T_s$ , located at  $z = 0$ , as shown in Fig. 3.27. A solidification front then moves upward, and the expected temperature profile when the front is at  $z = s$  is shown. Let  $\theta = (T - T_i)/(T_s - T_i)$ ; assuming constant properties, the temperature in the solid is governed by Fourier's equation,

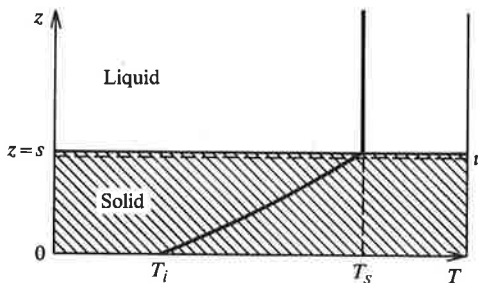
$$\frac{\partial \theta}{\partial t} = \alpha \frac{\partial^2 \theta}{\partial z^2} \quad (3.83)$$

with initial and boundary conditions

$$t = 0: \quad \theta = 1 \quad (3.84a)$$

$$z = 0: \quad \theta = 0 \quad (3.84b)$$

$$z = s: \quad \theta = 1 \quad (3.84c)$$



**Figure 3.27** Solidification from a liquid: coordinate system and instantaneous temperature profile.

The unknown location of the interface is determined from the interface energy balance, Eq. (3.18). Since there is no temperature gradient in the liquid phase, Eq. (3.18) reduces to

$$0 = k \left. \frac{\partial T}{\partial z} \right|_u + \dot{m}'' h_{fs} \quad (3.85)$$

where  $\dot{m}''$  [kg/m<sup>2</sup> s] is the solidification rate and is negative to be consistent with Eq. (3.18). With respect to the interface, the liquid flows across in the negative  $z$  direction. The speed at which the front moves is

$$V = \frac{ds}{dt} = -\frac{\dot{m}''}{\rho} \quad (3.86)$$

Substituting for  $T$  and  $\dot{m}''$  in Eq. (3.85) gives

$$k(T_s - T_i) \left. \frac{\partial \theta}{\partial z} \right|_u - \rho h_{fs} V = 0 \quad (3.87)$$

Based on our experience with the semi-infinite solid problem of Section 3.4.2, we might suspect that the solution has the form

$$\theta = A \operatorname{erf} \frac{z}{(4\alpha t)^{1/2}} \quad (3.88)$$

We know Eq. (3.88) satisfies the differential equation; the task is to see if it can fit the initial and boundary conditions. Equations (3.84a) and (3.84b) are satisfied since  $\operatorname{erf} \infty = 1$  and  $\operatorname{erf} 0 = 0$ ; Eq. (3.84c) requires that

$$A \operatorname{erf} \frac{s}{(4\alpha t)^{1/2}} = 1$$

which is possible only if  $s$  is proportional to  $t^{1/2}$ . To simplify the algebra, we set  $s = \lambda(4\alpha t)^{1/2}$ , where  $\lambda$  is a constant yet to be determined. Then  $A = 1/\operatorname{erf} \lambda$ , so that Eq. (3.88) gives the temperature distribution  $T(z, t)$  as

$$\frac{T - T_i}{T_s - T_i} = \theta = \frac{\operatorname{erf}[z/(4\alpha t)^{1/2}]}{\operatorname{erf} \lambda}$$

Also,

$$V = \frac{ds}{dt} = \lambda \left( \frac{\alpha}{t} \right)^{1/2} \quad (3.89)$$

the speed of the front.

The constant  $\lambda$  is now determined from the interface energy balance, Eq. (3.87). After some algebra (see Section 3.4.2 for differentiation of the error function), we obtain

$$\pi^{1/2} \lambda e^{\lambda^2} \operatorname{erf} \lambda = \frac{c(T_s - T_i)}{h_{fs}} \quad (3.90)$$

The right-hand side of this equation is a dimensionless group that characterizes heat transfer during phase change; it is called the **Jakob number**,  $Ja$ , or the Stefan number for a solid-liquid phase change. Equation (3.90) is an implicit relation for  $\lambda = \lambda(Ja)$  but is easily solved by specifying a range of  $\lambda$  values and then calculating the corresponding values of  $Ja$ . Figure 3.28 was prepared in this way.

Often the Jakob number is quite small; for example, when ice forms from water with  $T_s - T_i = 10$  K, the Jakob number is 0.058. For small Jakob numbers,  $e^{\lambda^2} \operatorname{erf} \lambda$  can be approximated as  $(2/\pi^{1/2})\lambda$ ; then

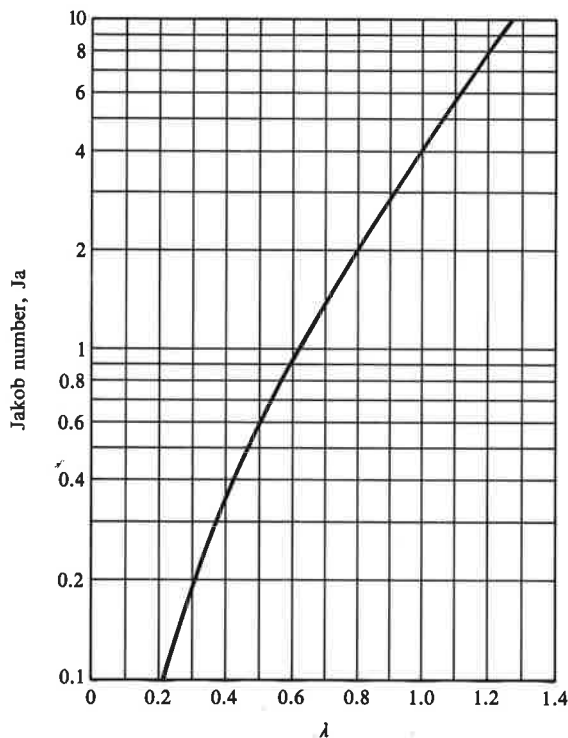
$$\lambda = \left(\frac{Ja}{2}\right)^{1/2}; \quad V = \left(\frac{Ja \alpha}{2t}\right)^{1/2} \quad (3.91)$$

This result corresponds to a linear temperature variation across the solid, as can be seen by substituting  $d\theta/dz = 1/s$  and  $V = ds/dt$  in Eq. (3.87) to give

$$\frac{ds}{dt} = \frac{\alpha Ja}{s}$$

or

$$s ds = \alpha Ja dt$$



**Figure 3.28** Solution of Eq. (3.90), namely,  $\pi^{1/2}\lambda e^{\lambda^2} \operatorname{erf} \lambda = Ja$ . The Jakob number  $Ja = c(T_s - T_i)/h_{fs}$ .

Integrating,

$$s^2 = 2\alpha Ja t \tag{3.92}$$

Equation (3.92) is called a *parabolic* growth law by metallurgists. Substituting back in Eq. (3.86) gives

$$V = \left( \frac{Ja \alpha}{2t} \right)^{1/2}$$

which is the same as Eq. (3.91). Notice that if, at the outset, we had simply assumed steady-state conduction, a linear temperature variation would have been obtained. Thus, the conduction can be said to be *quasi steady*, even though temperatures in the solid are changing with time. In terms of the physics of the problem, we are neglecting the heat loss required to cool the solid below the solidification temperature,  $T_s$ , in comparison with the enthalpy of fusion. The solid is said to be *subcooled* since its temperature is below the solid-liquid equilibrium value,  $T_s$ .

In closing, it is worthwhile to note that although the analytical solution Eq. (3.91) is for a very simple phase change problem, the result that the interface moves at a speed proportional to  $(\alpha/t)^{1/2}$  is found to apply in other geometries and in more complex situations (for example, bubble growth in some boiling heat transfer processes).

**EXAMPLE 3.12** An Ice-Making Process

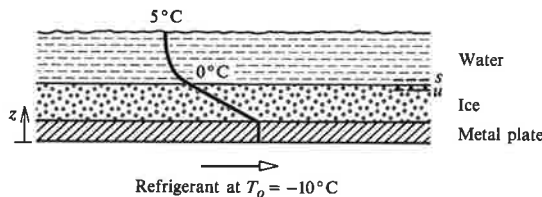
In an ice-making process, water at 5°C flows over a plate cooled by refrigerant at -10°C. When the ice layer is 2 mm thick, it is scraped off the plate, and the process repeats itself. Estimate the time interval required between scrapings. Take the overall heat transfer coefficient from the refrigerant to the plate-ice interface as 900 W/m² K. The enthalpy of fusion of ice is 335 kJ/kg.

**Solution**

**Given:** An ice-making process.

**Required:** Time to form an ice layer 2 mm thick.

- Assumptions:**
1. One-dimensional solidification.
  2. Quasi-steady conduction across the ice layer.
  3. Sensible heat loss of the water cooling from 5°C to 0°C is small compared with the enthalpy of fusion.



We have shown that the Jakob number for ice formation is small; hence, the conduction across the ice layer can be taken as quasi steady. We cannot use Eq. (3.92) for the thickness of the layer since  $T_i$  is not a constant in this problem. However, we can proceed in a similar manner. The surface energy at the ice-water interface is

$$k \frac{\partial T}{\partial z} \Big|_s = k \frac{\partial T}{\partial z} \Big|_u + \dot{m}'' h_{fs}$$

$$k \frac{\partial T}{\partial z} \Big|_s \approx 0 \quad \text{if the sensible heat loss of the water is neglected}$$

$$k \frac{\partial T}{\partial z} \Big|_u = -q = \frac{T_s - T_o}{s/k + 1/U} \quad \text{for two resistances in series}$$

$$\dot{m}'' = -\rho \frac{ds}{dt}$$

Substituting above,

$$\rho h_{fs} \frac{ds}{dt} = \frac{T_s - T_o}{s/k + 1/U}$$

This differential equation is easily solved. Separating variables and rearranging,

$$\frac{T_s - T_o}{\rho h_{fs}} dt = \left( \frac{s}{k} + \frac{1}{U} \right) ds$$

Integrating with  $s = 0$  at  $t = 0$ ,

$$\frac{T_s - T_o}{\rho h_{fs}} t = \frac{s^2}{2k} + \frac{s}{U}$$

From Table A.2 for ice at  $0^\circ\text{C}$ ,  $\rho = 910 \text{ kg/m}^3$ ,  $k = 2.22 \text{ W/m K}$ .

$$\frac{(0 - (-10))}{(910)(335 \times 10^3)} t = \frac{(0.002)^2}{(2)(2.22)} + \frac{0.002}{900}; \quad t = 95 \text{ s}$$

### Comments

1. A more complete solution for this type of problem is given by London and Seban [15].
2. The student should think about the design of an ice-making machine based on this process.

### 3.5.2 Steady-State Melting Ablation

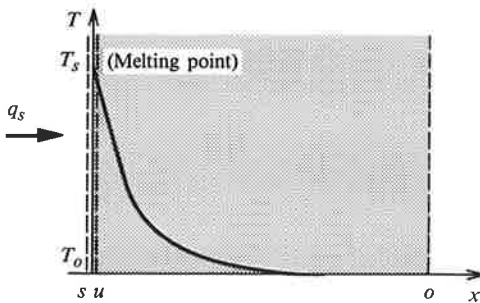
Ablative heat shields are widely used to protect structures from high heat fluxes. Heat shields are made from a great variety of materials, including refractory metals such as tungsten, Teflon, graphite, and silica-phenolic composites. The heat transfer analysis of a simple melting ablator is straightforward if it can be assumed that the



**Figure 3.29** A silica-phenolic nosecone after arc-jet testing, showing evidence of melting ablation. (Photograph courtesy of Mr. J. Courtney, TRW Systems, Redondo Beach.)

liquid melt is removed as fast as it is formed. On a reentry vehicle, the friction and pressure forces will cause the melt to flow backward over the vehicle, leaving only a thin film of negligible thermal resistance. The heat shield in Fig. 3.29 shows evidence of undergoing melting ablation. Alternatively, in some situations, gravity forces may be sufficient to ensure that the liquid drains quickly from the solid surface.

We consider the one-dimensional model of melting ablation shown in Fig. 3.30. It is assumed that the imposed heat flux  $q_s$  is a constant and is unaffected by the ablation process (most often  $q_s$  is affected by the ablation, and a coupled problem involving both the gas and solid phases must be considered). After time  $t = 0$ , there will be an initial transient as temperatures in the solid rise until a quasi-steady state is attained, with the surface temperature  $T_s$  at  $x = 0$  equal to the melting temperature. The melting rate is again denoted  $\dot{m}''$  [ $\text{kg}/\text{m}^2 \text{ s}$ ], and the surface recedes at a constant



**Figure 3.30** Schematic of one-dimensional melting ablation.



speed  $\dot{m}''/\rho$ , where  $\rho$  is the density of the solid. The relation between  $\dot{m}''$  and  $q_s$  can be obtained without knowing the temperature profile in the solid, as will now be demonstrated.

Figure 3.31 shows a control volume located between  $s$ - and  $o$ -surfaces. The  $s$ -surface is in the gas phase just adjacent to the solid. The  $o$ -surface is a fixed distance from the interface and is located deep enough into the solid for the temperature gradient there to be negligible. A  $u$ -surface is located in the solid phase adjacent to the gas-solid interface. Molten material is imagined to leave through the sides of the control volume between the  $s$ -surface and the interface at the rate  $\dot{m}''$  [ $\text{kg}/\text{m}^2 \text{ s}$ ]. Mass conservation requires that solid material should flow across the  $o$ -surface also at the rate  $\dot{m}''$ . The steady-flow energy equation, Eq. (1.4), applied to the  $s$ - $o$  control volume of cross-sectional area  $A$ , requires that:

Mass flow rate  $\times$  Change in enthalpy = Net rate of heat inflow

$$\dot{m}''A(h_s - h_o) = q_sA - 0$$

where  $h_s$  is the enthalpy of molten material at the interface temperature  $T_s$ , and  $h_o$  is the enthalpy of solid material at temperature  $T_o$ . The enthalpy of phase change is  $h_{fs}$ ; then  $h_s - h_u = h_{fs}$ , where  $h_u$  is the enthalpy of solid material at temperature  $T_s (= T_u)$ , and

$$q_s = \dot{m}''[h_{fs} + (h_u - h_o)]$$

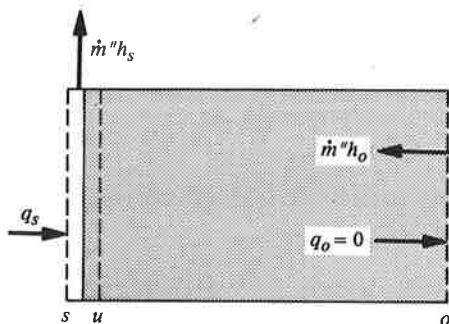
or

$$\dot{m}'' = \frac{q_s}{h_{fs} + (h_u - h_o)} \quad (3.93)$$

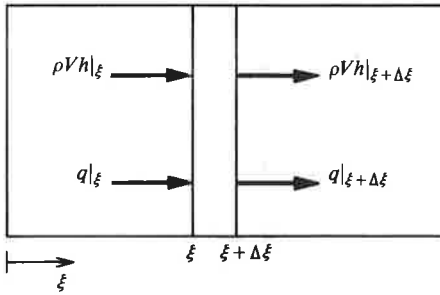
If the specific heat of the solid is taken to be constant, the final result is

$$\dot{m}'' = \frac{q_s}{h_{fs} + c_p(T_s - T_o)} \quad (3.94)$$

The speed at which the solid surface recedes is simply  $\dot{m}''/\rho$ .



**Figure 3.31** Control volume for the application of mass and energy conservation principles to steady-state melting ablation.



**Figure 3.32** Elemental control volume in a coordinate system located on the moving boundary for one-dimensional ablation.

To obtain the temperature profile in the solid, it is necessary to solve an appropriate form of the heat conduction equation. It is convenient to use first principles to derive a special form of the equation for which the coordinate axes are located on the moving surface, as shown in Fig. 3.32. The coordinate  $\xi$  is taken to be positive measured into the solid, so that the velocity  $V$  at which the solid moves (from right to left) has a negative value. For steady ablation, the temperature at any location  $\xi$  is unchanging with time. Application of the steady-flow energy equation, Eq. (1.4), to the elemental control volume  $A\Delta\xi$  located between  $\xi$  and  $\xi + \Delta\xi$  requires that:

Mass flow rate  $\times$  Change in enthalpy = Net rate of heat inflow by conduction

$$\rho VA[h|_{\xi+\Delta\xi} - h|_{\xi}] = qA|_{\xi} - qA|_{\xi+\Delta\xi}$$

Dividing by  $A\Delta\xi$  and letting  $\Delta\xi \rightarrow 0$  gives

$$\rho V \frac{dh}{d\xi} = -\frac{dq}{d\xi}$$

But

$$q = -k \frac{dT}{d\xi} \quad \text{and} \quad dh = c_p dT$$

Substituting and rearranging,

$$\frac{d}{d\xi} \left( k \frac{dT}{d\xi} \right) - \rho V c_p \frac{dT}{d\xi} = 0 \quad (3.95)$$

Taking the thermal conductivity  $k$  to be constant and  $c_p = c_v = c$  gives the equation governing the temperature distribution  $T(\xi)$ :

$$\frac{d^2 T}{d\xi^2} - \frac{V}{\alpha} \frac{dT}{d\xi} = 0; \quad \alpha = \frac{k}{\rho c} \quad (3.96)$$

Appropriate boundary conditions for this second-order ordinary differential equation are

$$\xi = 0: \quad T = T_s; \quad \xi \rightarrow \infty: \quad T \rightarrow T_o \quad (3.97a,b)$$

The solution of Eq. (3.96) is

$$T = C_1 e^{(V/\alpha)\xi} + C_2$$

and when the constants are evaluated from the boundary conditions, the result is

$$\frac{T - T_o}{T_s - T_o} = e^{(V/\alpha)\xi}; \quad (V \text{ is negative}) \quad (3.98)$$

That is, the temperature profile shows a simple exponential decay. The heat flux into the solid at the  $u$ -surface can be obtained using Fourier's law:

$$q_u = -k \left. \frac{dT}{d\xi} \right|_{\xi=0} = -k(T_s - T_o) \left( \frac{V}{\alpha} \right) = -\rho c V (T_s - T_o) \quad (3.99)$$

An energy balance on the control volume located between the  $s$ - and  $u$ -surfaces will show that  $q_s$  differs from  $q_u$  by the enthalpy of phase change absorbed at the interface.

Notice that Eq. (3.96) could have been derived from the heat conduction equation for one-dimensional transient conduction, Eq. (3.33), by an appropriate change of variables (see Exercise 3-89).

### EXAMPLE 3.13 Ablation of Stainless Steel

In an experiment to study laser heating, a stainless steel component is exposed to a powerful laser beam, and a jet of argon gas impinging on the surface sweeps away the molten metal. The component is initially at 300 K, and after a short transient the surface is measured to recede at a rate of 230  $\mu\text{m/s}$ . Estimate the total heat flux to the surface and the penetration of the thermal response into the solid. The stainless steel properties include  $\rho = 7800 \text{ kg/m}^3$ ,  $c = 600 \text{ J/kg K}$ ,  $\alpha = 4.0 \times 10^{-6} \text{ m}^2/\text{s}$ ,  $h_{fs} = 2.7 \times 10^5 \text{ J/kg}$ , and a melting temperature of 1670 K.

#### Solution

**Given:** Rate of surface recession of ablating stainless steel.

**Required:** Surface heat flux and depth of penetration of thermal response.

**Assumptions:** 1. One-dimensional heat flow.

2. Steady-state ablation.

3. The melt layer is thin enough for there to be a negligible temperature drop across it.

4. No chemical reactions, since the argon is inert.

The surface heat flux can be obtained from Eq. (3.94). Solving for  $q_s$ ,

$$\begin{aligned} q_s &= \dot{m}'' [h_{fs} + c_p(T_s - T_o)] \\ &= \{(7800)(230 \times 10^{-6})[2.7 \times 10^5 + 600(1670 - 300)]\} \\ &= 1.96 \times 10^6 \text{ W/m}^2 \quad (1.96 \text{ MW/m}^2) \end{aligned}$$

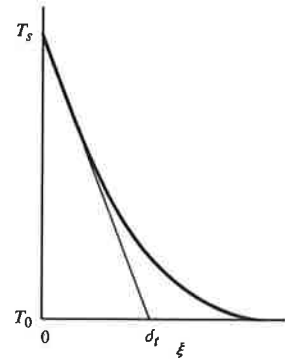
Referring to the figure, we can take  $\delta_r$  to be an estimate of the thermal penetration. Differentiating Eq. (3.98),

$$\left. \frac{dT}{d\xi} \right|_{\xi=0} = \frac{(T_s - T_o)V}{\alpha}$$

$$\delta_r = \frac{\alpha}{-V} = \frac{4.0 \times 10^{-6}}{230.0 \times 10^{-6}} = 0.017 \text{ m (1.7 cm)}$$

### Comments

The depth of thermal penetration is seen to be small.



## 3.6 NUMERICAL SOLUTION METHODS

Although many simple steady-state and transient heat conduction problems can be solved analytically, solutions for more complex problems are best obtained numerically. Numerical solution methods are particularly useful when the shape of the solid is irregular, when thermal properties are temperature- or position-dependent, and when boundary conditions are nonlinear. Numerical methods commonly used include the *finite-difference method*, the *finite-element method*, and the *boundary-element method*. The finite-difference method was the first numerical method to be used extensively for heat conduction. It remains a popular method, not because it is superior to other methods for heat conduction, but because it is easier to implement and is also the most useful numerical solution method for heat convection problems.

The first step in a finite-difference solution procedure is to discretize the spatial and time coordinates to form a *mesh of nodes*. Next, finite-difference approximations are made to the derivatives appearing in the heat conduction equation to convert the *differential* equation to an algebraic *difference* equation. Alternatively, the difference equation can be constructed by applying the energy conservation principle directly to a volume element surrounding the node. In steady-state problems, a set of linear algebraic equations is obtained with as many unknowns as the number of nodes in the mesh. These equations can be solved by matrix inversion or by iteration. For transient conduction, temperatures at the current time step may be found directly using values at the preceding time step. In some formulations, iteration may be required, since values at the current time step are also involved. In the first applications of finite-difference methods to heat conduction, the calculations were done by hand, limiting consideration to a coarse mesh with relatively few nodes. Because the accuracy of a finite-difference approximation increases with number of nodes, these solutions were inadequate.

The availability of mainframe digital computers in the late 1950s completely changed the picture, and by the 1960s, engineers could use as fine a grid as was necessary to meet their requirements. The 1970s saw increased use of the programmable calculator to obtain finite-difference solutions to heat conduction problems, which

meant that an engineer would write a computer program for the specific problem under consideration. In the 1980s and 1990s, powerful personal computers have become available. Furthermore, there is no longer the need, nor is it cost-effective, for engineers to write their own computer programs to implement a finite-difference solution method. There are many standard computer programs available for this purpose. Some examples are listed at the end of this chapter [16–19]. Thus, in Section 3.6, finite-difference methods are presented with the modest objective of giving the student an appreciation of the essential ideas involved, so that the available computer programs can be used intelligently. Any serious endeavor to develop engineering tools based on finite-difference solution procedures should be preceded by an appropriate course in numerical analysis.

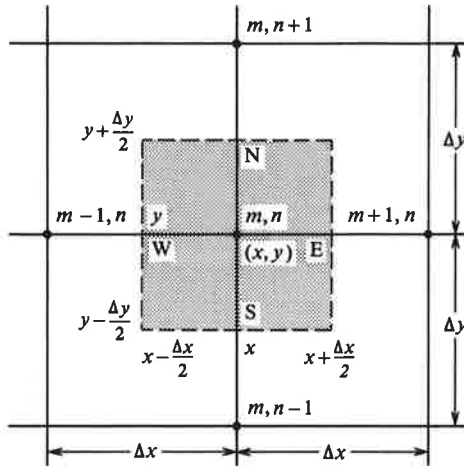
Finite-element methods are widely used in structural mechanics and are also applicable to heat conduction problems. An object is divided into discrete spatial regions called *finite elements*. The most common two-dimensional element is the triangle, and the most common three-dimensional element is the tetrahedron. The finite-element method allows the heat conduction equation to be satisfied in an average sense over the finite element; thus, the elements can be much larger than the control volumes used in finite-difference methods. The use of triangles or tetrahedrons for elements allows the approximation of complex and irregularly shaped objects. Application of the method leads to a set of algebraic equations, which are solved by matrix inversion or iteration. Compared to finite-difference methods, the formulation of these equations is considerably more involved and requires more effort, as does writing a computer program to implement the procedure. However, once written, finite-element computer programs tend to be more versatile than their finite-difference counterparts. Choice of which method to use is perhaps dictated by the objective rather than by the intrinsic virtues of the method. For example, calculation of temperature variations in solids is often required for the purpose of determining thermal stresses. Since the finite-element method is preeminent for stress calculations, many standard computer codes use the finite-element method to calculate both temperatures and stresses in one package.

A newer development is the boundary-element method, in which the boundary of the object is divided into finite elements, and there is no need to consider the interior at all. Although this method is attractive for simpler heat conduction problems, its versatility and generality have yet to be established.

### 3.6.1 A Finite-Difference Method for Two-Dimensional Steady Conduction

Consider two-dimensional steady conduction with volumetric heat generation and constant thermal properties. Using Cartesian coordinates, Fig. 3.33 shows a finite control volume  $\Delta x$  by  $\Delta y$  of unit depth surrounding node  $(m, n)$  within the solid. The  $m$  and  $n$  indices denote  $x$  and  $y$  locations, respectively, in a uniform mesh of node points. For convenience, we will use compass directions to denote the faces of the element (N, S, E, and W). The energy conservation principle, Eq. (1.2), applied to the finite control volume reduces to

$$0 = \dot{Q} + \dot{Q}_v$$



**Figure 3.33** Finite control volume  $\Delta x$  by  $\Delta y$  by 1 surrounding node  $(m, n)$  at the location  $(x, y)$  used to derive the difference equation for two-dimensional steady conduction.

The heat transfer  $\dot{Q}$  is by conduction across the four faces of the element; thus,

$$0 = \dot{Q}_x|_W + \dot{Q}_y|_S - \dot{Q}_x|_E - \dot{Q}_y|_N + \Delta\dot{Q}_v \quad (3.100)$$

since the sign convention in Eq. (1.2) requires heat transfer into the system to be positive. The heat conduction across the left-hand face of the element is

$$\dot{Q}_x|_W = -k \left. \frac{\partial T}{\partial x} \right|_W \Delta y \cdot 1$$

To approximate the derivative of  $T(x, y)$  we will assume a linear temperature gradient between the nodes  $(m-1, n)$  and  $(m, n)$ ; then

$$\dot{Q}_x|_W = -k \frac{T_{m,n} - T_{m-1,n}}{\Delta x} \Delta y$$

which is seen to be positive for  $T_{m-1,n} > T_{m,n}$ . Similarly, for the right-hand, bottom, and top faces,

$$\dot{Q}_x|_E = -k \frac{T_{m+1,n} - T_{m,n}}{\Delta x} \Delta y$$

$$\dot{Q}_y|_S = -k \frac{T_{m,n} - T_{m,n-1}}{\Delta y} \Delta x$$

$$\dot{Q}_y|_N = -k \frac{T_{m,n+1} - T_{m,n}}{\Delta y} \Delta x$$

The internal heat generation is simply  $\dot{Q}_v'''$  times the volume of the element:

$$\Delta\dot{Q}_v = \dot{Q}_v''' \Delta x \Delta y \cdot 1$$

Substituting in Eq. (3.100), multiplying by  $\Delta x/k\Delta y$ , and rearranging,

$$2(1 + \beta)T_{m,n} = T_{m-1,n} + T_{m+1,n} + \beta(T_{m,n-1} + T_{m,n+1}) + \frac{\dot{Q}_v'''}{k}\Delta x^2 \quad (3.101)$$

where  $\beta = (\Delta x/\Delta y)^2$  is a geometric mesh factor. For a square mesh  $\Delta x = \Delta y$ ,  $\beta = 1$ , and no internal heat generation,

$$4T_{m,n} = T_{m,n+1} + T_{m+1,n} + T_{m,n-1} + T_{m-1,n} \quad (3.102)$$

which simply states that the temperature at each node is the arithmetic average of the temperatures at the four nearest neighboring nodes.

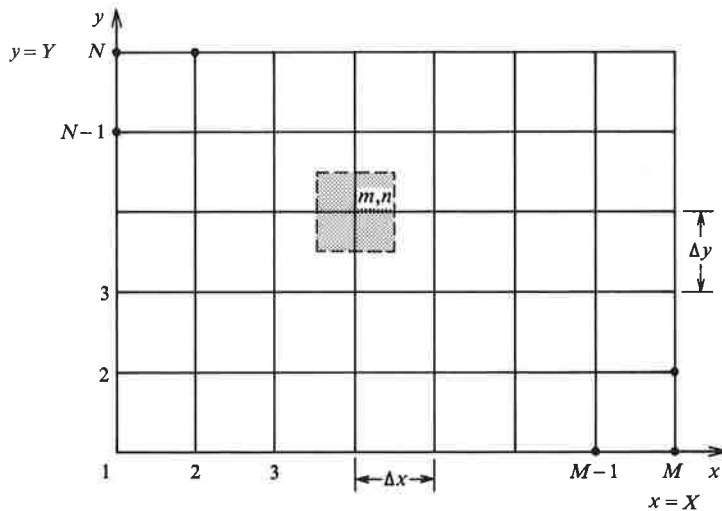
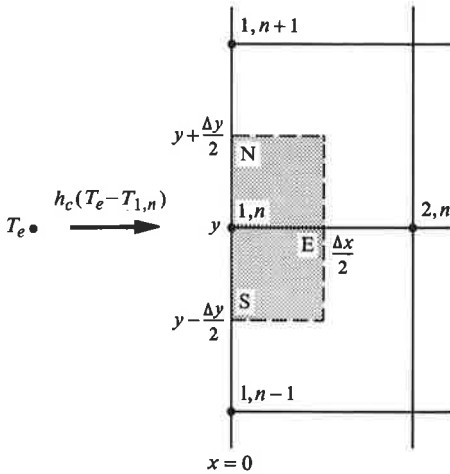


Figure 3.34 Nodal mesh for steady conduction in a rectangular plate.

### Boundary Conditions

Figure 3.34 shows a complete mesh for a rectangular plate of dimensions  $X, Y$ . There are  $M$  node points in the  $x$  direction and  $N$  node points in the  $y$  direction. If the boundary condition is one of prescribed temperature, the temperatures at the boundary nodes are known. If the boundary condition is one of prescribed heat flux or convection, then the finite-difference form of the condition is obtained by making an energy balance on a finite control volume adjacent to the boundary. For example, consider the convection boundary condition shown in Fig. 3.35, and assume  $\dot{Q}_v''' = 0$  for simplicity,

$$\text{Net heat conduction into the volume} + \text{Heat convection across face at } x = 0 = 0$$



**Figure 3.35** Finite control volume used to derive the difference equation for a convective boundary condition at  $x = 0$ : two-dimensional steady conduction.

As before,

$$\dot{Q}_x|_E = -k \frac{T_{2,n} - T_{1,n}}{\Delta x} \Delta y$$

$$\dot{Q}_y|_S = -k \frac{T_{1,n} - T_{1,n-1}}{\Delta y} \frac{\Delta x}{2}$$

$$\dot{Q}_y|_N = -k \frac{T_{1,n+1} - T_{1,n}}{\Delta y} \frac{\Delta x}{2}$$

and

$$\dot{Q}_x|_0 = h_c(T_e - T_{1,n})\Delta y$$

Substituting in the energy balance and taking  $\Delta x = \Delta y$ ,

$$T_{2,n} + \frac{1}{2}(T_{1,n-1} + T_{1,n+1}) - 2T_{1,n} + \frac{h_c \Delta x}{k}(T_e - T_{1,n}) = 0$$

A mesh Biot number is defined as  $\text{Bi} = h_c \Delta x / k$ ; then solving for  $T_{1,n}$  gives

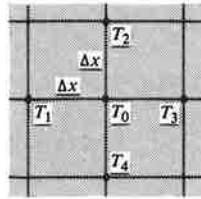
$$T_{1,n} = \frac{1}{2 + \text{Bi}} \left[ T_{2,n} + \frac{1}{2}(T_{1,n-1} + T_{1,n+1}) + \text{Bi} T_e \right] \quad (3.103)$$

Table 3.7 gives similar results for a variety of boundary conditions, including interior and exterior corners. In this table, a simplified node numbering scheme is used for clarity.



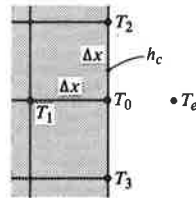
**Table 3.7** Finite-difference approximations for steady-state conduction, square mesh.

1. Interior node



$$T_0 = \frac{1}{4}[T_1 + T_2 + T_3 + T_4]$$

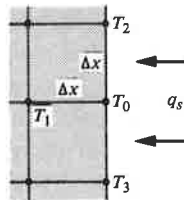
2. Plane surface, convection



$$T_0 = \frac{1}{2 + Bi} \left[ T_1 + \frac{1}{2}(T_2 + T_3) + BiT_e \right]$$

$$Bi = \frac{h_c \Delta x}{k}$$

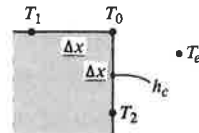
3. Plane wall, known heat flux



$$T_0 = \frac{1}{2}T_1 + \frac{1}{4}(T_2 + T_3) + \frac{q_s \Delta x}{2k}$$

(for an adiabatic surface or plane of symmetry set  $q_s = 0$ )

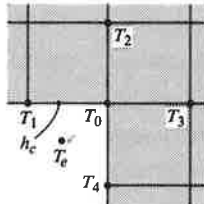
4. Exterior corner, convection



$$T_0 = \frac{1}{1 + Bi} \left[ \frac{1}{2}(T_1 + T_2) + BiT_e \right]$$

$$Bi = \frac{h_c \Delta x}{k}$$

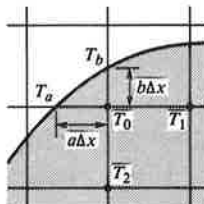
5. Interior corner, convection



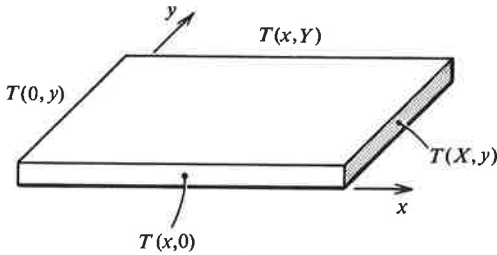
$$T_0 = \frac{1}{3 + Bi} \left[ T_2 + T_3 + \frac{1}{2}(T_1 + T_4) + BiT_e \right]$$

$$Bi = \frac{h_c \Delta x}{k}$$

6. Interior node near a curved non-isothermal surface



$$T_0 = \frac{1}{(1/a + 1/b)} \left[ \frac{T_1}{1 + a} + \frac{T_2}{1 + b} + \frac{T_a}{a(1 + a)} + \frac{T_b}{b(1 + b)} \right]$$



**Figure 3.36** Schematic of rectangular plate with prescribed edge temperatures.

### **Solution Procedures**

Consider the simplest case of a rectangular plate with prescribed boundary temperatures, as shown in Fig. 3.36. Referring to Fig. 3.34, the plate has dimensions  $X$  and  $Y$ , with  $M$  and  $N$  nodes in the  $x$  and  $y$  directions, respectively; then  $\Delta x = X/(M - 1)$ ,  $\Delta y = Y/(N - 1)$ . Equation (3.102) is a set of  $(M - 2) \times (N - 2)$  linear algebraic equations in the  $(M - 2) \times (N - 2)$  unknown interior nodal temperatures  $T_{m,n}$ . If a coarse mesh is chosen so that there are relatively few nodes, *matrix inversion* or *Gaussian elimination* can be used to solve the equation set. In writing a computer program to effect the solution, all that is required is to call on a standard subroutine. However, the accuracy of a finite-difference method will increase as the mesh size is reduced (provided round-off error in the numerical computations is not introduced). Thus, typically many nodes will be used, perhaps 100 or more. Then matrix inversion is uneconomical, and more sophisticated elimination methods should be used to take advantage of the sparseness of the matrix generated by the simple finite-difference approximations described here. Such methods are widely used in practice. Alternatively, iterative solution methods can be used. A simple and easily programmed iterative method is *Gauss-Seidel iteration*, which proceeds as follows:

1. A reasonable initial guess  $T_{m,n}^0$  is made for each of the unknown interior nodal temperatures. This is iteration zero.
2. New values  $T_{m,n}^1$  are calculated by applying Eq. (3.102) to each node sequentially. Initial  $T^0$  values or, if available, new  $T^1$  values are substituted in the right-hand side of the equation.
3. The mesh is swept repeatedly until, at iteration  $k$ , the temperatures at each node are seen to change by less than a prescribed small amount,

$$\left| 1 - \frac{T_{m,n}^k}{T_{m,n}^{k-1}} \right| < \varepsilon \quad (3.104)$$

The finite-difference solution is then said to have *converged* to the exact solution of the difference equation.

The system of linear algebraic equations, Eq. (3.102), is *diagonally dominant*; that is, when written in matrix form, the largest elements on each row of the coefficient matrix are on the main diagonal. The Gauss-Seidel procedure applied to

such a system always converges uniformly to the proper solution and never becomes unstable; however, for a large number of equations, the convergence can be slow. Many methods have been devised to obtain faster convergence, for example, the *alternating-direction implicit* and *successive over-relaxation methods*. Such methods are described in the references listed in the bibliography at the end of the text.

### Surface Heat Flux

Once the temperature field is obtained, it is sometimes necessary to determine the heat flux at a boundary surface. We make an energy balance on a finite control volume adjacent to the boundary, as shown in Fig. 3.37, and proceed as in the derivation of the boundary condition, Eq. (3.103).

$$\text{Net heat conduction into the volume} + \text{Heat flux across face at } x = 0 = 0$$

As before,

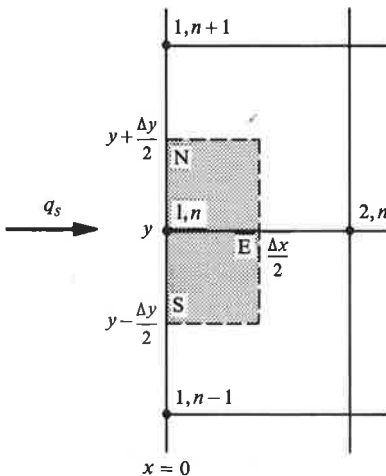
$$\dot{Q}_x|_E = -k \frac{T_{2,n} - T_{1,n}}{\Delta x} \Delta y$$

$$\dot{Q}_y|_S = -k \frac{T_{1,n} - T_{1,n-1}}{\Delta y} \frac{\Delta x}{2}$$

$$\dot{Q}_y|_N = -k \frac{T_{1,n+1} - T_{1,n}}{\Delta y} \frac{\Delta x}{2}$$

and

$$\dot{Q}_x|_0 = q_s \Delta y$$



**Figure 3.37** Finite control volume used to derive a difference equation for the surface heat flux: steady two-dimensional conduction.

Substituting in the energy balance, taking  $\Delta x = \Delta y$ , and solving for  $q_s$  gives

$$q_s = \frac{k}{\Delta x} \left[ 2T_{1,n} - T_{2,n} - \frac{1}{2}(T_{1,n-1} + T_{1,n+1}) \right] \tag{3.105}$$

Equation (3.105) is simply item 3 of Table 3.7 rearranged to give  $q_s$ . Equation (3.105) is quite general; however, for a convective boundary condition, the surface heat can be just as easily calculated from Newton’s law of cooling as  $q_s = h_c(T_e - T_{1,n})$ .

**EXAMPLE 3.14** Steady Conduction in a Square Plate

An  $8 \times 8$  cm square plate has one edge maintained at  $100^\circ\text{C}$ ; the other three edges are maintained at  $0^\circ\text{C}$ . Use the finite-difference method to determine the temperature distribution in the plate. Compare the result with the exact solution given in Section 3.3.1.

**Solution**

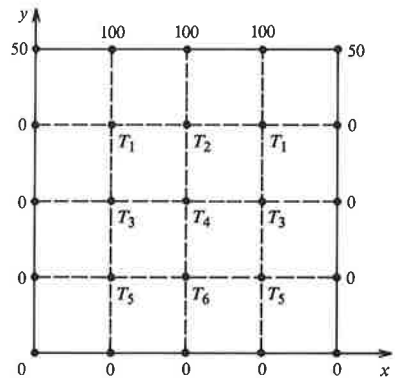
**Given:** Square plate with edge temperatures prescribed.

**Required:** Steady-state temperature distribution using the finite-difference method.

**Assumptions:** Temperatures are constant across the thickness of the plate to give a two-dimensional problem.

The figure shows the mesh and the prescribed temperatures along the edges. There are nine interior nodes, but symmetry about the centerline results in only six unknown temperatures, which are labeled  $T_1, T_2, \dots, T_6$  as shown. From Eq. (3.102), these temperatures are given by

$$\begin{aligned} T_1 &= \frac{1}{4}(T_3 + T_2 + 0 + 100) \\ T_2 &= \frac{1}{4}(T_4 + T_1 + T_1 + 100) \\ T_3 &= \frac{1}{4}(T_5 + T_4 + 0 + T_1) \\ T_4 &= \frac{1}{4}(T_6 + T_3 + T_3 + T_2) \\ T_5 &= \frac{1}{4}(0 + T_6 + 0 + T_3) \\ T_6 &= \frac{1}{4}(0 + T_5 + T_5 + T_4) \end{aligned}$$



For an initial guess, a linear variation in  $y$  is assumed, and the preceding equations are evaluated in order, using latest available values. For example, when  $T_2$  is evaluated, the new value of  $T_1$  just obtained is used. The process is repeated until the convergence is satisfactory. The following table shows 16 iterations. Also shown is the exact solution obtained by evaluating Eq. (3.30).

Temperature	$T_1$	$T_2$	$T_3$	$T_4$	$T_5$	$T_6$
Initial guess, °C	75	75	50	50	25	25
Iteration level:						
$k = 1$	56.25	65.62	32.81	39.06	14.45	16.99
$k = 2$	49.61	59.57	25.78	32.03	10.69	13.35
$k = 4$	44.61	54.43	20.51	26.76	8.02	10.70
$k = 8$	42.97	52.79	18.86	25.11	7.20	9.88
$k = 16$	42.86	52.68	18.75	25.00	7.14	9.82
Exact solution	43.20	54.05	18.20	25.00	6.80	9.54
Percent error	0.80	2.54	3.01	0.00	5.08	2.93

### Comments

1. Notice that the center temperature,  $T_4$ , is the average of the edge temperatures.
2. At the corners where the temperature is discontinuous, the average value of 50°C can be assigned. Assigning the average value of 50°C at the corners ensures a zero net heat flow into the corner control volume; however, these values are not used in the calculations.

### 3.6.2 Finite-Difference Methods for One-Dimensional Unsteady Conduction

Consider one-dimensional unsteady conduction with no internal heat generation and constant properties. Figure 3.38 shows a finite control volume  $\Delta x \cdot 1 \cdot 1$  surrounding node  $m$  at location  $x$  in the solid. Figure 3.39 shows the mesh where the time coordinate is discretized in steps  $\Delta t$  and the index  $i$  denotes time. The energy conservation principle, Eq. (1.1), is applied to the finite control volume over a time interval  $\Delta t$ , from time step  $i$  to step  $(i + 1)$ :

$$\Delta U = \dot{Q} \Delta t \quad (3.106)$$

The increase in internal energy from time step  $i$  to step  $(i + 1)$  is

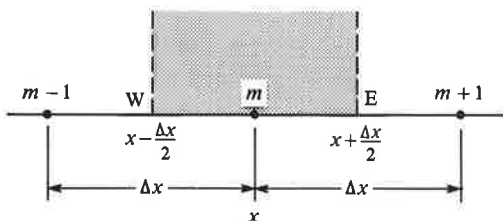
$$\Delta U = \rho c (\Delta x \cdot 1 \cdot 1) (T_m^{i+1} - T_m^i)$$

The conduction over the time interval  $\Delta t$  is taken as

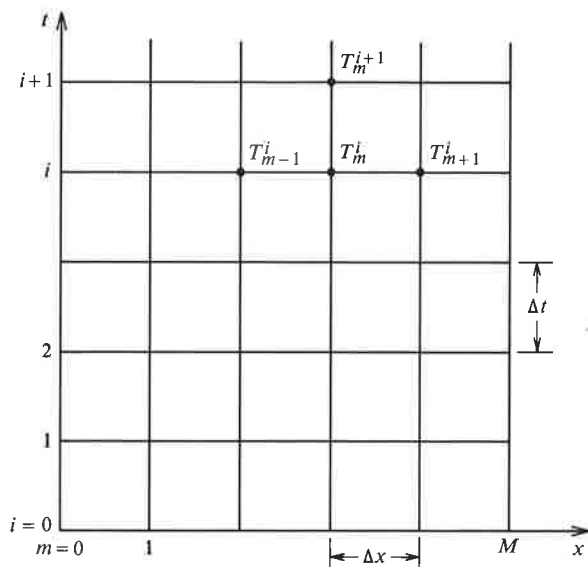
$$\dot{Q}_x|_W \Delta t = -k \frac{T_m^i - T_{m-1}^i}{\Delta x} (1 \cdot 1) \Delta t$$

$$\dot{Q}_x|_E \Delta t = -k \frac{T_{m+1}^i - T_m^i}{\Delta x} (1 \cdot 1) \Delta t$$

where the fluxes have been evaluated at time step  $i$ . Substituting in Eq. (3.106),



**Figure 3.38** Finite control volume  $\Delta x$  by 1 by 1 surrounding node  $m$  at location  $x$  used to derive the difference equation for one-dimensional unsteady conduction.



**Figure 3.39** Nodal mesh for one-dimensional unsteady conduction.

dividing by  $\Delta t$ , and rearranging gives

$$T_m^{i+1} = \text{Fo}(T_{m-1}^i + T_{m+1}^i) + (1 - 2\text{Fo})T_m^i \quad (3.107)$$

where  $\text{Fo} = \alpha\Delta t/\Delta x^2$  is the mesh Fourier number. Equation (3.107) is an explicit relation for  $T_m^{i+1}$ , the temperature of node  $m$  at the  $(i + 1)$ th time step, in terms of temperatures at the previous time step. In this *explicit* method, no iteration is required. Using given initial temperatures at time  $t = 0$ ,  $T_m^0$ , the new temperatures,  $T_m^1$ , can be calculated. Temperatures at the boundary nodes 0 and  $M$  are fixed by the specified boundary conditions. The process is then repeated, marching forward in time.

Although simple, the explicit method has a major drawback: the allowable size of time step is limited by stability requirements. To avoid divergent oscillations in the solution, the coefficient for  $T_m^i$  in Eq. (3.107) must not be negative. That is,

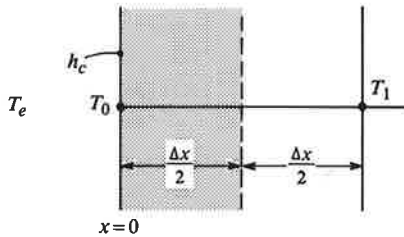
$$\text{Fo} \leq \frac{1}{2} \quad (3.108)$$

Since the spatial discretization step  $\Delta x$  is usually chosen to give a desired spatial resolution of the temperature profile, Eq. (3.108) sets a limit on the time step:

$$\Delta t \leq \frac{\Delta x^2}{2\alpha} \quad (3.109)$$

If the boundary condition is other than that of prescribed temperature, the associated stability requirement is more stringent than Eq. (3.109). Consider the convective boundary condition illustrated in Fig. 3.40. An energy balance requires that, during the time step  $\Delta t$ ,

$$\text{Increase in internal energy within volume} = \text{Net conduction into volume} + \text{Convection across boundary}$$



**Figure 3.40** Finite control volume used to derive the difference equation for a convective boundary condition at  $x = 0$ : one-dimensional unsteady conduction.

or

$$\rho c \frac{\Delta x}{2} (1 \cdot 1)(T_0^{i+1} - T_0^i) = k(1 \cdot 1) \frac{T_1^i - T_0^i}{\Delta x} \Delta t + h_c(1 \cdot 1)(T_e^i - T_0^i) \Delta t$$

Rearranging and solving for the new nodal temperature,  $T_0^{i+1}$ ,

$$T_0^{i+1} = 2\text{Fo}(T_1^i + \text{Bi}T_e^i) + (1 - 2\text{Fo} - 2\text{Fo}\text{Bi})T_0^i \quad (3.110)$$

where again  $\text{Bi} = h_c \Delta x / k$ . For stability, the coefficient of  $T_0^i$  must not be negative:

$$1 - 2\text{Fo} - 2\text{Fo}\text{Bi} \geq 0$$

or

$$\text{Fo} \leq \frac{1}{2(1 + \text{Bi})} \quad (3.111)$$

Since the Biot number is positive, Eq. (3.111) is always a more stringent stability condition than Eq. (3.108).

The stability criterion limits  $\Delta t$  to no more than  $(\Delta x)^2 / 2\alpha$ , and less if the mesh Biot number is not small. Thus, if we wish to improve accuracy by halving the mesh size  $\Delta x$ , the time step  $\Delta t$  must be divided by four. For accurate solutions using a fine spatial mesh size, alternative methods are available. The *implicit* method evaluates the conduction fluxes at time step  $(i + 1)$  rather than at step  $i$ :

$$\dot{Q}_x|_W \Delta t = -k \frac{T_m^{i+1} - T_{m-1}^{i+1}}{\Delta x} (1 \cdot 1) \Delta t$$

$$\dot{Q}_x|_E \Delta t = -k \frac{T_{m+1}^{i+1} - T_m^{i+1}}{\Delta x} (1 \cdot 1) \Delta t$$

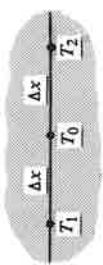
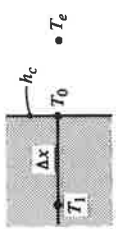
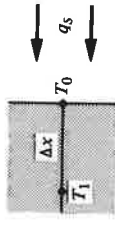
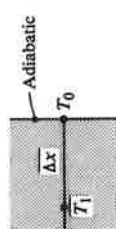
The new form of Eq. (3.107) is

$$T_m^{i+1} = \frac{\text{Fo}(T_{m+1}^{i+1} + T_{m-1}^{i+1}) + T_m^i}{1 + 2\text{Fo}} \quad (3.112)$$

There are three unknown temperatures in each nodal equation. The set of algebraic equations is *tridiagonal*; that is, when written in matrix form, all the elements of the coefficient matrix are zero except for those that are on or to either side of the main diagonal. To advance the solution through each time step, Gauss-Seidel iteration works well.<sup>4</sup> At time step  $(i + 1)$ , the nodal equations are swept repeatedly

<sup>4</sup> Direct methods, such as successive substitution, may also be used when the equation set is tridiagonal.

**Table 3.8** Finite-difference approximations for one-dimensional unsteady conduction.

Item	Configuration	Explicit Form and Stability Criterion	Implicit Form
1.	 <p>Interior node</p>	$T_0^{i+1} = \text{Fo}(T_1^i + T_2^i) + (1 - 2\text{Fo})T_0^i$ $\text{Fo} = \frac{\alpha \Delta t}{\Delta x^2} \leq \frac{1}{2}$	$T_0^{i+1} = \frac{\text{Fo}(T_1^{i+1} + T_2^{i+1}) + T_0^i}{1 + 2\text{Fo}}$
2.	 <p>Convection at surface</p>	$T_0^{i+1} = 2\text{Fo}(T_1^i + \text{Bi}T_e^i) + (1 - 2\text{Fo} - 2\text{FoBi})T_0^i$ $\text{Fo} \leq \frac{1}{2(1 + \text{Bi})}; \quad \text{Bi} = \frac{h_c \Delta x}{k}$	$T_0^{i+1} = \frac{2\text{Fo}(T_1^{i+1} + \text{Bi}T_e^{i+1}) + T_0^i}{1 + 2\text{Fo} + 2\text{FoBi}}$
3.	 <p>Known surface heat flux</p>	$T_0^{i+1} = 2\text{Fo} \left( T_1^i + \frac{q_s^i \Delta x}{k} \right) + (1 - 2\text{Fo})T_0^i$ $\text{Fo} \leq \frac{1}{2}$	$T_0^{i+1} = \frac{2\text{Fo}[T_1^{i+1} + (q_s^{i+1} \Delta x/k)] + T_0^i}{1 + 2\text{Fo}}$
4.	 <p>Adiabatic surface, or plane of symmetry</p>	$T_0^{i+1} = 2\text{Fo}T_1^i + (1 - 2\text{Fo})T_0^i$ $\text{Fo} \leq \frac{1}{2}$	$T_0^{i+1} = \frac{2\text{Fo}T_1^{i+1} + T_0^i}{1 + 2\text{Fo}}$



**Table 3.9** Finite-difference approximations and stability criteria for two-dimensional unsteady conduction, square mesh. For an adiabatic surface or plane of symmetry, set  $q_s = 0$  in item 3.

1. Interior node		<p>Explicit: <math>T_0^{i+1} = Fo(T_1^i + T_2^i + T_3^i + T_4^i) + (1 - 4Fo)T_0^i</math>; <math>Fo \leq \frac{1}{4}</math></p> <p>Implicit: <math>T_0^{i+1} = \frac{Fo(T_1^{i+1} + T_2^{i+1} + T_3^{i+1} + T_4^{i+1}) + T_0^i}{1 + 4Fo}</math></p>
2. Plane surface, convection		<p>Explicit: <math>T_0^{i+1} = 2Fo \left[ T_1^i + \frac{1}{2}(T_2^i + T_3^i) + BiT_e^i \right] + (1 - 4Fo - 2FoBi)T_0^i</math>; <math>Fo \leq \frac{1}{2(2 + Bi)}</math></p> <p>Implicit: <math>T_0^{i+1} = \frac{2Fo [T_1^{i+1} + (1/2)(T_2^{i+1} + T_3^{i+1}) + BiT_e^{i+1}] + T_0^i}{1 + 2Fo(2 + Bi)}</math></p>
3. Plane surface, known heat flux		<p>Explicit: <math>T_0^{i+1} = 2Fo \left[ T_1^i + \frac{1}{2}(T_2^i + T_3^i) + \frac{q_s^i \Delta x}{k} \right] + (1 - 4Fo)T_0^i</math>; <math>Fo \leq \frac{1}{4}</math></p> <p>Implicit: <math>T_0^{i+1} = \frac{2Fo [T_1^{i+1} + (1/2)(T_2^{i+1} + T_3^{i+1}) + (q_s^{i+1} \Delta x/k)] + T_0^i}{1 + 4Fo}</math></p>
4. Exterior corner, convection		<p>Explicit: <math>T_0^{i+1} = 2Fo(T_1^i + T_2^i + 2BiT_e^i) + (1 - 4Fo - 4FoBi)T_0^i</math>; <math>Fo \leq \frac{1}{4(1 + Bi)}</math></p> <p>Implicit: <math>T_0^{i+1} = \frac{2Fo(T_1^{i+1} + T_2^{i+1} + 2BiT_e^{i+1}) + T_0^i}{1 + 4Fo(1 + Bi)}</math></p>
5. Interior corner, convection		<p>Explicit: <math>T_0^{i+1} = \frac{4}{3}Fo \left[ \frac{1}{2}(T_1^i + T_4^i) + T_2^i + T_3^i + BiT_e^i \right] + (1 - 4Fo - \frac{4}{3}FoBi)T_0^i</math>; <math>Fo \leq \frac{3}{4(3 + Bi)}</math></p> <p>Implicit: <math>T_0^{i+1} = \frac{(4/3)Fo [(1/2)(T_1^{i+1} + T_4^{i+1}) + T_2^{i+1} + T_3^{i+1} + BiT_e^{i+1}] + T_0^i}{1 + 4Fo[1 + (1/3)Bi]}</math></p>

until convergence to sufficient accuracy is obtained. The implicit method is unconditionally stable, and the choice of the time step size  $\Delta t$  is dictated by accuracy rather than stability considerations. As mentioned in Section 3.6.1, there are iteration schemes that give faster convergence than Gauss-Seidel iteration, and these may be found in numerical methods texts. When the boundary condition is other than that of prescribed temperature, an energy balance must be used at the boundary control volumes, as was shown for the explicit method, but with spatial derivatives evaluated at time step  $(i + 1)$ . Table 3.8 lists both explicit and implicit forms for a variety of boundary conditions. Table 3.9 lists corresponding results for two-dimensional unsteady conduction.

In addition to the explicit and implicit methods, a third method often used is the *Crank-Nicolson* method. Whereas the explicit method evaluates conduction fluxes at the old time step  $i$ , and the implicit method uses the new time step  $(i + 1)$ , the Crank-Nicolson method uses an average of the values at time steps  $i$  and  $(i + 1)$ . The nodal equation is then more complicated (see Exercise 3-128). For a given mesh size, the Crank-Nicolson method gives more accurate results than either the explicit or implicit methods. Although oscillations can occur, they never become unstable.

### EXAMPLE 3.15 Convective Heating of a Resin Slab

An 8 cm-thick slab of resin is to be cured under an array of air jets at  $100^\circ\text{C}$ , as shown in the accompanying sketch. If the initial temperature of the resin is  $20^\circ\text{C}$ , determine the temperature of the back face after one hour. Take the heat transfer coefficient as  $40 \text{ W/m}^2 \text{ K}$ , and for the resin  $\rho = 2600 \text{ kg/m}^3$ ,  $c = 800 \text{ J/kg K}$ ,  $k = 1.0 \text{ W/m K}$ .

#### Solution

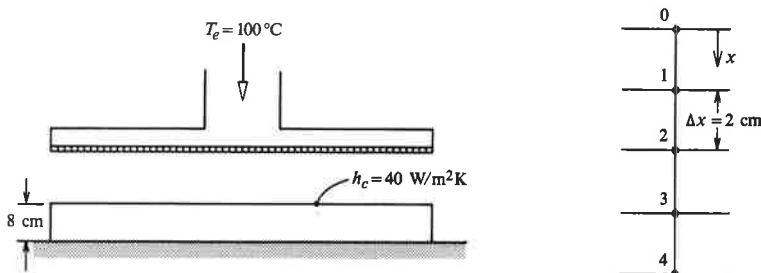
**Given:** Slab, convectively heated on one face.

**Required:** Back face temperature after one hour.

**Assumptions:** 1. The back face is well insulated.

2. The heat transfer coefficient  $h_c$  is uniform over the surface, and  $k$ ,  $\rho$ , and  $c$  are constant.

3. Edge losses are negligible.



The explicit finite-difference method will be used. Let  $\Delta x = 2$  cm; then the mesh size-based Biot number is

$$\text{Bi} = \frac{h_c \Delta x}{k} = \frac{(40)(0.02)}{1.0} = 0.8$$

The stability criterion, Eq. (3.111), is

$$\text{Fo} \leq \frac{1}{2(1 + \text{Bi})} = \frac{1}{2(1 + 0.8)} = 0.277$$

Choose  $\text{Fo} = 0.25$ , so that the time step is

$$\Delta t = \frac{\text{Fo}(\Delta x)^2}{\alpha} = \frac{(0.25)(0.02)^2}{1.0/(2600 \times 800)} = 208 \text{ s (3.47 min)}$$

Equation (3.107) for the interior nodes becomes

$$\begin{aligned} T_m^{i+1} &= [1 - (2)(0.25)]T_m^i + 0.25(T_{m-1}^i + T_{m+1}^i) \\ &= 0.5T_m^i + 0.25(T_{m-1}^i + T_{m+1}^i) \end{aligned}$$

and Eq. (3.110) for the surface node is

$$\begin{aligned} T_0^{i+1} &= (2)(0.25)(T_1^i + 0.8T_e) + [1 - 2(0.25) - 2(0.25)(0.8)]T_0^i \\ &= 0.5(T_1^i + 0.8T_e) + 0.1T_0^i \end{aligned}$$

To obtain an appropriate equation for node 4 at the adiabatic surface, we simply set  $\text{Bi} = 0$  in Eq. (3.110) to obtain

$$T_4^{i+1} = (2)(0.25)T_3^i + [1 - (2)(0.25)]T_4^i = 0.5(T_3^i + T_4^i)$$

The initial condition is  $T = 20^\circ\text{C}$ ; thus, the temperatures at the first time step are

$$\begin{aligned} T_0^1 &= 0.5[20 + (0.8)(100)] + 0.1(20) = 52 \\ T_1^1 &= 0.5(20) + 0.25(20 + 20) = 20 \\ T_2^1 &= 0.5(20) + 0.25(20 + 20) = 20 \\ T_3^1 &= 0.5(20) + 0.25(20 + 20) = 20 \\ T_4^1 &= 0.5(20 + 20) = 20 \end{aligned}$$

and at the second time step,

$$\begin{aligned} T_0^2 &= 0.5[20 + (0.8)(100)] + 0.1(52) = 55.2 \\ T_1^2 &= 0.5(20) + 0.25(52 + 20) = 28.0 \\ T_2^2 &= 0.5(20) + 0.25(20 + 20) = 20 \\ T_3^2 &= 0.5(20) + 0.25(20 + 20) = 20 \\ T_4^2 &= 0.5(20 + 20) = 20 \end{aligned}$$

and so on. The results for 20 time steps obtained using a programmable hand calculator are given in the following table. Also shown is the surface temperature  $T_0$ , calculated using computer program COND2, which is essentially exact.

Time step	Time min	$T_0$ °C	$T_1$ °C	$T_2$ °C	$T_3$ °C	$T_4$ °C	$T_0$ (exact) °C
0	0.00	20.00	20.00	20.00	20.00	20.00	20.00
1	3.47	52.00	20.00	20.00	20.00	20.00	46.32
2	6.93	55.20	28.00	20.00	20.00	20.00	53.30
3	10.40	59.52	32.80	22.00	20.00	20.00	57.68
4	13.87	62.35	36.78	24.20	20.50	20.00	60.85
5	17.33	64.63	40.03	26.42	21.30	20.25	63.32
6	20.80	66.48	42.78	28.54	22.32	20.78	65.33
7	24.27	68.04	45.14	30.54	23.49	21.55	67.01
8	27.73	69.37	47.22	32.43	24.77	22.52	68.45
9	31.20	70.55	49.06	34.21	26.12	23.64	69.71
10	34.67	71.58	50.72	35.90	27.52	24.88	70.82
11	38.13	72.52	52.23	37.51	28.96	26.20	71.81
12	41.60	73.37	53.62	39.05	30.41	27.58	72.72
13	45.07	74.15	54.92	40.53	31.86	28.99	73.54
14	48.53	74.87	56.13	41.96	33.31	30.43	74.31
15	52.00	75.55	57.27	43.34	34.75	31.87	75.02
16	55.47	76.19	58.36	44.68	36.18	33.31	75.69
17	58.93	76.80	59.40	45.97	37.59	34.75	76.32
18	62.40	77.38	60.39	47.23	38.97	36.17	76.92
19	65.87	77.93	61.35	48.46	40.34	37.57	77.50
20	69.33	78.47	62.27	49.65	41.67	38.95	78.05

### Comments

Notice that, for this crude calculation using  $\Delta x = 2$  cm, the stability criterion is not a significant limitation on the time step. However, if  $\Delta x$  were reduced to, say, 0.5 cm to improve spatial resolution of the temperature profile,  $\Delta t$  becomes only 13 s. Even this time step poses no problem to present-day personal computers.

---

### EXAMPLE 3.16 Quenching of a Slab with Nucleate Boiling

A 4 cm-thick slab of steel initially at 500 K is immersed in a water bath at 310 K and 1 atm. Under these conditions, *nucleate boiling* (see Chapter 7) occurs on the slab surface; the heat transfer coefficient is very large and is strongly dependent on temperature difference. An appropriate empirical equation for  $h_c$  under these conditions is  $h_c = 140(T - T_{\text{sat}})^2$  W/m<sup>2</sup> K, where  $T_{\text{sat}}$  is the saturation temperature (boiling point). Determine the temperature profile across the slab for a period of 30 s. For the steel, take  $k = 54$  W/m K,  $\alpha = 1.5 \times 10^{-5}$  m<sup>2</sup>/s.

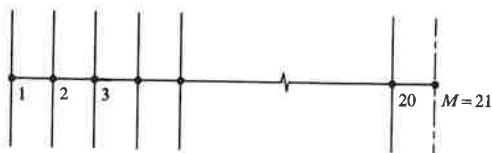
### Solution

**Given:** Slab immersed in water; nucleate boiling on surface.

**Required:** Temperature profiles.

**Assumption:** Edge effects negligible to give a one-dimensional problem.

The implicit finite-difference method will be used for this problem, and the results will be obtained using a computer. Since the problem is symmetrical about the center plane of the slab, node  $M = 21$  is located on the center plane as shown. Choosing a time step of 1 s, the mesh Fourier number is



$$Fo = \frac{\alpha \Delta t}{\Delta x^2} = \frac{(1.5 \times 10^{-5})(1)}{(0.02/20)^2} = 15$$

Temperatures at the interior nodes  $m = 2, \dots, M - 1$  are given by Eq. (3.112):

$$\begin{aligned} T_m^{i+1} &= \frac{1}{1 + (2)(15)} [15(T_{m+1}^{i+1} + T_{m-1}^{i+1}) + T_m^i] \\ &= \frac{1}{31} [15(T_{m+1}^{i+1} + T_{m-1}^{i+1}) + T_m^i] \end{aligned}$$

The temperature at node  $M$  is given in Table 3.8, item 4:

$$\begin{aligned} T_M^{i+1} &= \frac{1}{1 + (2)(15)} [(2)(15)T_{M-1}^{i+1} + T_M^i] \\ T_{21}^{i+1} &= \frac{1}{31} [30T_{20}^{i+1} + T_{21}^i] \end{aligned}$$

The temperature at the surface node  $m = 1$  is given in Table 3.8, item 2, with  $T_e$  replaced by  $T_{\text{sat}}$ :

$$T_1^{i+1} = \frac{2(15)(T_2^{i+1} + \text{Bi} T_{\text{sat}}) + T_1^i}{1 + 2(15) + (2)(15) \text{Bi}}$$

The Biot number is not a constant in this problem and, when the implicit formulation is used, must be evaluated at the current time step:

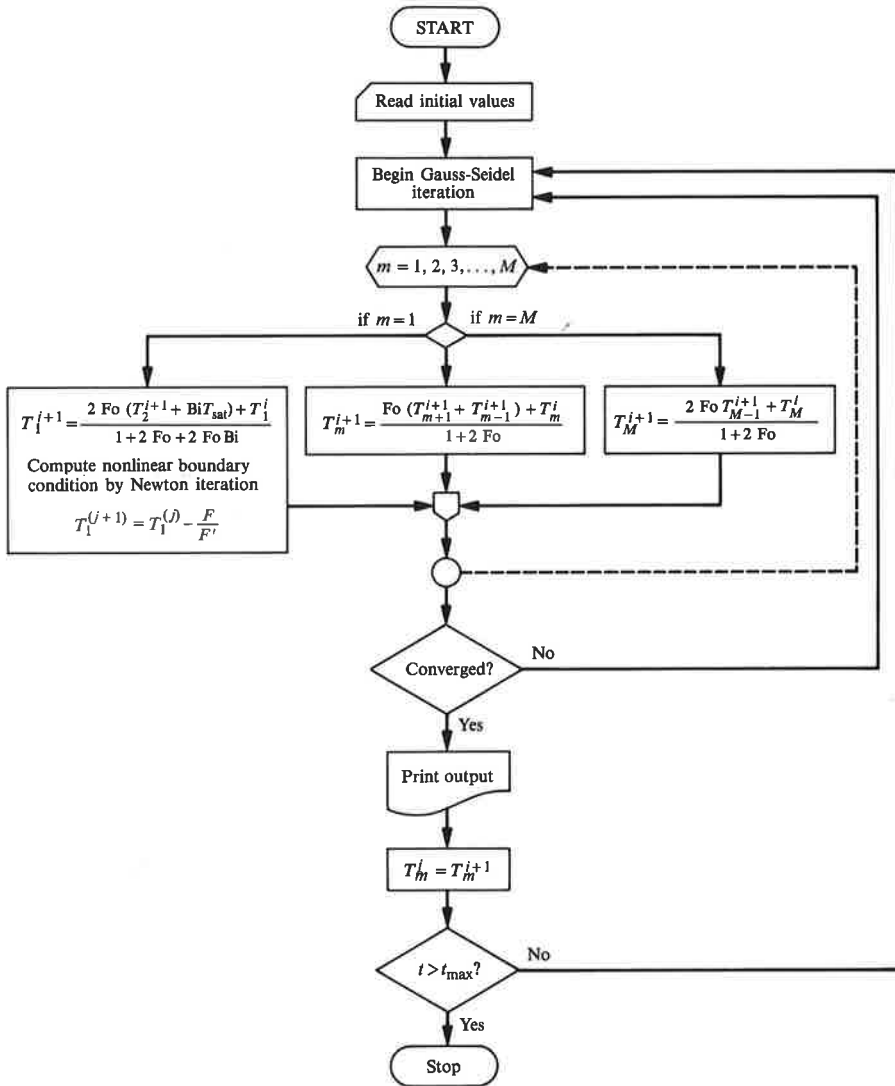
$$\text{Bi} = \frac{h_c \Delta x}{k} = \frac{140(T_1^{i+1} - T_{\text{sat}})^2 (0.02/20)}{54} = 2.59 \times 10^{-3} (T_1^{i+1} - T_{\text{sat}})^2$$

Thus,

$$T_1^{i+1} = \frac{30(T_2^{i+1} + 2.59 \times 10^{-3} (T_1^{i+1} - T_{\text{sat}})^2 T_{\text{sat}}) + T_1^i}{31 + 7.78 \times 10^{-2} (T_1^{i+1} - T_{\text{sat}})^2}$$

Since  $T_1^{i+1}$  appears on both sides of this equation, it should be solved for by iteration. A flow diagram for a simple program based on Gauss-Seidel and Newton iteration follows. Sample results are given in the accompanying table.

Node	1	6	11	16	21
Location $x$ , cm	0	0.5	1.0	1.5	2.0
Nodal temperatures, K:					
$t = 0$ s	500.0	500.0	500.0	500.0	500.0
1	394.9	471.0	492.0	497.6	498.8
2	390.8	451.2	481.2	492.8	495.6
5	387.6	425.8	455.1	472.4	478.0
10	385.4	409.4	429.3	442.4	447.0
20	382.5	393.3	402.3	408.2	410.2
30	380.5	385.6	389.8	392.6	393.5

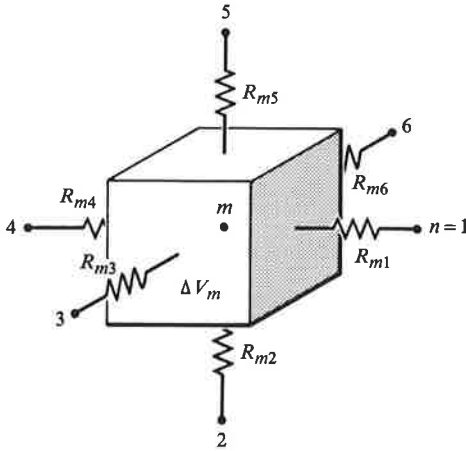


**Comments**

1. The effect of  $\Delta x$  and  $\Delta t$  on the accuracy of the solution should be explored.
2. The task of writing a computer program is given as Exercise 3–130.

**3.6.3 Resistance-Capacitance (RC) Formulation**

A useful alternative to the formulations for finite-difference numerical methods presented in the previous sections is the **resistance-capacitance** formulation. Consider multidimensional unsteady conduction with internal heat generation and variable thermal properties. Figure 3.41 shows the node of interest,  $m$ , surrounded by a volume



**Figure 3.41** Finite control volume  $\Delta V_m$  surrounding node  $m$ , with thermal resistances  $R_{mn}$ : resistance-capacitance formulation.

$\Delta V_m$  of thermal capacitance  $C_m = \rho_m c_m \Delta V_m$ . The surrounding nodes are denoted  $n$ , and conduction from the volume  $\Delta V_n$  into volume  $\Delta V_m$  is expressed in terms of a thermal resistance  $R_{mn}$ . An energy balance on volume  $\Delta V_m$  over the time interval  $\Delta t$  gives

$$C_m \frac{T_m^{i+1} - T_m^i}{\Delta t} = \sum_n \frac{T_n^i - T_m^i}{R_{mn}} + \dot{Q}_v''' \Delta V_m \quad (3.113)$$

where the superscript refers to the time step, as before. Equation (3.113) is an explicit formulation. Although written for an interior node, Eq. (3.113) can also be applied to boundary nodes with the resistances  $R_{mn}$  evaluated accordingly. The concepts involved here are, of course, identical to those introduced for elementary thermal networks in Sections 1.4 and 2.3. Notice that when properties are temperature-dependent, the capacitance  $C_m$ , resistances  $R_{mn}$ , and source  $\dot{Q}_v'''$  are evaluated at time step  $i$  to preserve the explicit formulation. If an implicit formulation is desired, the driving potentials  $(T_n - T_m)$  must be evaluated at time step  $(i + 1)$ . However, to have a *fully implicit* formulation,  $C_m$ ,  $R_{mn}$ , and  $\dot{Q}_v'''$  must also be evaluated at time step  $(i + 1)$ , which can slow down the required iteration procedure. Thus, the explicit formulation is usually preferred when this resistance-capacitance representation is used.

Solving Eq. (3.113) for  $T_m^{i+1}$  gives

$$T_m^{i+1} = \left( 1 - \frac{\Delta t}{C_m} \sum_n \frac{1}{R_{mn}} \right) T_m^i + \left( \dot{Q}_v''' \Delta V_m + \sum_n \frac{T_n^i}{R_{mn}} \right) \frac{\Delta t}{C_m} \quad (3.114)$$

Again, a satisfactory condition for stability is that the coefficient of  $T_m^i$  should not be negative:

$$1 - \frac{\Delta t}{C_m} \sum_n \frac{1}{R_{mn}} \geq 0 \quad (3.115)$$

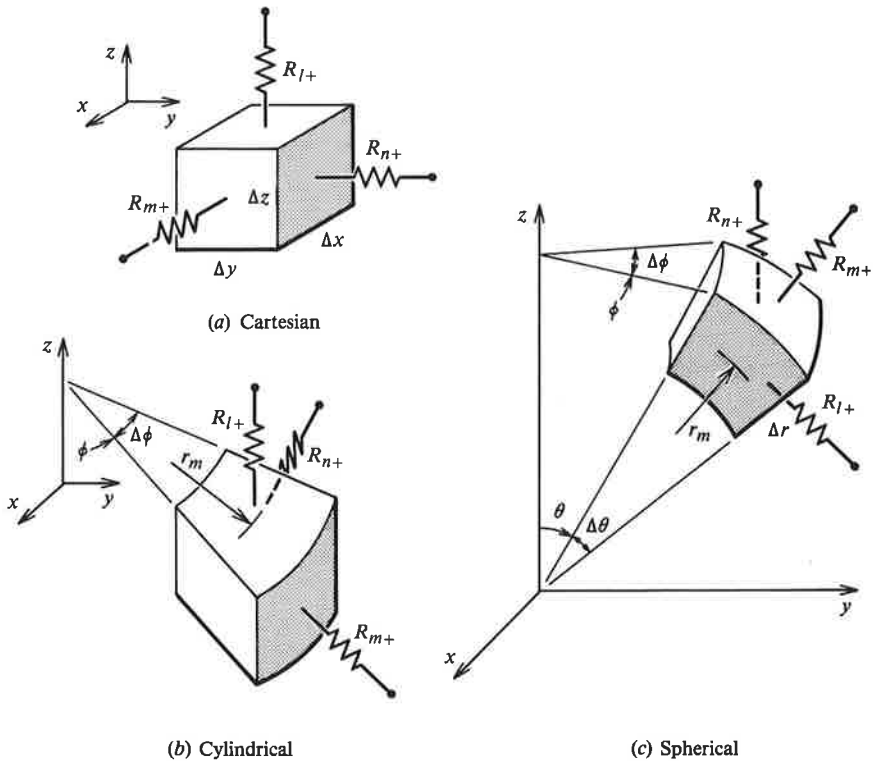
The resistance-capacitance representation is usually applied to problems that have complicated boundary conditions, that require a variation in the size and shape of volumes  $\Delta V_m$ , or for which thermal properties are temperature-dependent. Thus, the stability criterion must be evaluated for each node, and a time step chosen such that

$$\Delta t \leq \left( \frac{C_m}{\sum_n (1/R_{mn})} \right)_{\min} \quad (3.116)$$

That is, it is the most restrictive nodal equation that controls the allowable time step.

Table 3.10 gives the volumes  $\Delta V_m$  and resistances  $R$  for interior nodes in the Cartesian, cylindrical, and spherical coordinate systems shown in Fig. 3.42. Table 3.11 shows examples for boundary nodes in Cartesian coordinates.

The resistance-capacitance representation is also widely applied to systems-level thermal analysis. Figure 3.43 shows how a complicated system is divided into elements. At this level, the representation is equivalent to the lumped thermal capacity approach of Section 1.5. The major advantage of the  $RC$  representation is the versatility of resulting computer programs. The equation-solving routines can be written



**Figure 3.42** Finite control volumes  $\Delta V_m$  and resistances  $R$  in Cartesian, cylindrical, and spherical coordinates for the resistance-capacitance formulation.



**Table 3.10** Internal nodal resistances in Cartesian, cylindrical, and spherical coordinates.

	Coordinate System		
	Cartesian	Cylindrical	Spherical
Coordinates	$x, y, z$	$r, \phi, z$	$r, \phi, \theta$
Indices	$m, n, l$	$m, n, l$	$m, n, l$
Volume element	$\Delta x \Delta y \Delta z$	$r_m \Delta r \Delta \phi \Delta z$	$r_m^2 \sin \theta \Delta r \Delta \phi \Delta \theta$
$R_{m+}$	$\frac{\Delta x}{\Delta y \Delta z k}$	$\frac{\Delta r}{(r_m + \Delta r/2) \Delta \phi \Delta z k}$	$\frac{\Delta r}{(r_m + \Delta r/2)^2 \sin \theta \Delta \phi \Delta \theta k}$
$R_{m-}$	$\frac{\Delta x}{\Delta y \Delta z k}$	$\frac{\Delta r}{(r_m - \Delta r/2) \Delta \phi \Delta z k}$	$\frac{\Delta r}{(r_m - \Delta r/2)^2 \sin \theta \Delta \phi \Delta \theta k}$
$R_{n+}$	$\frac{\Delta y}{\Delta x \Delta z k}$	$\frac{r_m \Delta \phi}{\Delta r \Delta z k}$	$\frac{\Delta \phi \sin \theta}{\Delta r \Delta \theta k}$
$R_{n-}$	$\frac{\Delta y}{\Delta x \Delta z k}$	$\frac{r_m \Delta \phi}{\Delta r \Delta z k}$	$\frac{\Delta \phi \sin \theta}{\Delta r \Delta \theta k}$
$R_{l+}$	$\frac{\Delta z}{\Delta x \Delta y k}$	$\frac{\Delta z}{r_m \Delta \phi \Delta r k}$	$\frac{\Delta \theta}{\sin(\theta + \Delta \theta/2) \Delta r \Delta \phi k}$
$R_{l-}$	$\frac{\Delta z}{\Delta x \Delta y k}$	$\frac{\Delta z}{r_m \Delta \phi \Delta r k}$	$\frac{\Delta \theta}{\sin(\theta - \Delta \theta/2) \Delta r \Delta \phi k}$

in terms of the very general capacitance  $C_m$  and resistances  $R_{mn}$ , with specialization of these quantities relegated to subroutines prepared for a particular problem. It is usual practice to also allow for the possibility of radiation heat transfer between the volume elements; Eq. (3.113) then becomes

$$C_m \frac{T_m^{i+1} - T_m^i}{\Delta t} = \sum_n \frac{T_{n_i} - T_m^i}{R_{mn}^{\text{cond}}} + \sum_n \frac{T_n^i - T_m^i}{R_{mn}^{\text{rad}}} + \dot{Q}_v''' \Delta V_m \quad (3.117)$$

where  $R_{mn}^{\text{cond}}$  and  $R_{mn}^{\text{rad}}$  are conduction and radiation resistances, respectively. Referring to Section 1.3.2, Eq. (1.17) becomes

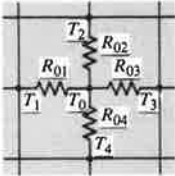
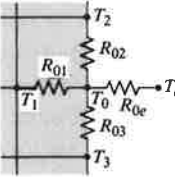
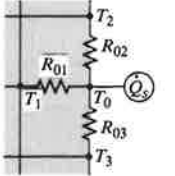
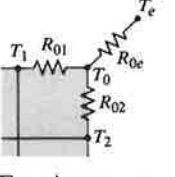
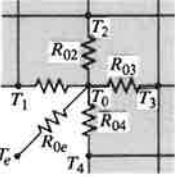
$$\begin{aligned} \dot{Q}_{nm} &= A_n \mathcal{F}_{nm} \sigma (T_n^4 - T_m^4) \\ &= A_n \mathcal{F}_{nm} \sigma (T_n^2 + T_m^2)(T_n + T_m)(T_n - T_m) \end{aligned}$$

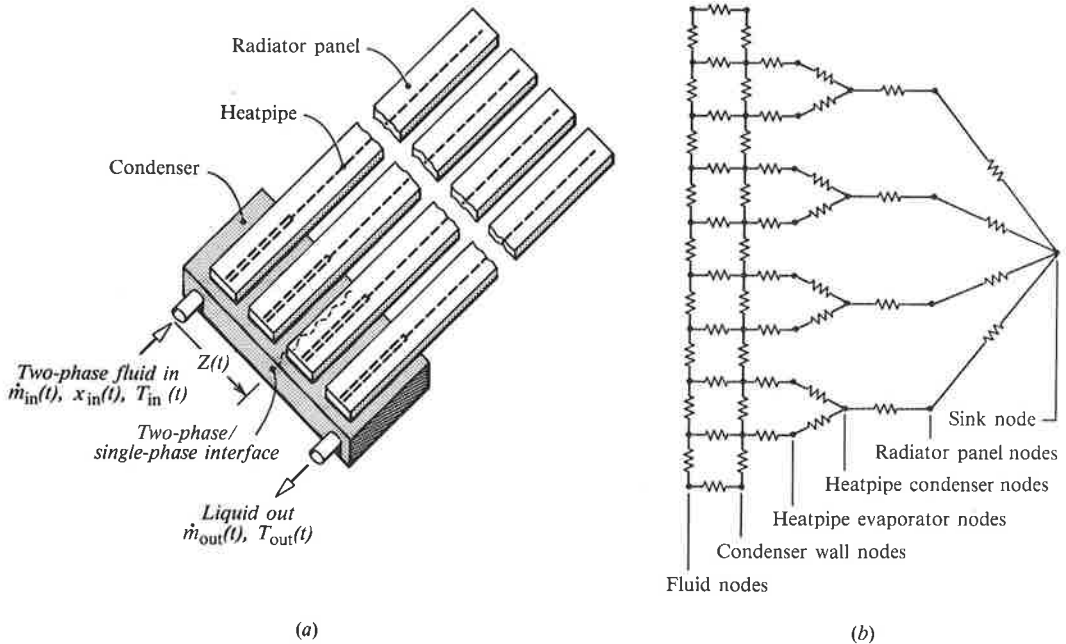
Hence,

$$R_{mn}^{\text{rad}} = \frac{1}{A_n \mathcal{F}_{nm} \sigma (T_n^2 + T_m^2)(T_n + T_m)} \quad (3.118)$$

In general, the transfer factors  $\mathcal{F}_{nm}$  depend on the geometry and emittances of all the surfaces making up an enclosure and are difficult to calculate. However, computer programs are available for this purpose (or simple approximations are used).

**Table 3.11** Control volumes and resistances for two-dimensional Cartesian coordinates,  $\Delta x = \Delta y$ .

Item	Configuration	Control Volume and Resistances
1.	 <p>Interior node</p>	$\Delta V = (\Delta x)^2$ $R_{01} = R_{02} = R_{03} = R_{04} = \frac{1}{k}$
2.	 <p>Plane surface, convection</p>	$\Delta V = \frac{(\Delta x)^2}{2}$ $R_{01} = \frac{1}{k}; \quad R_{02} = R_{03} = \frac{2}{k}$ $R_{0e} = \frac{1}{h_c \Delta x}$
3.	 <p>Plane surface, known heat flux</p>	$\Delta V = \frac{(\Delta x)^2}{2}$ $R_{01} = \frac{1}{k}; \quad R_{02} = R_{03} = \frac{2}{k}$ $\dot{Q}_s = q_s \Delta x$
4.	 <p>Exterior corner, convection</p>	$\Delta V = \frac{(\Delta x)^2}{4}$ $R_{01} = R_{02} = \frac{2}{k}$ $R_{0e} = \frac{1}{h_c \Delta x}$
5.	 <p>Interior corner, convection</p>	$\Delta V = \frac{3(\Delta x)^2}{4}$ $R_{01} = R_{04} = \frac{2}{k}$ $R_{02} = R_{03} = \frac{1}{k}$ $R_{0e} = \frac{1}{h_c \Delta x}$



**Figure 3.43** RC representation of a spacecraft heat rejection system. (a) The physical system. (b) The nodal network.

Computer programs based on the resistance-capacitance representation have found very wide industrial use, particularly in the aerospace industry. Popular examples include SINDA [16] and MITAS [17]. Although simple in concept, these programs have been refined over many years and are efficient, reliable, and convenient to use. Other software that can be used for conduction calculations include PHOENICS[18] and COMPACT[19].

### EXAMPLE 3.17 Asymmetrical Heating of a Cylindrical Rod

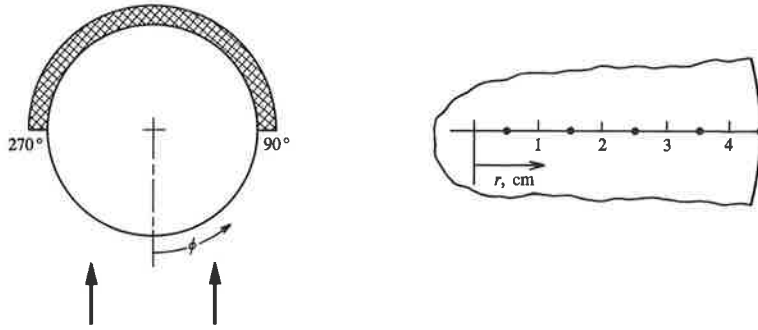
A long, 9 cm-diameter ceramic rod, initially at  $20^\circ\text{C}$ , is exposed to a radiation heat flux on one side such that  $q_s = 5000 \cos \phi$ ,  $270^\circ < \phi < 90^\circ$ , and is insulated on the other side,  $q_s = 0$ ,  $90^\circ < \phi < 270^\circ$ . Determine the temperature response of the rod. For the ceramic, take  $\rho = 3000 \text{ kg/m}^3$ ,  $k = 5 \text{ W/m K}$ , and  $c = 800 \text{ J/kg K}$ .

#### Solution

**Given:** Ceramic rod heated on one side, insulated on the other.

**Required:** Temperature response,  $T(r, \phi, t)$ .

**Assumptions:** 1. Constant properties.  
2. No axial variation of temperature.



The explicit resistance-capacitance formulation described in Section 3.6.3 will be used. Equation (3.114) gives the temperatures at the interior nodes; for  $\dot{Q}_v''' = 0$ ,

$$T_m^{i+1} = \left( 1 - \frac{\Delta t}{C_m} \sum_n \frac{1}{R_{mn}} \right) T_m^i + \frac{\Delta t}{C_m} \sum_n \frac{T_n^i}{R_{mn}}$$

Choosing  $\Delta r = 1$  cm,  $\Delta \phi = 30^\circ = 0.5236$  rad, and  $\Delta z = 1$  m, Table 3.10 gives the volume element as

$$\Delta V_m = r_m \Delta r \Delta \phi \Delta z = r_m (0.01)(0.5236)(1) = 5.236 \times 10^{-3} r_m$$

and  $C_m = \rho c \Delta V_m = (3000)(800)(5.236 \times 10^{-3}) r_m = 1.257 \times 10^4 r_m$ . Also from Table 3.10, the nodal resistances are

$$R_{m+} = \frac{\Delta r}{(r_m + \Delta r/2) \Delta \phi \Delta z k} = \frac{0.01}{(r_m + 0.005)(0.5236)(1)(5)} = \frac{3.820 \times 10^{-3}}{r_m + 0.005}$$

$$R_{m-} = \frac{\Delta r}{(r_m - \Delta r/2) \Delta \phi \Delta z k} = \frac{0.01}{(r_m - 0.005)(0.5236)(1)(5)} = \frac{3.820 \times 10^{-3}}{r_m - 0.005}$$

$$R_{n+} = \frac{r_m \Delta \phi}{\Delta r \Delta z k} = \frac{r_m (0.5236)}{(0.01)(1)(5)} = 10.47 r_m$$

$$R_{n-} = R_{n+} = 10.47 r_m$$

A surface node for  $270^\circ < \phi < 90^\circ$  is shown in the accompanying figure. For this half-volume,

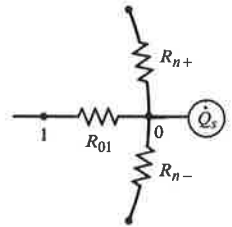
$$\begin{aligned} C_m &= \frac{1}{2} (1.257 \times 10^4) (0.045) \\ &= 282.8 \end{aligned}$$

$$R_{01} = \frac{\Delta r}{(r_0 - \Delta r/2) \Delta \phi \Delta z k} = \frac{0.01}{(0.045 - 0.005)(0.5236)(1)(5)} = 9.549 \times 10^{-2}$$

$$R_{n+} = \frac{r_0 \Delta \phi}{(\Delta r/2)(\Delta z)(k)} = \frac{(0.045)(0.5236)}{(0.005)(1)(5)} = 0.9425$$

$$R_{n-} = R_{n+} = 0.9425$$

$$\dot{Q}_s = q_s r_s \Delta \phi \Delta z = (5000 \cos \phi)(0.045)(0.5236)(1) = 117.8 \cos \phi$$



The same values of  $C_m$ ,  $R_{01}$ ,  $R_{n+}$ , and  $R_{n-}$  apply to the surface nodes for  $90^\circ < \phi < 270^\circ$ , but  $\dot{Q}_s = 0$ .

The stability criterion for the explicit method is given by Eq. (3.116):

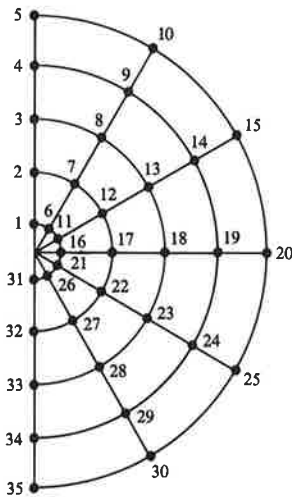
$$\Delta t \leq \left( \frac{C_m}{\sum_n (1/R_{mn})} \right)_{\min}$$

The minimum value is obtained for  $r_m = 0.005$  m, for which

$$\begin{aligned} \frac{C_m}{\sum_n (1/R_{mn})} &= \frac{(1.257 \times 10^4)(0.005)}{\frac{(0.005 + 0.005)}{(3.820 \times 10^{-3})} + \frac{(0.005 - 0.005)}{(3.820 \times 10^{-3})} + \frac{1}{(10.47)(0.005)} + \frac{1}{(10.47)(0.005)}} \\ &= 1.54 \text{ s} \end{aligned}$$

Hence, choose  $\Delta t = 1.0$  s.

Sample results are shown below.

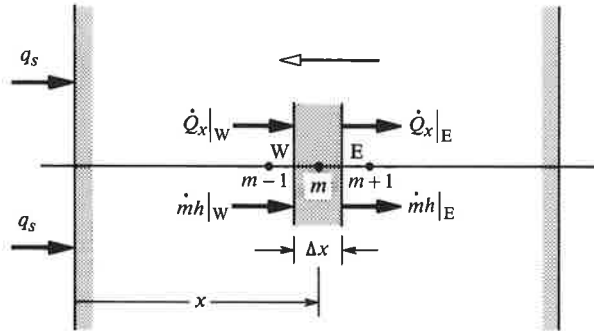


Time [s]	Nodal temperatures, °C					
	35	32	2	5	25	15
0	20.0	20.0	20.0	20.0	20.0	20.0
60	32.9	20.6	20.0	20.0	26.5	20.0
120	39.4	22.8	20.1	20.0	29.9	20.2
180	44.3	25.4	20.6	20.1	32.8	20.7
240	48.4	28.0	21.3	20.3	35.4	21.3
300	52.0	30.5	22.2	20.6	37.8	22.2
360	55.1	32.8	23.2	21.2	40.1	23.2
420	58.0	35.1	24.4	21.9	42.3	24.3
480	60.6	37.2	25.7	22.8	44.4	25.6
540	63.0	39.3	27.1	23.8	46.5	26.9
600	65.3	41.3	28.5	25.0	48.5	28.3

### 3.6.4 A Finite-Difference Method for Moving-Boundary Problems

Finite-difference methods have proven invaluable for analyzing moving-boundary problems. One important application has been the calculation of the thermal response of ablative heat shields on reentry vehicles. It is doubtful whether Project Apollo could have been successful without the use of such methods for the design of the heat shield on the command module. As an example, we will consider a simple one-dimensional transient ablation problem. The coordinate system is fixed to the surface so that the solid can be imagined to flow at a negative velocity  $V$  through the plane at  $x = 0$ , as shown in Fig. 3.44. A finite control volume  $\Delta x \cdot 1 \cdot 1$  surrounds node  $m$  at location  $x$ . An energy balance on the control volume over time interval  $\Delta t$  requires that

$$\text{Increase in internal energy within volume} = \text{Net conduction into volume} + \text{Net inflow of enthalpy} \quad (3.119)$$



**Figure 3.44** Finite control volume  $\Delta x$  by 1 by 1 surrounding node  $m$  at location  $x$  used to derive the difference equation for one-dimensional transient ablation.

Notice that Eq. (3.119) is a special form of the *unsteady-flow* energy equation for an open system. The increase in internal energy from time step  $i$  to step  $(i + 1)$  is

$$\Delta U = \rho c (\Delta x \cdot 1 \cdot 1) (T_m^{i+1} - T_m^i)$$

To obtain an implicit formulation, the conduction heat flows are evaluated at time step  $(i + 1)$ :

$$\dot{Q}_x|_W \Delta t = -k \frac{T_m^{i+1} - T_{m-1}^{i+1}}{\Delta x} (1 \cdot 1) \Delta t$$

$$\dot{Q}_x|_E \Delta t = -k \frac{T_{m+1}^{i+1} - T_m^{i+1}}{\Delta x} (1 \cdot 1) \Delta t$$

The enthalpy flow poses a special problem. Perhaps the obvious approach is to write

$$\dot{m}h|_W \Delta t = \rho c V \frac{T_{m-1}^{i+1} + T_m^{i+1}}{2} (1 \cdot 1) \Delta t$$

$$\dot{m}h|_E \Delta t = \rho c V \frac{T_m^{i+1} + T_{m+1}^{i+1}}{2} (1 \cdot 1) \Delta t$$

where the enthalpy flows across the planes at  $x - \Delta x/2$  and  $x + \Delta x/2$  have been evaluated in terms of the average temperature of adjacent nodes. This approach leads to what is called a *central-difference* scheme. On physical grounds, however, the enthalpy flow across a plane can be influenced by the temperature on the upwind side only; the temperature on the downwind side should not have an influence. Thus, the *upwind-difference* scheme requires that the enthalpy flows be written as

$$\dot{m}h|_W \Delta t = \rho c V T_m^{i+1} (1 \cdot 1) \Delta t$$

$$\dot{m}h|_E \Delta t = \rho c V T_{m+1}^{i+1} (1 \cdot 1) \Delta t$$

for velocity  $V$  negative, as is the case for our problem. Accuracy and stability considerations dictate which scheme is most appropriate. In fact, it is a common

practice to use a hybrid scheme in which central differencing is used when the velocity  $V$  is small, and upwind differencing is used when  $V$  is large. For simplicity, we will use the central-difference scheme only. Substituting in Eq. (3.119) and rearranging gives

$$T_m^{i+1} = \frac{\text{Fo}(T_{m+1}^{i+1} + T_{m-1}^{i+1}) - (1/2)\text{Fo Pe}(T_{m+1}^{i+1} - T_{m-1}^{i+1}) + T_m^i}{1 + 2\text{Fo}} \quad (3.120)$$

where  $\text{Pe}$  is the mesh *Peclet number*, which is defined as  $\text{Pe} = V\Delta x/\alpha$ . It is, in fact, the mesh Peclet number that determines whether central or upwind differencing should be used: upwind differencing should be used when  $|\text{Pe}| > 2$ .

### Boundary Conditions

Formulation of the finite-difference forms of the boundary conditions is similar to the procedure used for the implicit method described in Section 3.6.2. For the front face, shown in Fig. 3.45a, an energy balance requires that

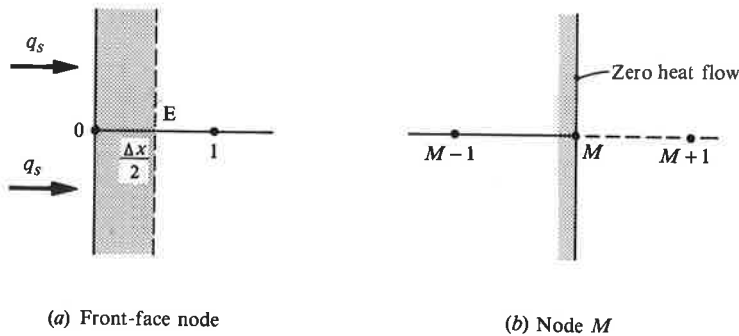
$$\rho c \left( \frac{\Delta x}{2} \cdot 1 \cdot 1 \right) (T_0^{i+1} - T_0^i) = (\dot{Q}_x|_0 - \dot{Q}_x|_E) \Delta t + (\dot{m}h|_0 - \dot{m}h|_E) \Delta t$$

$$\dot{Q}_x|_0 = q_s(1 \cdot 1); \quad \dot{Q}_x|_E = -k \frac{T_1^{i+1} - T_0^{i+1}}{\Delta x} (1 \cdot 1)$$

$$\dot{m}h|_0 = \rho c V T_0^{i+1} (1 \cdot 1); \quad \dot{m}h|_E = \rho c V \frac{T_1^{i+1} + T_0^{i+1}}{2} (1 \cdot 1)$$

Substituting and rearranging,

$$T_0^{i+1} = \frac{2\text{Fo}(T_1^{i+1} + q_s \Delta x/k) - \text{Fo Pe } T_1^{i+1} + T_0^i}{1 + 2\text{Fo} - \text{Fo Pe}} \quad (3.121)$$



**Figure 3.45** Nodal network and finite control volume for formulation of finite-difference forms of boundary conditions for one-dimensional transient ablation. (a) Front-face node. (b) Node  $M$ .

Referring to Fig. 3.45b we place node  $m = M$  at  $x = L$ , for  $L$  chosen sufficiently large to ensure zero heat flow. An appropriate finite difference form of this boundary condition can be derived in a number of ways. For example, the temperature at the *mirror-image* node ( $M + 1$ ) can be set equal to the temperature at node ( $M - 1$ ) to give a zero temperature gradient at  $x = L$ ,

$$T_{M+1}^{i+1} = T_{M-1}^{i+1}$$

Substituting in Eq. (3.120) for  $m = M$ ,

$$T_M^{i+1} = \frac{2\text{Fo}T_{M-1}^{i+1} + T_M^i}{1 + 2\text{Fo}} \quad (3.122)$$

Notice that this result is also given as item 4 of Table 3.8. Example 3.18 illustrates the implementation of this finite-difference solution procedure.

### EXAMPLE 3.18 Dust Erosion of a Plastic Heat Shield

A very thick plastic heat shield, initially at  $0^\circ\text{C}$ , is exposed simultaneously to a heat flux of  $160 \text{ kW/m}^2$  from a high-temperature radiation source and to a dust blast that erodes the surface at a rate of  $0.1 \text{ mm/s}$ . Determine the temperature response of the shield. For the plastic, take property values of  $\rho = 1200 \text{ kg/m}^3$ ,  $k = 0.3 \text{ W/m K}$ , and  $\alpha = 0.015 \times 10^{-6} \text{ m}^2/\text{s}$ .

#### Solution

**Given:** Transient conduction with a specified surface ablation rate.

**Required:** Temperature profiles  $T(x, t)$

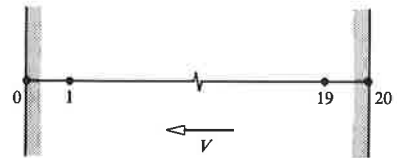
- Assumptions:**
1. One-dimensional conduction.
  2. Constant properties.
  3. The heat flow does not penetrate deeper than 2 mm.

Choose  $\Delta x = 0.1 \text{ mm}$ ,  $L = 2 \text{ mm}$ , and  $\Delta t = 0.1 \text{ s}$ ; then the mesh size-based Fourier number is

$$\text{Fo} = \frac{\alpha \Delta t}{\Delta x^2} = \frac{(0.015 \times 10^{-6})(0.1)}{(1 \times 10^{-4})^2} = 0.15$$

and the mesh size-based Peclet number is

$$\text{Pe} = \frac{V \Delta x}{\alpha} = \frac{(-10^{-4})(10^{-4})}{0.015 \times 10^{-6}} = -0.667$$



Equation (3.120) for the interior nodes  $m = 1, 2, \dots, 19$  is

$$\begin{aligned} T_m^{i+1} &= \frac{0.15(T_{m+1}^{i+1} + T_{m-1}^{i+1}) - (1/2)(0.15)(-0.667)(T_{m+1}^{i+1} - T_{m-1}^{i+1}) + T_m^i}{1 + (2)(0.15)} \\ &= 0.1539T_{m+1}^{i+1} + 0.07690T_{m-1}^{i+1} + 0.7692T_m^i \end{aligned}$$



Equation (3.121) for the front-face node,  $m = 0$ , is

$$\begin{aligned} T_0^{i+1} &= \frac{(2)(0.15)[T_1^{i+1} + (160 \times 10^3)(10^{-4})/(0.3)] - (0.15)(-0.667)T_1^{i+1} + T_0^i}{1 + (2)(0.15) - (0.15)(-0.667)} \\ &= 11.43 + 0.2857T_1^{i+1} + 0.7143T_0^i \end{aligned}$$

Equation (3.122) for node  $m = 20$ , is

$$\begin{aligned} T_{20}^{i+1} &= \frac{(2)(0.15)T_{19}^{i+1} + T_{20}^i}{1 + (2)(0.15)} \\ &= 0.2308T_{19}^{i+1} + 0.7692T_{20}^i \end{aligned}$$

As in Example 3.16, the Gauss-Seidel method can be used to solve the nodal equations. Sample temperature profiles are shown in the following table. Also given is the quasi-steady solution obtained from Eqs. (3.98) and (3.99). First, from Eq. (3.99),

$$q_u = -\rho c V (T_s - T_0)$$

$$T_s = T_0 - \frac{q_u}{\rho c V} = T_0 - \frac{\alpha q_u}{kV} = 0 - \frac{(0.015 \times 10^{-6})(160 \times 10^3)}{(0.3)(-10^{-4})} = 80^\circ\text{C}$$

and from Eq. (3.98),

$$T = T_0 + (T_s - T_0)e^{(V/\alpha)\xi} = 0 + (80 - 0)e^{-10^{-4}\xi/0.015 \times 10^{-6}} = 80e^{-6667\xi} \text{ }^\circ\text{C}$$

Time s	Nodal temperatures, $^\circ\text{C}$										
	0	2	4	6	8	10	12	14	16	18	20
0	0.0	→									
1	49.9	3.7	0.2	0.0	→						
2	61.9	8.4	0.8	0.1	0.0	→					
3	68.0	11.8	1.6	0.2	0.0	→					
4	71.6	14.0	2.3	0.3	0.0	→					
5	74.0	15.6	2.9	0.5	0.1	0.0	→				
6	75.6	16.7	3.3	0.6	0.1	0.0	→				
8	77.5	18.1	4.0	0.8	0.1	0.0	→				
10	78.5	18.9	4.4	1.0	0.2	0.0	→				
15	79.6	19.7	4.8	1.1	0.3	0.1	0.0	→			
20	79.9	19.9	4.9	1.2	0.3	0.1	0.0	→			
25	80.0	20.0	5.0	1.2	0.3	0.1	0.0	→			
$\infty$	80.0	21.1	5.6	1.5	0.4	0.1	0.0	→			

### Comments

The mesh size Peclet number is 0.667, so use of the central-difference scheme for the convective term was appropriate.

### 3.7 CLOSURE

The temperature distribution in a solid is governed by the general heat conduction equation. This partial differential equation can be solved using classical mathematical methods or using numerical methods. In either case, considerable effort is required to obtain the solution for a particular problem.

The use of the classical separation-of-variables method was demonstrated for both steady multidimensional conduction and unsteady one-dimensional conduction. The method of superposition of solutions was used to build up the solution of a problem with complicated boundary conditions from solutions for simple boundary conditions. A useful product rule allows the temperature response of a number of shapes of finite dimensions to be obtained as a product of the responses of simpler shapes with infinite dimensions. For example, the response for a finite-length cylinder is obtained from the response of an infinite cylinder and an infinite slab. The conduction shape factor is convenient for calculating two-dimensional heat conduction between two isothermal surfaces. Solutions for conduction into a semi-infinite solid are always applicable for times short enough for the penetration of the thermal response to be small compared to the body dimensions. The computer program COND1 is a useful tool for such calculations. Determining the temperature response of convectively cooled (or heated) slabs, cylinders, and spheres is made simple by the computer program COND2 and by the availability of results in graphical form as temperature response charts.

When the shape of a solid is irregular, or when boundary conditions are complex, solutions to the heat conduction equation are best obtained numerically. Standard computer programs for this purpose are widely available, and such programs should be used for any serious thermal design activity. Thus, numerical methods were not presented in great detail. Only the finite-difference method was considered, and then only with the objective of conveying the essential ideas involved. Actually, the heat conduction equation is one of the easiest equations to solve numerically, and even the simplest methods yield satisfactory results. At this level, the ideas involved are almost intuitive. However, any serious effort to develop versatile and efficient computer programs to solve the heat conduction equation should be preceded by an appropriate course in numerical analysis, so that questions concerning stability, rate of convergence, and accuracy are properly handled.

Many heat conduction problems involve a moving boundary. Both analytical and numerical solution methods were demonstrated for two such problems. Numerical methods are particularly relevant because some important moving-boundary problems, such as the ablation of a heat shield on a reentry vehicle, can involve strongly varying thermal properties, complicated surface boundary conditions, and chemical reactions. We chose to use coordinate axes fixed to the moving surface for the ablation problem in Sections 3.5.2 and 3.6.4. This approach has the effect of giving a *convection* term in the governing differential equation, Eq. (3.96) or (3.119), even though a solid rather than a fluid is involved. Similar terms will arise in the analysis of convection in Chapter 5.

## REFERENCES

1. Haberman, R., *Elementary Applied Partial Differential Equations*, 2nd ed., Prentice-Hall, Englewood Cliffs, N.J. (1987).
2. Boyce, W. E., and DiPrima, R. C., *Elementary Differential Equations and Boundary Value Problems*, 4th ed., John Wiley & Sons, New York (1986).
3. Kreyszig, E., *Advanced Engineering Mathematics*, 4th ed., John Wiley & Sons, New York (1979).
4. Fourier, J., *The Physical Theory of Heat*, Dover Publications, New York (1955). (Originally published in 1822.)
5. Carslaw, H. S., and Jaeger, J. C., *Conduction of Heat in Solids*, 2nd ed., Clarendon Press, Oxford (1959).
6. Emmons, H. W., "The numerical solution of heat conduction problems," *Trans. ASME*, 65, 607-615 (1943).
7. Kayan, C. F., "An electrical geometrical analogue for complex heat flow," *Trans. ASME*, 67, 713-718 (1945).
8. Karplus, W. J., and Soroka, W. W., *Analog Methods: Computation and Simulation*, 2nd ed., McGraw-Hill, New York (1959).
9. Myers, G. E., *Analytical Methods in Heat Conduction*, Genium Publishing Corporation, Schenectady, N.Y. (1987). <sup>Transfer</sup>
10. Gurney, H. P., and Lurie, J., "Charts for estimating temperature distributions in heating and cooling solid shapes," *Ind. Eng. Chem.*, 15, 1170-1172 (1923).
11. Rohsenow, W. M., Hartnett, J. P., and Ganic, E. N., eds., *Handbook of Heat Transfer Fundamentals*, 2nd ed., McGraw-Hill, New York (1985).
12. Schneider, P. J., *Temperature Response Charts*, John Wiley & Sons, New York (1963).
13. Heisler, M. P., "Temperature charts for induction and constant temperature heating," *Trans. ASME*, 69, 227-236 (1947).
14. Langston, L. S., "Heat transfer from multidimensional objects using one-dimensional solutions for heat loss," *Int. J. Heat Mass Transfer*, 25, 149-150 (1982).
15. London, A. L., and Seban, R. A., "Rate of ice formation," *Trans. ASME*, 65, 711-778 (1943).
16. SINDA (Systems Improved Numerical Differencing Analyzer), Lockheed Engineering and Management Services Company, Inc.

17. MITAS (Martin Marietta Interactive Thermal Analysis System), Martin Marietta Corporation.
18. PHOENICS (Parabolic, Hyperbolic or Elliptic Numerical Code Series), CHAM Ltd., 40 High Street, Wimbledon, London SW 19A4, England.
19. COMPACT, Innovative Research Inc., 2520 Broadway St., NE, Minneapolis, MN 55413.
20. Mitra, K., Kumar, S., Vedavarz, A., and Moallemi, M. K., "Experimental evidence of hyperbolic heat conduction in processed meat," *J. Heat Transfer*, 117, 568–573 (1995).

### EXERCISES

- 3-1. Derive the general heat conduction equation in cylindrical coordinates by applying the first law to the volume element shown in Fig. 3.3a.
- 3-2. Derive the general heat conduction equation in spherical coordinates by applying the first law to the volume element shown in Fig. 3.3b.
- 3-3. Use the methods of vector calculus to derive the general heat conduction equation. (*Hint:* Apply the first law to a volume  $V$  with surface  $S$ , and use the Gauss divergence theorem to convert the surface integral of heat flow across  $S$  to a volume integral over  $V$ .)
- 3-4. The cylindrical and spherical coordinate systems are examples of *orthogonal curvilinear coordinates*. In general, we can denote these coordinates by  $u_1, u_2, u_3$ , which are defined by specifying the Cartesian coordinates  $x, y, z$  as

$$x = x(u_1, u_2, u_3)$$

$$y = y(u_1, u_2, u_3)$$

$$z = z(u_1, u_2, u_3)$$

A coordinate system is orthogonal when the three families of surfaces  $u_1 = \text{Const}$ ,  $u_2 = \text{Const}$ ,  $u_3 = \text{Const}$  are orthogonal to one another. The figure shows an elemental parallelepiped whose faces coincide with planes  $u_1 = \text{Const}$  or  $u_2 = \text{Const}$  or  $u_3 = \text{Const}$ , with edge lengths  $h_1 du_1, h_2 du_2, h_3 du_3$  where  $h_1, h_2, h_3$  are called the *metric coefficients*. The length of a diagonal is given by

$$ds^2 = h_1^2 du_1^2 + h_2^2 du_2^2 + h_3^2 du_3^2$$

In terms of these coordinates, the components of the temperature gradient are

$$\frac{1}{h_1} \frac{\partial T}{\partial u_1}, \quad \frac{1}{h_2} \frac{\partial T}{\partial u_2}, \quad \frac{1}{h_3} \frac{\partial T}{\partial u_3}$$

